

*GASFLOW: A Computational
Fluid Dynamics Code for Gases,
Aerosols, and Combustion*

VOLUME 3
Assessment Manual

*J. W. Spore
P. Royl*
J. R. Travis*
E. D. Hughes
C. Müller
H. Wilkening**
W. Baumann*
G. F. Niederauer*

**Forschungszentrum Karlsruhe, Box 3640, 976021 Karlsruhe, Germany.
**ISPRA*

DISCLAIMER

This report was prepared as an account of work sponsored by an agency of the United States Government. Neither the United States Government nor any agency thereof, nor any of their employees, make any warranty, express or implied, or assumes any legal liability or responsibility for the accuracy, completeness, or usefulness of any information, apparatus, product, or process disclosed, or represents that its use would not infringe privately owned rights. Reference herein to any specific commercial product, process, or service by trade name, trademark, manufacturer, or otherwise does not necessarily constitute or imply its endorsement, recommendation, or favoring by the United States Government or any agency thereof. The views and opinions of authors expressed herein do not necessarily state or reflect those of the United States Government or any agency thereof.

DISCLAIMER

Portions of this document may be illegible electronic image products. Images are produced from the best available original document.

CONTENTS

	PAGE
ACKNOWLEDGMENTS	xiii
EXECUTIVE SUMMARY	xv
1.0. INTRODUCTION.....	1
1.1. Field Codes.....	1
1.2. GASFLOW	3
1.3. Objective.....	4
1.4. References.....	5
2.0. RESERVED FOR FUTURE USE.....	6
3.0. RESERVED FOR FUTURE USE.....	6
4.0. RESERVED FOR FUTURE USE.....	6
5.0. RESERVED FOR FUTURE USE.....	6
6.0. RESERVED FOR FUTURE USE.....	6
7.0. GASFLOW ASSESSMENT USING ANALYTICAL SOLUTIONS.....	7
7.1. Assessment Objectives	7
7.2. Assessment Problems	7
7.3. Significant Findings	7
7.4. Problem 1: Steady-State and Laminar Flow Startup	9
7.4.1. Summary.....	9
7.4.2. Problem Description and Solution.....	9
7.4.2.1. Problem Description.....	9
7.4.2.2. Equations and Analytical Solution.....	10
7.4.2.3. Analytical Results.....	11
7.4.2.4. Analytical Acceptance Parameters and Values.....	11
7.4.3. GASFLOW Calculations	11
7.4.3.1. GASFLOW Input Model.....	11
7.4.4. Conclusions and Recommendations.....	11
7.4.4.1. Input File Listing.....	13
7.5. Problem 2: Diffusion of Hydrogen into Air.....	16
7.5.1. Summary.....	16
7.5.2. Problem Description and Solution.....	16
7.5.2.1. Problem Description.....	16
7.5.2.2. Equations and Analytical Solution.....	16
7.5.2.3. Analytical Results.....	17
7.5.2.4. Analytical Acceptance Parameters and Values.....	17
7.5.3. GASFLOW Calculations	17
7.5.3.1. GASFLOW Input Model.....	17
7.5.4. Conclusions and Recommendations.....	18
7.5.4.1. Input File Listing.....	18
7.6. Problem 3: Flow past a Rectangular Block	22

CONTENTS (cont)

	PAGE
7.6.1. Summary.....	22
7.6.2. Problem Description and Solution.....	23
7.6.2.1. Problem Description.....	23
7.6.2.2. Analytical Results.....	23
7.6.2.3. Analytical Acceptance Parameters and Values.....	23
7.6.3. GASFLOW Calculations.....	23
7.6.3.1. GASFLOW Input Model.....	23
7.6.4. Conclusions and Recommendations.....	23
7.6.4.1. Input File Listing.....	26
7.7. Problem 4: Flow through a Variable Area Expansion.....	29
7.7.1. Summary.....	29
7.7.2. Problem Description and Solution.....	29
7.7.2.1. Problem Description.....	29
7.7.2.2. Equations and Analytical Solution.....	30
7.7.2.3. Analytical Acceptance Parameters and Values.....	30
7.7.3. GASFLOW Calculations.....	30
7.7.3.1. GASFLOW Input Model.....	30
7.7.4. Conclusions and Recommendations.....	30
7.7.4.1. Input File Listing.....	32
7.8. Problem 5: Abrupt Area Change; Flow through a Contraction.....	35
7.8.1. Summary.....	35
7.8.2. Problem Description and Solution.....	35
7.8.2.1. Problem Description.....	35
7.8.2.2. Equations and Analytical Solution.....	36
7.8.2.3. Analytical Acceptance Parameters and Values.....	36
7.8.3. GASFLOW Calculations.....	36
7.8.3.1. GASFLOW Input Model.....	36
7.8.4. Conclusions and Recommendations.....	37
7.8.4.1. Input File Listing.....	37
7.9. Problem 6: Flow with Friction in Constant-Area Ducts	40
7.9.1. Summary.....	40
7.9.2. Problem Description and Solution.....	40
7.9.2.1. Problem Description.....	40
7.9.2.2. Equations and Analytical Solution.....	41
7.9.2.3. Analytical Acceptance Parameters and Values.....	42
7.9.3. GASFLOW Calculations.....	42
7.9.3.1. GASFLOW Input Model.....	42
7.9.4. Conclusions and Recommendations.....	42
7.9.4.1. Input File Listing.....	42
7.10. Problem 7: Flow with Friction in Constant-Area Ducts, Part 2: Fluid Speed at Inlet Specified	45
7.10.1. Summary.....	45
7.10.2. Problem Description and Solution.....	45
7.10.2.1. Problem Description.....	45

CONTENTS (cont)

	PAGE
7.10.2.2. Equations and Analytical Solution	46
7.10.2.3. Analytical Acceptance Parameters and Values.....	46
7.10.3. GASFLOW Calculations	46
7.10.3.1. GASFLOW Input Model.....	46
7.10.4. Conclusions and Recommendations.....	47
7.10.4.1. Input File Listing.....	47
7.11. Problem 8: 1D Flow with an Orifice	50
7.11.1. Summary.....	50
7.11.2. Problem Description and Solution.....	50
7.11.2.1. Problem Description.....	50
7.11.2.2. Equations and Analytical Solution.....	51
7.11.2.3. Analytical Results.....	51
7.11.2.4. Analytical Acceptance Parameters and Values.....	51
7.11.3. GASFLOW Calculations	51
7.11.3.1. GASFLOW Input Model.....	51
7.11.4. Conclusions and Recommendations.....	51
7.11.4.1. Input File Listing.....	53
7.12. Problem 9: Uniform Energy Addition to Stagnant Fluid	56
7.12.1. Summary.....	56
7.12.2. Problem Description and Solution.....	56
7.12.2.1. Problem Description.....	56
7.12.2.2. Equations and Analytical Solution.....	57
7.12.2.3. Analytical Results.....	57
7.12.2.4. Analytical Acceptance Parameters and Values.....	57
7.12.3. GASFLOW Calculations	57
7.12.3.1. GASFLOW Input Model.....	57
7.12.4. Conclusions and Recommendations.....	57
7.12.4.1. Input File Listing.....	58
7.13. Problem 10: Specified Mass-Flow-Rate Boundary-Condition Function.....	62
7.13.1. Summary.....	62
7.13.2. Problem Description and Solution.....	62
7.13.2.1. Problem Description.....	62
7.13.2.2. Equations and Analytical Solution.....	63
7.13.2.3. Analytical Results.....	63
7.13.2.4. Analytical Acceptance Parameters and Values.....	63
7.13.3. GASFLOW Calculations	63
7.13.3.1. GASFLOW Input Model.....	63
7.13.4. Conclusions and Recommendations.....	63
7.13.4.1. Input File Listing.....	64
7.14. Problem 11: Filter with Turbulent Flow Losses	69
7.14.1. Summary.....	69
7.14.2. Problem Description and Solution.....	70
7.14.2.1. Problem Description.....	70

CONTENTS (cont)

	PAGE
7.14.2.2. Analytical Results	70
7.14.2.3. Analytical Acceptance Parameters and Values.....	70
7.14.3. GASFLOW Calculations	70
7.14.3.1. GASFLOW Input Model.....	70
7.14.4. Conclusions and Recommendations.....	70
7.14.4.1. Input File Listing.....	71
7.15. Problem 12: Filter with Laminar Flow Losses.....	74
7.15.1. Summary.....	74
7.15.2. Problem Description and Solution.....	74
7.15.2.1. Problem Description.....	74
7.15.2.2. Analytical Results	75
7.15.2.3. Analytical Acceptance Parameters and Values.....	75
7.15.3. GASFLOW Calculations	75
7.15.3.1. GASFLOW Input Model.....	75
7.15.4. Conclusions and Recommendations.....	75
7.15.4.1. Input File Listing.....	75
7.16. Problem 13: Filter with Laminar plus Turbulent Flow Losses	79
7.16.1. Summary.....	79
7.16.2. Problem Description and Solution.....	79
7.16.2.1. Problem Description.....	79
7.16.2.2. Analytical Results	80
7.16.2.3. Analytical Acceptance Parameters and Values.....	80
7.16.3. GASFLOW Calculations	80
7.16.3.1. GASFLOW Input Model.....	80
7.16.4. Conclusions and Recommendations.....	80
7.16.4.1. Input File Listing.....	80
7.17. Problem 14: Steady-State Heat Transfer through a Wall	84
7.17.1. Summary.....	84
7.17.2. Problem Description and Solution.....	84
7.17.2.1. Problem Description.....	84
7.17.2.2. Equations and Analytical Solution.....	85
7.17.2.3. Analytical Acceptance Parameters and Values.....	86
7.17.3. GASFLOW Calculations	86
7.17.3.1. GASFLOW Input Model.....	86
7.17.3.2. GASFLOW Results	86
7.17.4. Conclusions and Recommendations.....	87
7.17.4.1. Input File Listing.....	87
7.18. Problem 15: Pressure-Volume Work Term 1: Equilibrium Case	91
7.18.1. Summary.....	91
7.18.2. Problem Description and Solution.....	91
7.18.2.1. Problem Description.....	91
7.18.2.2. Equations and Analytical Solution.....	92
7.18.2.3. Analytical Acceptance Parameters and Values.....	93
7.18.3. GASFLOW Calculations	93

CONTENTS (cont)

	PAGE
7.18.3.1. GASFLOW Input Model.....	93
7.18.3.2. GASFLOW Results.....	93
7.18.4. Conclusions and Recommendations.....	93
7.18.4.1. Input File Listing.....	96
8.0. GASFLOW COMPARISON WITH DATA	99
8.1. Assessment Objectives	99
8.2. Assessment Problems	99
8.2.1. The BOM Spherical Combustion Chamber	99
8.2.1.1. Comparison of Computed Results.....	99
8.2.1.2. Conclusions.....	103
8.2.2. The SNL FLAME Experiment (FLAME Facility Test Problem).....	105
8.2.2.1. Background.....	105
8.2.2.2. GASFLOW Model of the FLAME Facility.....	106
8.2.2.3. Calculation Results and Comparison with Experiment.....	107
8.2.3. GX6 Battelle Test GX6	121
8.2.3.1. Summary	121
8.2.3.2. Test Description.....	121
8.2.3.3. GASFLOW Calculations.....	122
8.2.3.3.1.GASFLOW input model.....	122
8.2.3.3.2.GASFLOW results.....	122
8.2.3.4. Conclusions and Recommendations.....	122
8.2.3.5. Input File Listing.....	127
8.2.4. Battelle Containment HYJET Test JX7	143
8.2.4.1. Summary	143
8.2.4.2. Test Description.....	144
8.2.4.3. GASFLOW Calculations.....	145
8.2.4.3.1.GASFLOW Input Model	145
8.2.4.3.2.GASFLOW Results.....	145
8.2.4.4. Conclusions and Recommendations.....	145
8.2.4.5. Input File Listing.....	150
8.2.5. HDR Test T31.5.....	165
8.2.5.1. Summary	165
8.2.5.2. Test Description.....	165
8.2.5.3. GASFLOW Calculations	169
8.2.5.3.1.GASFLOW Input Model	169
8.2.5.3.2.GASFLOW Results.....	170
8.2.5.4. Conclusions and Recommendations.....	174
8.2.6. Phebus Test	175
8.2.6.1. Summary	175
8.2.6.2. Test Description.....	175
8.2.6.3. GASFLOW Calculations	179

CONTENTS (cont)

	PAGE
8.2.6.3.1.GASFLOW Input Model	179
8.2.6.3.2.GASFLOW Results.....	179
8.2.6.4. Conclusions and Recommendations.....	180
8.2.6.5. Input File Listing.....	180
8.3. References.....	185

FIGURES

	PAGE
Fig. 7-1. Sketch of laminar flow between parallel plates.....	12
Fig. 7-2. Comparison of GASFLOW predictions with a steady-state solution.	12
Fig. 7-3. Comparison of analytical solution and GASFLOW results at time 10 s.....	18
Fig. 7-4. The GASFLOW mesh for calculating a flow field behind a rectangular block.....	24
Fig. 7-5. Velocity vector plot.....	24
Fig. 7-6. Velocity as a function of time at i = 18, j = 3, and k = 2.....	25
Fig. 7-7. Velocity as a function of time at i = 17, j = 4, and k = 2.....	25
Fig. 7-8. Flow area as a function of distance along the channel	31
Fig. 7-9. Comparison of GASFLOW and analytical solution for the fluid speed	31
Fig. 7-10. Sketch of a 1D duct with abrupt contraction in the flow area.....	37
Fig. 7-11. Comparison of an analytical solution and GASFLOW results for the fluid speed	52
Fig. 7-12. Comparison of an analytical solution and GASFLOW results for the pressure	53
Fig. 7-13. Comparison of the analytical solution and GASFLOW results	58
Fig. 7-14. Comparison of analytical solution and GASFLOW results.....	64
Fig. 7-15. Temperature as a function of time	94
Fig. 7-16. Total mass as a function of time.....	95
Fig. 7-17. Pressure as a function of time	96
Fig. 8-1. 120-L flammability test sphere	101
Fig. 8-2. Pressure ratio vs hydrogen concentration.....	102
Fig. 8-3. Pressure ratio vs hydrogen concentration for quiescent mixtures of 1:1 ratios of hydrogen/nitrous oxide in air.....	102
Fig. 8-4. Pressure ratio vs hydrogen concentration for quiescent mixtures of 1:1 ratios of hydrogen/nitrous oxide in air compared with data with 1 and 2% added ammonia	104

FIGURES (cont)

	PAGE
Fig. 8-5. Absolute pressure vs time for 10% quiescent hydrogen/nitrous oxide mixtures in air.....	104
Fig. 8-6. Time rate of pressure change vs time for 10% quiescent hydrogen/nitrous oxide mixtures in air	105
Fig. 8-7. Schematic diagram of the SNL FLAME channel, showing the locations of hydrogen injection. The shaded area indicates the symmetrical region modeled in the computation.....	110
Fig. 8-8. Computational domain for the SNL FLAME simulation calculation, showing the variable mesh.....	111
Fig. 8-9. Two-dimensional view of the computational mesh used for the SNL FLAME calculation, showing the location where hydrogen is injected	112
Fig. 8-10. Plot of the calculated velocity vectors in the SNL FLAME experiment at the plane of injection 100 s after initiation of the hydrogen injection. The maximum velocity magnitude (averaged at cell centers) is 22.3 m/s....	113
Fig. 8-11. Contour plot of the calculated hydrogen volume fraction in the SNL FLAME experiment at the plane of injection at 100 s after the hydrogen injection begins, showing development of the buoyant plume.....	114
Fig. 8-12. Contour plot of the calculated hydrogen volume fraction in the SNL FLAME experiment at the plane of injection 200 s after the hydrogen injection begins. Note the gradual spreading of the buoyant plume.....	115
Fig. 8-13. Plot of the computed velocity vectors in the SNL FLAME experiment at the plane of injection at 487 s, which is immediately after the injection stops. The maximum velocity magnitude (averaged at cell centers) is 7.2 m/s	116
Fig. 8-14. Computed hydrogen volume fraction contours in the SNL FLAME experiment at the plane of injection at 487 s, which is immediately after the injection stops	117
Fig. 8-15. Calculated profile of hydrogen mole fraction in the SNL FLAME experiment as a function of distance from the bottom of the channel at 100 and 1800 s after the injection stops. The two experimental data points (with error bars) at 1800 s also are shown	118
Fig. 8-16. Calculated hydrogen volume fraction contours in the SNL FLAME experiment at the plane of injection 1800 s after the injection stops exhibiting vertical stratification of the hydrogen.....	119
Fig. 8-17. Time-history plots of the calculated hydrogen mole fraction in the SNL FLAME experiment at various locations. Note the merging of the curves for the two locations at the same height (i.e., same first-cell index, 9).....	120
Fig. 8-18. Scheme of the BMC for the Battelle GX tests (radial cut and unwrapped geometry of banana rooms).....	123

FIGURES (cont)

	PAGE
Fig. 8-19. GX6 source data and pressure transient GASFLOW 2.1 analysis with ducts for valve and leak simulations	124
Fig. 8-20. Calculated and measured gas temperatures in Battelle test GX6 with GASFLOW 2.1 and use of ducts for valve and leak simulations	125
Fig. 8-21. Calculated and measured hydrogen volume fractions in Battelle test GX6 with GASFLOW 2.1 and use of ducts for valve and leak simulations.....	126
Fig. 8-22. Helium jet in BMC during Hyjet test Jx7 at 50 s (GASFLOW-Kismet)	144
Fig. 8-23. He concentrations as a function of time at selected axial levels	146
Fig. 8-24. He concentrations as a function of time at two different positions.....	147
Fig. 8-25. He concentrations as a function of axial position at two different times	48
Fig. 8-26. He concentrations as a function of radial position from the jet center line at two different times and two different axial positions.....	149
Fig. 8-27. Cross-sectional view of the HDR containment building at two angles. The cross section on the right shows the standard staircase; the spiral staircase is visible on the left	168
Fig. 8-28. (a) Cross-sectional view of the HDR containment facility showing the blowdown room. The blowdown pipe can be seen in the middle, extending from the left side of the pressure vessel; (b) perspective drawing of the blowdown room; and (c) details of the blowdown pipe, gas injection pipe, and diffusor.....	169
Fig. 8-29. Noding diagram.....	172
Fig. 8-30. HDR test T31.5 pressures and temperatures; test data vs results from GASFLOW 2.1	173
Fig. 8-31. Light-gas (15% hydrogen, 95% helium) volume fractions in HDR test T31.5; test data vs results from GASFLOW 2.1.....	174
Fig. 8-32. Phebus Containment Vessel REPF 502.....	177
Fig. 8-33. Characteristic flow field from GASFLOW	179

TABLES

	PAGE
Table 7-1 Analytical Assessment Problems Summary.....	8
Table 8-1 Location of the X, Y, and Z gridlines in the GASFLOW model of the SNL FLAME Facility	107
Table 8-2 Time sequence of events in the HDR T31.5 experiment.....	167
Table 8-3 Parameters and Results for the Steady-State Thermal-Hydraulic Tests.....	178

ACKNOWLEDGMENTS

The authors would like to thank Lisa Rothrock and Ann Mascareñas for their careful preparation and technical editing of this document.

**GASFLOW: A Computational Fluid Dynamics Code for Gases,
Aerosols, and Combustion**

by

**J. W. Spore, P. Royl, J. R. Travis, E. D. Hughes, C. Müller,
H. Wilkening, W. Baumann, and G. F. Niederauer**

EXECUTIVE SUMMARY

Los Alamos National Laboratory (LANL) and Forschungszentrum Karlsruhe (FzK) are developing GASFLOW, a three-dimensional (3D) fluid dynamics field code as a best-estimate tool to characterize local phenomena within a flow field. Examples of 3D phenomena include circulation patterns; flow stratification; hydrogen distribution mixing and stratification; combustion and flame propagation; effects of noncondensable gas distribution on local condensation and evaporation; and aerosol entrainment, transport, and deposition.

An analysis with GASFLOW will result in a prediction of (1) the gas composition and discrete particle distribution in space and time throughout the facility and (2) the resulting pressure and temperature loadings on the walls and internal structures with or without combustion. A major application of GASFLOW is for predicting the transport, mixing, and combustion of hydrogen and other gases in nuclear reactor containments and other facilities. It has been applied to situations involving transporting and distributing combustible gas mixtures. It has been used to study gas dynamic behavior (1) in low-speed, buoyancy-driven flows, as well as sonic flows or diffusion dominated flows; and (2) during chemically reacting flows, including deflagrations. The effects of controlling such mixtures by safety systems can be analyzed.

The code version described in this manual is designated GASFLOW 2.1, which combines previous versions of the United States Nuclear Regulatory Commission code HMS (for Hydrogen Mixing Studies) and the Department of Energy and FzK versions of GASFLOW. The code was written in standard Fortran 90. This manual comprises three volumes. Volume I describes the governing physical equations and computational model. Volume II describes how to use the code to set up a model geometry, specify gas species and material properties, define initial and boundary conditions, and specify different outputs, especially graphical displays. Sample problems are included. Volume III contains some of the assessments performed by LANL and FzK. GASFLOW is under continual development, assessment, and application by LANL and FzK. This manual is considered a living document and will be updated as warranted.

GASFLOW is a finite-volume code based on robust computational fluid dynamics numerical techniques that solve the compressible Navier-Stokes equations for 3D

volumes in Cartesian or cylindrical coordinates. The code can model geometrically complex facilities with multiple compartments and internal structures in a computational domain of multiple 3D blocks of cells connected by one-dimensional flow paths. GASFLOW has transport equations for multiple gas species, liquid water droplets, and total fluid internal energy. A built-in library contains 23 gas species and 1 liquid water species.

GASFLOW can simulate the effects of two-phase dynamics with the homogeneous equilibrium model, two-phase heat transfer (steam condensation and water evaporation) to walls and internal structures, chemical kinetics from catalytic hydrogen recombination and combustion processes, and fluid turbulence. The code can model two-phase heat transfer to and from walls and internal structures by convection and mass diffusion.

Wall shear stress models are provided for bulk laminar and turbulent flow. Two turbulence models available: algebraic and κ - ϵ , which provide zero- and two-transport-equation models, respectively, that determine turbulent velocity and length scales needed to compute the turbulent viscosity. Terms for the turbulent diffusion of different species are included in the mass and internal energy equations.

Chemical energy of combustion involving hydrogen provides a source of energy within the gaseous regions. A one-step global chemical kinetics model based on a modified Arrhenius law accounts for local hydrogen and oxygen concentrations. A two-step chemical kinetics model divides the chemical reaction into two parts: (1) an induction phase, which builds radicals and releases little energy; and (2) an energy release phase, where the radicals recombine. Hydrogen is ignited using a generalized ignitor model that represents both spark- and glow-plug-type designs. A catalytic hydrogen combination with oxygen is modeled using data from both the Nuclear Ingenieur Service and Siemens recombiner box designs.

The aerosol model comprises the following models: Lagrangian discrete particle transport, stochastic turbulent particle diffusion, particle deposition, particle entrainment, and particle cloud. These models incorporate the physics of particle behavior to model discrete particle phenomena and allow the code user to track the transport, deposition, and entrainment of discrete particles, as well as clouds of particles.

GASFLOW 2.1 models have been extended beyond GASFLOW 1.0 with the following developments:

- independent multiblock computational domains;
- independent multiblocks connected on external boundaries by a ventilation system;
- a fractional area treatment to model flow areas smaller than a cell face area;

- accurate internal energy as a function of temperature to fourth-degree polynomials;
- gas properties library of thermochemical and transport extended to 30 species;
- homogeneous equilibrium model for fluid mixture;
- droplet depletion or "rainout";
- two-phase heat and mass transfer to structural components;
- both spark- and glow-plug ignitor models;
- empirical hydrogen combustion limits;
- hydrogen recombiner models; and
- transport, deposition, and entrainment of discrete particles.

Each version of GASFLOW is tested with a Standard Test Matrix of 126 problems in four categories: (1) feature tests for the computer science aspects of the code; (2) functional tests for code algorithms, equations, logic paths, and decision points; (3) comparisons with analytical solutions; and (4) comparisons with data. During the development of GASFLOW 2.1, many experiments were modeled and analyzed. All 19 analytical solutions and the following 6 experiments are documented in Volume III: (1) the Bureau of Mines Spherical Test Chamber; (2) the Sandia FLAME Experiment; (3) Battelle Model Containment (BMC) Test GX6; (4) Battelle Model Containment Test HYJET JX7; (5) Heißdampfreaktor (HDR) Test T31.5; and (6) Phebus Tests 4A, 4B, 6A, and 10A. All of the problems in the Standard Test Matrix and in the initial set of assessments were executed successfully by GASFLOW 2.1 without modification, and the results are in agreement with the analytical solution or the test data. For example, other assessment analyses of the HDR, BMC, Russian RUT, and LANL TA-55 facilities are documented in the literature.

The Bureau of Mines Spherical Test Chamber (having a volume of 120 L) has been used to investigate the flammability of hydrogen, ammonia, nitrous oxide, and air mixtures under quiescent and turbulent conditions. GASFLOW calculated combustion of mixtures of hydrogen concentrations for 5 to 40 vol % diluted in air, 1:1 ratios of hydrogen and nitrous oxide in air, and very low hydrogen and nitrous oxide concentrations in air with 1 and 2% ammonia added. Beginning with ambient temperature and pressure, GASFLOW accurately calculated that the behaviors of both fuel-lean and fuel-rich mixtures for hydrogen are (1) little pressure rise for very low hydrogen concentrations, (2) downward flame propagation and nearly complete combustion for approximately 8% hydrogen, and (3) a maximum pressure for a stoichiometric (29.6% hydrogen) mixture. Good results were obtained for the mixtures where nitrous oxide was added, although the pressure rise rate was conservatively high by up to 20%. In conclusion, the one-step finite-rate chemical kinetics model yields good results but is limited. For more complex combustion problems, a reduced set of chemical kinetics mechanisms or a two-step

method based on an induction parameter model should be used. Both improved models are derived from detailed chemical kinetics mechanisms.

The FLAME facility (1.8 m wide, 2.4 m high, 30 m long = 136 m³) at Sandia National Laboratories was used to study flame acceleration and deflagration-to-detonation transition of hydrogen-air mixtures. In experiment F-21, 13% hydrogen was added and mixed with a fan. After 30 min, gas samples indicated stratification ranging from 15% at an upper location to 10% at a lower location. The test was chosen to assess transient mixing and stratification calculations by GASFLOW, beginning with stagnant air and followed by hydrogen injection, mechanical mixing, and natural stratification. The algebraic turbulence model was used, and results were not very sensitive to the chosen turbulent length scale because mixing was largely achieved by molecular diffusion. GASFLOW showed that the hydrogen jet does not penetrate very far before it becomes a buoyant plume that gradually expands. At 100 s after injection ends, stratification is maximum (approximately 17% at the top and approximately 4% at the bottom) in the early part of the mixing phase, which lasted for 1800 s, or 30 min. When the gas samples were taken, GASFLOW calculated upper and lower volume fractions of 15.4% and 9.8%, respectively, within the reported uncertainty of 0.5%.

The Battelle Model Containment (BMC) Test GX6 was used to validate the catalytic recombiner model in GASFLOW. This test was conducted using the central cylindrical room R1/R3 and the annular segment compartments R5 through R8; these rooms were sealed off from the remainder of the BMC. Each compartment has a gas volume of 49 m³; the total for test GX6 was 209 m³. A Siemens catalytic recombiner was placed next to the inner wall of R5, not far from the opening to R6. Steam was injected into rooms R5, R6, and R7. Hydrogen was injected into R8. Ten hours of the test was calculated with GASFLOW. The calculated pressure was slightly higher than measured and stayed more level, indicating a combination of too much in-leakage in the calculation and slightly different boundary condition pressures. The drop in pressure at approximately 6 h into the transient, which was caused by terminating the inflow of steam, was calculated to be slightly earlier and larger. This drop indicated that the condensation rate in GASFLOW is slightly larger than is inferred from the test data. The overall agreement is good and captures the dominant trends in the data. Temperature comparisons at several different locations are excellent and capture dominant trends in the data. In particular, the temperature rise through the recombiner was calculated quite accurately.

The BMC Test JX7, also known as HYJET, was used to validate the capability to model small- and large-scale effects of a turbulent jet and convection with containment within one calculation. This test used all of the rooms in the BMC, except the annular segment compartment R7, which has a total gas volume of 600 m³. Near the bottom of R6, a helium mass of 9.25 kg was injected vertically under the openings to R5 and to the dome over a period of 200 s. The nozzle had a diameter of 95 mm and an average injection velocity of 42 m/s. The jet from the nozzle extended all the way from the source location into the dome region, where the helium then stratifies as a cloud. Using a model with 50,000 computational cells, GASFLOW calculated the helium concentrations at four sensor locations: in the dome, near the bottom of the central room, and in the upper and lower parts of the ring room. In general, GASFLOW predicts the dominate trends well and predicts the helium stratification consistently with the data. Good agreement was

obtained in the central room and in the lower part of the ring room. GASFLOW overpredicted the helium concentration in the dome region; this is attributed to insufficient air entrainment along the jet surface.

HDR Test T31.5, also known as an International Standard Problem, ISP-23, was used to validate the capability to model hydrogen and steam transport and distributions in a large-scale containment during a simulated large-break loss-of-coolant accident. The containment has a steel shell with a height of 60 m, an internal diameter of 20 m, and a free volume of 11,300 m³. The containment has 72 compartments connected with about 200 passageways below the approximately 5000-m³ volume of the open hemispherical-dome region. In this test, a blowdown from the pressure vessel injected 30,000 kg of a steam-water mixture over the first 50 s at the 22-m level. From 21 to 36 min, superheated steam was injected at a rate of 2.2 kg/s. From 36 to 48 min, a light gas (14% hydrogen and 85% helium) was injected. The GASFLOW model for T31.5 used 12,300 computational cells with obstacles and barriers to model all major floors and walls and all compartments. Heat structures were modeled extensively through the containment. An isentropic expansion model was used for the blowdown. GASFLOW predicts the dominate trends well for pressure, temperature, and concentration for this complex test.

Pressure peaks and rapid pressure equilibrium calculated by GASFLOW throughout the containment agreed quite well with the data. After 5 min, GASFLOW starts predicting a slower pressure decay, reaching a difference of 0.08 bars after about 15 min. One explanation is the lack of a film relocation model. The film vaporization model provides a continuous steam source that slows down the pressure decay; however, that should be cut off as dryout occurs. Calculated temperature histories reflect the somewhat higher asymptotic pressures. Calculated values are high by about 10°C in the middle and upper containment and by 20° to 25°C in the bottom containment. Three effects could cause high bottom temperatures; the most likely is that a significant amount of water collects in the bottom, creating an additional heat sink, especially after passing over cold surfaces on the way down. GASFLOW calculations of light-gas concentrations in the spiral staircase and in the dome are in excellent agreement with data. In two places, GASFLOW concentrations vary significantly from the data. One is near the source, where concentration gradients vary strongly and the computational mesh is not fine enough to resolve them well. Another is at the bottom, where the concentration is very low (only about 0.5%).

Four steady-state tests (4A, 4B, 6A, and 10A) in the Phebus facility were used to validate the condensation model in GASFLOW. The facility (approximately 5.7 m high and 1.8 m in diameter = 10 m³) has a insulated double skinned wall through which coolant flows to maintain a homogeneous inner wall temperature of approximately 110°C. Inside the top part of the facility is (1) a wet condenser, which consists of three steel rods internally cooled to a specific temperature, and (2) a dry condenser, which is heated to prevent condensation. Initial conditions were air diluted with 39 vol % steam at 110°C and 1.9 bars. Steam sources for this set of tests varied from 1 g/s at 114°C and 1.65 bar to 4 g/s at 125°C and 2.3 bar, directly vertically upward from the bottom. A GASFLOW model of 715 computational cells modeled a 60-degree sector. Condensation parameters were set to standard values. The calculated final pressures during the condensation process were found to agree with the data within 1% to 5% for the various cases.

1.0. INTRODUCTION

1.1. Field Codes

It is common to differentiate between two types of multidimensional fluid dynamics codes. A "field code" uses correlations for wall flow resistance and heat transfer. A "computational fluid dynamics (CFD) code" calculates the heat and momentum transfer through the boundary layer at a wall instead of using correlations. Although GASFLOW [1-1] is capable of calculating flow and heat-transfer gradients near surfaces, thus resolving boundary layers, noding for such calculations is too fine for practical analyses of full-size containment structures and other facilities. Thus, for most engineering analyses, GASFLOW is characterized as a field code.

In field codes, a model (e.g., a nuclear power plant containment) comprises relatively small control volumes (also called nodes or cells), perhaps hundreds or thousands per each compartment. Using many cells provides resolution of detail of primary quantities, such as temperature and momentum, within a compartment. Each control volume has three momentum equations and energy and mass conservation equations. Therefore, in a field code, momentum is advected along three axes locally as well as potentially at multiple points between compartments. Mass and energy are advected between cells within a compartment, as well as potentially at several points between adjacent compartments.

Field codes traditionally have been used for benchmark containment analysis and for investigating complex phenomena that were beyond the capabilities of lumped parameter codes. Field codes focus on predicting local parameters (e.g., concentration, temperature, and velocity). These codes represent a detailed approach to containment modeling. Field codes traditionally have been used for best-estimate calculations rather than conservative predictions.

Advantages of a field code:

- Full Navier-Stokes equations, providing detailed modeling capabilities and removing many of the assumptions inherent in lumped parameter code formulations.
- Capability to determine primary and local flow patterns that could improve on models for heat and mass transfer, thereby increasing accuracy.
- Capability to calculate countercurrent and multiple flow streams between compartments, rather than the single-flow direction and composition of a lumped parameter flow path.
- Capability to calculate local concentrations and concentration gradients across a compartment, as well as across a containment, for more accurate calculations of distributions of species and formation of phenomena such as

plumes, pockets, and stratification.

- Capability to calculate complex interactions among phenomena, such as local state conditions, flow fields, aerosol dynamics, combustion chemistry, and wall interactions of heat and mass transfer.
- Software structure that allows adding alternative theoretical and empirical models for various relations and phenomena, as well as numerical techniques, to study the effects of interactions with other code features, perform sensitivity and uncertainty studies, and perform benchmark studies against experiments.
- Inherent ability to predict 3D details of physical behavior, such as flow patterns and the formation and dissipation of such phenomena as plumes and stratification, thus providing a means to visualize and dissect the phenomena with sophisticated computer graphics.

Disadvantages of a field code:

- Protracted input setup times, requiring detailed facility data that may not be readily available.
- Long computational times, highly dependent on (1) the total number of nodes and complexity of physical models employed; and (2) a variety of platforms, including mainframes, workstations, and personal computers. Limits the ability to perform sensitivity studies. Vector and multiprocessing machines highly desirable.
- Lack of integrated models for certain systems, such as boiling-water reactor (BWR) pressure suppression, ice condenser, and AP600 external containment film flow, limits the types of analyses that can be performed.
- Potential user and numerical distortions can be amplified if the user is insufficiently experienced or prudent in using the code.
- Complex containment configurations, so simplifications of geometrical detail on predicted results could be significant, albeit less so than with a lumped parameter code.
- Limited assessment base relative to containment scenarios and phenomena, especially for specific models such as turbulence.
- Mesh size near structures is dependent on empirical-heat and mass-transfer correlations used.
- Technology is advancing quickly, thus mitigating or removing some of the disadvantages of field codes. Modern preprocessors with grid generators,

point and click operations, and databases can greatly reduce input setup times. The speed of workstations and personal computers continues to increase exponentially unabated. It will not be long before vector and multiprocessor workstations and personal computers become available and outstrip the performance of current vector supercomputer mainframes, as has already happened with scalar performance.

- Some types of sensitivity studies can be performed in parallel by using different computers, perhaps using CPUs that otherwise would be idle.
- Field codes are becoming commonplace in many industries. A wide variety of applications to many types of buildings and scenarios encompass many of the same phenomena found in a containment; thus, the general experience of the field is large and increasing. The experience in other larger industries needs to be tapped by the relatively small nuclear industry.

To gain more confidence in the results obtained from field codes, several issues need to be addressed. Software issues concern numerical uncertainty, adequacy of physical models, existence of compensating errors, and complex geometry. Assessing a code against experimental data is one means of gaining confidence in code results. One journal concerned about numerical accuracy in CFD codes (also applicable to field codes) has set forth 10 criteria for accepting papers, stating that such standards must be considered in practical engineering applications as well as in research projects. [1-2] User issues include guidelines for modeling complex geometry, determining nodalization, and selecting code options. User issues should be addressed in a users' manual and in reports on assessment. All of these issues must be addressed appropriately to qualify a code for its intended uses.

1.2. GASFLOW

Reflecting the advancement of nuclear power and other types of technology, GASFLOW has been modified and improved to consider various scenarios and phenomena that had not been previously introduced and hypothesized. As the need to understand more complicated phenomena more fully increases, the analytical models must become more sophisticated. GASFLOW was constructed to better characterize local phenomena within a flow field. Calculating detailed physical phenomena, GASFLOW is well suited for benchmark analysis and for examining issues requiring high physical resolution. Examples of 3D phenomena include circulation patterns; flow stratification; hydrogen distribution mixing and stratification; combustion and flame propagation; effects of noncondensable gas distribution on local condensation and evaporation; and aerosol entrainment, transport, and deposition.

An analysis with GASFLOW will result in a prediction of (1) the gas composition and discrete particle distribution in space and time throughout the facility and (2) the resulting pressure and temperature loadings on the walls and internal structures with or without combustion. A major application of GASFLOW is for predicting transport, mixing, and combustion of hydrogen and other gases in nuclear reactor containments

and other facilities. It has been applied to situations involving transporting and distributing combustible gas mixtures. It has been used to study gas dynamic behavior (1) in low-speed, buoyancy-driven flows, as well as sonic flows or diffusion dominated flows; and (2) during chemically reacting flows, including deflagrations.

In the future, improvements in software technology and new experimental data will be used to improve the modeling capabilities of GASFLOW. Improvements in hardware technology will increase computational speed, making GASFLOW more suitable for general use.

1.3. Objective

The primary objective of this document is to present and discuss some results of the GASFLOW assessment performed for the Nuclear Regulatory Commission (NRC). Here we define assessment as the process of evaluating the results of code calculations in comparison with analytical solutions and experimental data.

Experimental data to support code assessment are available from the Flame and Surtsey facilities at Sandia National Laboratories (SNL), the Battelle-Frankfurt Model Containment (BMC) and Heißdampfreaktor (HDR) facilities in Germany, the Phebus facility in France, the RUT facility in Russia, and other government and commercial facilities. Basic and separate effects data are available from various university and government laboratories. However, the experimental data for characterizing local phenomena, particularly detailed velocity vectors and transient gas concentration measurements, are sparse and can have significant uncertainties.

Each version of GASFLOW is tested with a Standard Test Matrix of 126 problems in four categories: (1) feature tests for the computer science aspects of the code; (2) functional tests for code algorithms, equations, logic paths, and decision points; (3) comparisons with analytical solutions; and (4) comparisons with data. During the development of GASFLOW 2.1, many experiments were modeled and analyzed. All 19 analytical solutions and 6 experiments are documented in this volume: (1) the Bureau of Mines Spherical Test Chamber, (2) the Sandia FLAME Experiment, (3) Battelle Model Containment (BMC) Test GX6, (4) Battelle Model Containment Test HYJET JX7, (5) Heißdampfreaktor (HDR) Test T31.5, and (6) Phebus Tests 4A, 4B, 6A, and 10A. All of the problems in the Standard Test Matrix and in the initial set of assessments were executed successfully by GASFLOW 2.1 without modification, and the results are in agreement with the analytical solution or the test data. Other assessment analyses of experiments in the HDR, BMC, Russian RUT, and Los Alamos TA-55 facilities, for example, are documented in the literature.

Testing and assessment of GASFLOW are ongoing activities associated with the continual code development of GASFLOW. Thus, this is expected to be a living document; new results will be added as the work is completed. Currently, this document contains only the introduction and two chapters on code assessment. The other chapters have been drafted and will be completed and added to this manual as funding becomes available.

1.4. References

- 1-1 J. R. Travis, J. W. Spore, P. Royl, K. L. Lam, T. L. Wilson, G. A. Necker, B. D. Nichols, R. Redlinger, E. D. Hughes, H. Wilkening, W. Baumann, and G. F. Niederauer, "GASFLOW: A Computational Fluid Dynamics Code for Gases, Aerosols, and Combustion; Vol. 1, Theory and Computational Model; Vol. 2, User's Manual; and Vol. 3, Assessment Manual," Los Alamos National Laboratory report LA-13357-MS (1998), and Forschungszentrum Karlsruhe report FZKA-5994 (1998).
- 1-2 C. J. Freitas, "Policy Statement on Control of Numerical Accuracy," *ASME Journal of Fluids Engineering* 115, pp. 339-340 (1993).

RESERVED FOR FUTURE USE (Sections 2.0 thru 6.0 – TBD)

7.0. GASFLOW ASSESSMENT USING ANALYTICAL SOLUTIONS

7.1. Assessment Objectives

Problems with analytical solutions provide an opportunity to test rigorously the equations and solution methods used in GASFLOW. However, these problems usually are limited to a small subset of the general models and methods in GASFLOW. Thus, although the success metric is both exact and complete, the coverage in terms of the total models and methods in GASFLOW will be very limited. In some cases, the 1D assessment problems can be run one at a time in the three coordinate directions, thus increasing the coverage; however, the basic problem still will be limited to the number of items tested.

Some problems with analytical solutions that have been used in the GASFLOW assessment are discussed in this section. A standard format has been adopted for reporting the results of the testing. The reporting format also will be used to record and present the results of other GASFLOW testing.

The advantages of using problems with analytical solutions include the fact that the problems are very narrowly focused and exact. These characteristics allow application of very stringent success matrix to the GASFLOW results. That is, the one or two terms that are the focus of each problem must be evaluated exactly by GASFLOW.

7.2. Assessment Problems

The assessment problems with analytical solutions are summarized in Table 7-1. The following information is shown in the table. The second column lists the terms in the model equations that are tested by the problems listed in the first column. In addition to the specific terms in the basic equations, each problem tests how boundary conditions are handled in GASFLOW.

7.3. Significant Findings

All of the problems listed in Table 7-1 were executed successfully by GASFLOW. All problems were run on GASFLOW 2.1.0.13 or 2.1.1.4 without modification. The success metric for these assessment tests that have an analytical solution is that the GASFLOW results will be in agreement with the analytical solution.

The only significant finding revealed by testing GASFLOW with these problems was that the boundary condition specification can change the results in GASFLOW. If the fluid speed is specified at the inlet, for example, the momentum flux is not calculated. If the pressure at the inlet is specified instead, the momentum flux is calculated. This is characteristic of a finite-volume differencing scheme. Specification of the velocity as a boundary condition implies that the momentum equation solution is replaced with the velocity boundary-condition specification and that the calculation of the momentum flux at the boundary therefore is not necessary.

TABLE 7-1 ANALYTICAL ASSESSMENT PROBLEMS SUMMARY

Problem Description	What is Tested
1. Laminar startup between parallel plates.	Gravity and momentum diffusion (shear stresses).
2. Transient diffusion in stagnant fluid.	Mass diffusion term.
3. Flow past a rectangular block.	Test van Leer differencing scheme.
4. Steady flow through a smooth area change (a nozzle).	Momentum flux (convection, advection) and pressure- gradient terms.
5. Steady flow through an abrupt area change (contraction).	Momentum flux and pressure gradient.
6. Steady flow in a constant-area channel with wall friction.	Wall friction and pressure gradient.
7. Steady flow in a constant-area change with wall friction with inlet velocity fixed.	Wall friction and pressure gradient with inlet velocity fixed.
8. One-dimensional flow through an orifice.	Momentum flux, orifice loss model, and pressure- gradient terms.
9. Uniform energy source in two 3D blocks with one connecting duct.	Volumetric energy source and time rate of change of energy.
10. Mass-flow-rate boundary condition specification.	Tests boundary condition specification by use of time-dependent function.
11. Test filter model with turbulent flow losses.	Test filter model.
12. Test filter model with laminar flow losses.	Test filter model.
13. Test filter model with both laminar and turbulent flow losses.	Test filter model.
14. Steady-state conduction through a plain wall.	Conduction equation solution and heat-transfer-coefficient evaluation.
15. Vapor condensation from bulk in mixture of air and water vapor.	Tests p-v work term and transient energy equation.

Other than this single finding, each assessment test met its success metric.

7.4. Problem 1: Steady-State and Laminar Flow Startup

7.4.1. Summary

Purpose

To validate the momentum diffusion (viscous stress) and gravity terms in the momentum balance equations. Convergence of the finite difference numerical solution method to the solution of the partial differential equations also will be demonstrated.

Success Matrix

The GASFLOW-calculated values for the velocity distribution will agree with the analytical values. The numerical solution will converge to the solution of the partial differential equations.

Problem Description

The laminar flow of an incompressible fluid between two parallel stationary walls will be analyzed. The flow is driven by a constant body force caused by gravity.

Relationship to Code Models and Methods

See Table 7-1.

Relationship to PIRT Phenomena

N/A.

Code Version and Modifications

GASFLOW 2.1.0.13, with no modifications.

Hardware and Operating System

Sun Ultra 2/200, Sun Microsystems Inc., Sun OS 5.5.1.

Compiler, Version, and Optimization Level

Edinburgh Portable Compilers' Fortran 90 Compiler, Version 1.5.1.6, Opt=O3.

Runtime Statistics: Total Run Time, Grind Time

The total problem used 3115.7 s of CPU time for an average of 373.5 ms/cell/cycle.

Results and Conclusions

The GASFLOW results agree with the analytical solution. The numerical solution converges to the solution of the partial differential equations.

7.4.2. Problem Description and Solution

7.4.2.1. Problem Description. A sketch of the flow between two parallel plates is shown in Figure 7-1. The plates are 8 cm apart, and gravity acts vertically downward. The test problem simulates the laminar flow of air between the plates at a Reynolds number of 100, where the Reynolds number is defined as

$$Re = \frac{u_{avg} H}{v} \quad (7-1)$$

The air viscosity is $v = 0.153 \text{ cm}^2/\text{s}$, and the value of the gravitational body force is $g = 0.054865 \text{ cm/s}^2$.

For completeness, the problem will be run such that the gravitational body force will act in each of the three coordinate directions.

7.4.2.2. Equations and Analytical Solution. For the laminar flow of an incompressible fluid between the plates in Figure 7-1, the Navier-Stokes equations reduce to

$$\frac{\partial w}{\partial t} = v \frac{\partial^2 w}{\partial y^2} + g \quad (7-2)$$

where the initial condition is

$$w = 0 \text{ for } 0 \leq y \leq H; t = 0 \quad (7-3)$$

and the boundary condition is

$$w = 0 \text{ at } y = 0; u = 0 \text{ at } y = H; t > 0. \quad (7-4)$$

As shown in Figure 7-1, y is the spatial coordinate extending from 0 at one wall to H at the other wall and g is the gravitational body force acting downward parallel to the direction of flow. The kinematic viscosity is v , and the time is t .

The analytical solution of Eqs. (7-2) through (7-4) is obtained by the method of separation of variables and is

$$w(y, t) = w_{ss}(y) + \sum_{n=1}^{\infty} C_n e^{-(\frac{n\pi}{H})^2 vt} \sin(n\pi \frac{y}{H}) \quad (7-5)$$

where

$$C_n = -\frac{2}{H} \int_0^H w_{ss}(y') \sin\left(\frac{n\pi}{H} y'\right) dy' \quad (7-6)$$

and the steady-state solution is

$$w_{ss}(y) = \frac{gy}{2v} (H - y) \quad (7-7)$$

The average speed of the fluid, obtained by the average of Equation (7-7) over the flow channel, is

$$w_{avg} = \frac{gH^2}{12v} \quad (7-8)$$

Equation (7-7) can be written as

$$w_{ss}(y) = 6w_{avg} \left[\frac{y}{H} - \left(\frac{y}{H} \right)^2 \right] \quad (7-9)$$

The maximum fluid speed is

$$w_{max} = \frac{gH^2}{8v} \quad (7-10)$$

For the specified conditions, $w_{avg} = 1.9125 \text{ cm/s}$, and the Reynolds number of Equation (7-1) is $Re = 100$.

7.4.2.3. Analytical Results. The steady-state distribution of the fluid velocity between the parallel plates is given in Figure 7-2. As shown in the figure, The GASFLOW calculations accurately predict the steady-state analytical results.

7.4.2.4. Analytical Acceptance Parameters and Values. As shown in Figure 7-2, the GASFLOW numerical solution accurately predicts the steady-state solutions. The first or dominant decay constant for the analytical solution is $v(\Pi/H)^2 = 0.0236 \text{ s}^{-1}$, whereas the GASFLOW prediction is 0.0235 s^{-1} .

7.4.3. GASFLOW Calculations

7.4.3.1. GASFLOW Input Model. The calculations were performed with GASFLOW, Version 2.1.0.13. No local updates or modifications were made to the code. The space between the plates in Figure 7-1 was represented by 33 cells in the transverse y direction and 25 cells in the axial z direction. No-slip boundary conditions were used at the $y = 0$ and $y = H$ walls, free-slip boundary conditions were used in the x direction, the pressure was specified at the entrance to the plates in the z direction, and continuative boundary conditions were specified at the exit from the plates.

7.4.4. Conclusions and Recommendations

GASFLOW, Version 2.1.0.13, accurately predicted the analytical solution, as required by the success metric.

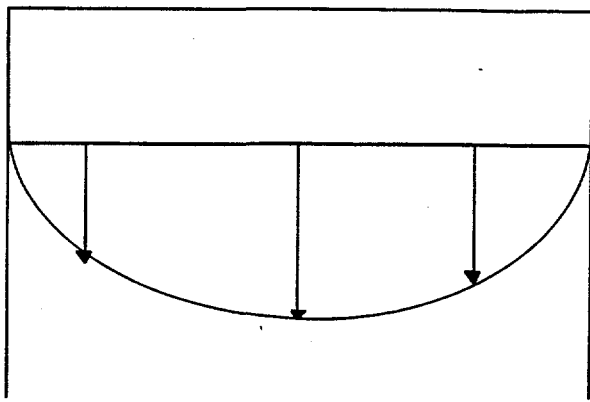


Fig. 7-1. Sketch of laminar flow between parallel plates.

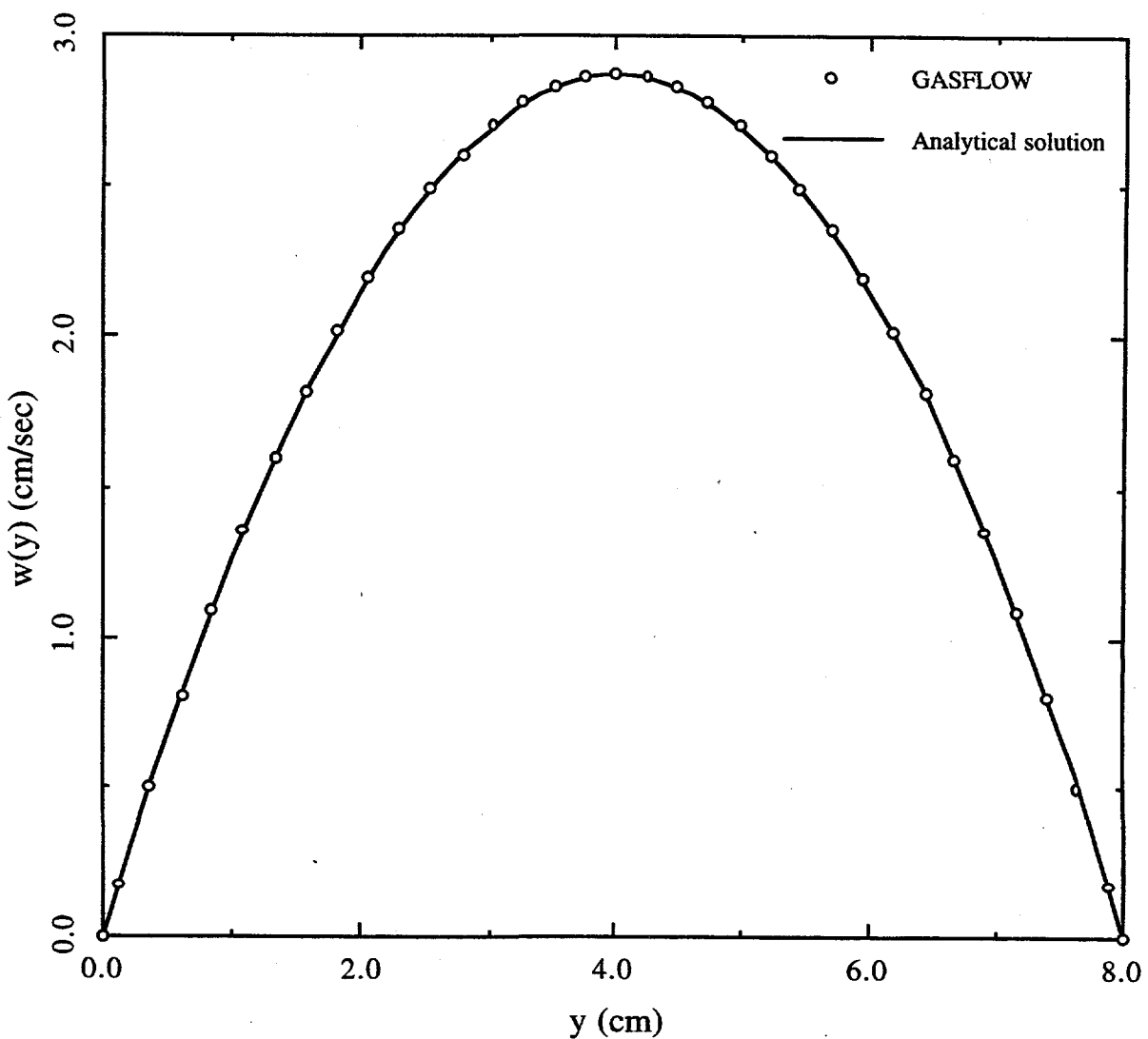


Fig. 7-2. Comparison of GASFLOW predictions with a steady-state solution.

7.4.4.1. Input File Listing.

2D laminar gravity driven flow
TSA10 JWS
GASFLOW V2.1
NOTES:

\$Source: /home/inrrisc4/jspore/gasflow/gf2/input/RCS/2D_laminar.ingf,v \$
\$Date: 1997/06/17 13:22:53 \$

* 23 MAY 97
* func3d.ar on /089534/gasflow/gf2/test_problems/func3d.ar
* 1 3D block -- 2D flow in the y-z direction
* air
* BLOCK #1
 4 x 8 x 100 cm
 1 x 33 x 25 = 825 cells
* Top boundary is fixed pressure.
* Bottom boundary is continuative,
* North and South boundaries are rigid no-slip.
* West and East boundaries are rigid free-slip.

NET WORK INPUT

\$innet
\$end

BASIC INPUT

\$xput

pamb0 = 1.0e+06,
idiffmom = 1,

autot = 1.0, cyl = 0.0,
delt0 = 0.10000,
deltmin = 1.000e-08,
deltmax = 1.000e-00,
epsi0 = 1.000e-08,
epsimax = 1.000e-08,
epsimin = 1.000e-08,
gz = -0.054865,
iobpl = 0,
itdowndt = 25,
itupdt = 100,
itmax = 100,
lpr = 1,
maxcyc = 8000,
ittyfreq = 5,
nu = 0.153,
pltdt = 20.00,
prtdt = 20.000,
twfin = 405.00,
tddt = 1000.0000,
velmx = 1.5,
ibw = 1,
ibe = 1,
ibs = 2,
ibn = 2,

```

ibb      = 3,
ibt      = 5,
mat = 'air',
gasdef(1,1) = 1 , 'im1', 1 , 'jm1', 1 , 'km1', 1 , ; I.C.
              1.0e6, 300.0, 1, 0., 0., 'air', 1.00000,
gasdef(1,2) = 0 , 1, 1 , 'jm1', 01 , 'km1', 1 , ; west B.C.
              1.0e6, 300.0, 1, 0., 1.0e+99, 'air', 1.00000,
gasdef(1,3) = 'im1','imax', 1 , 'jm1', 1 , 'km1', 1 , ; east B.C.
              1.0e6, 300.0, 1, 0., 1.0e+99, 'air', 1.00000,
gasdef(1,4) = 1 , 'im1', 0 , 1, 1 , 'km1', 1 , ; south B.C.
              1.0e6, 300.0, 1, 0., 1.0e+99, 'air', 1.00000,
gasdef(1,5) = 1 , 'im1','jm1','jmax', 1 , 'km1', 1 , ; north B.C.
              1.0e6, 300.0, 1, 0., 1.0e+99, 'air', 1.00000,
gasdef(1,6) = 1 , 'im1', 1 , 'jm1', 0 , 1, 1 , ; bttm B.C.
              1.0e6, 300.0, 1, 0., 1.0e+99, 'air', 1.00000,
gasdef(1,7) = 1 , 'im1', 1 , 'jm1','km1','kmax', 1 , ; top B.C.
              1.0e6, 300.0, 1, 0., 1.0e+99, 'air', 1.00000,

```

\$end

M E S H

```

$meshgn
iblock = 1,
nkx=1, nky = 1, nkz = 1,
xl(1) = 0.0, xc(1) = 0.0, nxl(1)=0, nxr(1)=1, dxmn(1)=1.e9, xl(2)=4.0,
yl(1) = 0.0, yc(1) = 0.0, nyl(1)=0, nyr(1)=33, dymn(1)=1.e9, yl(2)=8.0,
zl(1) = 0.0, xc(1) = 0.0, nzl(1)=0, nzr(1)=25, dzmn(1)=1.e9, zl(2)=100.0,
$end
$meshgn
$end

```

G R A P H I C S

```

$grafic
pnt(1, 1) = 2,      1,      10, 1,
              2, 'jm1',    10, 1,
              2,      1,      2, 1,
              2, 'jm1',    2, 1,
              2,      1,      1, 1,
              2, 'jm1', 'km1', 1,
p1d      = 1, 2,      'vn', 0,
              3, 4,      'vn', 0,
              1, 2,      'vn', 0,
              3, 4,      'vn', 0,
v2d      = 5, 6,      1,
thdt = 0.1,
thp(1,1) = 2, 16, 2, 1, 'vn', 0,
              2, 16, 2, 1, 'vn', 0,
              2, 16, 10, 1, 'vn', 0,
              2, 16, 24, 1, 'vn', 0,

```

\$end

P A R T I C L E S

\$parts
\$end
\$rheat
\$end
\$special
\$end
\$specialp
\$end

7.5. Problem 2: Diffusion of Hydrogen into Air

7.5.1. Summary

Purpose
To validate the specie diffusion equation for a 1D problem.
Success Matrix
The GASFLOW-calculated values for the hydrogen concentration as a function of time and space will agree with the analytical solution.
Problem Description
Hydrogen diffusion into air is modeled in a 1D duct.
Relationship to Code Models and Methods
See Table 7-1.
Relationship to PIRT Phenomena
N/A.
Code Version and Modifications
GASFLOW 2.1.0.13, with no modifications.
Hardware and Operating System
Sun Ultra 2/200, Sun Microsystems Inc., Sun OS 5.5.1.
Compiler, Version, and Optimization Level
Edinburgh Portable Compilers' Fortran 90 Compiler, Version 1.5.1.6, Opt=O3.
Runtime Statistics: Total Run Time, Grind Time
The total problem used 59.1 s of CPU time for an average of 282.7 ms/cell/cycle.
Results and Conclusions
The GASFLOW results agree with the analytical solution.

7.5.2. Problem Description and Solution

7.5.2.1. Problem Description. The transient diffusion of hydrogen into air is simulated in a 1D duct. Air fills the duct and at time zero, the left face of the duct is exposed to hydrogen. The problem is run for 10 s of simulation time.

7.5.2.2. Equations and Analytical Solution. The diffusion equation for the concentration of hydrogen is

$$\frac{\partial f}{\partial t} = D_{AB} \frac{\partial^2 f}{\partial x^2}, \quad (7-11)$$

where the initial condition is

$$f(x, t) = f_0; 0 \leq x \leq \infty, t = 0 \quad (7-12)$$

and the boundary condition is

$$f(x, t) = f_b; x = 0, t > 0 \quad (7-13)$$

The mass diffusivity for hydrogen diffusion into air is taken to be $0.754 \text{ cm}^2/\text{s}$, $f_0 = 0$, and $f_b = 1.0$.

The solution of Equation (7-11) is

$$\Delta f = erfc(\xi) \quad (7-14)$$

where $erfc$ is the complementary error function

$$\Delta f = \frac{f - f_0}{f_b - f_0} \quad (7-15)$$

and

$$\xi = \frac{x}{2\sqrt{D_{AB}t}} \quad (7-16)$$

7.5.2.3. Analytical Results. The analytical solution for the hydrogen concentration along the duct at 10 s is shown in Figure 7-3, along with the GASFLOW results.

Comparisons for other times will be prepared as time permits.

7.5.2.4. Analytical Acceptance Parameters and Values. As shown in Figure 7-3, the GASFLOW numerical solution accurately predicts the transient analytical solution.

7.5.3. GASFLOW Calculations

7.5.3.1. GASFLOW Input Model. The calculations were performed with GASFLOW, Version 2.1.0.13. No local updates or modifications were made to the code. The 1D duct contained 100 cells that were each 0.10 cm long; the total length of the duct was 10 cm. The diffusion-limit stability criterion for the GASFLOW numerical methods is

$$\frac{D_{AB}\Delta t}{\Delta x^2} < \frac{1}{2} \quad (7-17)$$

For the present calculation, the diffusion number, the left side of Equation (7-13), is ~0.377. Temporal and spatial convergence studies were not conducted.

7.5.4. Conclusions and Recommendations

GASFLOW, Version 2.1.0.13 accurately predicted the analytical solution, as required by the success metric.

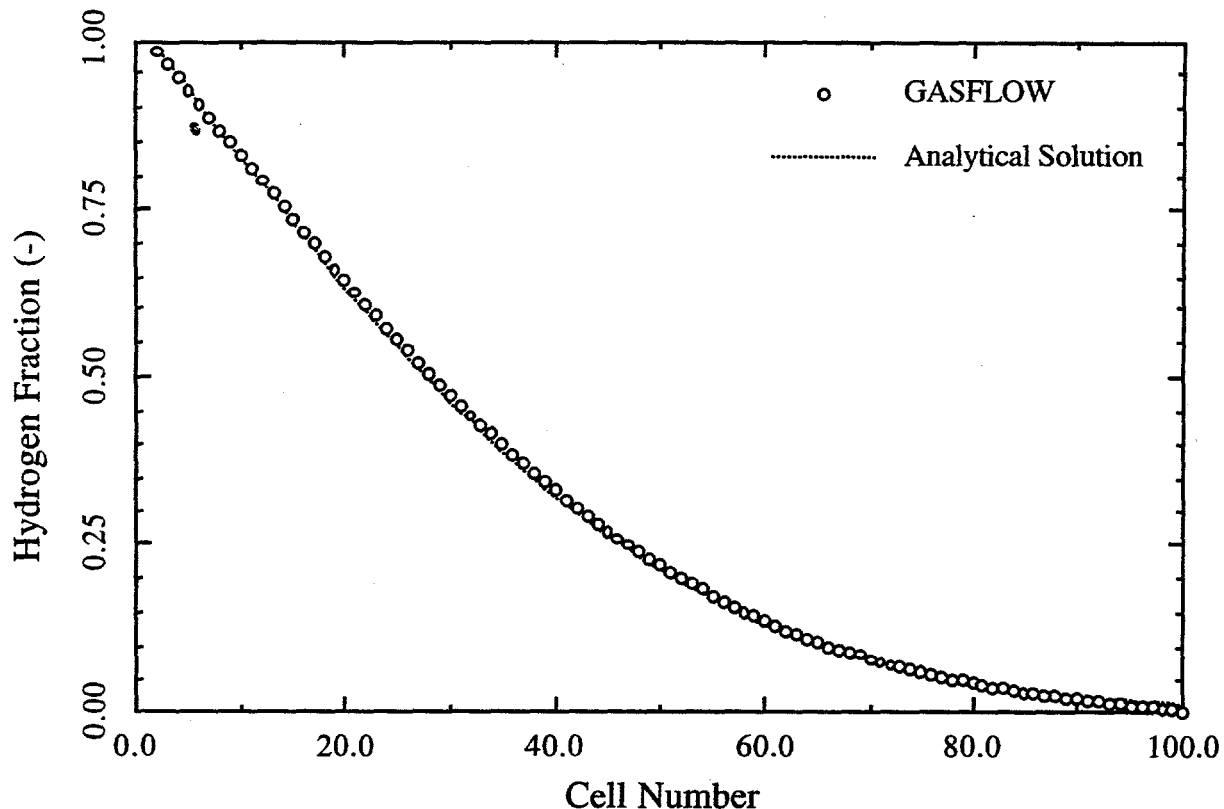


Fig. 7-3. Comparison of analytical solution and GASFLOW results at time 10 s

7.5.4.1. Input File Listing.

1 Duct / 0 Junction Test

TSA-6 JWS

GF2

\$Source: /home/inrrisc4/jspore/gasflow/gf2/input/RCS/diffuse.ingf,v \$
\$Date: 1997/06/17 13:28:42 \$

NOTES

* DIFFUSE.AR test case

* 10/21/94 developed

```
* 1 ducts, 0 jct
* file: INGF stored in a library on
*       /089534/gasflow/gf2/test_problems/diffuse.ar
* duct 1: 0.1 x 100 = 10 cm
* Number of real cells = 100
* Cartesian coordinates, uniform grid
* Working fluid: air
* WEST  B.C.: specified velocity VBC = 0.
* EAST  B.C.: specified velocity VBC = 0.
```

```

node 1           node 2
VBC           VBC
+---+-----+-----+-----+-----+-----+-----+-----+-----+-----+-----+
. 1 | 2 | 3 | 4 | 5 | 6 | 7 | 8 | 9 | conts 10-101 | 102.
. B |     |     |     |     |     |     |     |     |           B .
+---+-----+-----+-----+-----+-----+-----+-----+-----+-----+-----+

```

NETWORK PARAMETERS

```

$innet
  netopt      = 2,
  iwshear    = 0,
  ductdef(1,1) =  0.0,    0.0, 100.0, 100.0, 100.0, 100.0, 1, 2,100,
                  1.0,      0,      0,
  cpnt       =      0.0 ,      0.0 ,      0.0 ,
                  10.0 ,      0.0 ,      0.0 ,

```

Send

BASIC INPUT

\$xput

```

muoption = 1,
nu       = 0.754 ,
cmasssd  = 0.754 ,
gz       = -000.0,
autot   = 1.0,
delt0   = 0.0005,
deltmin = 1.000e-05,
deltmax = 5.000e-03,
idiffme = 1,
nrsdump = 0,
epsi0   = 1.000e-08,
epsimax = 1.000e-08,
epsimin = 1.000e-08,
itdowndt = 024,
itupdt   = 024,
itmax    = 050,
maxcyc  =      20000,
twfin   =      10.000,
lpr      = 1,

```

```

iobpl    = 1,
ittyfreq = 100,
pltdt   = 5.000,
prttdt   = 5.0 ,
tddt     = 5000.00,
velmx    = 1.5,

mat = 'air' , 'h2',

gasdef(1,1) = 0, 102, 1, -1, -1, -1, 1 ,
1.0000000000e6, 300.00, 1, 0., 0.,
'air' , 1.00000,

gasdef(1,2) = 0, 1, 1, -1, -1, -1, 1 ,
1.0000000000e6, 300.00, 1, 0., 9999999.,
'h2' , 1.00000,

gasdef(1,3) = 101, 102, 1, -2, -2, -2, 1 ,
1.0000000000e6, 300.00, 1, 0., 9999999.,
'air' , 1.00000,

vvalue = 0.0,

pbc(1,1) = 1, 0, 1,-1, -1, -1, 0, 0.0, 99999.,
; pbc(1,2) = 2, 0, 1,-1, -1, -1, 0, 0.0, 99999.,
vbc(1,1) = 2, 0, 1, 0, 0, 0, 0, 1, 0.0, 99999.,
; vbc(1,2) = 1, 0, 1, 0, 0, 0, 0, 1, 0.0, 99999.,

```

\$end

M E S H

```

$meshgn
$end

```

G R A P H I C S

\$grafic

```

pnt(1,1) = 1, 1, -1, -1,
pnt(1,2) = 101, 1, -1, -1,

pld(1,1) = 1, 2, 'mf', 'h2',
pld(1,2) = 1, 2, 'mf', 'air',

pld(1,1) = 1, 2, 'vf', 'h2',
pld(1,2) = 1, 2, 'vf', 'air',

thdt = 1.000,

thp(1,1) = 1, 1,-1,-1, 'un' , 0,
thp(1,2) = 5, 1,-1,-1, 'un' , 0,
thp(1,3) = 10, 1,-1,-1, 'un' , 0,

thp(1,4) = 1, 1,-1,-1, 'mf' , 'h2',
thp(1,5) = 5, 1,-1,-1, 'mf' , 'h2',
thp(1,6) = 10, 1,-1,-1, 'mf' , 'h2',

thp(1,7) = 1, 1,-1,-1, 'mf' , 'air',
thp(1,8) = 5, 1,-1,-1, 'mf' , 'air',

```

thp(1,9) = 10, 1,-1,-1, 'mf' , 'air',

\$end

P A R T I C L E S

\$parts

\$end

H E A T T R A N S F E R & C O N D E N S A T I O N

\$rheat

\$end

S P E C I A L

\$special

\$end

7.6. Problem 3: Flow past a Rectangular Block

7.6.1. Summary

Purpose

A qualitative assessment of the numerical representation of the momentum-advection and bulk-shear-stress terms in GASFLOW. The second-order van Leer method is used for the momentum-advection terms.

Success Matrix

The GASFLOW-calculated flow field will be in qualitative agreement experimental results and calculations with other CFD codes.

Problem Description

Flow of air at normal temperature and pressure past a rectangular block in the x-y Cartesian geometry. The flow channel surrounding the block is 20 cm long by 24 cm high, and the block, located in the center of the channel, is 1 cm thick by 2 cm high. The Reynolds number, based on the free-stream fluid speed and the height of the block, is 30.

Relationship to Code Models and Methods

See Table 7-1.

Relationship to PIRT Phenomena

N/A.

Code Version and Modifications

GASFLOW 2.1.0.13, with no modifications.

Hardware and Operating System

Sun Ultra 2/200, Sun Microsystems Inc., Sun OS 5.5.1.

Compiler, Version, and Optimization Level

Edinburgh Portable Compilers' Fortran 90 Compiler, Version 1.5.1.6, Opt=O3.

Runtime Statistics: Total Run Time, Grind Time

The total problem used 5368.2 s of CPU time for an average of 985.8 ms/cell/cycle.

Results and Conclusions

The GASFLOW results are in qualitative agreement with the expected results.

7.6.2. Problem Description and Solution

7.6.2.1. **Problem Description.** The computational domain, as shown in Figure 7-4, has 44 cells in the x and y directions, with smaller cells used near the block. The working fluid is air, and the initial condition is zero velocity everywhere. The air speed at the inlet plane and the pressure at the outlet are specified as boundary conditions. The fluid speed at the inlet is 2.3 cm/s, and the pressure at the outlet is 1.0×10^6 dynes/cm². The problem is run for 80 s of simulation time. Free-slip boundary conditions are used at the walls of the channel and no-slip conditions at the surfaces of the block.

An initial perturbation in the inlet velocity is used to reduce the time needed to develop the final flow pattern downstream of the block.

The timestep size for the calculation satisfied the Courant criterion for numerical stability.

7.6.2.2. **Analytical Results.** Experimental data and other calculations for flow past a rectangular block indicate that a vortex street does not form at low-speed flow corresponding to $Re = 30$. That is, the flow behind the block should approach steady, nonoscillatory values. On the other hand, the presence of vortex streets will be indicated by oscillatory fluid velocity components downstream of the block.

7.6.2.3. **Analytical Acceptance Parameters and Values.** GASFLOW predicts that a pair of counter-rotating eddies will form behind the block, as indicated in Figure 7-5. As shown in Figures 7-6 and 7-7, the GASFLOW numerical solution predicts a flow field that is approaching steady state and not a vortex street at $Re = 30$.

7.6.3. GASFLOW Calculations

7.6.3.1. **GASFLOW Input Model.** The calculations were performed with GASFLOW, Version 2.1.0.13. No local updates or modifications were made to the code.

7.6.4. Conclusions and Recommendations

GASFLOW, Version 2.1.0.13 results are in qualitative agreement with the expected results, as required by the success metric.

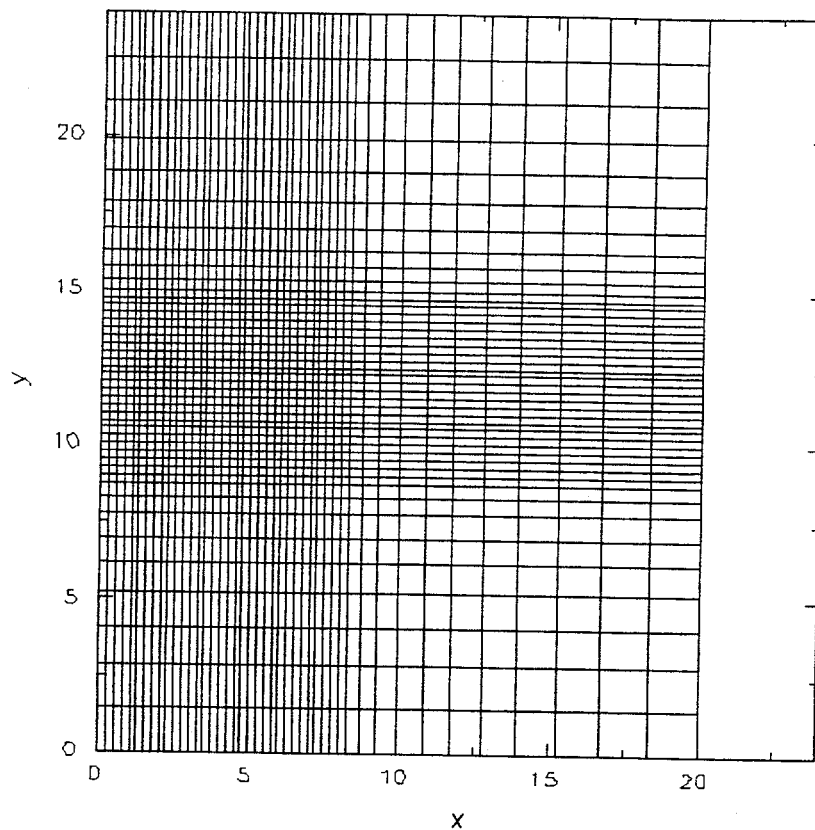


Fig. 7-4. The GASFLOW mesh for calculating a flow field behind a rectangular block

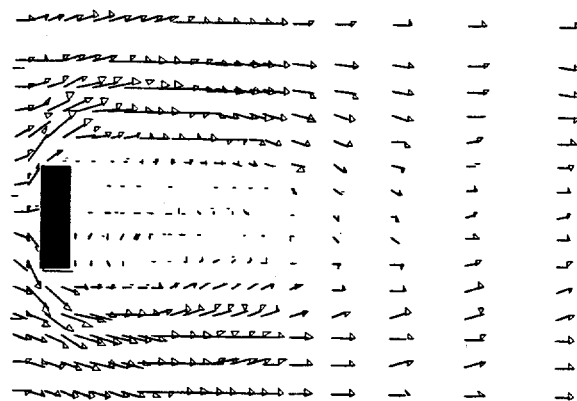


Fig. 7-5. Velocity vector plot

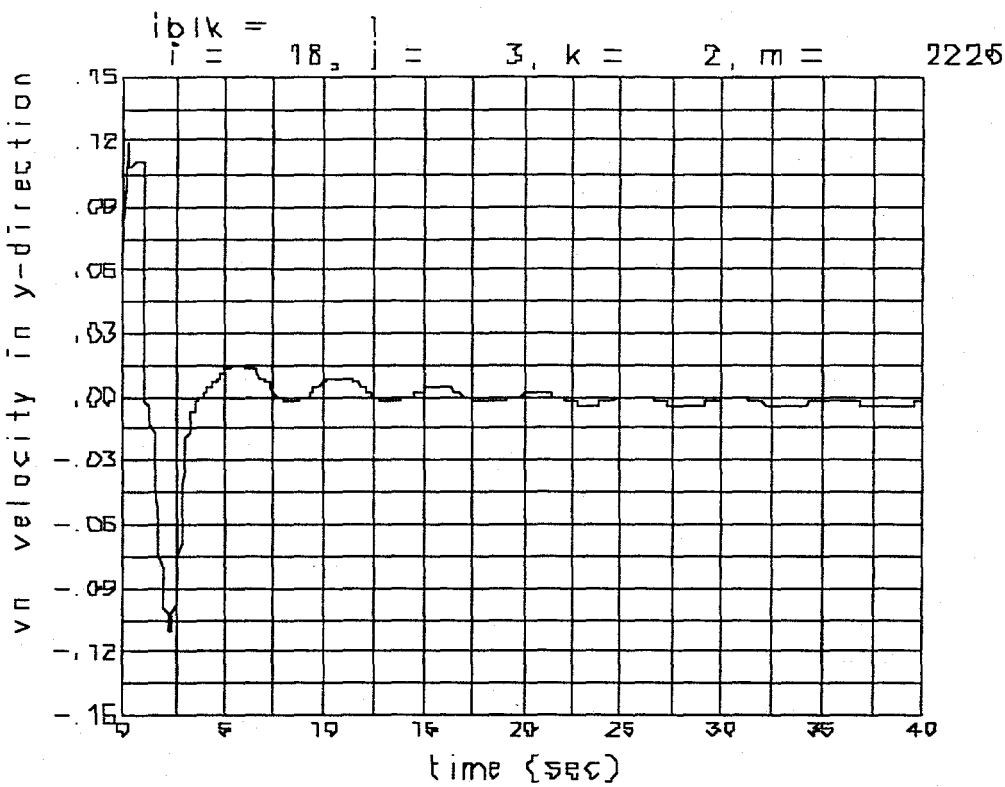


Fig. 7-6. Velocity as a function of time at $i = 18, j = 3$, and $k = 2$

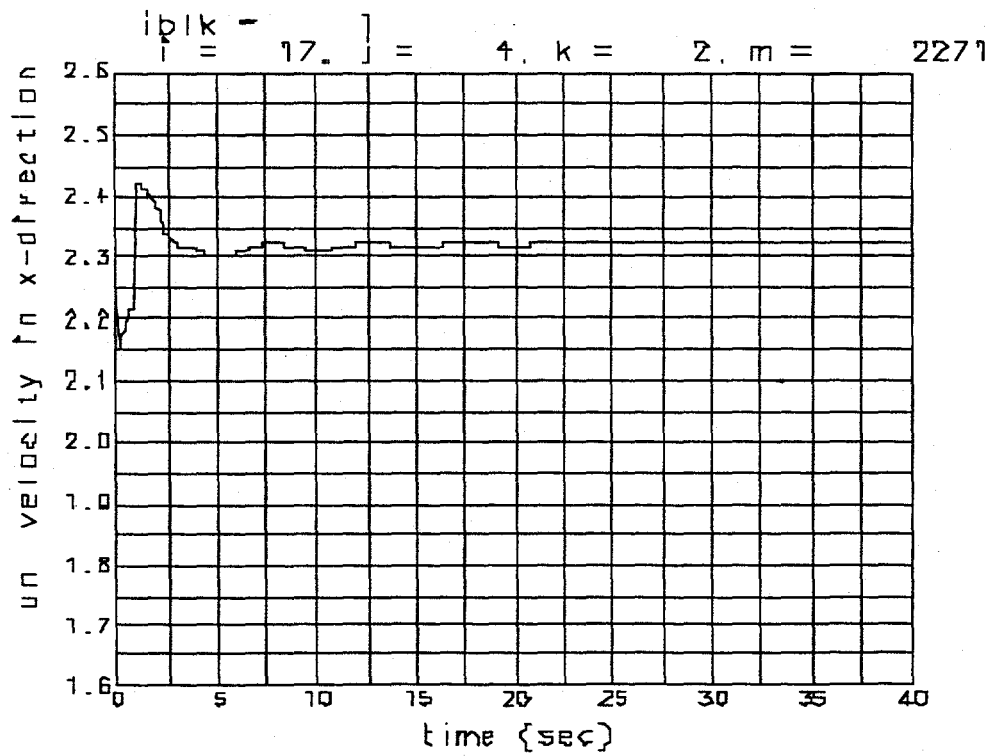


Fig. 7-7. Velocity as a function of time at $i = 17, j = 4$, and $k = 2$

7.6.4.1. Input File Listing.

Flow past block, Re = 30

HMS-93

TSA-8 Lam

HMS-vk.block

NOTES: Obstacle (2cm tall, 1cm thick) in channel 24cm tall, 20 cm long.

Obstacle to channel height ratio is 1/12

Variable mesh spacing: 2 zones in x and 3 zones in y.

Number of real cells = 44 x 44 x 1.

\$Id: von_Karmon.ingf,v 1.3 1997/06/18 09:57:14 jspose Exp \$
\$Log: von_Karmon.ingf,v \$

```
$innet
$end
$xput
nrsdump = 0,
ifvl = 1, ; Turn on van Leer advection scheme
autot = 1.0,
delt0 = 0.025,
deltmin = 1.000e-04,
deltmax = 1.000e-00,
eps10 = 1.000e-05,
epsimax = 1.000e-05,
epsimin = 1.000e-05,
gz = -000.0,
iobpl = 1,
itdowndt = 499,
itupdt = 498,
itmax = 500,
lpr = 1,
maxcyc = 900056,
ittyfreq = 100,
nu = 0.153,
muoption = 1,
pltdt = 50.0,
prtdt = 40.0,
twfin = 40.0,
tddt = 500.0,
velmx = 1.5,
ibb = 1,
ibn = 1,
ibs = 1,
ibw = 1,
ibe = 1,
ibt = 1,
idiffmom = 1,
nslipdef(1,1) = 5, 9, 19, 19, 1, 2, 1, 'both',
nslipdef(1,2) = 5, 9, 27, 27, 1, 2, 1, 'both',
nslipdef(1,3) = 5, 5, 19, 27, 1, 2, 1, 'both',
nslipdef(1,4) = 9, 9, 19, 27, 1, 2, 1, 'both',
vvalue = 2.3, 1.2, ; Inlet velocity, Perturbed velocity
vbc(1,1) = 01, 01, 1, 23, 1, 02, 1, 1, 0.0, 2.5e+03, ; Inlet, upper half
vbc(1,2) = 01, 01, 23, 45, 01, 02, 1, 2, 0.0, 1.0e+00, ; Perturb.,lower half
vbc(1,3) = 01, 01, 23, 45, 01, 02, 1, 1, 1.0, 2.5e+03, ; Inlet, lower half
```

```
pbc(1,1) = 45, 45, 1, 45, 01, 02, 1, 00.0, 2.5e+03,  
mat = 'air',  
gasdef(1,1) = 1, 45, 1, 45, 1, 2, 1,  
1.0132500000e6, 300.00, 1, 0., 0.,  
'air', 1.00000,  
gasdef(1,2) = 0, 1, 1, 45, 1, 2, 1,  
1.0132500000e6, 300.00, 1, 0., 2.5e+03,  
'air', 1.00000,  
gasdef(1,3) = 45, 46, 1, 45, 1, 2, 1,  
1.0132500000e6, 300.00, 1, 0., 2.5e+03,  
'air', 1.00000,  
mobs = 5, 9, 19, 27, 1, 2, 1,
```

\$end

M E S H

\$meshgn

```
iblock = 1,  
nkx = 02,  
xl(1) = 0.0, xc(1) = 0.0, nxl(1) = 0, nxr(1) = 32, dxmn(1) = 1000.0,  
xl(2) = 8.0, xc(2) = 8.0, nxl(2) = 0, nxr(2) = 12, dxmn(2) = 0.3,  
xl(3) = 20.0,  
  
nky = 03,  
yl(1) = 0.0, yc(1) = 9.0, nyl(1) = 10, nyx(1) = 0, dymn(1) = 0.3,  
yl(2) = 9.0, yc(2) = 9.0, nyl(2) = 0, nyx(2) = 24, dymn(2) = 9999.9,  
yl(3) = 15.0, yc(3) = 15.0, nyl(3) = 0, nyx(3) = 10, dymn(3) = 0.3,  
yl(4) = 24.,  
  
nkz = 01,  
zl(1) = 0.0, zc(1) = 0.0, nzl(1) = 0, nzr(1) = 01, dzmn(1) = 1000.0,  
zl(2) = 10.0,
```

\$end

G R A P H I C S

\$grafic

```
igrid = 1,  
thdt = 0.05,  
  
thp(1,1) = 18, 3, 2, 1, 'vn', 0,  
thp(1,2) = 18, 6, 2, 1, 'vn', 0,  
thp(1,3) = 36, 3, 2, 1, 'vn', 0,  
thp(1,4) = 36, 6, 2, 1, 'vn', 0,  
thp(1,5) = 41, 3, 2, 1, 'vn', 0,  
thp(1,6) = 41, 6, 2, 1, 'vn', 0,  
thp(1,7) = 45, 3, 2, 1, 'vn', 0,  
thp(1,8) = 45, 6, 2, 1, 'vn', 0,  
thp(1,9) = 17, 4, 2, 1, 'un', 0,
```

```
thp(1,10) = 17, 6, 2, 1, 'un', 0,  
thp(1,11) = 17,24, 2, 1, 'un', 0,  
thp(1,12) = 37, 4, 2, 1, 'un', 0,  
thp(1,13) = 37, 6, 2, 1, 'un', 0,  
thp(1,14) = 37,24, 2, 1, 'un', 0,  
thp(1,15) = 42, 6, 2, 1, 'un', 0,  
thp(1,16) = 42,24, 2, 1, 'un', 0,
```

```
pnt(1,1) = 1, 1, 2, 1,  
pnt(1,2) = 45, 45, 2, 1,  
pnt(1,3) = 9, 1, 2, 1,  
pnt(1,4) = 9, 45, 2, 1,  
pnt(1,5) = 21, 1, 2, 1,  
pnt(1,6) = 21, 45, 2, 1,  
pnt(1,7) = 37, 1, 2, 1,  
pnt(1,8) = 37, 45, 2, 1,  
pnt(1,9) = 42, 1, 2, 1,  
pnt(1,10) = 42, 45, 2, 1,  
pnt(1,11) = 45, 1, 2, 1,  
pnt(1,12) = 45, 45, 2, 1,  
9, 15, 2, 1,  
37, 31, 2, 1,
```

```
v2d(1,1) = 1, 2, 1,  
13,14, 1,
```

```
iinc = 2,  
jinc = 2,
```

```
$end
```

P A R T I C L E S

```
$parts
```

```
$end  
$rheat
```

```
$end  
$special  
$end
```

7.7. Problem 4: Flow through a Variable Area Expansion

7.7.1. Summary

Purpose

To validate the momentum flux terms for 1D flow in a variable-area flow channel.

Success Matrix

The GASFLOW-calculated values for the fluid speed and pressure distribution in the channel will agree with the analytical values.

Problem Description

1D frictionless flow through a variable-area expansion with the fluid velocity specified at the inlet and the pressure specified at the outlet.

Relationship to Code Models and Methods

See Table 7-1.

Relationship to PIRT Phenomena

N/A.

Code Version and Modifications

GASFLOW 2.1.1.4, with no modifications.

Hardware and Operating System

Sun SPARC 10, Sun Microsystems Inc., Sun OS 5.5.1.

Compiler, Version, and Optimization Level

SUN Fortran 90 Compiler, Version 1.2 patch 104366-04, Opt=O3.

Runtime Statistics: Total Run Time, Grind Time

The total problem used 26.7 s of CPU time for an average of 1391.3 ms/cell/cycle.

Results and Conclusions

The GASFLOW results agree with the analytical solution for the momentum equation and the continuity equation.

7.7.2. Problem Description and Solution

7.7.2.1. Problem Description. The distribution of the flow area along the channel is shown in Figure 7-8. The duct is 1200 cm long, and the change in the flow area occurs between 400 and 800 cm from the inlet. The flow area upstream of the expansion is 10,000 cm² and downstream is 40,000 cm². The pressure at the outlet is specified to be

1.00×10^6 dynes/cm², and the fluid speed at the inlet is specified to be 200.0 cm/s. GASFLOW calculates the fluid velocity and pressure throughout the duct.

7.7.2.2. Equations and Analytical Solution. The fluid speed at the inlet is specified as a boundary condition. The continuity equation gives the fluid speed as a function of the flow area

$$u(z) = \frac{U_{in} A_{in}}{A(z)} \quad (7-18)$$

The distribution of the fluid speed is given in Figure 7-9. As seen in the figure, GASFLOW accurately calculates the fluid speed.

The pressure distribution in the channel is caused by the change in the momentum flux. The Bernoulli equation gives the relationship between the pressure and the fluid speed as

$$p_1 + \frac{1}{2} \rho v_1^2 = p_2 + \frac{1}{2} \rho v_2^2 \quad (7-19)$$

Equation (7-19) predicts a pressure drop of 347 dynes/cm² across the duct.

7.7.2.3. Analytical Acceptance Parameters and Values. The fluid speed and pressure distribution along the channel, using Equations (7-18) and (7-19), should be predicted by the GASFLOW calculation. GASFLOW, Version 2.1.1.4 predicts a pressure drop of 347.9 dynes/cm² across the duct.

7.7.3. GASFLOW Calculations

7.7.3.1. GASFLOW Input Model. The calculations were performed with GASFLOW, Version 2.1.1.4. No local updates or modifications were made to the code. The duct was represented by 12 cells, each 100.0 cm long.

7.7.4. Conclusions and Recommendations

GASFLOW, Version 2.1.1.4 correctly solves the continuity equation and the momentum equation.

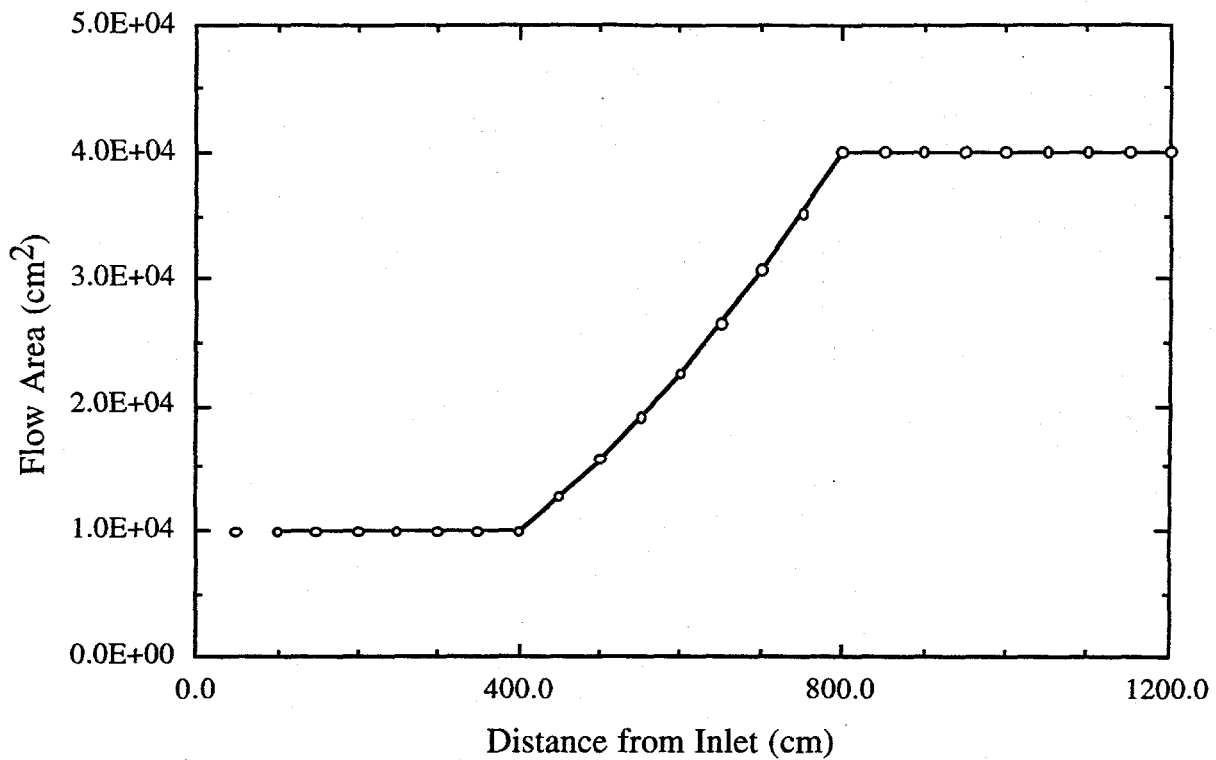


Fig. 7-8. Flow area as a function of distance along the channel

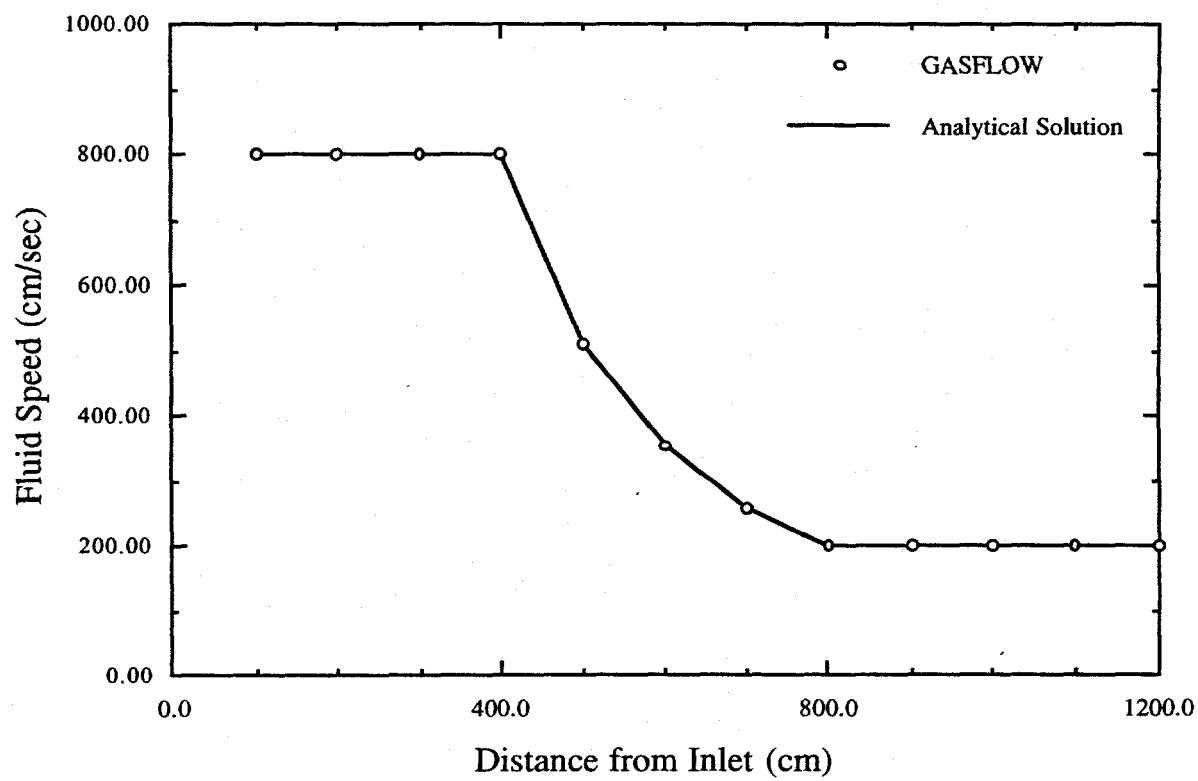


Fig. 7-9. Comparison of GASFLOW and analytical solution for the fluid speed

7.7.4.1. Input File Listing.

1 Ducts / 0 Junction Test

TSA-6 JWS

```
c $Source: /home/inrrisc4/jspore/gasflow/gf2/input/RCS/1duct_2.ingf,v $
c $Date: 1996/12/18 09:57:22 $
```

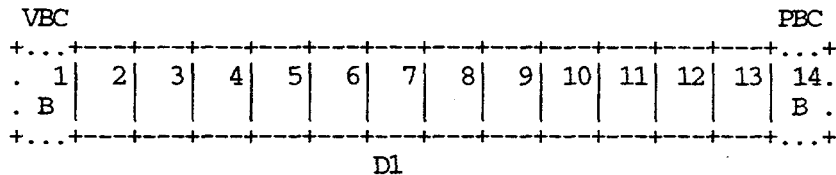
GF2

NOTE S

- * 1DUCT_2.AR test input
- * 1DUCT_2.AR is the mirror image of 1DUCT_1.AR
- * 13 SEP 93 -- date of latest change
- * 31 AUG 94 -- Modified input to be consistent with GF2
- * 1 duct
- * file: INGF stored in library file
- * /089534/gasflow/gf2/test_problems/1duct_2.ar
- * duct 1: 12 x 100 = 1200 cm
- * Number of real cells = 12
- * Cartesian coordinates, uniform grid
- * Working fluid: air
- * Smooth area change from 10000.0 cm**2 to 40000.0 cm**2
- * Smooth area change is to occur from 400 cm to 800 cm.
- * No smooth area change losses calculated.
- * Flow loss of 1.0 is applied at cell edge 12.
- * WEST B.C.: specified pressure
- * EAST B.C.: specified pressure

node 1

node 2



NETWORK PARAMETERS

\$innet

```
netopt = 2,
ductdef(1,1) = 0.0, 0.0, 100.0, 200.0, 100.0, 200.0, 1, 2, 12,
           1.0, 16, 400.0,
cpnt = 0.0 , 0.0 , 0.0 ,
       1200.0 , 0.0 , 0.0 ,
flossdef(1,1) = 11 , 12 , 1 , 1 , 1.0, 1.0,
iwshear = 0,
```

\$end

BASIC INPUT

\$put

```
muoption = 1,
nu = 0.150 ,
```

```

gz      = -000.0,
autot  = 1.0,
delt0  = 0.1000,
deltmin = 1.000e-04,
deltmax = 1.000e-00,
nrsdump = 0,
epsi0   = 1.000e-08,
epsimax = 1.000e-08,
epsimin = 1.000e-08,
itdowndt = 024,
itupdt  = 024,
itmax   = 025,
maxcyc  =      2000,
twfin   = 50.000,
lpr      = 1,
iobpl   = 1,
ittyfreq = 20,
pltdt   = 020.000,
prtdt   = 10.0 ,
tddt    = 5000.00,
velmx   = 1.5,
mat = 'air' ,
gasdef(1,1) = 0, 14, 1, -1, -1, -1, 1 ,
               1.000000000e6, 300.00, 1, 0., 0.,
               'air' , 1.00000,
gasdef(1,2) = 0, 1, 1, -1, -1, -1, 1 ,
               1.000000000e6, 300.00, 1, 0., 9999999.,
               'air' , 1.00000,
gasdef(1,3) = 13, 14, 1, -2, -2, -2, 1 ,
               1.000100000e6, 300.00, 1, 0., 9999999.,
               'air' , 1.00000,
vvalue = 800.00,
pbc(1,1) = 2, 14, 1,-1, -1, -1, 1, 0.0, 99999.,
vbc(1,1) = 1, 1, 1,-1, -1, -1, 1, 1, 0.0, 99999.,
;      pbc(1,2) = 2, 14, 1,-2, -2, -2, 1, 0.0, 99999.,
$end

```

M E S H

\$meshgn

\$end

G R A P H I C S

\$grafic

pnt(1,1) = 1, 1, -1, -1,
pnt(1,2) = 5, 1, -1, -1,

thdt = 0.0100,

thp(1,1) = 1, 1,-1,-1, 'un' , 0,
thp(1,2) = 5, 1,-1,-1, 'un' , 0,

\$end

P A R T I C L E S

\$parts

\$end

H E A T T R A N S F E R & C O N D E N S A T I O N

\$rheat

\$end

S P E C I A L

\$special

\$end

7.8. Problem 5: Abrupt Area Change; Flow through a Contraction

7.8.1. Summary

Purpose

To validate the model equations for 1D flow in a channel containing a local flow perturbation. This example is a channel with an abrupt contraction.

Success Matrix

The GASFLOW-calculated values for the velocity downstream of the contraction and the pressure at the channel inlet will agree with the analytical values.

Problem Description

1D, frictionless flow through an abrupt contraction with the fluid velocity specified at the inlet and the pressure specified at the outlet.

Relationship to Code Models and Methods

See Table 7-1.

Relationship to PIRT Phenomena

N/A.

Code Version and Modifications

GASFLOW 2.1.1.4, with no modifications.

Hardware and Operating System

Sun SPARC 10, Sun Microsystems Inc., Sun OS 5.5.1.

Compiler, Version, and Optimization Level

SUN Fortran 90 Compiler, Version 1.2 patch 104366-04, Opt=O3.

Runtime Statistics: Total Run Time, Grind Time

The total problem used 27.0 s of CPU time for an average of 1402.4 ms/cell/cycle.

Results and Conclusions

The GASFLOW results agree with the analytical solution for the momentum equation and the continuity equation.

7.8.2. Problem Description and Solution

7.8.2.1. Problem Description. A sketch of the flow in a 1D duct with an abrupt contraction in flow area is shown in Figure 7-10. The duct is 1200 cm long, and the change in the flow area occurs 800 cm from the inlet. The flow area upstream of the contraction is 40,000 cm² and downstream 10,000 cm². The pressure at the outlet is specified to be 1.00×10^6 dynes/cm², and the fluid speed at the inlet is specified to be 200.0 cm/s. GASFLOW calculates the fluid velocity and pressure throughout the duct.

7.8.2.2. Equations and Analytical Solution. The fluid speed at the inlet is specified as a boundary condition. The continuity equation gives the fluid speed downstream of the contraction as

$$u_2 = u_1 \frac{A_1}{A_2} \quad (7-20)$$

The area ratio $\beta = A_2/A_1$ and Equation (7-20) can be written as

$$u_2 = u_1 / \beta \quad (7-21)$$

The pressure drop across the flow channel is the sum of the change in the momentum flux plus the pressure loss at the abrupt contraction. In terms of the specified boundary conditions and channel geometry, the inlet pressure is

$$p_1 = p_2 + \frac{1}{2} \rho \frac{1}{\beta^2} u_1^2 [k + 1 - \beta^2] \quad (7-22)$$

The loss coefficient for an abrupt contraction is

$$k = 0.45 (1 - \beta) \quad (7-23)$$

where

$$\beta = 0.25 \text{ and } = 0.3375.$$

The density is $\rho = 0.001157 \text{ g/cm}^3$.

7.8.2.3. Analytical Acceptance Parameters and Values. The fluid speed downstream of the contraction, Equation (7-21), and the pressure at the inlet, Equation (7-23), should be predicted by the GASFLOW calculation. For the specified conditions, $u_2 = 800.0 \text{ cm/s}$, and the inlet pressure is $p_1 = 1,000,472.0 \text{ dynes/cm}^2$.

GASFLOW correctly predicts the fluid speed downstream of the contraction. The inlet pressure predicted by GASFLOW is $p_1 = 1,000,477.8 \text{ dynes/cm}^2$.

7.8.3. GASFLOW Calculations

7.8.3.1. GASFLOW Input Model. The calculations were performed with GASFLOW, Version 2.1.1.4. No local updates or modifications were made to the code. The duct was represented by 12 cells, 8 in the larger section upstream of the contraction and 4 in the smaller section of the contraction. Each cell is 100.0 cm long.

7.8.4. Conclusions and Recommendations

GASFLOW, Version 2.1.1.4 correctly solves the continuity equation and momentum equation solution.

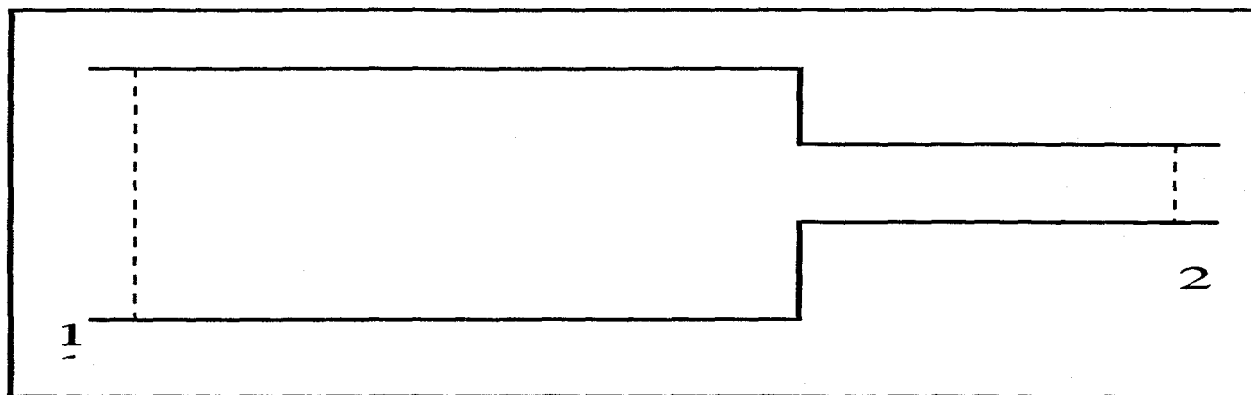


Fig. 7-10. Sketch of a 1D duct with abrupt contraction in the flow area

7.8.4.1. Input File Listing.

1 Ducts / 0 Junction Test

TSA-6 JWS

```
c $Source: /home/inrrisc4/jspore/gasflow/gf2/input/RCS/1duct_3.ingf,v $  
c $Date: 1996/12/18 09:57:22 $  
GF2
```

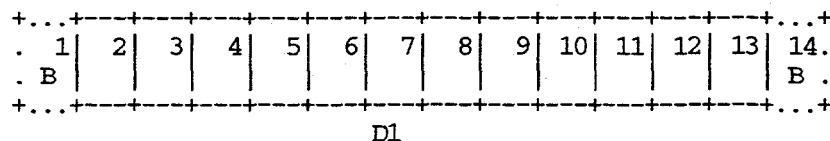
NOTES

- * 1DUCT_3.AR test input
- * 21 SEP 93 -- date of latest change
- * 31 AUG 94 -- Modified to be consistent with GF2
- * 1 duct
- * file: INGF stored in library file
- * /089534/gasflow/gf2/test_problems/1duct_3.ar
- * duct 1: 12 x 100 = 1200 cm
- * Number of real cells = 12
- * Cartesian coordinates, uniform grid
- * Working fluid: air
- * Abrupt area change from 40000.0 cm**2 to 10000.0 cm**2
- * Abrupt area change is to occur at 800 cm.
- * No smooth area change losses calculated.
- * WEST B.C.: specified pressure
- * EAST B.C.: specified pressure

node 1

node 2

PBC



N E T W O R K P A R A M E T E R S

\$innet

```
netopt      = 2,
iwshear    = 0,
ductdef(1,1) = 0.0, 0.0, 200.0, 100.0, 200.0, 100.0, 1, 2, 12,
                1.0,    7, 800.0,
cpnt       = 0.0 , 0.0 , 0.0 ,
                1200.0 , 0.0 , 0.0 ,
```

\$end

B A S I C I N P U T

\$xput

```
muoption = 1,
nu       = 0.150 ,

gz       = -000.0,

autot    = 1.0,
delt0    = 0.1000,
deltmin  = 1.000e-04,
deltmax  = 1.000e-00,

nrsdump  = 0,
eps10    = 1.000e-08,
epsimax  = 1.000e-08,
epsimin  = 1.000e-08,

itdowndt = 024,
itupdt   = 024,
itmax    = 025,

maxcyc   = 2000,
twfin    = 50.000,

lpx       = 1,
iobpl    = 1,
ittyfreq = 20,
pltdt   = 020.000,
prtddt  = 10.0 ,
tddt    = 5000.00,
velmx   = 1.5,

mat = 'air' ,

gasdef(1,1) = 0, 14, 1, -1, -1, -1, 1 ,
                1.0000000000e6, 300.00, 1, 0., 0.,
                'air' , 1.00000,
gasdef(1,2) = 0, 1, 1, -1, -1, -1, 1 ,
                1.0001000000e6, 300.00, 1, 0., 9999999.,
                'air' , 1.00000,
gasdef(1,3) = 13, 14, 1, -2, -2, -2, 1 ,
                1.0000000000e6, 300.00, 1, 0., 9999999.,
                'air' , 1.00000,
vvalue = 200.00,
```

```
pbc(1,1) = 2, 14, 1,-1, -1, -1, 1, 0.0, 99999.,  
vbc(1,1) = 1, 1, 1,-1, -1, -1, 1, 1, 0.0, 99999.,  
; pbc(1,2) = 2, 14, 1,-2, -2, -2, 1, 0.0, 99999.,
```

\$end

M E S H

\$meshgn

\$end

G R A P H I C S

\$grafic

```
pnt(1,1) = 1, 1, -1, -1,  
pnt(1,2) = 5, 1, -1, -1,
```

thdt = 0.0100,

```
thp(1,1) = 1, 1,-1,-1, 'un' , 0,  
thp(1,2) = 5, 1,-1,-1, 'un' , 0,
```

\$end

P A R T I C L E S

\$parts

\$end

H E A T T R A N S F E R & C O N D E N S A T I O N

\$rheat

\$end

S P E C I A L

\$special

\$end

7.9. Problem 6: Flow with Friction in Constant-Area Ducts

7.9.1. Summary

Purpose
To validate the wall friction terms in the momentum equation for flow in a constant-area, 1D duct.
Success Matrix
The GASFLOW-calculated values for the fluid speed and pressure distribution in the channel will agree with the analytical values.
Problem Description
1D flow through a constant-area duct with the pressure specified at the inlet and outlet.
Relationship to Code Models and Methods
See Table 7-1.
Relationship to PIRT Phenomena
N/A.
Code Version and Modifications
GASFLOW 2.1.0.13, with no modifications.
Hardware and Operating System
Sun Ultra 2/200, Sun Microsystems Inc., Sun OS 5.5.1
Compiler, Version, and Optimization Level
Edinburgh Portable Compilers' Fortran 90 Compiler, Version 1.5.1.6, Opt=O3.
Runtime Statistics: Total Run Time, Grind Time
The total problem used 32.2 s of CPU time for an average of 596.7 ms/cell/cycle.
Results and Conclusions
The GASFLOW results agree with the analytical solution for the momentum equation.

7.9.2. Problem Description and Solution

7.9.2.1. Problem Description. The flow channel is made up of two 1D ducts connected by a junction. There are eight real cells, each 100.0 cm long, in the problem. The pressure is specified at the inlet and outlet, and GASFLOW calculates the fluid speed and pressure distribution along the ducts.

7.9.2.2. **Equations and Analytical Solution.** The momentum balance for the duct is

$$p_{in} - p_{out} = \frac{1}{2} \frac{f_w L}{D} \rho u |u| \quad (7-24)$$

where

p_{in} = the pressure at the duct inlet,
 p_{out} = the pressure at the duct outlet,
 f_w = the friction factor,
 L = the length of the duct,
 ρ = the density of the fluid, and
 u = the fluid speed.

The friction factor is given by

$$f_w = \frac{0.3164}{Re^{0.25}} \quad (7-25)$$

where the Reynolds number is

$$Re = \frac{Du}{v} \quad (7-26)$$

Putting Equation (7-26) into Equation (7-25) and that result into Equation (7-24) gives

$$p_{in} - p_{out} = \frac{(0.5)(0.3164)}{D^{1.25}} (v^{0.25}) L \rho u^{1.75} \quad (7-27)$$

which can be solved for the fluid speed for the given problem.

For the duct length of 900 cm, Equation (7-27) yields

$$u = 1370.073131 \text{ cm/s}$$

and GASFLOW calculates

$$u = 1368.92 \text{ cm/s.}$$

The agreement between the analytical and GASFLOW solutions is very good.

An examination of the GASFLOW output shows the pressure distribution along the ducts to be linear, as expected.

7.9.2.3. Analytical Acceptance Parameters and Values. The fluid speed and the pressure distribution along the channel should be predicted by the GASFLOW calculation.

GASFLOW correctly predicts the fluid speed and the pressure distribution.

7.9.3. GASFLOW Calculations

7.9.3.1. GASFLOW Input Model. The calculations were performed with GASFLOW, Version 2.1.0.13. No local updates or modifications were made to the code. The ducts are represented by eight cells, each 100.0 cm long.

7.9.4. Conclusions and Recommendations

GASFLOW, Version 2.1.0.13 correctly solves the momentum equation for this problem only if the boundary cells are included in the duct length.

Users should be made aware of the way GASFLOW handles pressure-specified boundary conditions for ducts with wall friction.

7.9.4.1. Input File Listing.

3.3.1.1. Input File Existing 2 Ducts / 1 Junction Test

TSA-6 JWS

652

NOTES

\$Source: /home/inrrisc4/jspore/gasflow/gf2/input/RCS/wshear.ingf,v \$
\$Date: 1996/12/19 10:33:39 \$

* WSHEAR.AR test case
* 10 AUG 93 -- date of latest change
* 30 AUG 94 -- Changed input to be consistent with GF2
* 2 ducts, 1 jct
* file: INGF stored in an ar library file on
* /089534/gasflow/gf2/test_problems/wshear.ar
* duct 1: $4 \times 100 = 400$ cm, duct 2: $3 \times 100 = 300$ cm, jct 1: 100 cm/side
* Number of real cells = $4 + 3 + 1 = 8$
* Cartesian coordinates, uniform grid
* Working fluid: air
* Wall shear calculation on.
* WEST B.C.: specified pressure
* EAST B.C.: specified pressure

NETWORK PARAMETERS

\$innet

```
netopt      = 2,
ductdef(1,1) = 0.0, 0.0, 100.0, 100.0, 100.0, 100.0, 1, 2, 4,
               1.0, 0, 0,
ductdef(1,2) = 0.0, 0.0, 100.0, 100.0, 100.0, 100.0, 2, 3, 3,
               1.0, 0, 0,
defjct(1,1)  = 100.0, 100.0, 100.0, 2,
cpnt(1,1)    = 0.0, 0.0, 0.0,
cpnt(1,2)    = 450.0, 0.0, 0.0,
cpnt(1,3)    = 800.0, 0.0, 0.0,
iwshear = 1,
```

\$end

BASIC INPUT

\$xput

```
muoption = 1,
nu       = 0.150 ,
gz       = -000.0,
autot    = 1.0,
delt0    = 0.1000,
deltmin  = 1.000e-04,
deltmax  = 1.000e-00,
nrsdump  = 0,
epsi0    = 1.000e-08,
epsimax  = 1.000e-08,
epsimin  = 1.000e-08,
itdowndt = 024,
itupdt   = 024,
itmax    = 025,
maxcyc   = 8000,
twfin    = 100.000,
lpr       = 1,
iobpl    = 1,
ittyfreq = 20,
pltdt   = 200.000,
prttdt   = 50.0 ,
tddt     = 5000.00,
velmx   = 1.5,
mat = 'air' ,
gasdef(1,1) = 0, 6, 1, -1, -1, -1, 1,
               1.0000000000e6, 300.00, 1, 0., 0.,
               'air' , 1.00000,
gasdef(1,2) = 0, 5, 2, -2, -2, -2, 1,
               1.0000000000e6, 300.00, 1, 0., 0.,
               'air' , 1.00000,
gasdef(1,3) = 0, 1, 1, -1, -1, -1, 1,
               1.0001000000e6, 300.00, 1, 0., 9999999.,
               'air' , 1.00000,
```

```
gasdef(1,4) = 4, 5, 2, -2, -2, -2, 1,  
1.0000000000e6, 300.00, 1, 0., 999999.,  
'air' , 1.00000,
```

```
vvalue = 123.45,
```

```
pbc(1,1) = 1, 1, 1,-1, -1, -1, 1, 0.0, 99999.,  
pbc(1,2) = 2, 4, 2,-2, -2, -2, 1, 0.0, 99999.,
```

```
$end
```

M E S H

```
$meshgn
```

```
$end
```

G R A P H I C S

```
$grafic
```

```
pnt(1,1) = 1, 1, -1, -1,  
pnt(1,2) = 5, 1, -1, -1,
```

```
thdt = 0.0100,
```

```
thp(1,1) = 1, 1,-1,-1, 'un' , 0,  
thp(1,2) = 5, 1,-1,-1, 'un' , 0,  
thp(1,3) = 1, 2,-2,-2, 'un' , 0,  
thp(1,4) = 4, 2,-2,-2, 'un' , 0,
```

```
$end
```

P A R T I C L E S

```
$parts
```

```
$end
```

H E A T T R A N S F E R & C O N D E N S A T I O N

```
$rheat
```

```
$end
```

S P E C I A L

```
$special
```

```
$end
```

7.10. Problem 7: Flow with Friction in Constant-Area Ducts, Part 2: Fluid Speed at Inlet Specified

7.10.1. Summary

Purpose

To validate the wall friction terms in the momentum equation for flow in constant area, 1D ducts.

Success Matrix

The GASFLOW-calculated values for the pressure distribution in the channel will agree with the analytical values.

Problem Description

1D flow through constant-area ducts with the fluid speed specified at the inlet and the pressure specified at the outlet.

Relationship to Code Models and Methods

See Table 7-1.

Relationship to PIRT Phenomena

N/A.

Code Version and Modifications

GASFLOW 2.1.1.4, with no modifications.

Hardware and Operating System

Sun SPARC 10, Sun Microsystems Inc., Sun OS 5.5.1.

Compiler, Version, and Optimization Level

SUN Fortran 90 Compiler, Version 1.2 patch 104366-04, Opt=O3.

Runtime Statistics: Total Run Time, Grind Time

The total problem used 33.0 s of CPU time for an average of 1279.0 ms/cell/cycle.

Results and Conclusions

The GASFLOW results compare well with the analytical solution for the momentum equation.

7.10.2. Problem Description and Solution

7.10.2.1. Problem Description. The flow channel is made up of two 1D ducts connected by a junction. There are eight real cells, each 100.0 cm long, in the problem. The fluid speed is specified at the inlet and the pressure at the outlet. GASFLOW determines the pressure distribution in the ducts.

7.10.2.2. Equations and Analytical Solution. The momentum balance, neglecting the momentum flux, gives the pressure distribution

$$p(z) = p_{out} + \frac{1}{2} \frac{f_w(L-z)}{D} \rho u |u| \quad , \quad (7-28)$$

where

$p(z)$ = the pressure at distance z from the duct inlet,
 p_{out} = the pressure at the duct outlet,
 f_w = the friction factor,
 L = the length of the duct,
 ρ = the density of the fluid, and
 u = the fluid speed.

The fluid speed at the inlet was specified to be 3000.0 cm/s.

The friction factor is given by

$$f_w = \frac{0.3164}{Re^{0.25}} \quad , \quad (7-29)$$

where the Reynolds number is

$$Re = \frac{Du}{v} \quad . \quad (7-30)$$

For the conditions of the problem, $Re = 2.0 \times 10^6$ and $f_w = 0.00841354$. If f_w and the other numerical values, $D = 100.0$ cm, $v = 0.15$ cm²/s, $\rho = 0.0011569$ g/cm³, $L = 850.0$ cm, and $u = 3000.0$ cm/s, are put into Equation (7-28), then

$$p(z) = p_{out} + 0.43799(L-z) \quad . \quad (7-31)$$

7.10.2.3. Analytical Acceptance Parameters and Values. The pressure distribution along the channel given by Equation (7-31) should be predicted by the GASFLOW calculation.

7.10.3. GASFLOW Calculations

7.10.3.1. GASFLOW Input Model. The calculations were done with GASFLOW, Version 2.1.0.13. No local updates or modifications were made to the code. The ducts are represented by eight cells, each 100.0 cm long. The two 1D ducts are connected by a junction, also 100 cm long.

7.10.4. Conclusions and Recommendations

At $z = 0$ cm, Equation (7-31) predicts a pressure of 1,000,350 dynes/cm² and GASFLOW calculates 1,000,352 dynes/cm², which is in good agreement.

7.10.4.1. Input File Listing.

2 Ducts / 1 Junction Test

TSA-6 jws

GF2

NOTES

\$Source: /home/inrrisc4/jspore/gasflow/gf2/input/RCS/wshear.ingf,v \$
\$Date: 1996/12/19 10:33:39 \$

* WSHEAR.AR test case
* 10 AUG 93 -- date of latest change
* 30 AUG 94 -- Changed input to be consistent with GF2
* 2 ducts, 1 jct
* file: INGF stored in an ar library file on
* /089534/gasflow/gf2/test_problems/wshear.ar
* duct 1: $4 \times 100 = 400$ cm, duct 2: $3 \times 100 = 300$ cm, jct 1: 100 cm/side
* Number of real cells = $4 + 3 + 1 = 8$
* Cartesian coordinates, uniform grid
* Working fluid: air
* Wall shear calculation on.
* WEST B.C.: specified pressure
* EAST B.C.: specified pressure

NETWORK PARAMETERS

```

$innet
  netopt      = 2,
  ductdef(1,1) =  0.0,    0.0, 100.0, 100.0, 100.0, 100.0, 1, 2, 4,
                  1.0,      0,      0,
  ductdef(1,2) =  0.0,    0.0, 100.0, 100.0, 100.0, 100.0, 2, 3, 3,
                  1.0,      0,      0,
  defjct(1,1)  = 100.0, 100.0, 100.0,      2,
  cpnt(1,1)    =  0.0,    0.0,  0.0,
  cpnt(1,2)    = 450.0,   0.0,  0.0,
  cpnt(1,3)    = 800.0,   0.0,  0.0,
  iwshear = 1,
$end

```

BASIC INPUT

\$xput

```

muoption = 1,
nu      = 0.150 ,
gz      = -000.0,
autot   = 1.0,
delt0   = 0.1000,
deltmin = 1.000e-04,
deltmax = 1.000e-00,
nrsdump = 0,
epsi0   = 1.000e-08,
epsimax = 1.000e-08,
epsimin = 1.000e-08,
itdowndt = 024,
itupdt   = 024,
itmmax   = 025,
maxcyc  = 8000,
twfin    = 20.000,
lpr      = 1,
iobjpl  = 1,
ittyfreq = 20,
pltdt   = 10.000,
prtddt  = 20.0 ,
tddt    = 5000.00,
velmax  = 1.5,
mat = 'air' ,
gasdef(1,1) = 0, 6, 1, -1, -1, -1, 1 ,
               1.0000000000e6, 300.00, 1, 0., 0.,
               'air' , 1.00000,
gasdef(1,2) = 0, 5, 2, -2, -2, -2, 1 ,
               1.0000000000e6, 300.00, 1, 0., 0.,
               'air' , 1.00000,
gasdef(1,3) = 0, 1, 1, -1, -1, -1, 1 ,
               1.0003500000e6, 300.00, 1, 0., 9999999.,
               'air' , 1.00000,
gasdef(1,4) = 4, 5, 2, -2, -2, -2, 1 ,
               1.0000000000e6, 300.00, 1, 0., 9999999.,
               'air' , 1.00000,
vvalue = 3000.0,
pbc(1,1) = 2, 4, 2,-1, -1, -1, 1, 0.0, 99999.,
vbc(1,1) = 1, 1, 1,-1, -1, -1, 1, 1, 0.0, 99999.,
;      pbc(1,2) = 2, 4, 2,-2, -2, -2, 1, 0.0, 99999.,

```

Send

M E S H

\$meshgn
\$end

G R A P H I C S

\$grafic

pnt(1,1) = 1, 1, -1, -1,
pnt(1,2) = 5, 1, -1, -1,

thdt = 0.1000,

thp(1,1) = 1, 1,-1,-1, 'un' , 0,
thp(1,2) = 5, 1,-1,-1, 'un' , 0,
thp(1,3) = 1, 2,-2,-2, 'un' , 0,
thp(1,4) = 4, 2,-2,-2, 'un' , 0,

\$end

P A R T I C L E S

\$parts

\$end

H E A T T R A N S F E R & C O N D E N S A T I O N

\$rheat

\$end

S P E C I A L

\$special

\$end

7.11. Problem 8: 1D Flow with an Orifice

7.11.1. Summary

Purpose
To validate the orifice-loss model in the momentum equations.
Success Matrix
The GASFLOW-calculated values for the fluid pressure and temperature distribution along the channel will agree with the analytical solution.
Problem Description
A stagnant fluid in two 3D blocks connected by a single-duct geometry is heated by a uniform energy source.
Relationship to Code Models and Methods
See Table 7-1.
Relationship to PIRT Phenomena
N/A.
Code Version and Modifications
GASFLOW 2.1.0.13, with no modifications.
Hardware and Operating System
Sun Ultra 2/200, Sun Microsystems Inc., Sun OS 5.5.1.
Compiler, Version, and Optimization Level
Edinburgh Portable Compilers' Fortran 90 Compiler, Version 1.5.1.6, Opt=O3.
Runtime Statistics: Total Run Time, Grind Time
The total problem used 10.4 s of CPU time for an average of 3541.4 ms/cell/cycle.
Results and Conclusions
The GASFLOW results agree with the analytical solution.

7.11.2. Problem Description and Solution

7.11.2.1. Problem Description. The 1D frictionless flow of air in a straight channel in which an orifice is located. The orifice is the only flow resistance present. The channel is 1100.0 cm long and is represented by 11 nodes, each 100 cm long. The orifice is located 200 cm from the inlet of the channel. The flow area through the orifice is 0.10 in the flow area for the channel. The outlet pressure is specified to be 1.0×10^6 dyne/cm², and the inlet fluid speed is specified to be 100.0 cm/s. The pressure and fluid speed distributions along the channel are calculated by GASFLOW.

7.11.2.2. Equations and Analytical Solution. The loss coefficient for the orifice based on the flow area of the orifice is

$$K_l = 2.7(1.0 - \beta)(1.0 - \beta^2) \quad (7-32)$$

where

$$\beta = 0.10 \text{ and } K_l = 2.4057.$$

The fluid speed is constant, neglecting the small effects of compressibility of the air, and at the orifice location, $u = u_{in}/0.10$, where u_{in} is the specified speed of the fluid at the inlet.

The pressure drop across the orifice is given by

$$\Delta p_l = \frac{1}{2} \rho K_l u^2 \quad (7-33)$$

where $\rho = 0.001158 \text{ g/cm}^3$. Equation (7-33) gives the pressure drop across the orifice as $\Delta p_l = 1352.61 \text{ dyne/cm}^2$.

The pressure at the inlet to the channel is then the specified outlet pressure plus this pressure drop across the orifice.

7.11.2.3. Analytical Results. The fluid speed and pressure distribution along the channel are shown in Figures 7-11 and 7-12, respectively.

7.11.2.4. Analytical Acceptance Parameters and Values. As shown in Figures 7-11 and 7-12, the GASFLOW numerical solution predicts the analytical solution with good accuracy.

The small differences between the GASFLOW solution and the analytical solution may be caused by compressibility effects not included in the analytical solution.

7.11.3. GASFLOW Calculations

7.11.3.1. GASFLOW Input Model. The calculations were performed with GASFLOW, Version 2.1.0.13. No local updates or modifications were made to the code.

7.11.4. Conclusions and Recommendations

GASFLOW, Version 2.1.0.13 reasonably predicted the analytical solution, as required by the success metric.

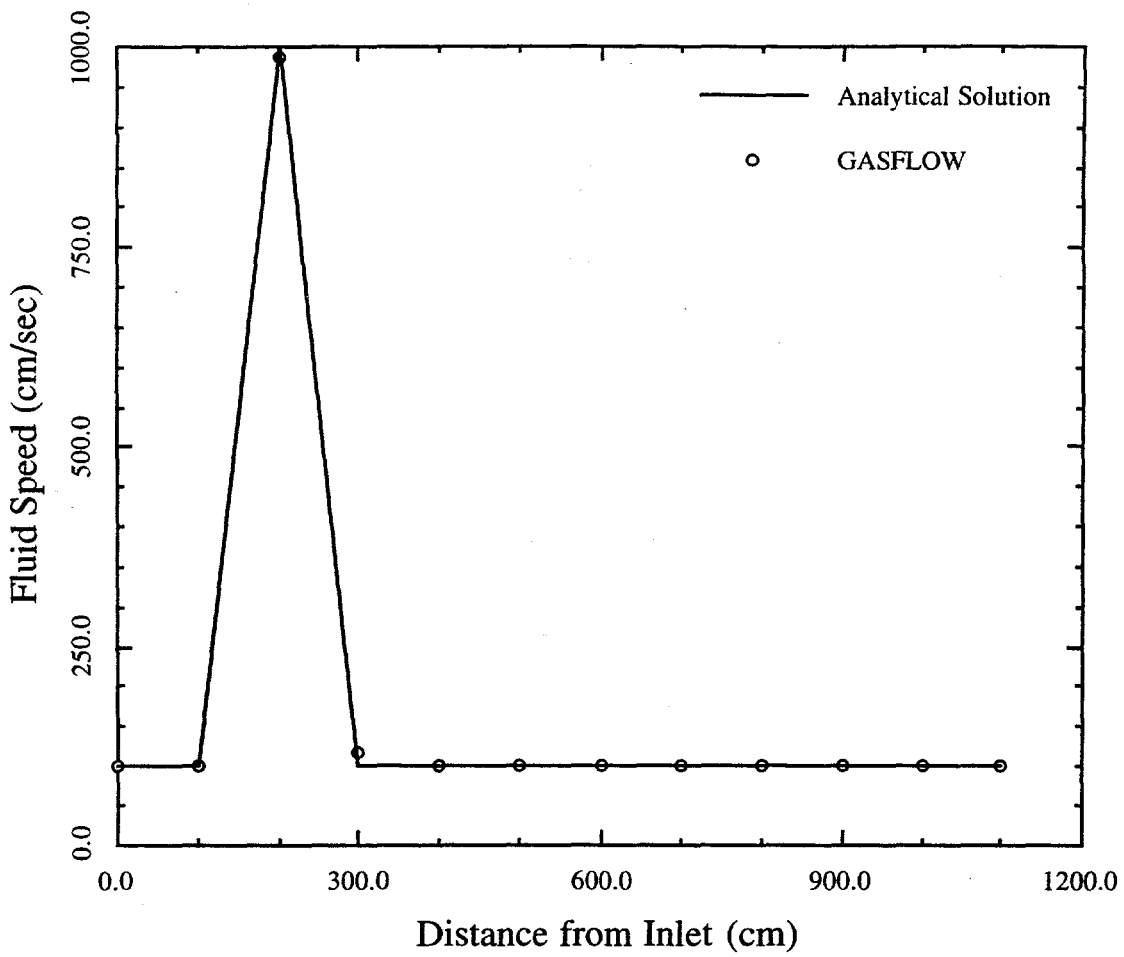


Fig. 7-11. Comparison of an analytical solution and GASFLOW results for the fluid speed

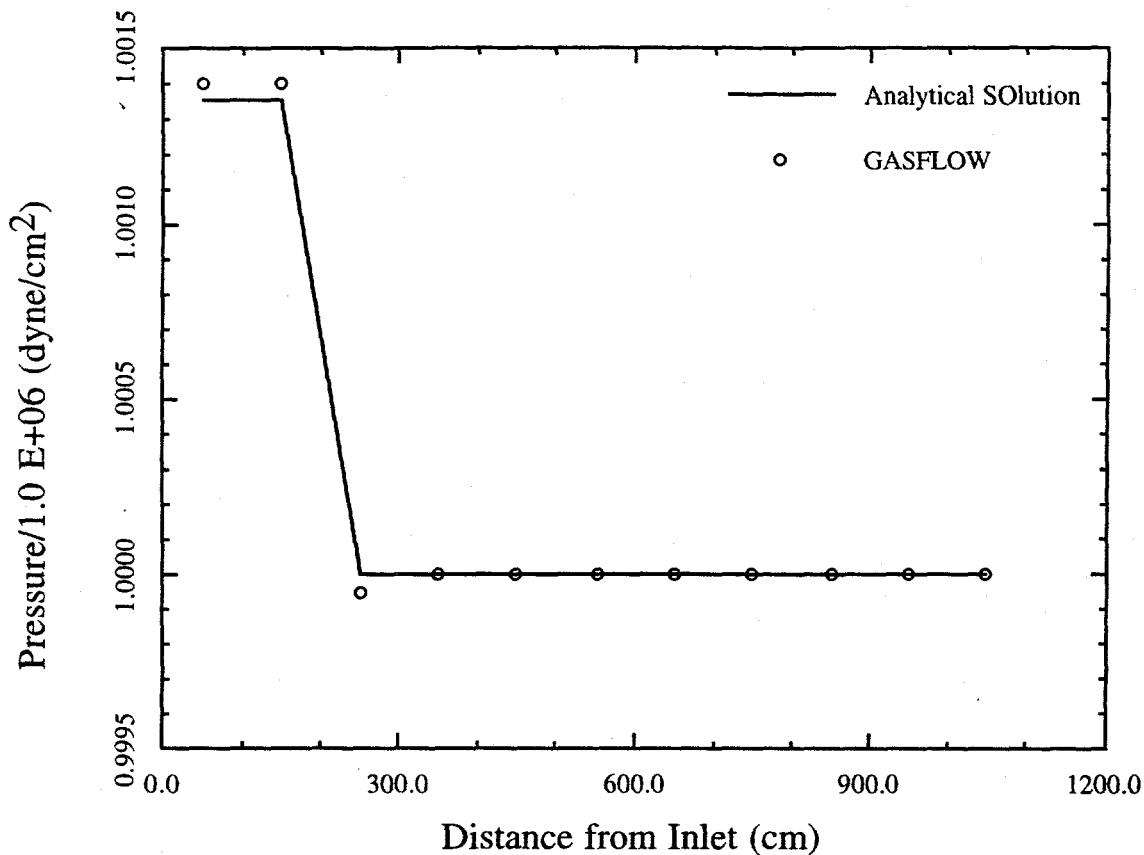


Fig. 7-12. Comparison of an analytical solution and GASFLOW results for the pressure

7.11.4.1. Input File Listing.

Channel flow with arearatio - x direction
 TSA10 SPORE Feb. 13 96
 gf2-ar

\$Header: /home/inrrisc4/jspore/gasflow/gf2/input/RCS/aratiox.ingf,v 1.1 1996/12/18
 10:51:53 jspore Exp \$

Orifice loss model gives a loss of 2.467
 Delta-P imposed across channel = 1000 dynes/cm²
 Density = 0.001158 gm/cm³

V = sqrt(2*1000/(0.001158*2.467))
 = 836.7 cm/s

\$innet
 \$end
 \$xput

iburn = 0,
 nrsdump = 0,
 autot = 1.0,

```

cyl      = 0.0,
delt0    = 0.00010,
deltmin  = 1.000e-06,
deltmax  = 1.000e-00,
epsi0    = 1.000e-05,
epsimax  = 1.000e-05,
epsimin  = 1.000e-05,
gz       = 0000.0,
iobpl   = 1,
itdowndt = 500,
itupdt   = 500,
itmax    = 1000,
lpr      = 1,
maxcyc  = 900000,
ittyfreq = 20,
nu       = 0.15,
prandtl1 = 0.7,
schmidt  = 0.45,
muoption = 1,
idiffmom = 0,
idiffme  = 1,
pltdt   = 0000.100,
prtdt   = 1.00,
twfin   = 1.000,
tddt    = 1200.0000,
velmx   = 5.0,
mat = 'air',
areardef(1,1) = 3,3,1,2,1,2,1,0.1,
gasdef(1,1)= 1, 12, 1, 02, 1, 02,1,1.000e+6, 300.00,2,0.,0.,
           'air',1.0,
gasdef(1,2)= 0, 1, 1, 02, 1, 02,1,1.001e+6, 300.00,2,0.,99999.,
           'air',1.0,
gasdef(1,3)= 12, 13, 1, 02, 1, 02,1,1.000e+6, 300.00,2,0.,99999.,
           'air',1.0,
vvalue = 100.00,
pbc(1,1) = 12, 12, 1, 2, 1, 2, 1, 0.0, 1.0e+99,
vbc(1,1) = 1, 1, 1, 2, 1, 2, 1, 0.0, 99999.,
; pbc(1,2) = 12, 12, 1, 2, 1, 2, 1, 0.0, 1.0e+99,
$end
-----
          heat - transfer
-----
$rheat
$end
-----
      mesh
-----
$meshgn
iblock = 1,
xgrid =
0.0, 100.0, 200.0, 300.0, 400.0, 500.0, 600.0, 700.0, 800.0, 900.0, 1000.0, 1100.0,

```

```
ygrid =  
0.0000e+00, 1.0000e+02,  
zgrid =  
0.0000e+00, 1.0000e+02,
```

```
$end
```

```
$meshgn  
$end
```

g r a p h i c s

```
$grafic
```

```
thdt = 1.e-2,
```

```
igrid = 0,
```

```
pnt = 1, 2, 02, 1,  
12, 02, 02, 1,
```

```
pld = 1, 2, 'tk', 0,  
1, 2, 'pn', 0,  
1, 2, 'un', 0,
```

```
thp(1,1) = 02, 02, 02, 1, 'pn', 0,  
02, 02, 02, 1, 'tk', 0,  
02, 02, 02, 1, 'un', 0,  
03, 02, 02, 1, 'un', 0,
```

```
$end
```

```
$special
```

```
$end  
$parts
```

```
$end
```

7.12. Problem 9: Uniform Energy Addition to Stagnant Fluid

7.12.1. Summary

Purpose

To validate the energy storage and energy source terms in the fluid energy equation.

Success Matrix

The GASFLOW-calculated values for the fluid temperature as a function of time will agree with the analytical solution.

Problem Description

A stagnant fluid in two 3D blocks connected by a single-duct geometry is heated by a uniform energy source.

Relationship to Code Models and Methods

See Table 7-1.

Relationship to PIRT Phenomena

N/A.

Code Version and Modifications

GASFLOW 2.1.0.13, with no modifications.

Hardware and Operating System

Sun Ultra 2/200, Sun Microsystems Inc., Sun OS 5.5.1.

Compiler, Version, and Optimization Level

Edinburgh Portable Compilers' Fortran 90 Compiler, Version 1.5.1.6, Opt=O3.

Runtime Statistics: Total Run Time, Grind Time

The total problem used 24.2 s of CPU time for an average of 481.1 ms/cell/cycle.

Results and Conclusions

The GASFLOW results agree with the analytical solution.

7.12.2. Problem Description and Solution

7.12.2.1. Problem Description. A sketch of the two 3D blocks and a connecting duct is given in the input file listing. There is no flow into or out of the flow field; the fluid is stagnant in the blocks and duct. A constant energy source of 8325.2 ergs/cm³-s was distributed uniformly throughout the flow field. The problem is run for 20 s of simulation time.

7.12.2.2. Equations and Analytical Solution. For a stagnant, constant-property fluid with a uniformly distributed energy source, the GASFLOW energy equation for the fluid is

$$\rho C_v \frac{dT}{dt} = Q \quad (7-34)$$

which gives the temperature as a function of time as

$$T(t) = T_0 + \frac{Qt}{\rho C_v} \quad (7-35)$$

where

$$T_0 = 300 \text{ K},$$

$$Q = 8325.2 \text{ ergs}/(\text{cm}^3 \cdot \text{s}),$$

$$\rho = 0.00116144 \text{ g/cm}^3, \text{ and}$$

$$C_v = 7.16802 \times 10^6 \text{ ergs/g-K}$$

Equation (7-35) gives the fluid temperature at 20 s to be $T = 320 \text{ K}$.

The fluid density is not exactly constant during the transient. Putting the final fluid density of $\rho = 0.00115664 \text{ g/cm}^3$ into Equation (7-35) will show that the effect of the density change on the temperature can be neglected.

7.12.2.3. Analytical Results. The fluid temperature as a function of time is shown in Figure 7-13.

7.12.2.4. Analytical Acceptance Parameters and Values. As shown in Figure 7-13, the GASFLOW numerical solution accurately predicts the transient analytical solution.

7.12.3. GASFLOW Calculations

7.12.3.1. GASFLOW Input Model. The calculations were performed with GASFLOW, Version 2.1.0.13. No local updates or modifications were made to the code. As shown in the sketch in the input listing, the 3D blocks contained nine cells and the connecting duct was modeled with four cells.

7.12.4. Conclusions and Recommendations

GASFLOW, Version 2.1.0.13 accurately predicted the analytical solution, as required by the success metric.

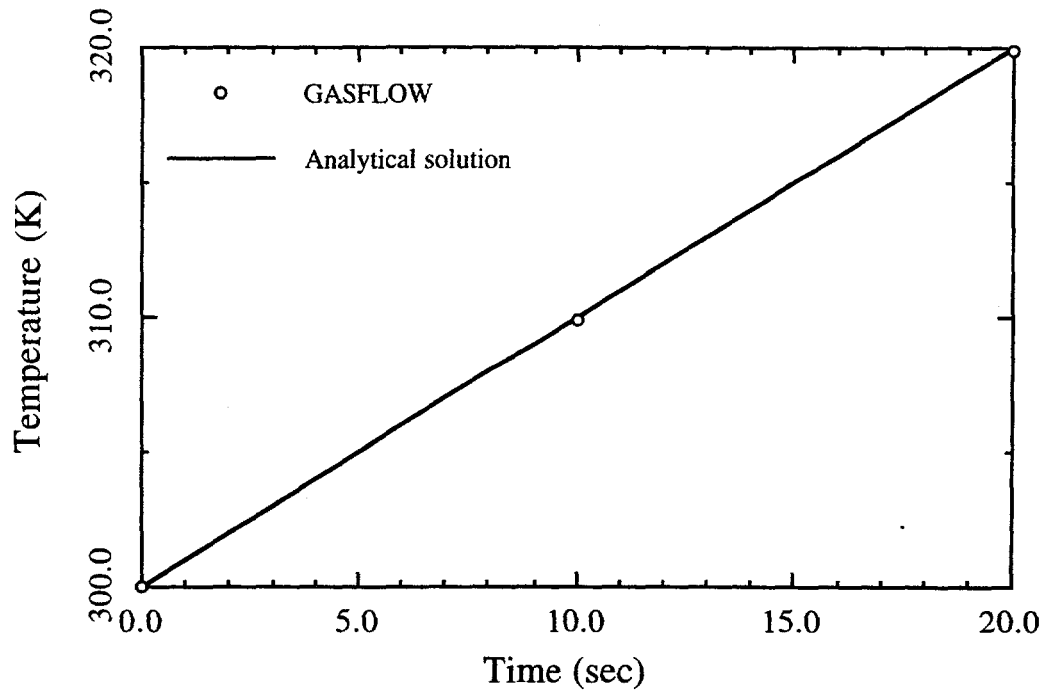


Fig. 7-13. Comparison of the analytical solution and GASFLOW results

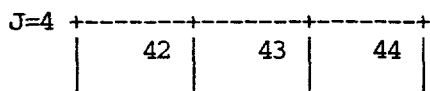
7.12.4.1. Input File Listing.

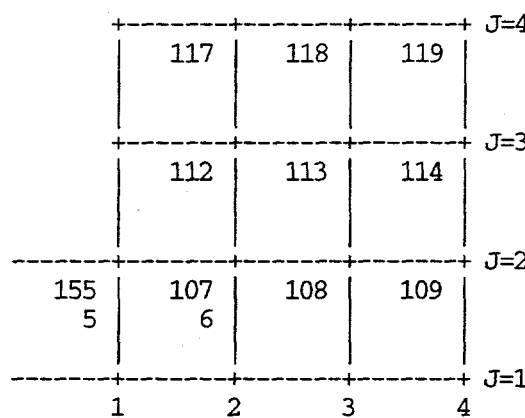
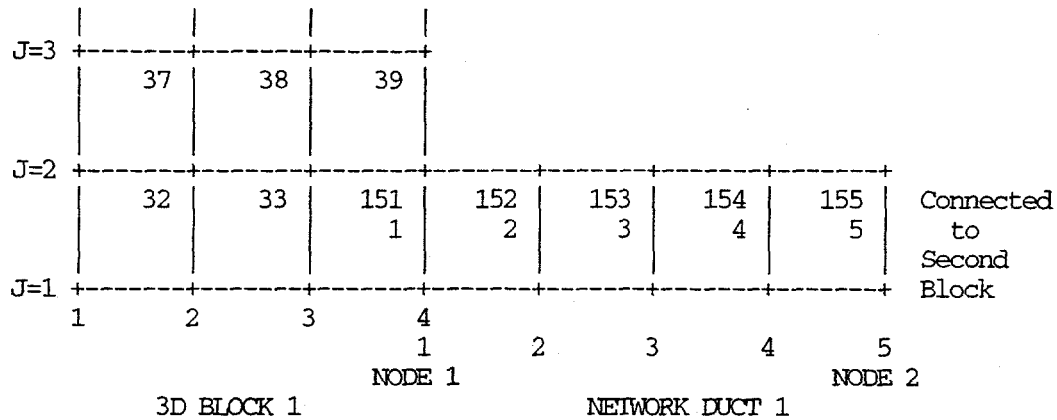
1D/3D Problem ESDEF test problem
 TSA6 jws
 GASFLOW V2.0

c \$Source: /home/inrrisc4/jspore/gasflow/gf2/input/RCS/2B_1D_esdef.ingf,v \$
 c \$Date: 1996/12/18 09:57:22 \$

NOTES:

- * 12/13/94
- * 2B_1D_esdef on ODIN in directory /home/jspore/gasflow/gf2/test_problems
- * 2 3D block, 1 duct
- * air
- * Uniform energy source term of 8325.2 ergs/cm³
- * BLOCK #1
 - 300 x 300 x 100 cm
 - 3 x 3 x 1 = 9 real cells m222 = 32
 - 5 x 5 x 3 = 75 total cells mrrr = 44
- * DUCT #1
 - 400 x (100 x 100) cm
 - 4 cells
 - W end: connected to 3D block
 - E end: connected to 3D block
- * BLOCK #2
 - 300 x 300 x 100 cm
 - 3 x 3 x 1 = 9 real cells m222 = 32
 - 5 x 5 x 3 = 75 total cells mrrr = 44





NETWORK INPUT

```

$innet
cpnt = 300.0, 50.0, 50.0,
       700.0, 50.0, 50.0,
ductdef = 100.0, 100.0, 100.0, 100.0, 100.0, 100.0,
           1,      2,      4,      1.0,    0.0,    0.0,
netopt  = 2,
kopt1d3d = 1,
nwcx = 4, 4, 1, 2, 1, 2, 1, 1,
       1, 1, 1, 2, 1, 2, 2, 2,
iwshear = 0,
$end

```

BASIC INPUT

```
$xput
; pbc(1,1) = 2, 0, 1, 0, 0, 0, 0, 0.00, 1.e99,
  vvalue = 1000.0,-500.0,
; vbc(1,1) = 1, 1, 1, 2, 1, 2, 1, 1, 0.00, 1.e99,
autot = 1.0, cyl = 0.0, omg = 34.0,
delt0 = 00.10000,
```

```

deltmin = 1.000e-08,
deltmax = 1.000e-00,
eps10 = 1.000e-08,
epsimax = 1.000e-08,
epsimin = 1.000e-08,
gz = -000.0,
iobpl = 0,
itdowndt = 25,
itupdt = 100,
itmax = 100,
lpr = 1,
maxcyc = 02000,
ittyfreq = 5,
nu = 0.15 ,
pltdt = 100.00,
prtdt = 010.000,
twfin = 020.00,
tddt = 100.0000,
velmx = 1.5,
ibw = 1,
ibe = 1,
ibs = 1,
ibn = 1,
ibb = 1,
ibt = 1,
mat = 'air',

; 3D BLOCK # 1-----
gasdef(1,1) = 1 , 'im1', 1 , 'jml' , 1 , 'kml' , 1 , ; I.C.
1.00000000e6, 300.0, 1, 0., 0.,
'air', 1.00000,
; 3D BLOCK # 2-----
gasdef(1,2) = 1 , 'im1', 1 , 'jml' , 1 , 'kml' , 2 , ; I.C.
1.00000000e6, 300.0, 1, 0., 0.,
'air', 1.00000,
; 1D NETWORK -----
gasdef(1,3) = 0 , 6, 1 , 0 , 0 , 0 , 0 , ; D#1 I.C.
1.00000000e6, 300.0, 1, 0., 0.,
'air', 1.00000,
esdef(1,1) = 1, 5, 1, 0, 0, 0, 8325.2, 0.0, 99999.0,
esdef(1,2) = 1, 4, 1, 4, 1, 2, 1, 8325.2, 0.0, 99999.0,
esdef(1,3) = 1, 4, 1, 4, 1, 2, 2, 8325.2, 0.0, 99999.0,

```

\$end

M E S H

```

$meshgn
iblock = 1,
xgrid = 0.0, 100.0, 200.0, 300.0,
ygrid = 0.0, 100.0, 200.0, 300.0,
zgrid = 0.0, 100.0,
$end
$meshgn
iblock = 2,

```

```
xgrid = 0.0, 100.0, 200.0, 300.0,  
ygrid = 0.0, 100.0, 200.0, 300.0,  
zgrid = 0.0, 100.0,  
$end  
$meshgn  
$end
```

G R A P H I C S

```
$grafic  
  
thdt = 1.0,  
thp(1,1) = 4, 2, 2, 1, 'tk', 0,  
           4, 3, 2, 1, 'tk', 0,  
           4, 2, 2, 2, 'tk', 0,  
           4, 3, 2, 2, 'tk', 0,  
           2, 1, 0, 0, 'tk', 0, ; duct #1  
           5, 1, 0, 0, 'tk', 0, ; duct #1  
           2, 1, 0, 0, 'pn', 0, ; duct #1  
           5, 1, 0, 0, 'pn', 0, ; duct #1  
  
$end
```

P A R T I C L E S

```
$parts  
$end  
$rheat  
$end  
$special  
$end  
$specialp  
$end
```

7.13. Problem 10: Specified Mass-Flow-Rate Boundary-Condition Function

7.13.1. Summary

Purpose
To validate the specified mass-flow-rate boundary-condition function.
Success Matrix
The GASFLOW-calculated values for the fluid velocity as a function of time will agree with the analytical evaluation of the specified function.
Problem Description
A fluid in two 3D blocks and three 1D ducts with the mass flow rate specified as a function of time at a cell face. Air is the working fluid.
Relationship to Code Models and Methods
See Table 7-1.
Relationship to PIRT Phenomena
N/A.
Code Version and Modifications
GASFLOW 2.1.0.13, with no modifications.
Hardware and Operating System
Sun Ultra 2/200, Sun Microsystems Inc., Sun OS 5.5.1.
Compiler, Version, and Optimization Level
Edinburgh Portable Compilers' Fortran 90 Compiler, Version 1.5.1.6, Opt=O3.
Runtime Statistics: Total Run Time, Grind Time
The total problem used 29.2 s of CPU time for an average of 447.5 ms/cell/cycle.
Results and Conclusions
The GASFLOW results agree with the analytical solution.

7.13.2. Problem Description and Solution

7.13.2.1. Problem Description. A sketch of the two 3D blocks and associated 1D ducts is given in the input file listing. The mass flow rate is specified as a function of time at the x face of cell 1,2,2 in 3D block 1.

7.13.2.2. Equations and Analytical Solution. The mass flow rate at the x face of cell 1,2,2 is specified as a function of time as

$$W=10.0 t^* - 20.0 t^{*2} + 40.0 t^{*3} - 20.0 t^{*4} , \quad (7-36)$$

where

$$t^* = (t-t_0)/(t_f-t_0),$$

$$t_0 = 0.00 \text{ s, and}$$

$$t_f = 50.0 \text{ s.}$$

With the mass flow rate from Equation (7-36) and the channel flow area and fluid density, the fluid speed is

$$v = W/(\rho A) , \quad (7-37)$$

where

$$\rho = 0.00116144 \text{ g/cm}^3 \text{ and}$$

$$A = 10000.0 \text{ cm}^2$$

7.13.2.3. Analytical Results. The fluid velocity as a function of time is shown in Figure 7-14.

7.13.2.4. Analytical Acceptance Parameters and Values. As shown in Figure 7-14, GASFLOW correctly evaluates the specified mass-flow-rate function.

7.13.3. GASFLOW Calculations

7.13.3.1. GASFLOW Input Model. The calculations were performed with GASFLOW, Version 2.1.0.13. No local updates or modifications were made to the code. As shown in the sketch in the input listing, the 3D blocks contained nine cells and the connecting ducts were modeled with four cells.

7.13.4. Conclusions and Recommendations

GASFLOW, Version 2.1.0.13 correctly evaluates the specified mass-flow-rate function, as required by the success metric.

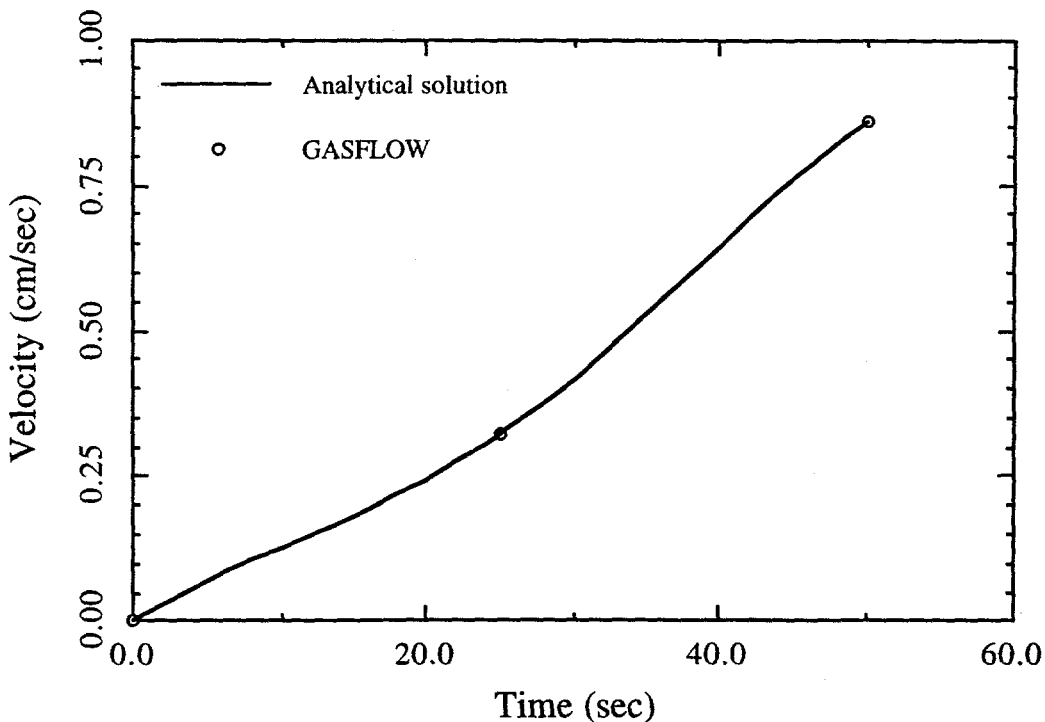


Fig. 7-14. Comparison of analytical solution and GASFLOW results

7.13.4.1. Input File Listing.

1D/3D Problem 2 Blocks & 3 Ducts with mbc BC.

TSA6 jws

GASFLOW V2.0

```
c $Source: /home/inrrisc4/jspore/gasflow/gf2/input/RCS/2B_3D_mbc.ingf,v $
c $Date: 1997/06/17 13:30:33 $
```

NOTES:

- * 20 DEC 94
- * 2B_3D_mbc on ODIN in directory /home/jspore/gasflow/gf2/test_problems
- * 2 3D block, 3 duct
- * air
- * BLOCK #1
 - 300 x 300 x 100 cm
 - 3 x 3 x 1 = 9 real cells m222 = 32
 - 5 x 5 x 3 = 75 total cells mrrr = 44
 - mbc at the x-face of cell 1,2,2
- * DUCT #1
 - 400 x (100 x 100) cm
 - 4 cells
 - W end: connected to 3D block 1
 - E end: connected to junction 1
- * DUCT #2
 - 400 x (100 x 100) cm
 - 4 cells
 - W end: connected to junction 1
 - E end: connected to 3D block 2

* DUCT #3

400 x (100 x 100) cm

4 cells

W end: connected to PBC.

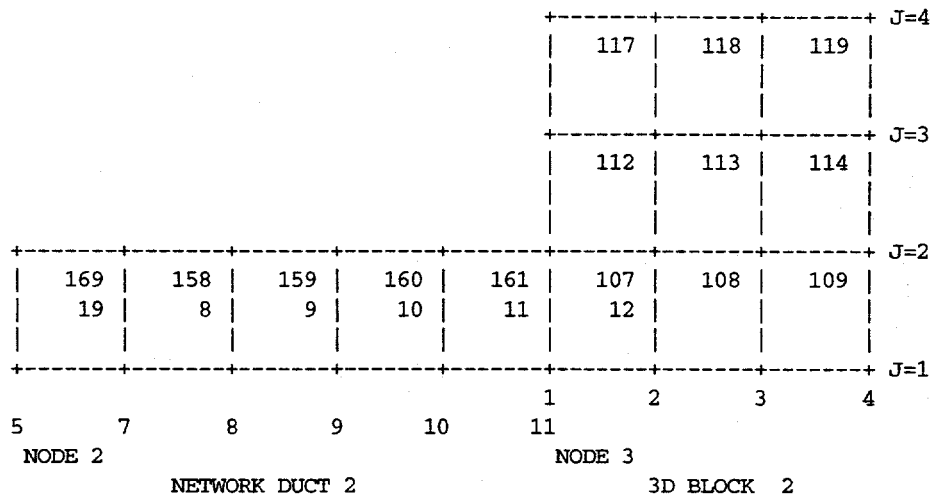
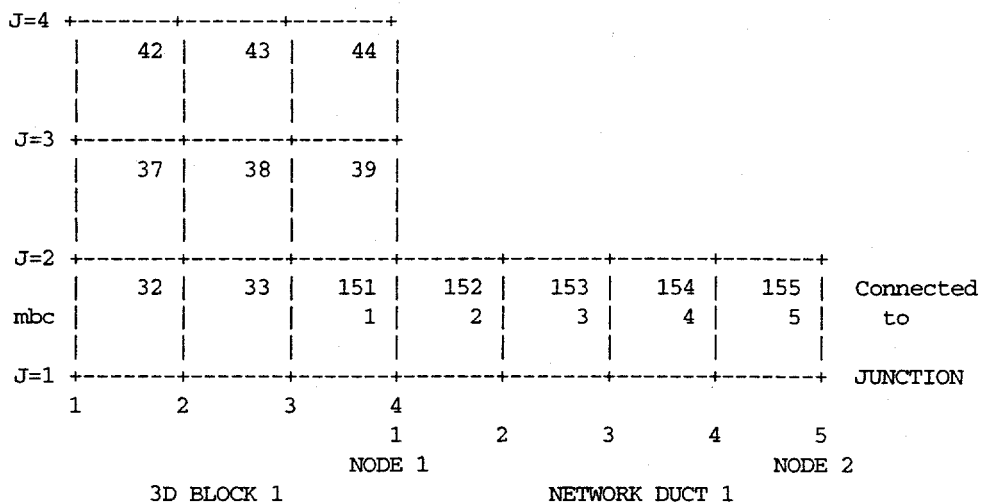
E end: connected to 3D block 2

* BLOCK #2

300 x 300 x 100 cm

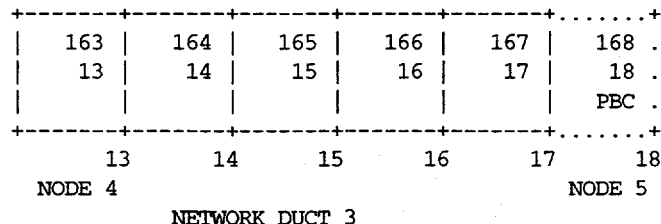
$3 \times 3 \times 1 = 9$ real cells $m222 = 32$

$$5 \times 5 \times 3 = 75 \text{ total cells}$$



3D cell

109



NET WORK INPUT

```
$innet
cpnt = 300.0, 50.0, 50.0,
       700.0, 50.0, 50.0,
       1100.0, 50.0, 50.0,
       1500.0, 50.0, 50.0,
       1900.0, 50.0, 50.0,
ductdef = 100.0, 100.0, 100.0, 100.0, 100.0, 100.0,
           1, 2, 4, 1.0, 0.0, 0.0,
           100.0, 100.0, 100.0, 100.0, 100.0, 100.0,
           2, 3, 4, 1.0, 0.0, 0.0,
           100.0, 100.0, 100.0, 100.0, 100.0, 100.0,
           4, 5, 4, 1.0, 0.0, 0.0,
defjct(1,1) = 100.0, 100.0, 100.0, 2,
netopt = 2,
kopt1d3d = 1,

nwcx = 4, 4, 1, 2, 1, 2, 1, 1,
       1, 1, 1, 2, 1, 2, 2, 3,
       4, 4, 1, 2, 1, 2, 2, 4,

iwshear = 0,
$end
```

BASIC INPUT

```
$xput
pbc(1,1) = 2, 0, 3, 4, 1, 2, 0, 0.00, 1.e99,
mvalue = 1000.0,-500.0,0.0,
mbc(1,1) = 1, 1, 1, 2, 1, 2, 1, 143, 0.00, 50.2,
mfunc(1,1) = 10.0, -20.0, 40.0, -20.0,

autot = 1.0, cyl = 0.0, omg = 34.0 ,
delt0 = 00.10000 ,
deltmin = 1.000e-08,
deltmax = 1.000e-00,
epsi0 = 1.000e-08,
epsimax = 1.000e-08,
epsimin = 1.000e-08,
gz = -000.0,
iobpl = 0,
itdowndt = 25,
itupdt = 100,
itmax = 100,
lpr = 1,
maxcyc = 02000,
ittyfreq = 20,
nu = 0.15 ,
pltdt = 100.00,
prtdt = 025.000,
twfin = 050.00,
tdt = 100.0000,
```

```

velmx = 1.5,
ibw = 1,
ibe = 1,
ibs = 1,
ibn = 1,
ibb = 1,
ibt = 1,

mat = 'air',

; 3D BLOCK # 1 -----
gasdef(1,1) = 1, 'im1', 1, 'jm1', 1, 'km1', 1, ;I.C.
1.00000000e6, 300.0, 1, 0., 0.,
'air', 1.00000,

; 3D BLOCK # 2 -----
gasdef(1,2) = 1, 'im1', 1, 'jm1', 1, 'km1', 2, ;I.C.
1.00000000e6, 300.0, 1, 0., 0.,
'air', 1.00000,

; 1D NETWORK DUCT # 1 -----
gasdef(1,3) = 0, 6, 1, 0, 0, 0, 0, ;D#1 I.C.
1.00000000e6, 300.0, 1, 0., 0.,
'air', 1.00000,

; 1D NETWORK DUCT # 2 -----
gasdef(1,4) = 0, 6, 2, 0, 0, 0, 0, ;D#2 I.C.
1.00000000e6, 300.0, 1, 0., 0.,
'air', 1.00000,

; 1D NETWORK DUCT # 2 -----
gasdef(1,5) = 0, 6, 3, 0, 0, 0, 0, ;D#3 I.C.
1.00000000e6, 300.0, 1, 0., 0.,
'air', 1.00000,

; 3D BLOCK # 1 -----
gasdef(1,6) = 0, 1, 1, 'jm1', 1, 'km1', 1, ;West B.C.
1.00000000e6, 300.0, 1, 0., 99999.,
'air', 1.00000,

; 1D NETWORK DUCT # 3 -----
gasdef(1,7) = 5, 6, 3, 0, 0, 0, 0, ; East B.C.
1.00000000e6, 300.0, 1, 0., 99999.,
'air', 1.00000,

```

\$end

M E S H

```

$meshgn
iblock = 1,
xgrid = 0.0, 100.0, 200.0, 300.0,
ygrid = 0.0, 100.0, 200.0, 300.0,
zgrid = 0.0, 100.0,

```

```
$end
$meshgn
  iblock = 2,
  xgrid = 0.0, 100.0, 200.0, 300.0,
  ygrid = 0.0, 100.0, 200.0, 300.0,
  zgrid = 0.0, 100.0,
$end
$meshgn
$end
```

GRAPHICS

```
$grafic
thdt = 1.0,
thp(1,1) = 4, 2, 2, 1, 'pn' , 0,
  4, 2, 2, 1, 'un' , 0,
  1, 2, 2, 1, 'un' , 0,
  1, 2, 2, 1, 'mdotx', 0,
  2, 1, 0, 0, 'mdotx', 0, ;duct #1
  5, 1, 0, 0, 'mdotx', 0, ;duct #1
  2, 1, 0, 0, 'un' , 0, ;duct #1
  5, 1, 0, 0, 'un' , 0, ;duct #1
  2, 2, 0, 0, 'mdotx', 0, ;duct #2
  5, 2, 0, 0, 'mdotx', 0, ;duct #2
  2, 2, 0, 0, 'un' , 0, ;duct #2
  5, 2, 0, 0, 'un' , 0, ;duct #2
  2, 3, 0, 0, 'mdotx', 0, ;duct #3
  5, 3, 0, 0, 'mdotx', 0, ;duct #3
  2, 3, 0, 0, 'un' , 0, ;duct #3
  5, 3, 0, 0, 'un' , 0, ;duct #3
```

```
$end
```

PARTICLES

```
$parts
$end
$rheat
$end
$special
$end
$specialp
$end
```

7.14. Problem 11: Filter with Turbulent Flow Losses

7.14.1. Summary

Purpose

Validation of the local pressure loss for turbulent flow through a filter.

Success Matrix

The GASFLOW-calculated fluid speed through the ducts and filter will agree with the analytical value.

Problem Description

Flow of air at normal temperature and pressure in 1D ducts with a filter in the first duct. The loss coefficient for the filter is specified by the user.

Relationship to Code Models and Methods

See Table 7-1.

Relationship to PIRT Phenomena

N/A.

Code Version and Modifications

GASFLOW 2.1.0.13, with no modifications.

Hardware and Operating System

Sun Ultra 2/200, Sun Microsystems Inc., Sun OS 5.5.1.

Compiler, Version, and Optimization Level

Edinburgh Portable Compilers' Fortran 90 Compiler, Version 1.5.1.6, Opt=O3.

Runtime Statistics: Total Run Time, Grind Time

The total problem used 7.1 s of CPU time for an average of 817.1 ms/cell/cycle.

Results and Conclusions

The GASFLOW results agree with the analytical solution.

7.14.2. Problem Description and Solution

7.14.2.1. Problem Description. Air flow through two 1D ducts with a filter located in the first duct. The pressure drop across the ducts is specified, and the code will calculate the fluid speed.

7.14.2.2. Analytical Results.

The pressure drop across the filter for turbulent flow is

$$(\Delta p)_{\text{filter}} = \frac{1}{2} k_t \rho \left(\frac{u}{\beta} \right)^2, \quad (7-38)$$

where

k_t = user-specified loss coefficient for turbulent flow and
 β = flow-area fraction for the filter.

Solving for the fluid speed Equation (7-38) gives

$$u = \sqrt{\frac{2(\Delta p)_{\text{filter}} \beta^2}{\rho k_t}}. \quad (7-39)$$

For the test problem,

$$\begin{aligned} \Delta p_{\text{filter}} &= 100 \text{ dynes/cm}^2, \\ \rho &= 0.00115676 \text{ g/cm}^3, \\ k_t &= 1.0, \text{ and} \\ \beta &= 1.0. \end{aligned}$$

Putting these values into Equation (7-39) gives the fluid speed upstream of the filter to be $u = 415.81 \text{ cm/s}$.

7.14.2.3. Analytical Acceptance Parameters and Values. The GASFLOW numerical solution predicts the fluid speed upstream of the filter to be 415.808503 cm/s .

7.14.3. GASFLOW Calculations

7.14.3.1. GASFLOW Input Model. The calculations were performed with GASFLOW, Version 2.1.0.13. No local updates or modifications were made to the code.

7.14.4. Conclusions and Recommendations

GASFLOW, Version 2.1.0.13 results are in agreement with the analytical results, as required by the success metric.

7.14.4.1. Input File Listing.

2 Ducts / 1 Junction Test

TSA6 JWS

GF2

\$Source: /home/inrrisc4/jspore/gasflow/gf2/input/RCS/filter.ingf,v \$
\$Date: 1996/12/19 09:00:12 \$

NOTES

```
* FILTER.AR test case
* 10 AUG 93 -- date of latest change
* 30 AUG 94 -- Made input compatible with GF2 input.
* 2 ducts, 1 jct
* file: INGF stored in an ar library file on
*       /089534/gasflow/gf2/test_problems/filter.ar
* duct 1: 4 x 100 = 400 cm, duct 2: 3 x 100 = 300 cm, jct 1: 100 cm/side
* Number of real cells = 4 + 3 + 1 = 8
* Cartesian coordinates, uniform grid
* Working fluid: air
* One filter at cell 3 duct 1, with turbulent only losses.
* WEST B.C.: specified pressure
* EAST B.C.: specified pressure
```

PBC										PBC	
+	+	+	+	+	+	+	+	+	+	+	+
.	1	2	3	4	5	12	8	9	10	11	.
.	B					J1				B	.
+	+	+	+	+	+	+	+	+	+	+	+
D1						D2					

NETWORK PARAMETERS

\$innet

```

netopt      = 2,
ductdef(1,1) = 0.0,    0.0, 100.0, 100.0, 100.0, 100.0, 1, 2, 4,
                1.0,      0,      0,
ductdef(1,2) = 0.0,    0.0, 100.0, 100.0, 100.0, 100.0, 2, 3, 3,
                1.0,      0,      0,
defjct(1,1)  = 100.0, 100.0, 100.0,      2,
cpnt(1,1)    = 0.0,    0.0,    0.0,
cpnt(1,2)    = 450.0,   0.0,    0.0,
cpnt(1,3)    = 800.0,   0.0,    0.0,
iwshear = 0,
filtrdef(1,1) = 2, 3, 1, 1,
                0, 1, 1.00,

```

\$end

BASIC INPUT

\$xput

muoption = 1,
nu = 0.150 ,

```

gz      = -000.0,

autot  = 1.0,
delt0  = 0.1000,
deltmin = 1.000e-04,
deltmax = 1.000e-00,

nrsdump = 0,
epsi0   = 1.000e-08,
epsimax = 1.000e-08,
epsimin = 1.000e-08,

itdowndt = 024,
itupdt   = 024,
itmax    = 025,

maxcyc  =      2000,
twfin   = 50.000,

lpr      = 1,
iobpl   = 1,
ittyfreq = 20,
pltdt   = 020.000,
prtdt   = 10.0 ,
tddt    = 5000.00,
velmx   = 1.5,

mat = 'air' ,

gasdef(1,1) = 0, 6, 1, -1, -1, -1, 1 ,
               1.0000000000e6, 300.00, 1, 0., 0.,
               'air' , 1.00000,
gasdef(1,2) = 0, 5, 2, -2, -2, -2, 1 ,
               1.0000000000e6, 300.00, 1, 0., 0.,
               'air' , 1.00000,
gasdef(1,3) = 0, 1, 1, -1, -1, -1, 1 ,
               1.0001000000e6, 300.00, 1, 0., 9999999.,
               'air' , 1.00000,
gasdef(1,4) = 4, 5, 2, -2, -2, -2, 1 ,
               1.0000000000e6, 300.00, 1, 0., 9999999.,
               'air' , 1.00000,
vvalue = 123.45,
pbc(1,1) = 1, 1, 1,-1, -1, -1, 1, 0.0, 99999.,
pbc(1,2) = 2, 4, 2,-2, -2, -2, 1, 0.0, 99999.,

```

\$end

M E S H

\$meshgn
\$end

G R A P H I C S

\$grafic

pnt(1,1) = 1, 1, -1, -1,
pnt(1,2) = 5, 1, -1, -1,

thdt = 0.0100,

thp(1,1) = 1, 1,-1,-1, 'un' , 0,
thp(1,2) = 5, 1,-1,-1, 'un' , 0,
thp(1,3) = 1, 2,-2,-2, 'un' , 0,
thp(1,4) = 4, 2,-2,-2, 'un' , 0,

\$end

P A R T I C L E S

\$parts

\$end

H E A T T R A N S F E R & C O N D E N S A T I O N

\$rheat

\$end

S P E C I A L

\$special

\$end

7.15. Problem 12: Filter with Laminar Flow Losses

7.15.1. Summary

Purpose
Validation of the local pressure loss for laminar flow through a filter.
Success Matrix
The GASFLOW-calculated fluid speed through the ducts and filter will agree with the analytical value.
Problem Description
Flow of air at normal temperature and pressure in 1D ducts with a filter in the second duct. The loss coefficient for the filter is specified by the user.
Relationship to Code Models and Methods
See Table 7-1.
Relationship to PIRT Phenomena
N/A.
Code Version and Modifications
GASFLOW 2.1.0.13, with no modifications.
Hardware and Operating System
Sun Ultra 2/200, Sun Microsystems Inc., Sun OS 5.5.1.
Compiler, Version, and Optimization Level
Edinburgh Portable Compilers' Fortran 90 Compiler, Version 1.5.1.6, Opt=O3.
Runtime Statistics: Total Run Time, Grind Time
The total problem used 8.5 s of CPU time for an average of 755.7 ms/cell/cycle.
Results and Conclusions
The GASFLOW results agree with the analytical solution.

7.15.2. Problem Description and Solution

7.15.2.1. Problem Description. Air flow through two 1D ducts with a filter located in the second duct. The pressure drop across the ducts is specified, and the code will calculate the fluid speed.

7.15.2.2. Analytical Results. The pressure drop across the filter for turbulent flow is

$$(\Delta p)_{\text{filter}} = k_l \mu u / D \beta^2 \quad (7-40)$$

where

k_l = user-specified loss coefficient for laminar flow,
 β = flow-area fraction for the filter,
 μ = fluid viscosity, and
 D = duct diameter.

Solving for the fluid speed Equation (7-40) gives

$$u = \frac{(\Delta p)_{\text{filter}} D \beta^2}{\mu k_l} \quad (7-41)$$

For the test problem,

$\Delta p_{\text{filter}} = 100 \text{ dynes/cm}^2$,
 $\rho = 0.00115676 \text{ g/cm}^3$,
 $k_l = 10.0$,
 $D = 100.0 \text{ cm}$,
 $\mu = \rho v = (0.00115676)(0.150) \text{ g/(cm-s)}$, and
 $\beta = 0.01$

Putting these values into Equation (7-41) gives the fluid speed upstream of the filter to be
 $u = 576.322 \text{ cm/s}$.

7.15.2.3. Analytical Acceptance Parameters and Values. The GASFLOW numerical solution predicts the fluid speed upstream of the filter to be 576.049 cm/s.

7.15.3. GASFLOW Calculations

7.15.3.1. GASFLOW Input Model. The calculations were performed with GASFLOW, Version 2.1.0.13. No local updates or modifications were made to the code.

7.15.4. Conclusions and Recommendations

GASFLOW, Version 2.1.0.13 results are in agreement with the analytical results, as required by the success metric.

7.15.4.1. Input File Listing.

2 Ducts / 1 Junction Test
TSA-6 jws
GF2

\$Source: /home/inrrisc4/jspore/gasflow/gf2/input/RCS/filter_1.ingf,v \$
\$Date: 1996/12/19 09:00:12 \$

NOTES

```
* FILTER_1.AR test case
* 10 AUG 93 -- date of latest change
* 31 AUG 93 -- Modified input to be consistent with GF2
* 2 ducts, 1 jct
* file: INGF stored in an ar library file on
*       /089534/gasflow/gf2/test_problems/filter_1.ar
* duct 1: 4 x 100 = 400 cm, duct 2: 3 x 100 = 300 cm, jct 1: 100 cm/side
* Number of real cells = 4 + 3 + 1 = 8
* Cartesian coordinates, uniform grid
* Working fluid: air
* One filter at cell 2 duct 2 with laminar only losses.
* WEST B.C.: specified pressure
* EAST B.C.: specified pressure
```

The diagram shows a 1D chain of 11 sites, labeled 1 through 11. The chain is represented by a horizontal line with vertical dashed lines at each site. The boundary conditions are periodic, indicated by 'PBC' at both ends. Site 11 is connected to site 1. The chain is divided into two regions: D1 (sites 1-5) and D2 (sites 6-11). Site 5 is labeled 'J1'. The chain is shown in a 2D grid with 3 rows and 11 columns.

NETWORK PARAMETERS

```

$innet
netopt      = 2,
ductdef(1,1) = 0.0,    0.0, 100.0, 100.0, 100.0, 100.0, 1, 2, 4,
                1.0,    0,    0,
ductdef(1,2) = 0.0,    0.0, 100.0, 100.0, 100.0, 100.0, 2, 3, 3,
                1.0,    0,    0,
defjct(1,1)  = 100.0, 100.0, 100.0,      2,
cpnt(1,1)    = 0.0,    0.0,    0.0,
cpnt(1,2)    = 450.0,  0.0,    0.0,
cpnt(1,3)    = 800.0,  0.0,    0.0,
iwshear = 0,
filtrdef(1,1) = 1, 2, 2, 1,
                10., 0., 0.01,

```

\$end

BASIC INPUT

\$xput

```

muoption = 1,
nu        = 0.150 ,
gz        = -000.0,
autot    = 1.0,
delt0    = 0.1000,
deltmin  = 1.000e-04,
deltmax  = 1.000e-00.

```

```

nrsdump = 0,
eps10 = 1.000e-08,
epsimax = 1.000e-08,
epsimin = 1.000e-08,

itdowndt = 024,
itupdt = 024,
itmax = 025,

maxcyc = 2000,
twfin = 50.000,

lpr = 1,
iobpl = 1,
ittyfreq = 20,
pltdt = 020.000,
prttdt = 10.0 ,
tddt = 5000.00,
velmx = 1.5,

mat = 'air' ,

gasdef(1,1) = 0, 6, 1, -1, -1, -1, 1 ,
1.0000000000e6, 300.00, 1, 0., 0.,
'air' , 1.00000,
gasdef(1,2) = 0, 5, 2, -2, -2, -2, 1 ,
1.0000000000e6, 300.00, 1, 0., 0.,
'air' , 1.00000,
gasdef(1,3) = 0, 1, 1, -1, -1, -1, 1 ,
1.0001000000e6, 300.00, 1, 0., 9999999.,
'air' , 1.00000,
gasdef(1,4) = 4, 5, 2, -2, -2, -2, 1 ,
1.0000000000e6, 300.00, 1, 0., 9999999.,
'air' , 1.00000,
vvalue = 123.45,
pbc(1,1) = 1, 1, 1,-1, -1, -1, 1, 0.0, 99999.,
pbc(1,2) = 2, 4, 2,-2, -2, -2, 1, 0.0, 99999.,

```

\$end

M E S H

\$meshgn
\$end

G R A P H I C S

\$grafic

```

pnt(1,1) = 1, 1, -1, -1,
pnt(1,2) = 5, 1, -1, -1,
thdt = 0.0100,
thp(1,1) = 1, 1,-1,-1, 'un' , 0,

```

thp(1,2) = 5, 1,-1,-1, 'un' , 0,
thp(1,3) = 1, 2,-2,-2, 'un' , 0,
thp(1,4) = 4, 2,-2,-2, 'un' , 0,

\$end

P A R T I C L E S

\$parts

\$end

H E A T T R A N S F E R & C O N D E N S A T I O N

\$rheat

\$end

S P E C I A L

\$special

\$end

7.16. Problem 13: Filter with Laminar plus Turbulent Flow Losses

7.16.1. Summary

Purpose

Validation of the combined laminar plus turbulent local-pressure loss for flow through a filter.

Success Matrix

The GASFLOW-calculated fluid speed through the ducts and filter will agree with the analytical value.

Problem Description

Flow of air at normal temperature and pressure in 1D ducts with a filter in the second duct. The laminar and turbulent loss coefficients for the filter are specified by the user.

Relationship to Code Models and Methods

See Table 7-1.

Relationship to PIRT Phenomena

N/A.

Code Version and Modifications

GASFLOW 2.1.0.13, with no modifications.

Hardware and Operating System

Sun Ultra 2/200, Sun Microsystems Inc., Sun OS 5.5.1

Compiler, Version, and Optimization Level

Edinburgh Portable Compilers' Fortran 90 Compiler, Version 1.5.1.6, Opt=O3

Runtime Statistics: Total Run Time, Grind Time

The total problem used 3.6 s of CPU time for an average of 1717.2 ms/cell/cycle.

Results and Conclusions

The GASFLOW results agree with the analytical solution.

7.16.2. Problem Description and Solution

7.16.2.1. Problem Description. Air flow through two 1D ducts with a filter located in the second duct. The pressure drop across the ducts is specified, and the code will calculate the fluid speed. A sketch of the flow is shown in the input file listing.

7.16.2.2. Analytical Results. The pressure drop across the filter for turbulent flow is

$$\Delta p = \frac{1}{2} k_t \rho \left(\frac{u}{\beta} \right)^2 + k_l \mu u / D \beta^2 \quad (7-42)$$

where

k_t = the user-specified loss coefficient for turbulent flow,

k_l = the user-specified loss coefficient for laminar flow,

β = the flow-area fraction for the filter,

μ = the fluid viscosity, and

D = the duct diameter.

For the test problem,

$$\Delta p = 100 \text{ dynes/cm}^2,$$

$$\rho = 0.00115676 \text{ g/cm}^3,$$

$$k_t = 1.0,$$

$$k_l = 1.0,$$

$$D = 100.0 \text{ cm},$$

$$\mu = \rho v = (0.00115676)(0.150) \text{ g/(cm-s), and}$$

$$\beta = 0.20.$$

Putting these values into Equation (7-42) gives the fluid speed through the ducts and filter to be $u = 83.16023 \text{ cm/s}$.

7.16.2.3. Analytical Acceptance Parameters and Values. The GASFLOW numerical solution predicts the fluid speed upstream of the filter to be 83.1607 cm/s.

7.16.3. GASFLOW Calculations

7.16.3.1. GASFLOW Input Model. The calculations were performed with GASFLOW, Version 2.1.0.13. No local updates or modifications were made to the code.

7.16.4. Conclusions and Recommendations

GASFLOW, Version 2.1.0.13 results are in agreement with the analytical results, as required by the success metric.

7.16.4.1. Input File Listing. 2

Ducts / 1 Junction Test

TSA-6 jws

GF2

```
$Source: /home/inrrisc4/jspore/gasflow/gf2/input/RCS/filter_1.ingf,v $  
$Date: 1996/12/19 09:00:12 $
```

NOTES

```
* FILTER_1.AR test case
* 10 AUG 93 -- date of latest change
* 31 AUG 93 -- Modified input to be consistent with GF2
* 2 ducts, 1 jct
* file: INGF stored in an ar library file on
*       /089534/gasflow/gf2/test_problems/filter_1.ar
* duct 1: 4 x 100 = 400 cm, duct 2: 3 x 100 = 300 cm, jct 1: 100 cm/side
* Number of real cells = 4 + 3 + 1 = 8
* Cartesian coordinates, uniform grid
* Working fluid: air
* One filter at cell 2 duct 2 with laminar only losses.
* WEST B.C.: specified pressure
* EAST B.C.: specified pressure
```

The diagram shows a 1D chain of 11 sites, labeled node 1 through node 11. The chain is represented by a horizontal line with vertical bars at each site. The boundary conditions are periodic (PBC), indicated by arrows at the ends. Site 1 is at the left end, and site 11 is at the right end. Site 5 is labeled J_1 . The chain is divided into two regions: p_1 on the left and p_2 on the right.

NETWORK PARAMETERS

```

$innet
    netopt      = 2,
    ductdef(1,1) = 0.0,    0.0, 100.0, 100.0, 100.0, 100.0, 1, 2, 4,
                      1.0,    0,    0,
    ductdef(1,2) = 0.0,    0.0, 100.0, 100.0, 100.0, 100.0, 2, 3, 3,
                      1.0,    0,    0,
    defjct(1,1) = 100.0, 100.0, 100.0,      2,
    cpnt(1,1)   = 0.0,    0.0,    0.0,
    cpnt(1,2)   = 450.0,   0.0,    0.0,
    cpnt(1,3)   = 800.0,   0.0,    0.0,
    iwshear = 0,
    filtrdef(1,1) = 1, 2, 2, 1,
                      10, 0, 0.01.

```

Send

BASIC INPUT

\$xput

```

muoption = 1,
nu       = 0.150 ,
gz       = -000.0,
autot   = 1.0,
delt0   = 0.1000,
deltmin = 1.000e-04,
deltmax = 1.000e-00,
nrsdump = 0,
epsi0   = 1.000e-08,
epsimax = 1.000e-08,
epsimin = 1.000e-08,

```

```

itdowndt = 024,
itupdt  = 024,
itmax   = 025,

maxcyc  =      2000,
twfin   = 50.000,

lpr      = 1,
iobpl   = 1,
ittyfreq = 20,
pltdt   = 020.000,
prtdt   = 10.0 ,
tddt    = 5000.00,
velmx   = 1.5,

mat = 'air' ,

gasdef(1,1) = 0, 6, 1, -1, -1, -1, 1 ,
1.000000000e6, 300.00, 1, 0., 0.,
'air' , 1.00000,
gasdef(1,2) = 0, 5, 2, -2, -2, -2, 1 ,
1.000000000e6, 300.00, 1, 0., 0.,
'air' , 1.00000,
gasdef(1,3) = 0, 1, 1, -1, -1, -1, 1 ,
1.000100000e6, 300.00, 1, 0., 9999999.,
'air' , 1.00000,
gasdef(1,4) = 4, 5, 2, -2, -2, -2, 1 ,
1.000000000e6, 300.00, 1, 0., 9999999.,
'air' , 1.00000,
vvalue = 123.45,
pbc(1,1) = 1, 1, 1,-1, -1, -1, 1, 0.0, 99999.,
pbc(1,2) = 2, 4, 2,-2, -2, -2, 1, 0.0, 99999.,

```

\$end

M E S H

\$meshgn
\$end

G R A P H I C S

\$grafic

```

pnt(1,1) = 1, 1, -1, -1,
pnt(1,2) = 5, 1, -1, -1,
thdt = 0.0100,
thp(1,1) = 1, 1,-1,-1, 'un' , 0,
thp(1,2) = 5, 1,-1,-1, 'un' , 0,
thp(1,3) = 1, 2,-2,-2, 'un' , 0,
thp(1,4) = 4, 2,-2,-2, 'un' , 0,

```

\$end

P A R T I C L E S

\$parts

\$end

H E A T T R A N S F E R & C O N D E N S A T I O N

\$rheat

\$end

S P E C I A L

\$special

\$end

7.17. Problem 14: Steady-State Heat Transfer through a Wall

7.17.1. Summary

Purpose
To validate the heat-transfer-coefficient models and 1D conduction heat transfer through a wall.
Success Matrix
The GASFLOW-calculated values for the heat transfer through the wall will agree with the analytical solution.
Problem Description
Cocurrent flow of air on both sides of a rectangular wall. The fluid speed is the same for both streams, one of which has an inlet temperature of 350.0 K and the other 300.0 K.
Relationship to Code Models and Methods
See Table 7-1.
Relationship to PIRT Phenomena
N/A.
Code Version and Modifications
GASFLOW 2.1.0.13, with no modifications.
Hardware and Operating System
Sun Ultra 2/200, Sun Microsystems Inc., Sun OS 5.5.1.
Compiler, Version, and Optimization Level
Edinburgh Portable Compilers' Fortran 90 Compiler, Version 1.5.1.6, Opt=O3.
Runtime Statistics: Total Run Time, Grind Time
The total problem used 903.5 s of CPU time for an average of 1505.8 ms/cell/cycle.
Results and Conclusions
The GASFLOW results agree with the analytical solution.

7.17.2. Problem Description and Solution

7.17.2.1. Problem Description. 1D flow in the y direction of air on each side of a rectangular wall. The wall is 4.0 cm thick. The fluid nodes are 1000.0 cm on a side, and there are two nodes in the x direction, three nodes in the y direction, and a single node in the z direction. The outlet pressure is specified to be 1.0×10^6 dyne/cm², and the inlet fluid speed is specified to be 300.0 cm/s in the y direction. One fluid stream has an inlet temperature of 350.0 K and the other 300.0 K. The pressure, temperature, and fluid speed

distributions along the channel are calculated by GASFLOW. The heat transfer through the wall and the wall-surface temperatures also are calculated. A sketch of the flow channel is given in the input file listing.

7.17.2.2. Equations and Analytical Solution. For steady-state 1D heat conduction through a rectangular wall, the overall heat transfer factor is

$$U = \frac{1}{\frac{1}{h_h} + \frac{t_w}{k_w} + \frac{1}{h_c}}, \quad (7-43)$$

where

h_h = the heat-transfer coefficient on the hot side,

t_w = the thickness of the wall (4.0 cm),

k_w = the thermal conductivity of the wall (5.0×10^6 ergs/cm s), and

h_c = the heat-transfer coefficient on the cold side.

The heat transfer through the wall is

$$Q_w = UA_w(T_h - T_c), \quad (7-44)$$

where

T_h = the hot-stream temperature,

T_c = the cold-stream temperature,

and the wall heat-transfer area is $A_w = 1.0 \times 10^6$ cm².

For turbulent flow conditions, the heat-transfer coefficients in GASFLOW are calculated from

$$h = \frac{4.0 \rho C_p |u_c|}{\left[2.19 \ln \left(\frac{y_c |u_c|}{v} \right) + 0.76 \right]^2} \text{Pr}^{-\frac{2}{3}}, \quad (7-45)$$

where the conditions for the problem of interest are summarized in Table 7-2.

Table 7-2. Heat-Transfer Conditions

Quantity	Hot Side	Cold Side
Temperature, T	350.0 K	300.0 K
Density, ρ	0.00099165 g/cm ³	0.0011564 g/cm ³
Specific Heat, C_p	1.00 J/g K	1.00 J/g K
Fluid Speed, u_c	300.0 cm/s	300.0 cm/s
Prandtl Number, Pr	1.00	1.00
Distance from Wall, y_c	500.00 cm	500.00 cm
Viscosity, ν	0.150 cm ² /s	0.150 cm ² /s

The heat-transfer coefficients are

$$h = 12411.1 \text{ ergs/cm}^2 \text{ s} \text{ for the hot side, and}$$

$$h = 14473.0098 \text{ ergs/cm}^2 \text{ s} \text{ for the cold side.}$$

Putting the heat-transfer coefficients and the wall properties into Equation (7-43) gives

$$U = 6645.95937 \text{ ergs/cm}^2 \text{ s,}$$

and the heat transfer through the wall from Equation (7-44) is

$$Q = 3.3084E+11 \text{ ergs/s.}$$

7.17.2.3. Analytical Acceptance Parameters and Values. The GASFLOW numerical solution will predict the analytical solution for the heat transfer through the wall.

7.17.3. GASFLOW Calculations

7.17.3.1. GASFLOW Input Model. The calculations were performed with GASFLOW, Version 2.1.0.13. No local updates or modifications were made to the code.

7.17.3.2. GASFLOW Results. The problem must be run for a sufficient amount of time for steady-state conditions to be attained. For the problem specified, approximately 12.5 h of simulated time were needed to attain steady state.

The code calculates the heat transfer through the wall to range from 3.2943E+11 ergs/s to 3.3361E+11 ergs/s, which is in very good agreement with the analytical solution given above in Section 1.17.2.2.

7.17.4. Conclusions and Recommendations

GASFLOW, Version 2.1.0.13 predicted the analytical solution, as required by the success metric.

7.17.4.1. Input File Listing.

Heat transfer test problem thin wall test.

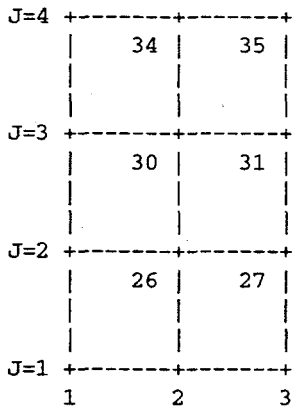
TSA6 jws

GASFLOW V1.0

NOTES:

```
$Source: /home/inrrisc4/jspore/gasflow/gf2/input/RCS/ht_1.ingf,v $  
$Date: 1996/12/19 09:00:12 $
```

```
* 20 JAN 95  
* 1 3D block  
* air  
* BLOCK #1  
 2000 x 3000 x 1000 cm  
 2 x 3 x 1 = 6 real cells m221 = 26  
 4 x 5 x 3 = 60 total cells mrrr = 35  
* PBC across the north boundary.  
* VBC across the south boundary.  
* Wall at i = 2, flow of different temperatures on each side  
of the wall.
```



NETWORK INPUT

```
$innet  
; cpnt = 300.0, 50.0, 50.0,  
; 700.0, 50.0, 50.0,  
; ductdef = 100.0, 100.0, 100.0, 100.0, 100.0, 100.0,  
; 1, 2, 4, 1.0, 0.0, 0.0,  
; netopt = 2,  
; kopt1d3d = 1,  
; nwcx = 4, 4, 1, 2, 1, 2, 1, 1,  
; iwshear = 0,  
$end
```

BASIC INPUT

```
$xput  
pbc(1,1) = 1, 3, 5, 5, 1, 2, 1, 0.00, 1.e99,
```

```

vvalue = 300.0,-500.0,
vbc(1,1) = 1, 3, 1, 1, 1, 2, 1, 1, 0.00, 1.e99,

autot = 1.0, cyl = 0.0, omg = 58.0 ,
delt0 = 00.01000 ,
deltmin = 1.000e-08,
deltmax = 1.000e-00,
epsi0 = 1.000e-08,
epsimax = 1.000e-08,
epsimin = 1.000e-08,
gz = -000.0,
iobpl = 0,
itdowndt = 20,
itupdt = 25,
itmax = 100,
lpr = 1,
maxcyc = 60000,
ittyfreq = 100,
nu = 0.15 ,
pltdt = 4000.00,
prtdt = 5000.00,
twfin = 56000.00,
tddt = 4000.00,
velmx = 1.5,
ibw = 1,
ibe = 1,
ibs = 1,
ibn = 5,
ibb = 1,
ibt = 1,

mat = 'air',

gasdef(1,1) = 1 , 'im1', 1 , 'jml', 1 , 'kml', 1 , ; I.C.
1.0000000e6, 300.0, 1, 0., 0.,
'air', 1.00000,

gasdef(1,2) = 1 , 'im1', 4 , 5, 1 , 'kml', 1 , ; North B.C.
1.0000000e6, 300.0, 1, 0., 99999.,
'air', 1.00000,

gasdef(1,3) = 1 , 2, 0 , 1, 1 , 'kml', 1 , ; SW B.C.
1.0000000e6, 350.0, 1, 0., 99999.,
'air', 1.00000,

gasdef(1,4) = 2 , 3, 0 , 1, 1 , 'kml', 1 , ; SE B.C.
1.0000000e6, 300.0, 1, 0., 99999.,
'air', 1.00000,

walls = 2, 2, 1, 4, 1, 2, 1, 1,

```

\$end

M E S H

```

$meshgn
iblock = 1,
xgrid = 0.0, 1000.0, 2000.0,
ygrid = 0.0, 1000.0, 2000.0, 3000.0,
zgrid = 0.0, 1000.0,

```

```
$end
$meshgn
$end
```

G R A P H I C S

```
$grafic
pnt(1, 1) = 1, 1, 2, 1,
              2, 'jml', 2, 1,
              1, 2, 2, 1,
              2, 2, 2, 1,
              2, 2, 2, 1, ;
              3, 2, 2, 1, ;

p1d = 3, 4, 'vn', 0,
      3, 4, 'pn', 0,
      5, 6, 'vn', 0, ;
      5, 6, 'pn', 0, ;

v2d = 1, 2, 1,

thdt = 1.0 ,
thp(1,1) = 2, 2, 2, 1, 'pn', 0,
              2, 2, 2, 1, 'vn', 0,
              2, 2, 2, 1, 'rn', 0,
              2, 2, 2, 1, 'tk', 0,

htthp = 2, 4, 2, 1, 'wall', 'east',
        2, 3, 2, 1, 'wall', 'east',
        2, 2, 2, 1, 'wall', 'east',
        3, 4, 2, 1, 'wall', 'west',
        3, 3, 2, 1, 'wall', 'west',
        3, 2, 2, 1, 'wall', 'west',

ht1dp = 2, 4, 2, 1, 'wall', 'east',
        2, 3, 2, 1, 'wall', 'east',
        2, 2, 2, 1, 'wall', 'east',
        3, 4, 2, 1, 'wall', 'west',
        3, 3, 2, 1, 'wall', 'west',
        3, 2, 2, 1, 'wall', 'west',
```

```
$end
```

P A R T I C L E S

```
$parts
$end
$rheat

ihtflag = 1,
nhtewall = 4,
tslab0 = 325.0,
tsink0 = 325.0,
twall0 = 325.0,
walldef(1,1) = 2, 4.0,
```

slabthk = 3.,

\$end
\$special
\$end
\$specialp
\$end

7.18. Problem 15: Pressure-Volume Work Term 1: Equilibrium Case

7.18.1. Summary

Purpose

To validate the pressure-volume work term in the GASFLOW energy equation.

Success Matrix

The GASFLOW-calculated values for the temperature as a function of time will be similar to the analytical solution, since GASFLOW does not use a condensation rate model consistent with the analytical solution. The final state will agree with the analytical solution.

Problem Description

A single-cell, closed-box model in which the vapor condenses out of a mixture of water vapor and air.

Relationship to Code Models and Methods

See Table 7-1.

Relationship to PIRT Phenomena

N/A.

Code Version and Modifications

GASFLOW 2.1.0.13, with no modifications.

Hardware and Operating System

Sun Ultra 2/200, Sun Microsystems Inc., Sun OS 5.5.1.

Compiler, Version, and Optimization Level

Edinburgh Portable Compilers' Fortran 90 Compiler, Version 1.5.1.6, Opt=O3.

Runtime Statistics: Total Run Time, Grind Time

The total problem used 84.3 s of CPU time for an average of 8435.0 ms/cell/cycle.

Results and Conclusions

GASFLOW and the analytical solution are in excellent agreement in terms of the final state. The transient behavior and the analytical solution are similar, but different due to the differences in the condensation models between the analytical solution and the GASFLOW solution.

7.18.2. Problem Description and Solution

7.18.2.1. Problem Description. A closed box (10.0 cm on each side) modeled with a single GASFLOW cell contains a mixture of water vapor and air at 1.0186×10^6 dynes/cm² pressure at a temperature of 373.15 K. The mixture is stagnant, and there is no flow

through the box. On a mole basis, the mixture is composed of 50% water vapor and 50% air. The walls of the box are maintained at 200 K. The water vapor condenses onto the cold walls, and a special input flag prevents heat transfer from the bulk mixture to the walls.

7.18.2.2. Equations and Analytical Solution. Because the box is closed, only the mass and energy equations are needed in the analysis. The mass conservation equation for the water vapor is

$$\frac{d}{dt}m_{h2o} = -km_{h2o}, \quad (7-46)$$

where k is a time constant that determines the rate of change of vapor to liquid. The solution of Equation (7-46) for the mass of water vapor as a function of time is

$$m_{h2o}(t) = (m_{h2o}^0)e^{-kt}, \quad (7-47)$$

and the sum of the air plus water vapor mass is

$$m = m_{air} + m_{h2o}(t), \quad (7-48)$$

The energy equation reduces to

$$\frac{dT}{dt} + \frac{km_{h2o}(t)R_{h2o}}{m_{h2o}(t)C_{v,h2o} + m_{air}C_{v,air}} T = 0 \quad (7-49)$$

The solution of Equation (7-49) is

$$T = T_0 e^{-\tau t} \quad (7-50)$$

where

$$\tau = \frac{1}{ak} [kt - \ln(a + be^{kt})] + \frac{1}{ak} \ln(a + b), \quad (7-51)$$

where

$$a = \frac{C_{v,h2o}}{kR_{h2o}} \quad (7-52)$$

and

$$b = \frac{m_{air} C_{v,air}}{k(m^0_{h2o}) R_{h2o}} \quad (7-53)$$

The numerical values are

$$k = 0.138629 \text{ 1/s},$$

$$R_{h2o} = 0.46152,$$

$$C_{v,h2o} = 1.4108,$$

$$C_{v,air} = 0.716802,$$

and given the mole fractions, total pressure, and the temperature for the problem, the mass of air and the initial mass of water vapor are

$$m_{air} = 0.47556216 \text{ g and}$$

$$m^0_{h2o} = 0.29574483 \text{ g.}$$

The solutions for the water-vapor mass and the temperature give the pressure as a function of time as

$$p(t) = (N_{air0} + \frac{m_{h2o}(t)}{Mm_{h2o}}) * R_c * T(t) / V \quad (7-54)$$

where R_c is the universal gas constant and N_{air} is the number of moles of air in the mixture.

7.18.2.3. Analytical Acceptance Parameters and Values. GASFLOW should approximately predict the time dependence of the mass of Equation (7-48), the temperature of Equation (7-50), and the pressure of Equation (7-54), since the analytical model condensation rate is not consistent with the condensation rate models in GASFLOW. However, the final state predicted by the analytical model and GASFLOW must be the same.

7.18.3. GASFLOW Calculations

7.18.3.1. GASFLOW Input Model. The calculations were performed with GASFLOW, Version 2.1.0.13. No local updates or modifications were made to the code. A single cell with no flow was used in the calculation.

7.18.3.2. GASFLOW Results. The analytical solution of Equation (7-50) for the temperature as a function of time and the GASFLOW results is shown in Figure 7-15. The total mass of Equation (7-48) and the pressure of Equation (7-54) are shown in Figures 1-16 and 7-17, respectively.

7.18.4. Conclusions and Recommendations

The GASFLOW results are in excellent agreement with the analytical solution in terms of the final state, as required by the success metric. Due to differences in the condensation models between GASFLOW and analytical solution the transient behavior differences are expected.

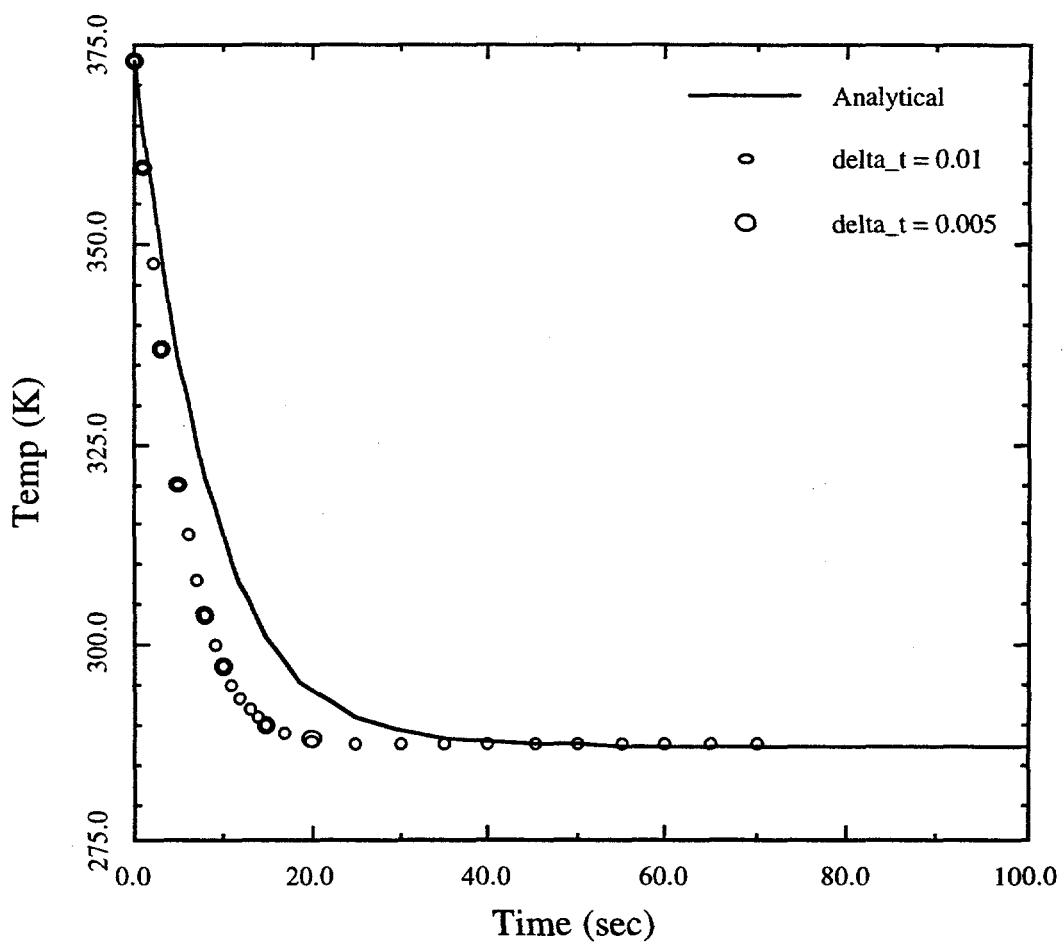


Fig. 7-15. Temperature as a function of time

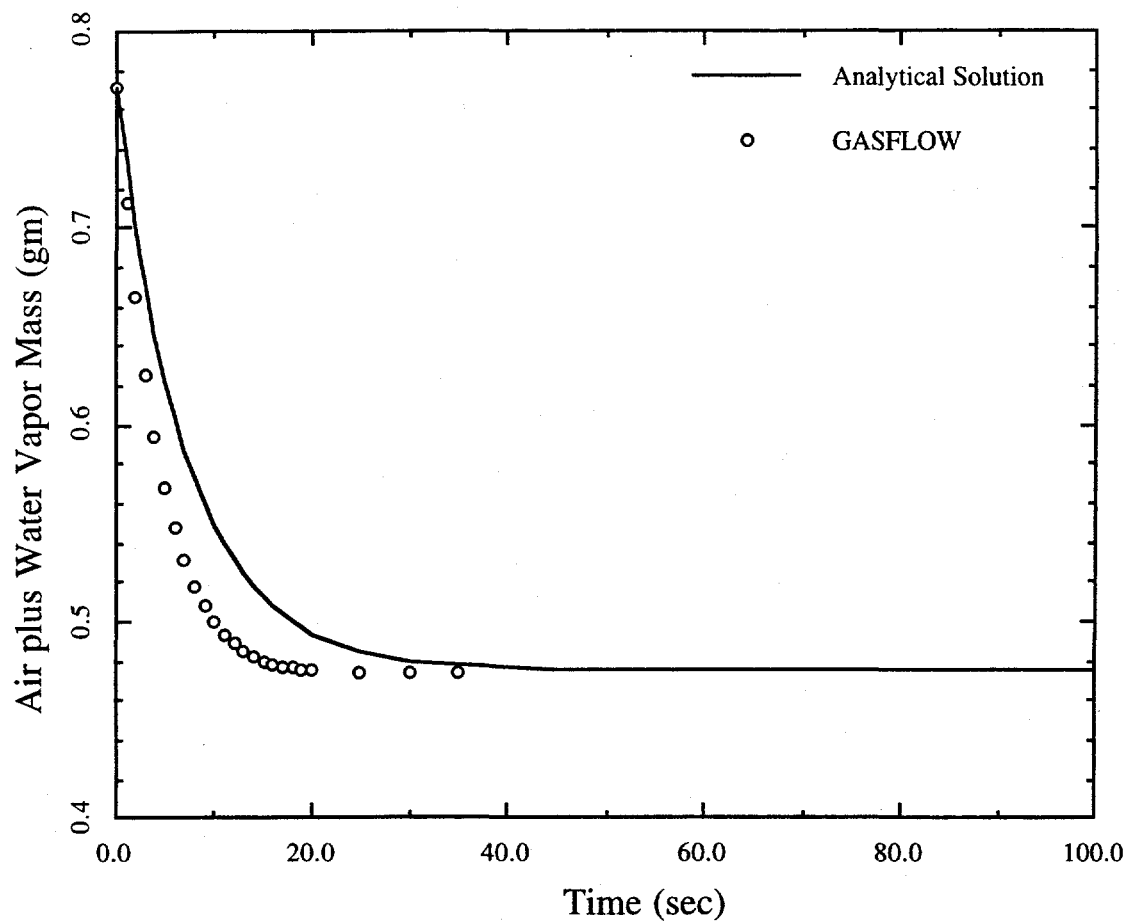


Fig. 7-16. Total mass as a function of time

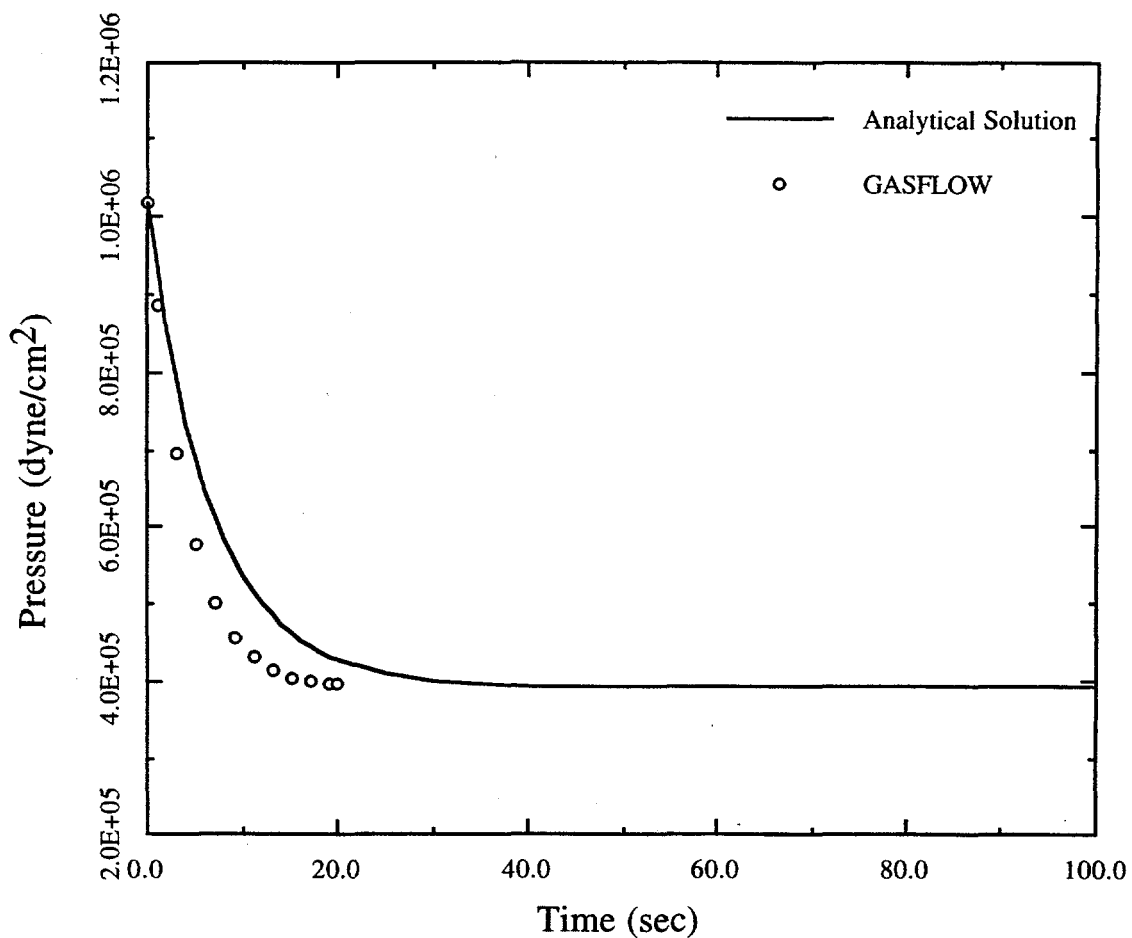


Fig. 7-17. Pressure as a function of time

7.18.4.1. Input File Listing.

Condensation on Sink (11/29/96)

FZK jtravis

GASFLOW

NOTES: Single cell problem used to verify the pressure-volume work term when condensation occurs on cold structures, or vaporization occurs from liquid film.

Assumptions: No heat transfer to structures
No bulk phase change

```

$innet
$end
$xput

cyl = 0,
iburn = 0,
idiffmom = 0,
idiffme = 0,
ieopt = 1,

```

```

trange = 'low',
icopt = 0,
itopt = 3,

; nu = 0.150 ,
; prandtl = 0.70,
; schmidt = 0.25,

tmodel = 'none',

autot = 0.0,
delt0 = 00.010,
deltmin = 1.000e-07,
deltmax = 1.000e-02,

epsi0 = 1.000e-05,
epsimax = 1.000e-05,
epsimin = 1.000e-05,

; gz = -980.0,

itdowndt = 100,
itupdt = 100,
itmax = 500,

lpr = 1,
ittyfreq = 100,
pltdt = 1.000,
prtddt = 100.0,
tddt = 1000.0,
velmx = 3.0,

maxcyc = 900001,
twfin = 100.000,

mat = 'h2o', 'air',

gasdef(1,1) = 1, 02, 1, 02, 1, 02, 1,
              1.018600e6, 373.15, 2, 0., 0.,
              'h2o', 0.5000, 'air', 0.5000,

```

\$end

M E S H

\$meshgn

```

iblock = 1,
nkx=1,
  xl(1)= 0.0, xc(1) = 0.000 , nxl(1)= 0, nxr(1)=01 , dxmn(1)= 9999.,
  xl(2)= 010.0,
nky=1,
  yl(1)= 0., yc(1) = 0.000 , nyl(1)= 0, nyx(1)=01 , dymn(1)= 9999.,
  yl(2)= 010.0,
nkz=1,
  zl(1)=0.0000, xc(1) = 0.0000, nzl(1)= 0, nzr(1)= 01, dzmn(1)= 9999.,
  zl(2)= 10.,

```

\$end

G R A P H I C S

\$grafic

```
thdt = 0.10,  
  
thp = 02, 02, 2, 1, 'pn', 0,  
      02, 02, 2, 1, 'tk', 0,  
      02, 02, 2, 1, 'vf', 'h2o',  
      02, 02, 2, 1, 'vf', 'air',
```

\$end

P A R T I C L E S

\$parts

\$end

H E A T T R A N S F E R & C O N D E N S A T I O N

\$rheat

```
ihtflag = 1,  
  
matbdy = 0,  
  
cbulkrlx = 0.0,  
iliq = 0,  
  
iwh2o = 0,  
iconv = 0,  
  
nhtesink = 20,  
  
sinkdef = 1,2, 1,2, 1,2, 1, 3, 100.0, 0.5, 200.0, 200.0,  
tsink0=200.0,  
$end
```

S P E C I A L

\$special

\$end

8.0. GASFLOW COMPARISON WITH DATA

8.1. Assessment Objectives

Assessment using separate-effects test data provides an opportunity to focus on the few physical phenomena that dominate these kinds of tests. The models and methods in GASFLOW should map one to one with the dominant physical phenomena present in these data. Some of the separate-effects experiments that have been used in the assessment of GASFLOW are discussed in this section.

8.2. Assessment Problems

The separate-effects test data reported in this section that have been used for assessment of GASFLOW include those from the

Bureau of Mines (BOM) spherical combustion chamber,
SNL Flame Acceleration Measurement and Experiments (FLAME) Facility
experiment,
GX6 experiment,
HYJET experiment, and
T31.5 experiment.

Each of these experiments and associated GASFLOW calculations is discussed in the following paragraphs.

8.2.1. The BOM Spherical Combustion Chamber

At the request of the Department of Energy and Westinghouse Hanford Company, the BOM has investigated the flammability of hydrogen, ammonia, nitrous oxide, and air mixtures. The tests were performed in a spherical chamber under quiescent and turbulent conditions.

This section describes combustion calculations using GASFLOW and compares the calculated pressure ratios with the experiments mentioned above. GASFLOW is a finite-volume computer code that solves the transient, 3D, compressible fluid, Navier-Stokes equations with multiple species coupled with finite-rate chemical kinetics. The computational results show good agreement with the experimental data and confirm that GASFLOW is a valuable tool for evaluating the above combustion process.

8.2.1.1. Comparison of Computed Results. GASFLOW was used to calculate predicted results for the BOM experiments. Mixture compositions considered were hydrogen concentrations from 5 to 40 vol % diluted in air, 1:1 ratios of hydrogen and nitrous oxide in air, and very low hydrogen and nitrous oxide concentrations in air with 1 and 2% ammonia added. The initial conditions were set to the ambient temperature and pressure. The spherical chamber shown in Figure 8-1 was considered to be adiabatic on the time scales of complete combustion. The computational volume consists of 3D cells in Cartesian coordinates and is enclosed within rigid, free-slip walls, which means that the gradient of the tangential velocity components on the boundaries is zero. In

these calculations, the internal energy was approximated with fourth-order fits and the specific constant volume heat capacity was computed with coefficients from Gordon and McBride.⁸⁻¹ The transport properties were approximated with fourth-order fits.

In Figure 8-2, the pressure ratio (the ratio of the final to the initial pressure) is shown as a function of the hydrogen concentration ranging from 5 to 40 vol % diluted in air. The line represents the GASFLOW results, whereas the solid diamonds show the experimental data from Ref. 8-2.

The calculated results agree well with experimental data and show the correct behavior for both fuel-lean and fuel-rich mixtures, where the maximum pressure ratio is reached for the stoichiometric mixture (29.6% hydrogen). For very low hydrogen concentrations (5 to 7%), the results indicate almost no pressure rise. This reflects the lower flammability limits (LFLs) for quiescent mixtures observed in the experiments. There is a rapid increase in the pressure ratio at ~8% hydrogen, where the mixture is rich enough to allow downward flame propagation and nearly complete combustion of the available hydrogen.

A second series of experiments, which is presented in Figure 8-3, was carried out using equal volume percentages of hydrogen and nitrous oxide mixtures diluted with air. The GASFLOW-calculated results are shown to be in good agreement with the experimental data. Near the LFL, the calculated results are shown to be higher than those observed. Theoretically determining the exact LFL is an extremely difficult, if not impossible, task. We chose to be conservative in our modeling approach near the LFL. With the one-step chemical kinetics equation model discussed above, we allow combustion reactions to occur, when in fact the observed data indicate that combustion does not occur.

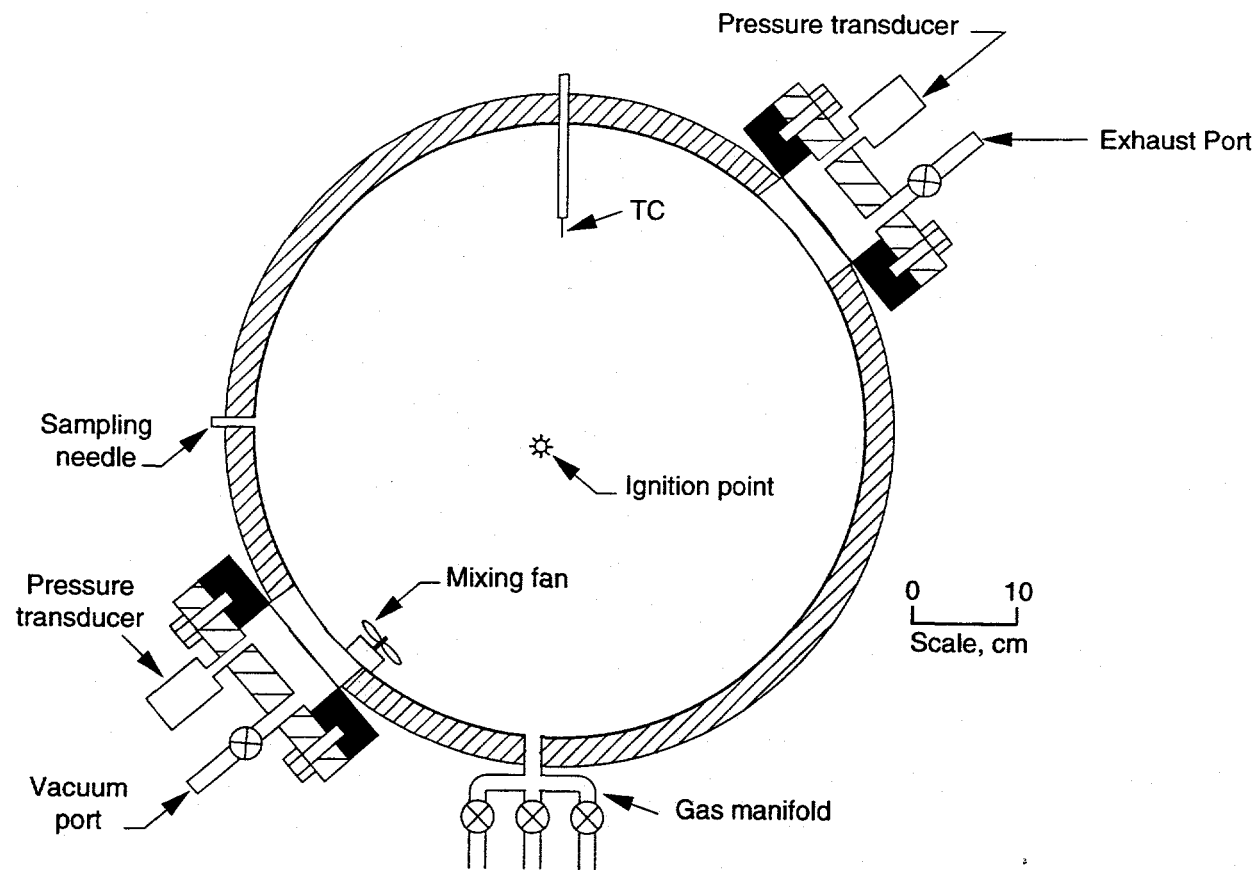


Fig. 8-1. 120-L flammability test sphere

Hydrogen - Air (quiescent, spark)

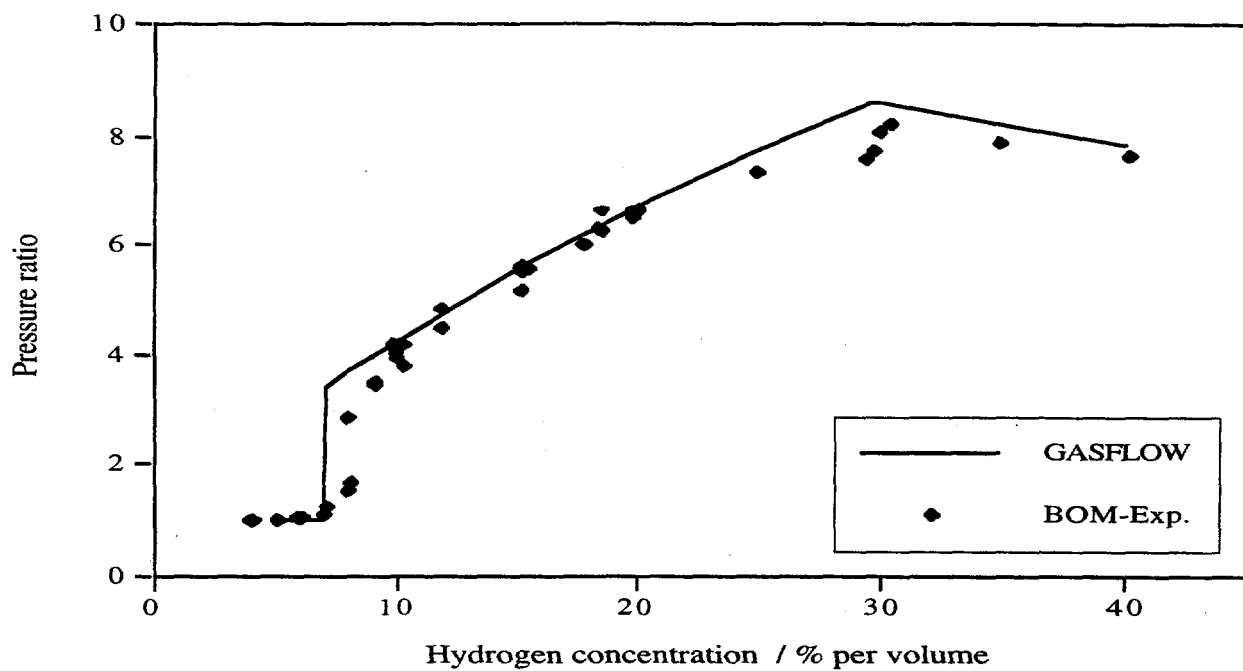


Fig. 8-2. Pressure ratio vs hydrogen concentration

$\text{H}_2 - \text{N}_2\text{O} - \text{Air}$ (quiescent, spark)

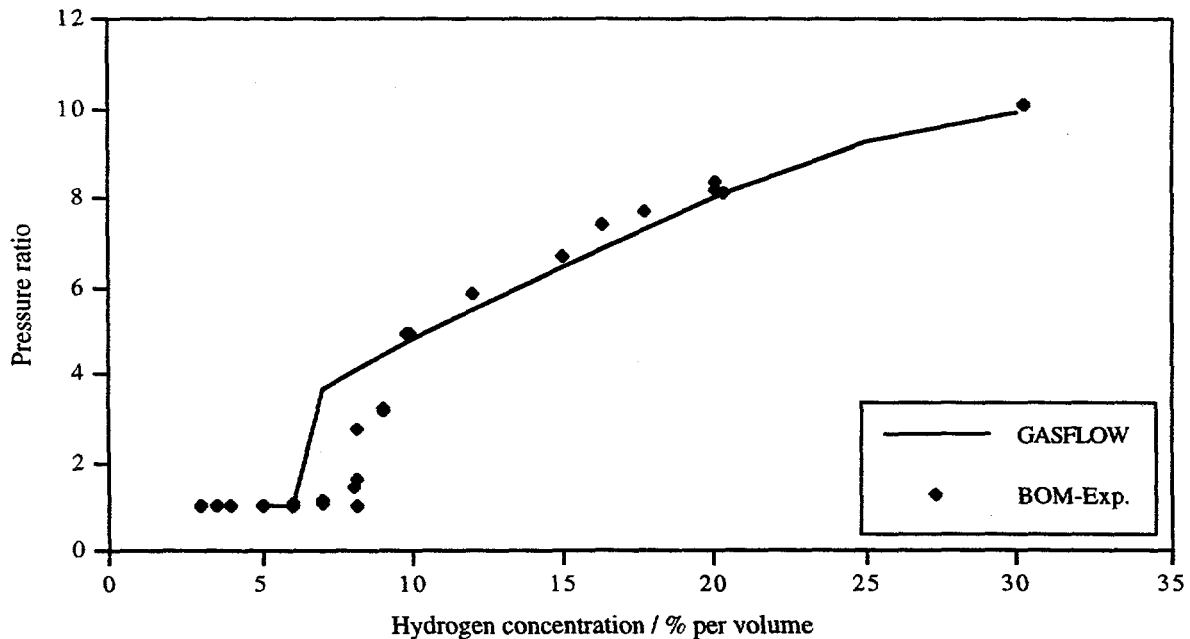


Fig. 8-3. Pressure ratio vs hydrogen concentration for quiescent mixtures of 1:1 ratios of hydrogen/nitrous oxide in air

In a third series of experiments, which is presented in Figure 8-4, we show the same equal volume percentages of hydrogen and nitrous oxide mixed with air, as seen in Figure 8-3, as well as the additional experiments and calculations of adding 1 and 2% ammonia. Again, GASFLOW's calculated results are shown to be in good agreement with the experimental data above the LFL. Near the LFL, the calculated results once again are shown to be higher than those observed. However, the calculations are conservative near the combustion LFL. When small amounts of ammonia are added to the hydrogen/nitrous oxide/air mixtures, the experiments indicated that the LFL of downward propagation is lowered. The calculation results follow this tendency.

In Figures 8-5 and 8-6, we present a comparison between GASFLOW and an experiment involving 10% hydrogen and 10% nitrous oxide in air. The actual pressure trace or time history for the experiment and calculated pressure history is shown in the first of these figures, whereas in the second figure, the time derivative of the pressure behavior is given. From the pressure traces, we note that the rise time from ignition to maximum pressure is longer in the calculation than what was observed in the experiment. The time rate of rise shown in Figure 8-6 indicates that in the early phase of combustion and immediately following ignition, the calculation is delayed in comparison to the experiment, whereas during the terminal phase of combustion, the calculation shows that the time rate of rise is ~20% higher than the observed rise rate. Although there are tradeoffs between the actual pressure rise time and the time rate of pressure rise, it is felt generally that the time rate of pressure rise is the most critical parameter for driving the structural dynamics response to combustion. In this instance, the calculated pressure is conservative because the maximum rate of pressure rise is ~20% higher than that observed.

In a parametric study we changed the activation energies and preexponential coefficients in the Arrhenius equations. We found that the lag in the pressure jump could be reduced but that the comparison of the calculated time rate of pressure change compared with the observed data was in poor agreement.

8.2.1.2. Conclusions. The combustion results computed with GASFLOW are shown overall to agree well with the BOM experimental data. The maximum combustion pressures above the LFL are within 5% of the data. Near the LFL, the approach is conservative, but the correct behavior can be seen. At concentrations lower than the LFL, no combustion occurs. The time rate of pressure rise is found to be in reasonable agreement with the experimental observations.

We conclude that the one-step finite-rate chemical kinetics model we used yields good results but is limited. For more complex problems, we suggest using reduced chemical kinetics mechanisms or a two-step method based on an induction parameter model. Both of these improved models are derived from detailed chemical kinetics mechanisms.

$H_2 - N_2O - Air - NH_3$ (quiescent, spark)

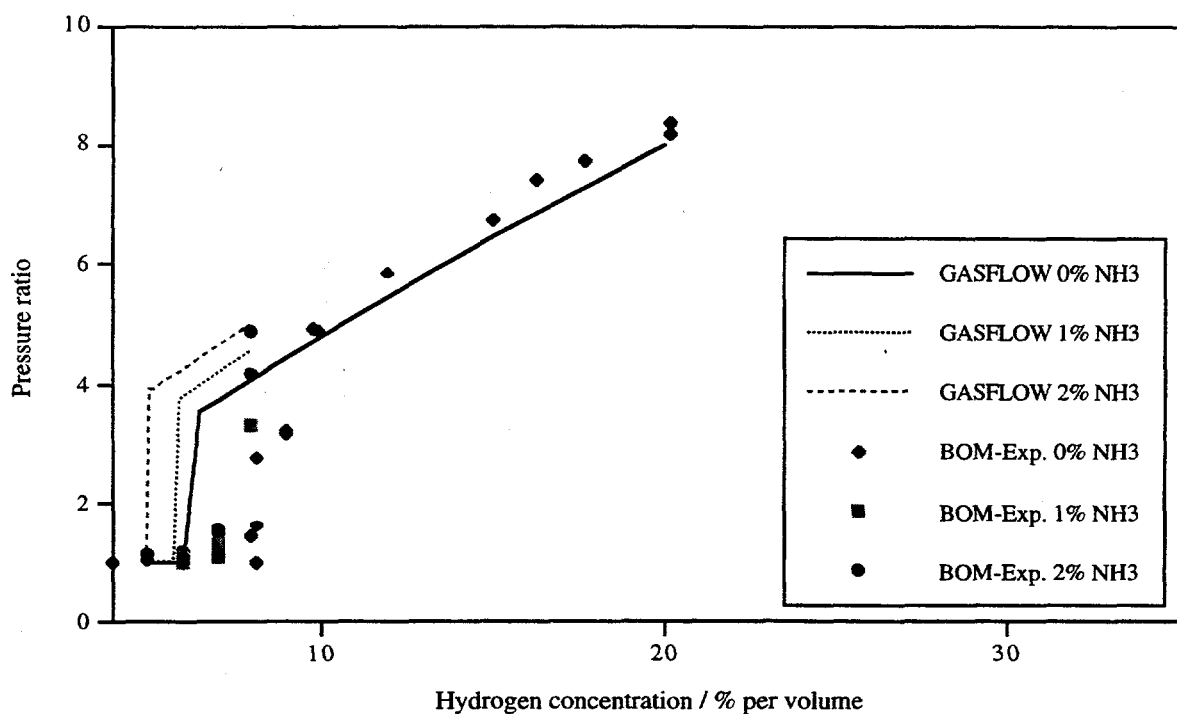


Fig. 8-4. Pressure ratio vs hydrogen concentration for quiescent mixtures of 1:1 ratios of hydrogen/nitrous oxide in air compared with data with 1 and 2% added ammonia

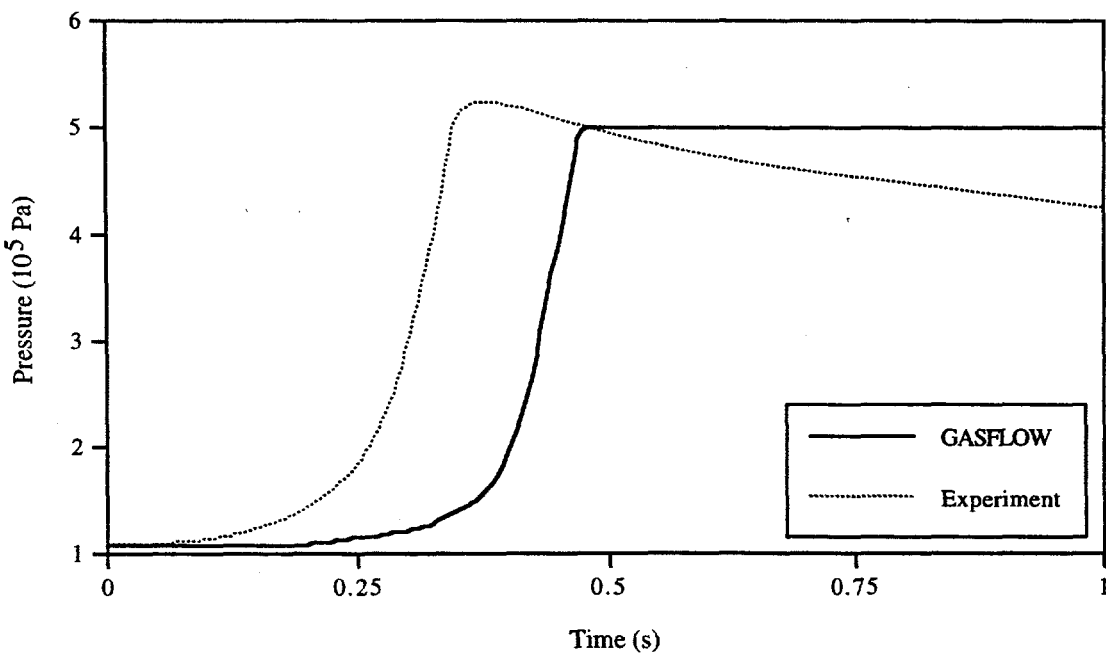


Fig. 8-5. Absolute pressure vs time for 10% quiescent hydrogen/nitrous oxide mixtures in air

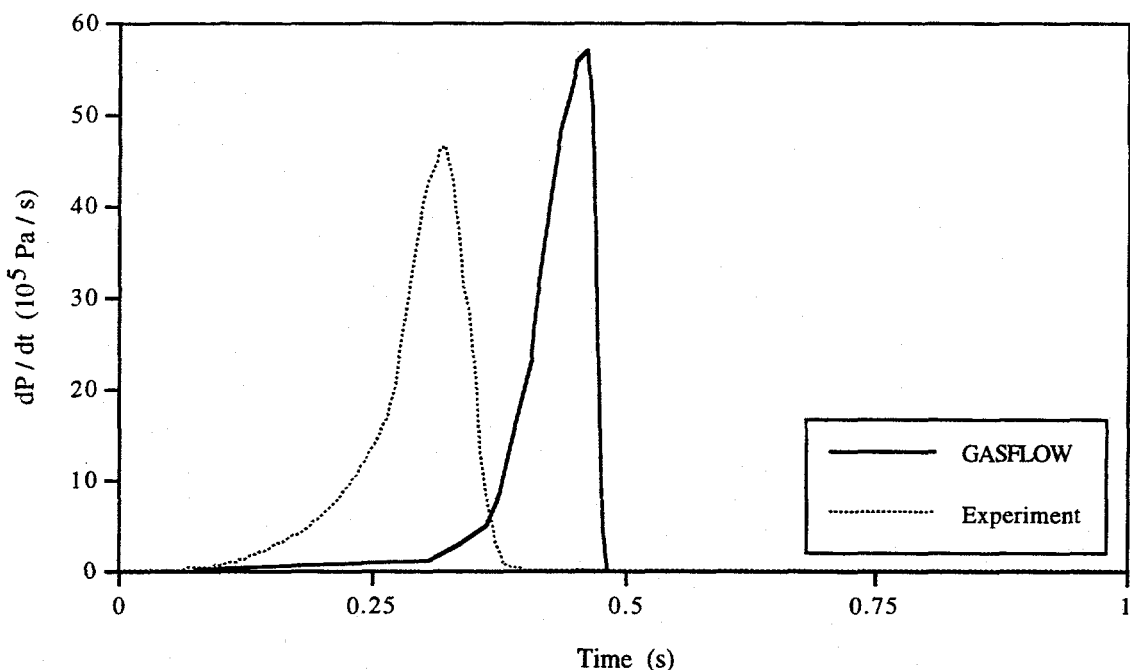


Fig. 8-6. Time rate of pressure change vs time for 10% quiescent hydrogen/nitrous oxide mixtures in air

8.2.2. The SNL FLAME Experiment (FLAME Facility Test Problem)

8.2.2.1. Background. The FLAME Facility (Ref. 8-3) is a large, horizontal, rectangular channel made of heavily reinforced concrete that was designed and built by SNL for the USNRC. The dimensions (1.83 m wide, 2.44 m high, and 30.5 m long, giving a total volume of 136 m³) were selected to be half of the scale of the upper-plenum region of an ice-condenser pressurized-water-reactor (PWR) containment. The upper plenum of the ice-condenser PWR containment is an annular region of rectangular cross sections extending ~350° around the containment. Thus, FLAME differs from the upper plenum because it is straight rather than curved. The main use of the facility was to study flame acceleration and deflagration-to-detonation transition of premixed hydrogen-air compositions.

A diagram of the FLAME channel showing its plan (top, side, and end views) is presented in Figure 8-7, which shows the three ports along the length of the channel through which hydrogen was injected. The direction of hydrogen injection is horizontal, as shown in the top- and end-view diagrams. Plastic bags were attached to one end of channel to take up the volume gained by adding the hydrogen. Expansion of the bags allowed the experimenters to visualize the hydrogen injection process.

In most experiments, hydrogen was injected into the channel until the desired amount was reached. Air-driven mixing fans along the channel walls were used to give a homogeneous mixture of hydrogen and air. The premixed gas at the prescribed

hydrogen concentration then was ignited at one end of the channel to study flame acceleration and detonation behaviors. In one experiment, F-21, the air supply to the mixing fans was cut off because an error occurred in preparing the test. Hydrogen was injected near the bottom into the test chamber until the hydrogen occupied 13% of the entire volume. Thirty minutes after the injection of hydrogen, analysis of gas samples taken at the upper locations indicated a hydrogen volume fraction of 15%, whereas gas samples at the lower locations had a hydrogen volume fraction of 10%, with an uncertainty of ~0.5% in the measurement. The SNL personnel speculated that a hydrogen plume probably developed, and without the aid of mechanical mixing fans, stratification of hydrogen concentration could have developed.

The focus of all SNL FLAME experiments was on flame acceleration and transition from deflagration to detonation. Temperature and pressure were measured during flame propagation. Hydrogen was injected to introduce the correct amount of the gas into the channel before the hydrogen mixture was ignited. In a normal experiment, the hydrogen was well mixed in the air by mixing fans. Therefore, no extensive measurement of hydrogen concentration was made other than an analysis of gas samples taken at a lower and an upper location in the channel before the ignition. Test F-21 was interesting because the hydrogen stratified after the mixing fans failed to operate. It was chosen to assess the GASFLOW code's prediction of hydrogen mixing and the resulting level of stratification as a function of time. However, only two experimental data points are available for comparison with the calculations—the volume fraction of hydrogen at 0.3 m above the channel floor and at 0.3 m below the channel ceiling (or 2.14 m from the channel floor), which were 10% and 15%, respectively, at 30 min after the end of the hydrogen injection.

8.2.2.2. GASFLOW Model of the FLAME Facility. Hydrogen was injected transversely at one side of the channel through three 2.54-cm-diam holes that are widely separated along the length of the channel, as shown in Figure 8-7. To preserve the hydrogen jet momentum and dynamics, we must model a small opening with an area equivalent to a 2.54-cm-diam hole in a computational volume that is 30.5 m long, 2.44 m high, and 1.83 m wide. To optimize computational resources, we modeled only one-sixth of the length of the channel. Symmetry was assumed about a plane cutting through the center of any one of the three injection holes, as well as about a plane halfway between any two adjacent injection ports. These planes of symmetry are shown as dotted lines in the side view of the channel depicted in Figure 8-7, in which the shaded areas indicate the part being modeled. Therefore, the computational volume has a cross section of 1.83 m (width) x 2.44 m (height) and is 5.08 m in the third dimension, which has been reduced by a factor of 6 because of the symmetry assumption.

The 3D computational domain is illustrated in Figure 8-8. In the coordinate system, X represents the vertical direction, Y represents the longitudinal direction, and Z represents the transverse direction. Therefore the X-Z plane represents the cross section of the channel, with hydrogen injected in the Z direction. Figure 8-9 shows the mesh of the X-Z plane, indicating the location where hydrogen is injected. Table 8-1 gives the location of grid lines in all three dimensions. The number of computational cells is 16 in the X direction, 15 in the Y direction, and 10 in the Z direction, giving a total of 2400.

Because many operations in the GASFLOW code have been arranged to take advantage of vectorization on X-Y planes of data, having the most number of cells in the X and Y directions is computationally more efficient.

8.2.2.3. Calculation Results and Comparison with Experiment. The calculation began with the injection phase. First, the computational volume was initialized with stagnant air at 27°C and 1 atm. Hydrogen then was injected as a horizontal jet in the transverse or Z direction ~23 cm from the bottom of the channel at a velocity of 28 m/s and for a duration of 487 s (8.1 min) to obtain an average air-hydrogen mixture with 13% hydrogen by volume. The mixing phase began at 487 s, when the jet was then shut off, and lasted for 1800 s (30 min) until 2287 s, corresponding to the time when gas samples were taken for analysis and ignition occurred. The calculation ended before ignition.

TABLE 8-1 LOCATION OF THE X, Y, AND Z GRIDLINES IN THE GASFLOW MODEL OF THE SNL FLAME FACILITY

Grid Line Number	Position of X or Vertical Grid Line (cm)	Position of Y or Longitudinal Grid Line (cm)	Position of Z or Transverse Grid Line (cm)
1	0.000	0.000	0.00
2	8.001	1.125	18.00
3	14.175	3.375	36.00
4	18.585	6.525	54.00
5	21.735	10.935	72.00
6	23.985	17.109	90.00
7	27.135	25.753	108.00
8	31.545	37.854	126.00
9	37.719	54.795	144.00
10	46.363	78.513	162.00
11	58.464	111.718	182.88
12	75.405	158.206	
13	99.123	222.288	
14	132.328	314.403	
15	169.499	411.202	
16	206.670	508.000	
17	243.840		

In the calculation, the hydrogen jet was injected through a rectangular opening with a cross section of $2.25\text{ cm} \times 1.125\text{ cm}$, which has an area equivalent to half that of the 2.54-cm-diam hydrogen injection port in the experiment. Therefore, the (full) jet Reynolds number is 4.6×10^4 . The automatic timestep-control option of the code was turned on to determine dynamically the timestep size for the calculations. For the injection phase, the timestep was controlled by the Courant limit because of the high injection velocity. We used 297,132 cycles for the 487 s of the injection phase calculation, giving an average timestep size of $1.64 \times 10^{-3}\text{ s}$. For the 1800-s mixing phase calculation, the timestep was largely determined by the diffusion limit, and the total number of cycles was 16,606, giving an average timestep size of 0.108 s.

For this problem, the specified kinematic viscosity was $0.153\text{ cm}^2/\text{s}$. The binary mass diffusivity of hydrogen in air was specified as $0.754\text{ cm}^2/\text{s}$, a value that is estimated from the kinetic theory of gases at low pressures. [The measured mass diffusivity of hydrogen in nitrogen at 20°C and 1 atm is $0.784\text{ cm}^2/\text{s}$ (Ref. 8-4). If air were pure nitrogen, the calculation would underpredict the molecular mixing rate because it would have used a lower mass diffusivity.] Both the viscosity and the mass diffusivity were assumed to be constant throughout the calculations. The algebraic turbulence model was used to account for turbulent mixing. The other two turbulence models, which are more advanced and computationally more intensive, were not used in this problem. These models will be assessed separately with experiments that provide extensive measurement of velocity and calculation. For the algebraic turbulence model, the most important parameter required is the turbulence length scale, which was set to 50 cm in the calculations. The length of this scale was selected to represent the size of the large eddies in the flow, which are responsible for most of the turbulent transport of mass and momentum. As discussed in the following paragraphs, the calculated results were not very sensitive to the magnitude of the chosen turbulent length scale because mixing was achieved largely by molecular diffusion.

Figure 8-10 is the velocity-vector plot in the channel cross section at the injection plane (i.e., the X-Z plane at $Y = 0$) 100 s after the injection begins. Velocity-vector plots at other times during the injection phase basically look the same. Note that because of its buoyancy, the hydrogen jet does not penetrate very far into the channel before it turns upward to the ceiling. The buoyant plume at 100 s also can be visualized by means of contours of hydrogen volume fraction, as shown in Figure 8-11. The injection location and distances in terms of equivalent jet diameters are shown, as well. Figure 8-12 shows the hydrogen contours at 200 s. Note the gradual expansion of the plume. Figures 8-13 and 8-14 show the velocity-vector plot and the hydrogen-volume-fraction contour at 487 s, the instant immediately after the injection ended.

The next set of figures show calculated results in the mixing phase. Figure 8-15 shows the calculated profile of the hydrogen mole fraction as a function of distance from the bottom of the channel at two time instants. At 100 s into the mixing phase (i.e., after the injection has stopped), the minimum hydrogen-volume fraction is ~4% at the bottom and the maximum is ~17% at the top (dotted curve). The level of stratification is gradually decreased by diffusion. At 1800 s (30 min), the minimum volume fraction is 9.15% and the maximum is 15.44% (solid curve). The experimental measurements—10%

at a lower location and 15% at an upper location—compare well with the respective calculated volume fractions of 9.8% and 15.4%. The reported uncertainty in the experimental measurement was 0.5% (in absolute hydrogen volume fraction), which is shown in Figure 8-15. It can be seen that the calculated and experimental results fall within the uncertainty of the measurement.

The calculated profile of the hydrogen volume fraction at 1800 s (dashed curve) with no turbulent diffusion is plotted in Figure 8-15. Because the mixing phase does not involve mechanical mixing (i.e., no stirring action due to fans), results of calculations with and without a turbulent diffusion are roughly the same, as indicated in the figure. However, comparing the solid curve and dashed curves shows that the calculation with turbulent diffusion gives a slightly more uniform hydrogen distribution than the calculation with only molecular diffusion. The turbulence length scale in the turbulence model was varied from 50 to 91 cm in the calculations with negligible differences in the results; therefore, most of the mixing was achieved by the molecular diffusion process.

The calculated vertical profiles of the hydrogen volume fraction presented in Figure 8-16 are taken from a location at the center of the horizontal computational plane. Where the profile is taken exactly does not matter because calculations show that the gas is roughly well mixed horizontally soon into the mixing phase. Figure 8-16 depicts the hydrogen contours at the plane of injection 1800 s into the mixing phase, showing the stratification of the hydrogen concentration vertically. Note that the contour lines are perfectly straight. Similar plots at any other vertical planes show identical results, so the hydrogen distribution on any horizontal plane is uniform at this time. Figure 8-17 shows the time-history plot of the computed hydrogen mole fraction at several locations in the channel. Note that the curves for the two locations at the same height (first of the three indices indicating cell location) merge only a short time into the mixing phase.

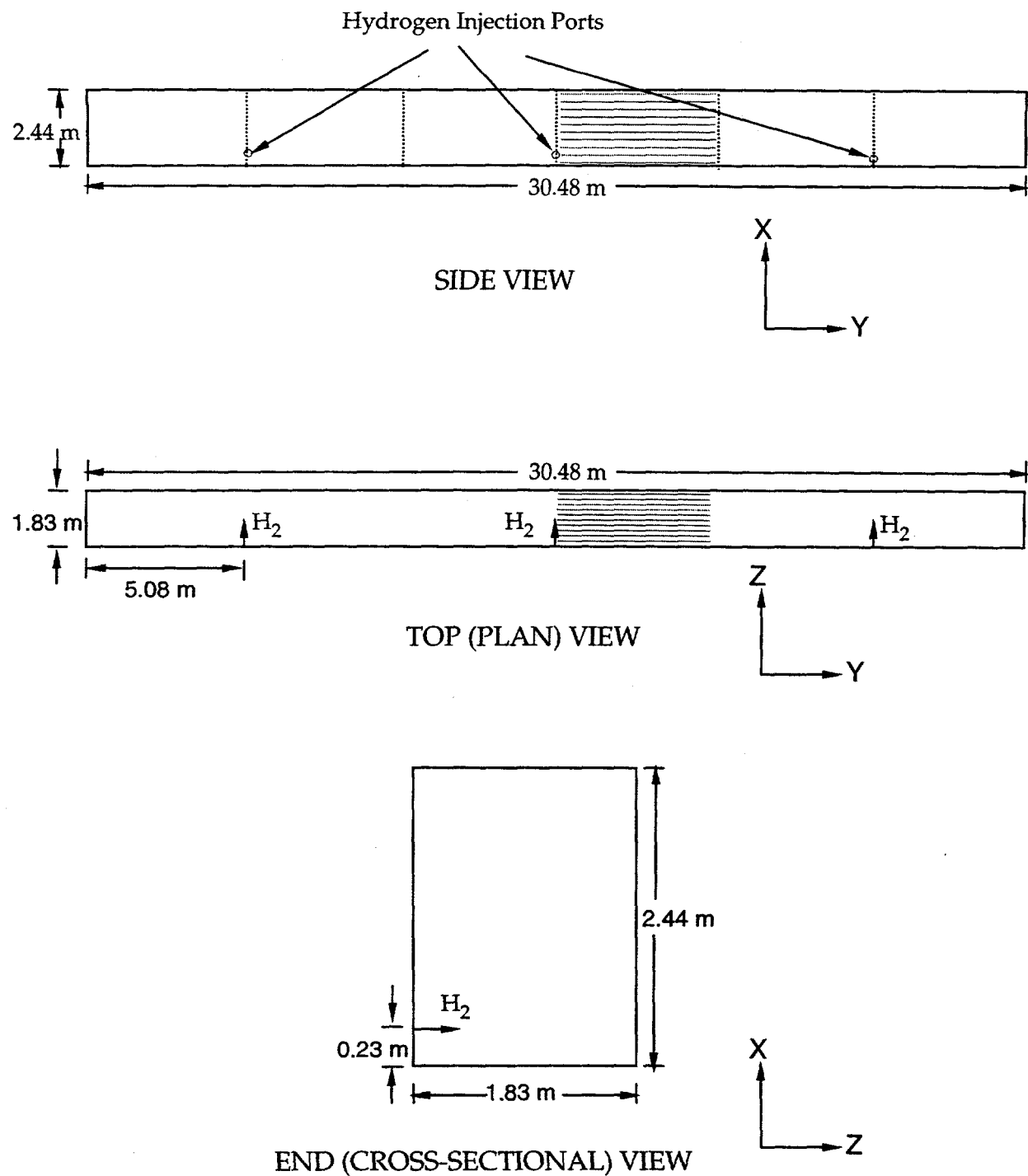


Fig. 8-7. Schematic diagram of the SNL FLAME channel, showing the locations of hydrogen injection. The shaded area indicates the symmetrical region modeled in the computation

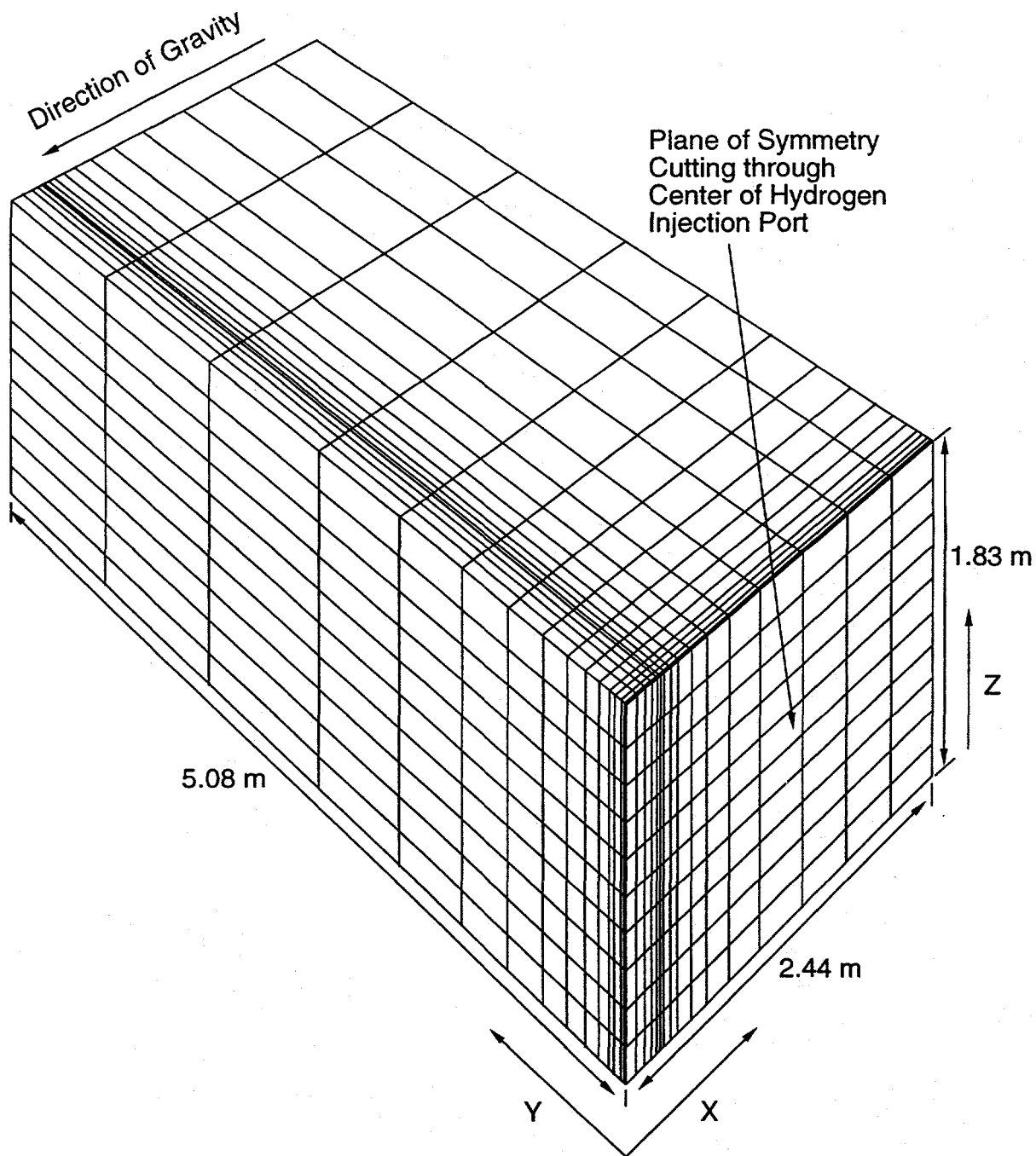


Fig. 8-8. Computational domain for the SNL FLAME simulation calculation, showing the variable mesh

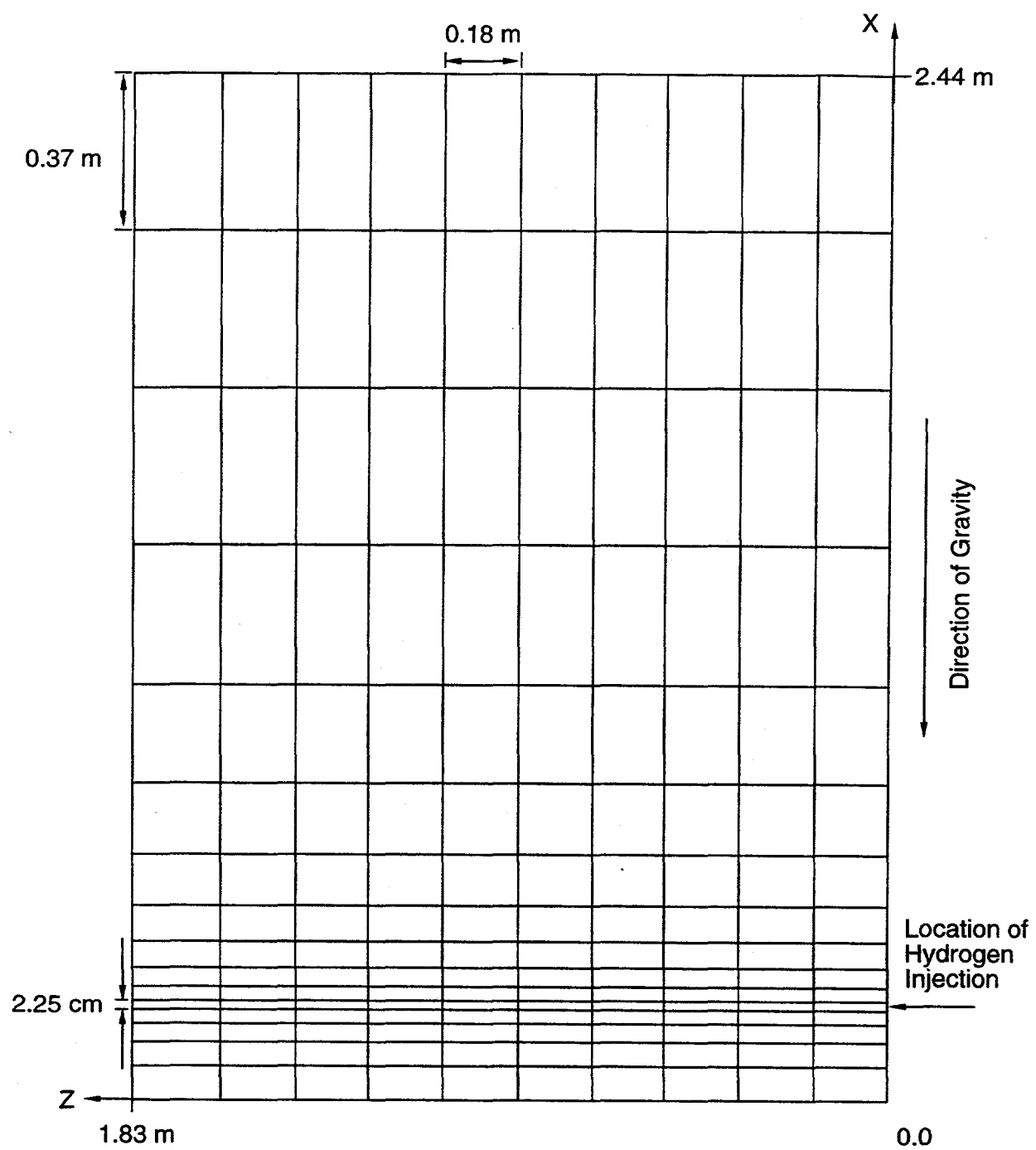


Fig. 8-9. Two-dimensional view of the computational mesh used for the SNL FLAME calculation, showing the location where hydrogen is injected

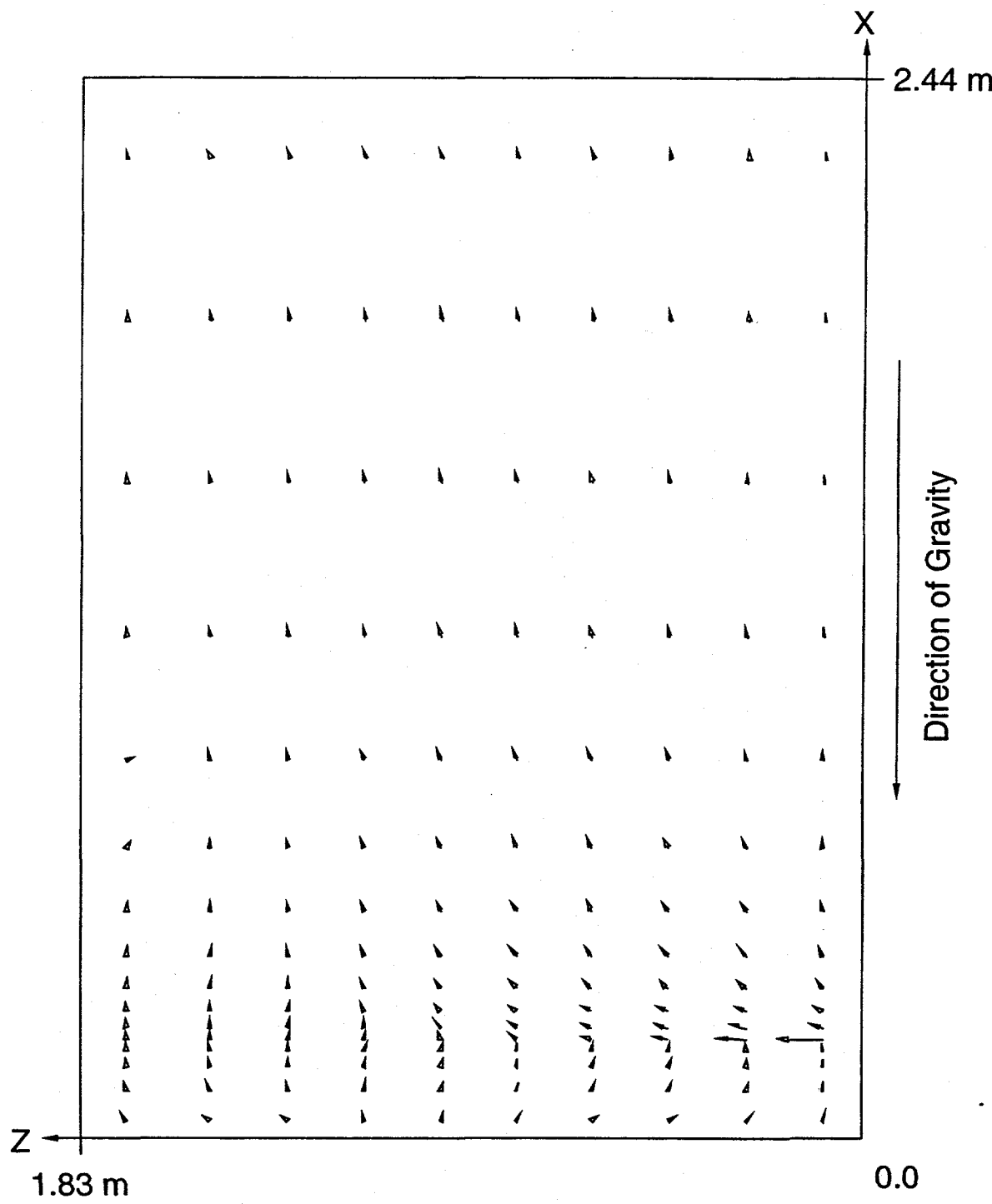


Fig. 8-10. Plot of the calculated velocity vectors in the SNL FLAME experiment at the plane of injection 100 s after initiation of the hydrogen injection. The maximum velocity magnitude (averaged at cell centers) is 22.3 m/s

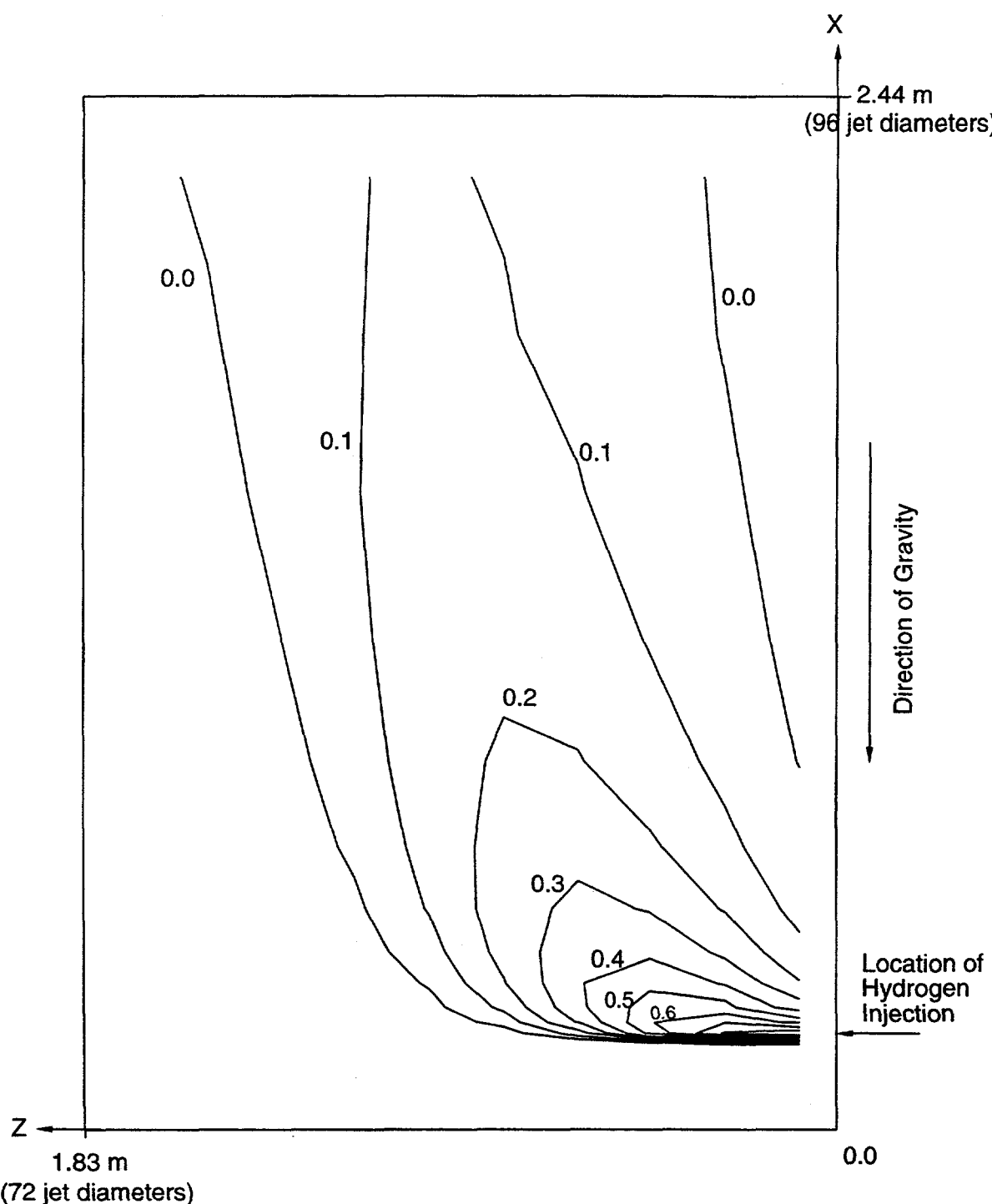


Fig. 8-11. Contour plot of the calculated hydrogen volume fraction in the SNL FLAME experiment at the plane of injection at 100 s after the hydrogen injection begins, showing development of the buoyant plume

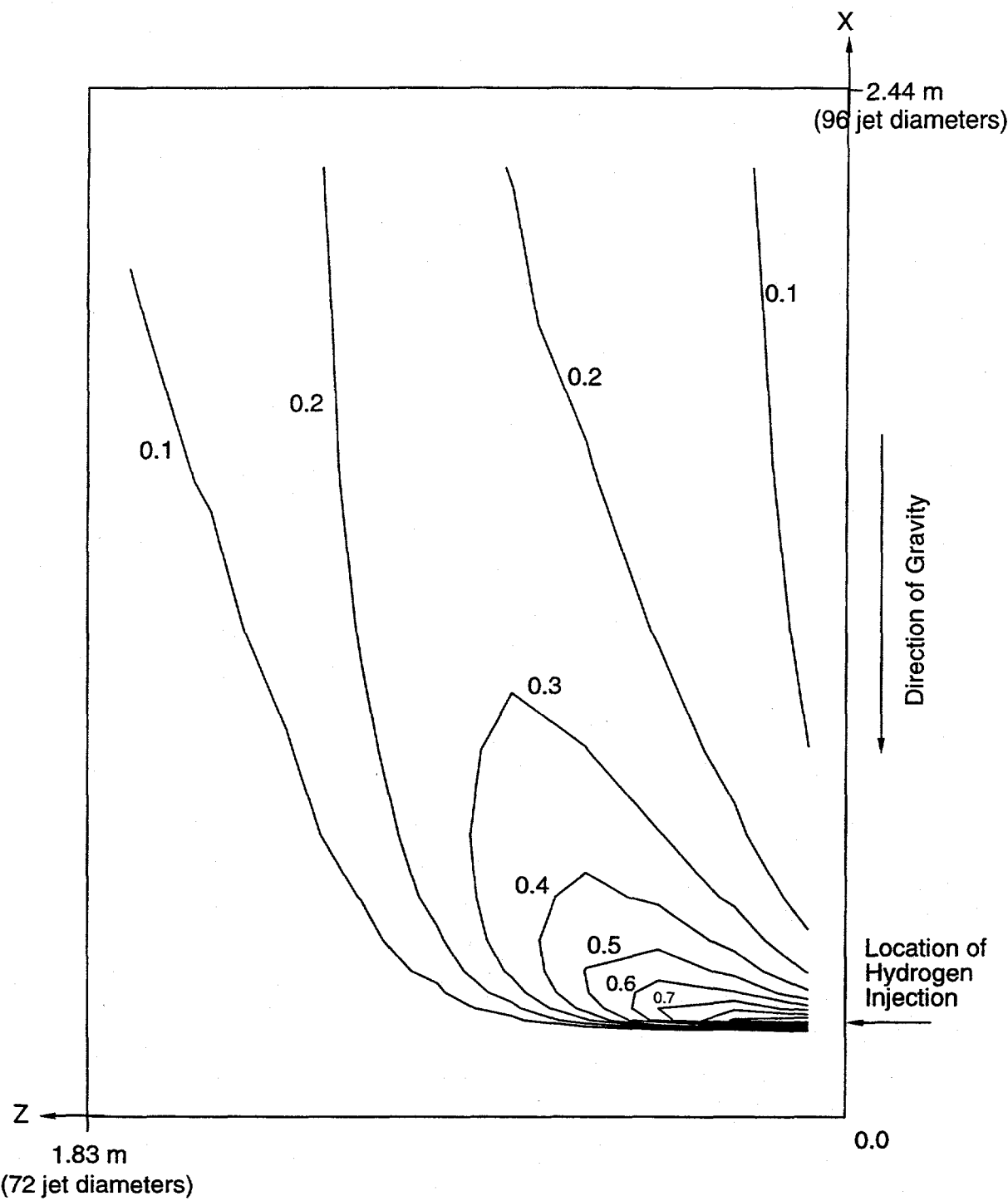


Fig. 8-12. Contour plot of the calculated hydrogen volume fraction in the SNL FLAME experiment at the plane of injection 200 s after the hydrogen injection begins. Note the gradual spreading of the buoyant plume

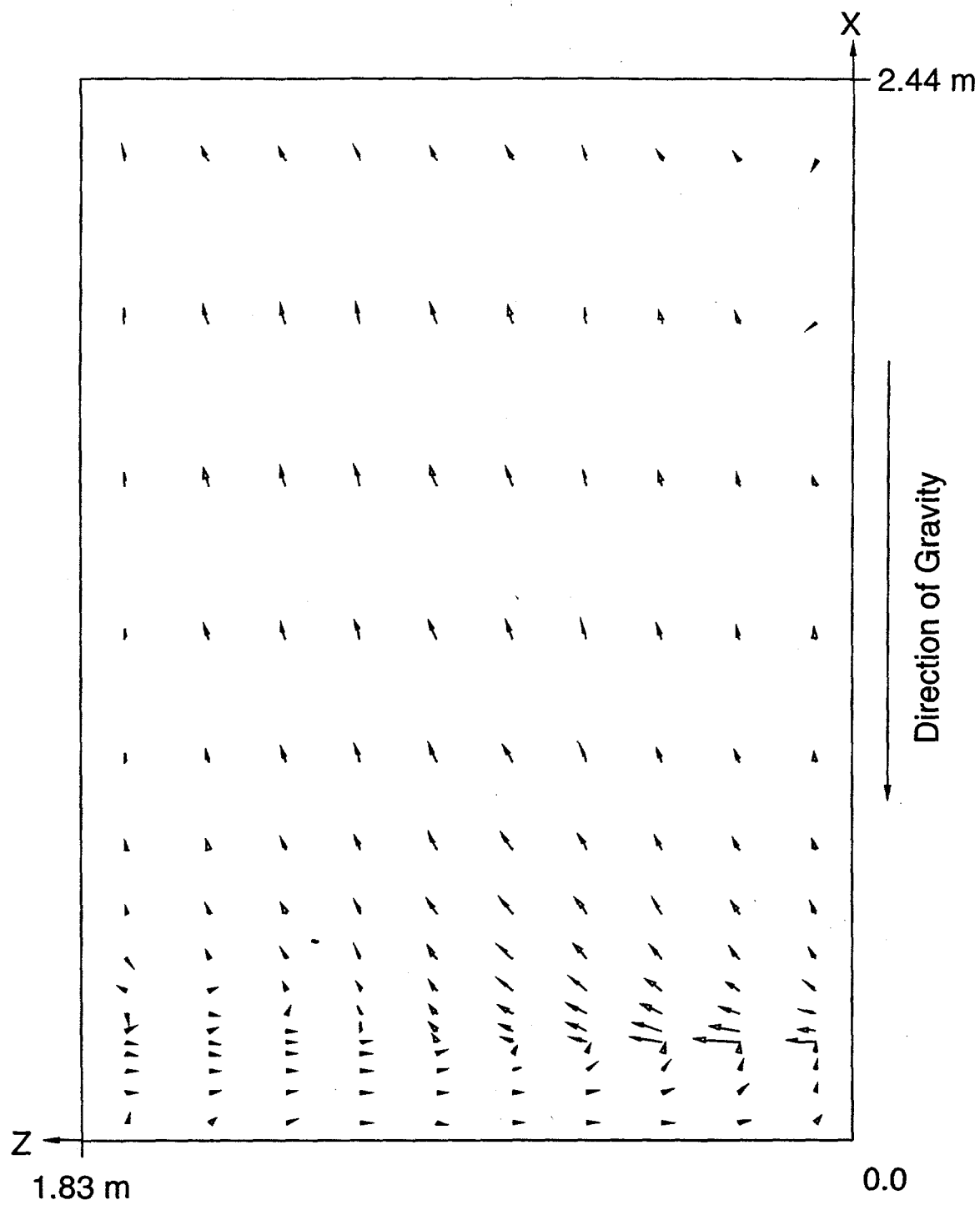


Fig. 8-13. Plot of the computed velocity vectors in the SNL FLAME experiment at the plane of injection at 487 s, which is immediately after the injection stops. The maximum velocity magnitude (averaged at cell centers) is 7.2 m/s

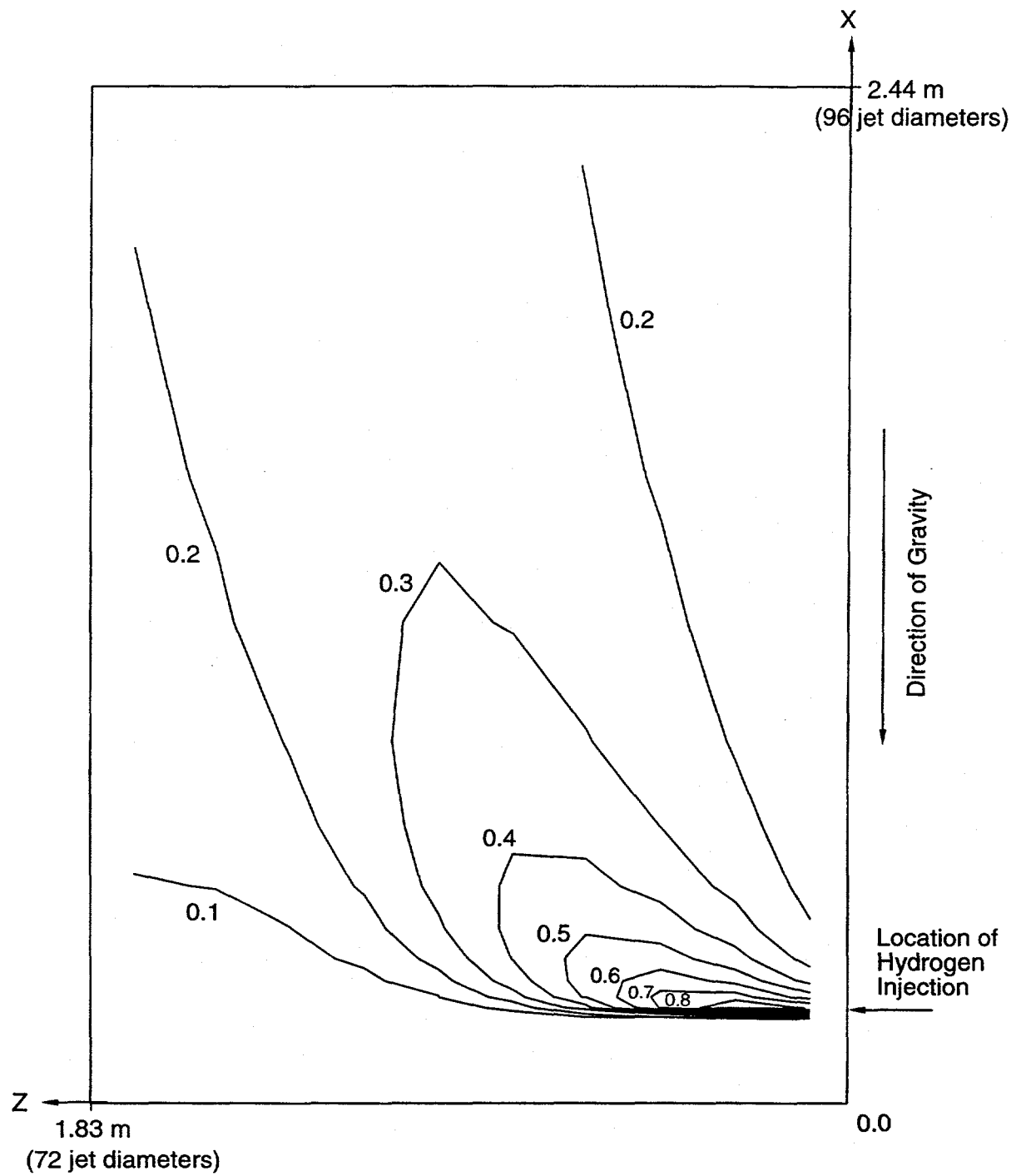


Fig. 8-14. Computed hydrogen volume fraction contours in the SNL FLAME experiment at the plane of injection at 487 s, which is immediately after the injection stops

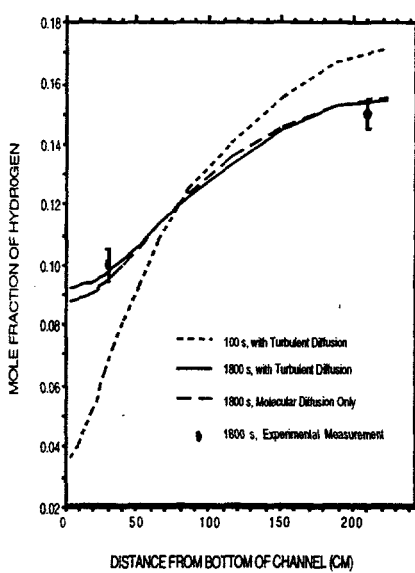


Fig. 8-15. Calculated profile of hydrogen mole fraction in the SNL FLAME experiment as a function of distance from the bottom of the channel at 100 and 1800 s after the injection stops. The two experimental data points (with error bars) at 1800 s also are shown

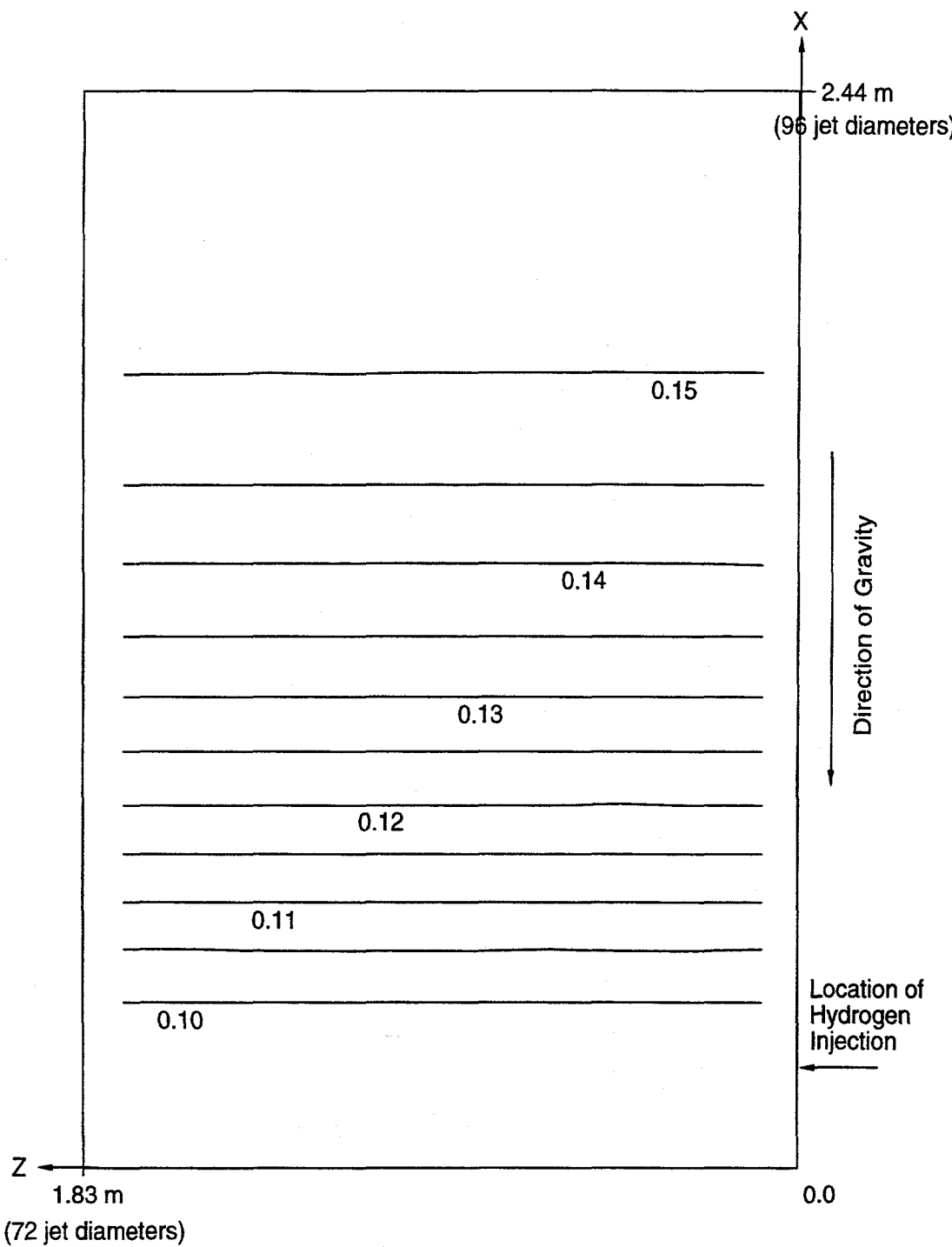


Fig. 8-16. Calculated hydrogen volume fraction contours in the SNL FLAME experiment at the plane of injection 1800 s after the injection stops exhibiting vertical stratification of the hydrogen

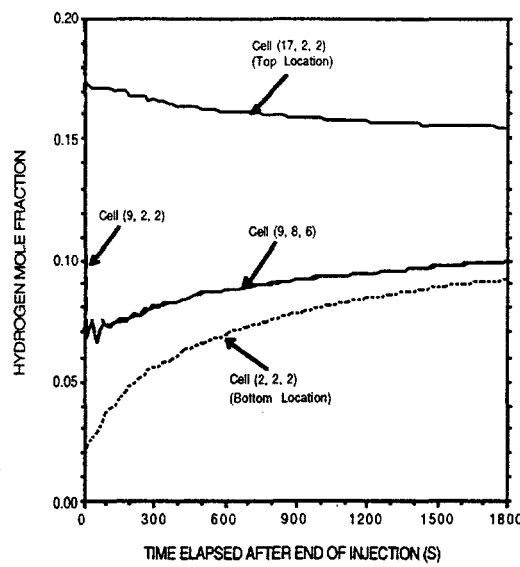


Fig. 8-17. Time-history plots of the calculated hydrogen mole fraction in the SNL FLAME experiment at various locations. Note the merging of the curves for the two locations at the same height (i.e., same first-cell index, 9)

8.2.3. GX6 Battelle Test GX6

8.2.3.1. Summary.

Purpose

Validation of the capability to model catalytic recombiners.

Success Metrics

The GASFLOW-calculated hydrogen concentrations will agree with the experimental measured hydrogen concentrations in the Battelle model containment (BMC).

Problem Description

For the GX6 test, hydrogen and steam are injected into the BMC facility, which included a Siemens catalytic recombiner. The GX6 test was performed in the BMC facility in annular compartments ("banana rooms") R5 to R8 and the central cylindrical room R1/R3. A plug on top of the central room R1/R3 and closed openings on the outside of the banana rooms sealed off this inner containment from the ring room and the dome of the BMC (see Figure 8-18). The total gas volume of the participating rooms was 209 m³, and each banana room R5 to R8 had a gas volume of 49 m³. The recombiner was positioned next to the inner wall of R5, not far from the overflow opening to R6. For the GX6 test, steam was nearly evenly injected into rooms R5, R6, and R7. Hydrogen was injected into room R8. Figure 8-19 gives the steam and hydrogen injection rates and times during which fans and valves were operated.

Relationship to Code Models and Methods

See Table 7-1.

Relationship to PIRT Phenomena

Code Version and Modifications

GASFLOW 2.1.0.11 with no updates.

Hardware and Operating System

CRAY-J90 UNICOS operating system.

Compiler, Version, and Optimization Level

CRAY Fortran 90, Version 3.0.0.1.

Runtime Statistics: Total Run Time, Grind Time

Problem took 1 month to complete.

Results and Conclusions

The GASFLOW results agree with experimental results.

8.2.3.2. Test Description. For the GX6 test, hydrogen and steam were injected into the BMC facility, which included a Siemens catalytic recombiner. The GX6 test was

performed in the BMC facility in banana rooms R5 to R8 and the central cylindrical room R1/R3. A plug on top of the central room R1/R3 and closed openings on the outside of the banana rooms sealed off this inner containment from the ring room and the dome of the BMC (see Figure 8-18). The total gas volume of the participating rooms was 209 m³, and each banana room R5 to R8 had a gas volume of 49 m³. The recombiner was positioned next to the inner wall of R5, not far from the overflow opening to R6. For the GX6 test, steam was nearly evenly injected into rooms R5, R6, and R7. Hydrogen was injected into room R8. Figure 8-19 gives the steam and hydrogen injection rates and times during which fans and valves were operated.

8.2.3.3. GASFLOW Calculations.

8.2.3.3.1. GASFLOW input model. The calculations were performed with GASFLOW, Version 2.1.0.11. No local updates or modifications were made to the code.

8.2.3.3.2. GASFLOW results. Figure 8-19 is a comparison of the calculated and measured pressure for the GX6. The calculated pressure depends on the condensation rate, boundary condition pressures, and leakage models. The calculated pressure before ~6 h into the transient is slightly higher than the measured data. This indicates a difference in the boundary condition pressures for the GASFLOW model and the actual pressure seen by the test facility. After ~6 h into the transient, the calculated pressure is still higher than the measured pressure, which indicates a combination of too much in-leakage in the calculation and slightly different boundary condition pressures. The drop in pressure at ~6 h is caused by termination of the inflow of steam into the test facility and the condensation of steam already in the test facility. The GASFLOW-calculated timing for this drop in pressure is slightly earlier and slightly larger than the measured pressure. This indicates that the condensation model in GASFLOW is predicting a condensation rate slightly larger than is inferred in the test data. The overall agreement is good and captures the dominant trends in the data.

Figure 8-20 is a comparison of the calculated and measured temperatures for the GX6 test at several different locations within the test facility. The temperature comparisons are excellent and capture the dominant trends in the data. In addition, the prediction of the temperature above the recombiner foils (i.e., the temperature rise through the recombiner) is predicted quite accurately.

Figure 8-21 is a comparison of the calculated and measured hydrogen concentrations of the GX6 test at several different locations within the test facility. The comparisons are excellent and demonstrate that GASFLOW accurately calculates the rise in the hydrogen concentration as the hydrogen is injected into the test facility and the reduction in the hydrogen concentration as the recombiner removes hydrogen from the test facility.

8.2.3.4. Conclusions and Recommendations. The GASFLOW, Version 2.1.0.11 results are in agreement with the test results, as required by the success metric.

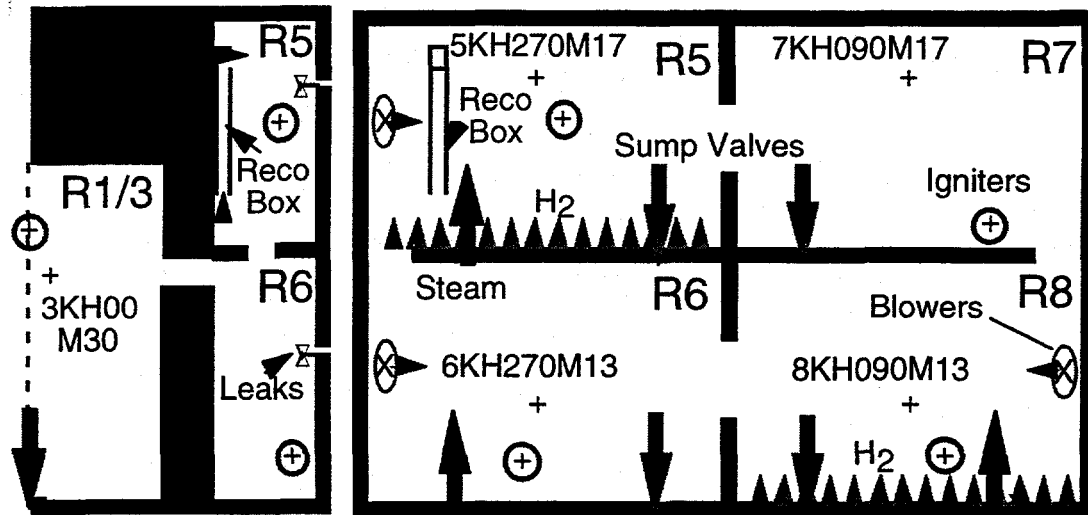


Fig. 8-18. Scheme of the BMC for the Battelle GX tests (radial cut and unwrapped geometry of banana rooms)

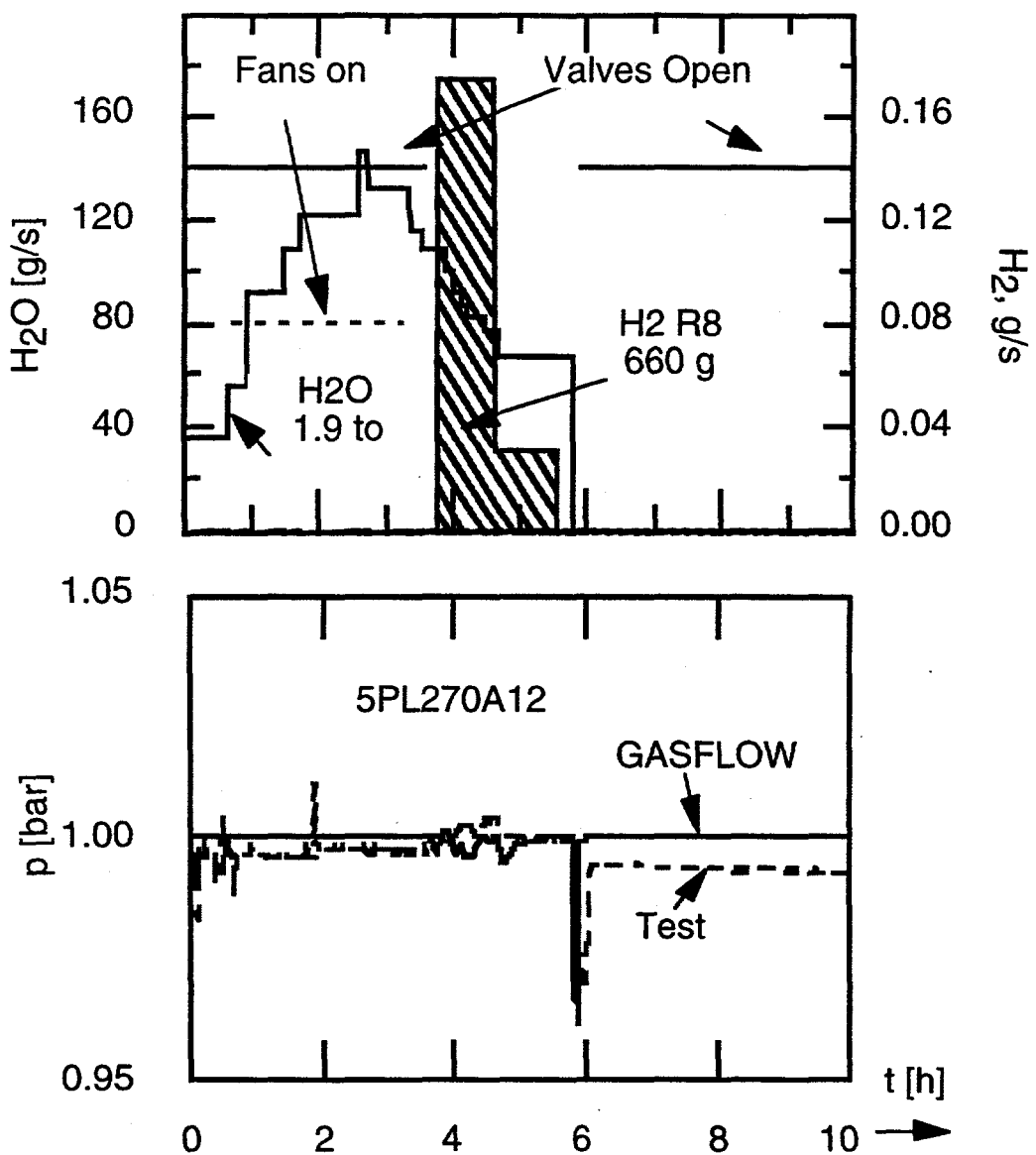


Fig. 8-19. GX6 source data and pressure transient GASFLOW 2.1 analysis with ducts for valve and leak simulations

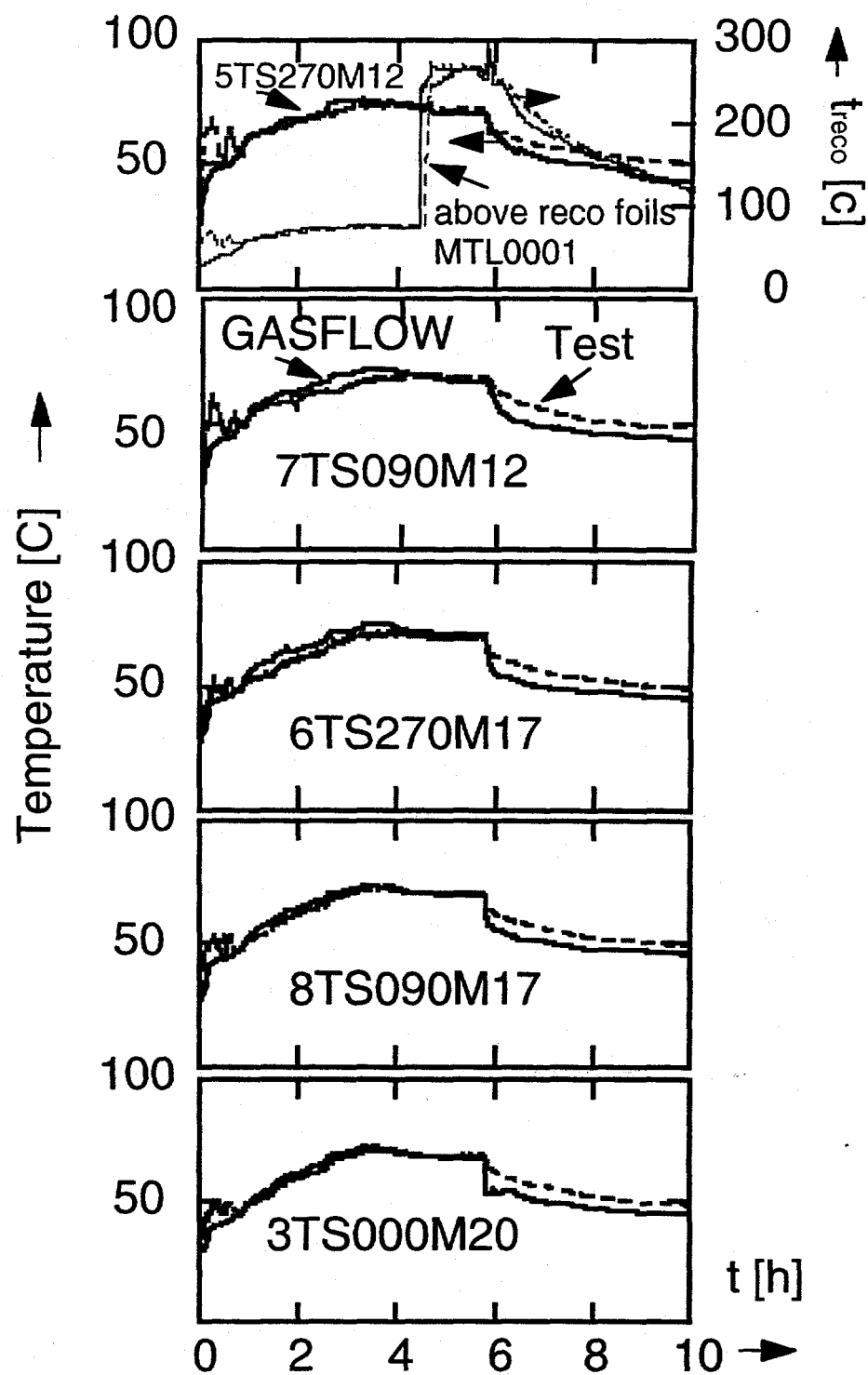


Fig. 8-20. Calculated and measured gas temperatures in Battelle test GX6 with GASFLOW 2.1 and use of ducts for valve and leak simulations

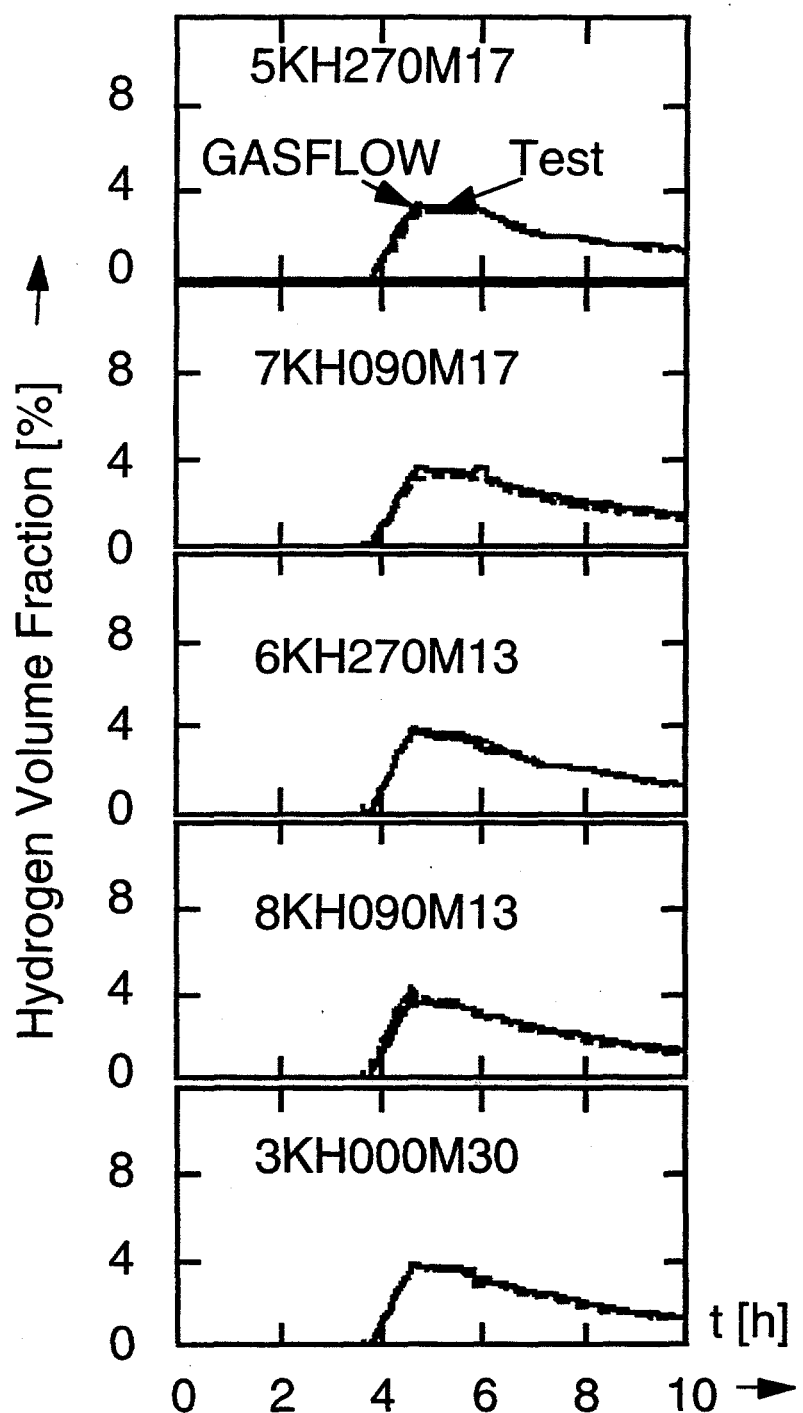


Fig. 8-21. Calculated and measured hydrogen volume fractions in Battelle test GX6 with GASFLOW 2.1 and use of ducts for valve and leak simulations

8.2.3.5. Input File Listing.

ingf GX6 free slip bc correct gravity head and valve areas in banana rooms
royl9.10.97

NOTES: 3-D domain

Number of fluid cells = $10 \times 27 \times 18 = 4860$ for the coordinate dimension r, theta, and z, respectively.

Fixed pbc's and vbc's to be consistent - 4/97 - JWS.

Added damper to represent valve at 2,3,1 - 5/97 - JWS.

Added leakage path models to represent flow around instrument tubes - 6/97 - JWS.

Added new recombiner model - 6/97 - JWS.

imax = 11

jmax = 28

kmax = 19

imaxjmax = 308

Total number of 3D cells = $11 \times 28 \times 19 = 5852$

duct 1 is the valve connected at 2,3,1.

Leakage paths with annular gap of 0.1 cm on a diameter of 10 cm through a wall of 30 cm.

Duct #	m	i	j	k
2	1946	10	9	7
3	2012	10	15	7
4	2034	10	17	7
5	2100	10	23	7
6	2254	10	9	8
7	2331	10	16	8
8	2408	10	23	8
9	3497	10	10	12
10	3552	10	15	12
11	3563	10	16	12
12	3640	10	23	12
13	4366	10	5	15
14	4784	10	15	16

\$innet

```
;           dxw  dxe  dyw  dye      dzw  dze  west  east  ncells  betax
ductdef(1,1) = 0.0, 0.0, 6.5000, 6.5000, 0.0, 0.0, 1, 2, 4, 1.0, 0, 0,
ductdef(1,2) = 0.0, 0.0, 30.0000, 30.0000, 30.0, 30.0, 3, 4, 4, 1.0, 0, 0,
ductdef(1,3) = 0.0, 0.0, 30.0000, 30.0000, 30.0, 30.0, 5, 6, 4, 1.0, 0, 0,
ductdef(1,4) = 0.0, 0.0, 30.0000, 30.0000, 30.0, 30.0, 7, 8, 4, 1.0, 0, 0,
ductdef(1,5) = 0.0, 0.0, 30.0000, 30.0000, 30.0, 30.0, 9, 10, 4, 1.0, 0, 0,
ductdef(1,6) = 0.0, 0.0, 30.0000, 30.0000, 30.0, 30.0, 11, 12, 4, 1.0, 0, 0,
ductdef(1,7) = 0.0, 0.0, 30.0000, 30.0000, 30.0, 30.0, 13, 14, 4, 1.0, 0, 0,
ductdef(1,8) = 0.0, 0.0, 30.0000, 30.0000, 30.0, 30.0, 15, 16, 4, 1.0, 0, 0,
```

```

ductdef(1,9) = 0.0, 0.0, 30.0000, 30.0000, 30.0, 30.0, 17, 18, 4,1.0,0,0,
ductdef(1,10)= 0.0, 0.0, 30.0000, 30.0000, 30.0, 30.0, 19, 20, 4,1.0,0,0,
ductdef(1,11)= 0.0, 0.0, 30.0000, 30.0000, 30.0, 30.0, 21, 22, 4,1.0,0,0,
ductdef(1,12)= 0.0, 0.0, 30.0000, 30.0000, 30.0, 30.0, 23, 24, 4,1.0,0,0,
ductdef(1,13)= 0.0, 0.0, 30.0000, 30.0000, 30.0, 30.0, 25, 26, 4,1.0,0,0,
ductdef(1,14)= 0.0, 0.0, 30.0000, 30.0000, 30.0, 30.0, 27, 28, 4,1.0,0,0,

;
      x      y      z
cpnt(1,1)  = 0.0, 0.0, 0.0, ; Points to define duct 1
cpnt(1,2)  = 500.0, 0.0, 0.0,
cpnt(1,3)  = 430.0, 90.0, 150.0, ; Points to define duct 2
cpnt(1,4)  = 550.0, 90.0, 150.0,
cpnt(1,5)  = 430.0, 180.0, 150.0, ; Points to define duct 3
cpnt(1,6)  = 550.0, 180.0, 150.0,
cpnt(1,7)  = 430.0, 210.0, 150.0, ; Points to define duct 4
cpnt(1,8)  = 550.0, 210.0, 150.0,
cpnt(1,9)  = 430.0, 300.0, 150.0, ; Points to define duct 5
cpnt(1,10) = 550.0, 300.0, 150.0,
cpnt(1,11) = 430.0, 90.0, 190.0, ; Points to define duct 6
cpnt(1,12) = 550.0, 90.0, 190.0,
cpnt(1,13) = 430.0, 195.0, 190.0, ; Points to define duct 7
cpnt(1,14) = 550.0, 195.0, 190.0,
cpnt(1,15) = 430.0, 300.0, 190.0, ; Points to define duct 8
cpnt(1,16) = 550.0, 300.0, 190.0,
cpnt(1,17) = 430.0, 105.0, 300.0, ; Points to define duct 9
cpnt(1,18) = 550.0, 105.0, 300.0,
cpnt(1,19) = 430.0, 180.0, 300.0, ; Points to define duct 10
cpnt(1,20) = 550.0, 180.0, 300.0,
cpnt(1,21) = 430.0, 195.0, 300.0, ; Points to define duct 11
cpnt(1,22) = 550.0, 195.0, 300.0,
cpnt(1,23) = 430.0, 300.0, 300.0, ; Points to define duct 12
cpnt(1,24) = 550.0, 300.0, 300.0,
cpnt(1,25) = 430.0, 55.0, 390.0, ; Points to define duct 13
cpnt(1,26) = 550.0, 55.0, 390.0,
cpnt(1,27) = 430.0, 180.0, 414.0, ; Points to define duct 14
cpnt(1,28) = 550.0, 180.0, 414.0,

;
      i1      i2      iduct    iblk    itab    flowloss    flowarea    areafraction
      ; @ time=0.0
dampdef(1,1) = 1,      2,      1,      1,      1,      1.0,      30.00,      1.0,
;

      time(s)    area fraction
dmptb(1,1,1) = 0.0,      1.0,
                12960.0,      1.0,
                12961.0,      0.0,
                20952.0,      0.0,
                20953.0,      1.0,
                24806.0,      1.0,
                24807.0,      0.0,
                40000.0,      0.0,
;

; Annular flow losses for 1D leakage paths

flossdef(1,1) = 2, 3, 2, 1, -10.10, 10.0,
flossdef(1,2) = 2, 3, 3, 1, -10.10, 10.0,

```

```

flossdef(1,3) = 2, 3, 4, 1, -10.10, 10.0,
flossdef(1,4) = 2, 3, 5, 1, -10.10, 10.0,
flossdef(1,5) = 2, 3, 6, 1, -10.10, 10.0,
flossdef(1,6) = 2, 3, 7, 1, -10.10, 10.0,
flossdef(1,7) = 2, 3, 8, 1, -10.10, 10.0,
flossdef(1,8) = 2, 3, 9, 1, -10.10, 10.0,
flossdef(1,9) = 2, 3,10, 1, -10.10, 10.0,
flossdef(1,10)= 2, 3,11, 1, -10.10, 10.0,
flossdef(1,11)= 2, 3,12, 1, -10.10, 10.0,
flossdef(1,12)= 2, 3,13, 1, -10.10, 10.0,
flossdef(1,13)= 2, 3,14, 1, -10.10, 10.0,

```

; Network to 3D block connections,

	i1	I2	J1	J2	K1	K2	B#	N#	1D/3D connections
nwcx(1, 1)	= 1,	2,	2,	3,	1,	1,	1,	2, , ;	Damper to position 2,3,1
nwcx(1, 2)	=10,	10,	8,	9,	6,	7,	1,	3, , ;	Leakage duct 2
nwcx(1, 3)	=10,	10,	14,	15,	6,	7,	1,	5, , ;	Leakage duct 3
nwcx(1, 4)	=10,	10,	16,	17,	6,	7,	1,	7, , ;	Leakage duct 4
nwcx(1, 5)	=10,	10,	22,	23,	6,	7,	1,	9, , ;	Leakage duct 5
nwcx(1, 6)	=10,	10,	8,	9,	7,	8,	1,	11, , ;	Leakage duct 6
nwcx(1, 7)	=10,	10,	15,	16,	7,	8,	1,	13, , ;	Leakage duct 7
nwcx(1, 8)	=10,	10,	22,	23,	7,	8,	1,	15, , ;	Leakage duct 8
nwcx(1, 9)	=10,	10,	9,	10,	11,	12,	1,	17, , ;	Leakage duct 9
nwcx(1,10)	=10,	10,	14,	15,	11,	12,	1,	19, , ;	Leakage duct 10
nwcx(1,11)	=10,	10,	15,	16,	11,	12,	1,	21, , ;	Leakage duct 11
nwcx(1,12)	=10,	10,	22,	23,	11,	12,	1,	23, , ;	Leakage duct 12
nwcx(1,13)	=10,	10,	4,	5,	14,	15,	1,	25, , ;	Leakage duct 13
nwcx(1,14)	=10,	10,	14,	15,	15,	16,	1,	27, , ;	Leakage duct 14

\$end

\$xput

```

nrsdump = 0,
sortami = 1,
iburn = 0,
cyl = 1.,
idiffmom = 0,
idiffme = 0,
ieopt = 1,
trange = 'low',
icopt = 2,
itopt = 1,
tmodel = 'none',
autot = 1.0,
delt0 = 0.100,
deltmin = 1.000e-6,
deltmax = 1.0,
epsi0 = 1.000e-06,

```

```

epsimax = 1.000e-06,
epsimin = 1.000e-06,
itdowndt = 350,
itupdt = 350,
itmax = 1000,

gx = 0.0,
gy = 0.0,
gz = -980.0,

lpr = 1,
ittyfreq = 100,
pltdt = 4000.0,
prttdt = 36000.0,
tddt = 2000.,
velmx = 25.5,

maxcyc = 10000000,
twfin = 36000.,

ibs = 1,
ibn = 1,
ibe = 1,
ibw = 1,
ibb = 1,
ibt = 1.

mobs = 3, 04, 2, 26, 1, 02, 1, 1, ;graben
      5, 07, 11, 13, 1, 02, 1, 1, ;graben
      5, 07, 19, 21, 1, 02, 1, 1, ;graben
      9, 10, 02, 26, 1, 02, 1, 1, ;graben
      3, 10, 1, 2, 1, 18, 1, 1, ;room4
      3, 10, 26, 27, 01, 18, 1, 1, ;room4
      8, 10, 2, 26, 02, 04, 1, 1, ;canyon
      3, 05, 2, 26, 08, 09, 1, 1, ;ceiling
      5, 06, 5, 26, 08, 09, 1, 1, ;ceiling
      6, 08, 5, 23, 08, 09, 1, 1, ;ceiling
      6, 09, 24, 26, 08, 09, 1, 1, ;ceiling
      8, 09, 02, 23, 08, 09, 1, 1, ;ceiling
      9, 10, 2, 26, 08, 09, 1, 1, ;ceiling
      1, 03, 01, 27, 12, 18, 1, 1, ;plug on r3
      3, 4, 2, 26, 2, 3, 1, 1, ; ring around r1/r3
      3, 4, 2, 15, 3, 4, 1, 1,
      3, 4, 2, 3, 4, 5, 1, 1,
      3, 4, 5, 10, 4, 5, 1, 1,
      3, 4, 11, 19, 4, 5, 1, 1,
      3, 4, 20, 24, 4, 5, 1, 1,
      3, 4, 25, 26, 4, 5, 1, 1,
      3, 4, 2, 26, 5, 6, 1, 1,
      3, 4, 2, 26, 6, 7, 1, 1,
      3, 4, 2, 7, 7, 8, 1, 1,

```

3,	4,	8,	13,	7,	8,1,1,				
3,	4,	14,	19,	7,	8,1,1,				
3,	4,	20,	26,	7,	8,1,1,				
3,	4,	2,	26,	8,	9,1,1,				
3,	4,	2,	26,	9,	10,1,1,				
3,	4,	2,	26,	10,	11,1,1,				
3,	4,	2,	26,	11,	12,1,1,				
3,	4,	2,	26,	12,	13,1,1,				
3,	4,	2,	26,	13,	14,1,1,				
3,	4,	2,	26,	14,	15,1,1,				
3,	4,	2,	26,	15,	16,1,1,				
3,	4,	2,	26,	16,	17,1,1,				
3,	4,	2,	26,	17,	18,1,1,				
walls =	4,	06,	15,	15,	09,	18,	1,	1,	;ue57
	6,	09,	15,	15,	15,	18,	1,	1,	
	9,	10,	15,	15,	09,	18,	1,	1,	
	4,	07,	15,	15,	02,	08,	1,	1,	;ue68
	7,	08,	15,	15,	02,	05,	1,	1,	
	8,	09,	15,	15,	04,	05,	1,	1,	
	7,	09,	15,	15,	06,	08,	1,	1,	
	9,	10,	15,	15,	04,	08,	1,	1,	
	5,	05,	05,	06,	10,	16,	1,	2,	; recoleft
	4,	05,	05,	05,	10,	17,	1,	2,	; recoeast
	4,	05,	06,	06,	10,	17,	1,	2,	; recowest
	4,	05,	05,	06,	17,	17,	1,	2,	; recotop
	3,	03,	15,	26,	03,	04,	1,	1,	; source left
	3,	04,	15,	26,	04,	04,	1,	1,	; source top
	7,	08,	05,	15,	08,	08,	1,	3,	; h2r5 bottom
	8,	08,	05,	08,	08,	09,	1,	3,	; h2r5 east
	8,	08,	08,	15,	08,	09,	1,	3,	; h2r5 east
	7,	07,	05,	15,	08,	09,	1,	3,	; h2r5 west
	7,	08,	05,	05,	08,	09,	1,	3,	; h2r5 south
	7,	08,	15,	15,	08,	09,	1,	3,	; h2r5 north
	4,	05,	02,	26,	02,	02,	1,	4,	; smp Graben
	5,	07,	02,	11,	02,	02,	1,	4,	; smp Graben
	5,	07,	13,	19,	02,	02,	1,	4,	; smp Graben
	5,	07,	21,	26,	02,	02,	1,	4,	; smp Graben
	7,	08,	02,	26,	02,	02,	1,	4,	; smp Graben
;	8,	10,	08,	10,	08,	08,	1,	3,	; h2o r5bottom
;	8,	10,	08,	08,	08,	09,	1,	3,	; h2o r5south
;	8,	10,	10,	10,	08,	09,	1,	3,	; h2o r5north
;	8,	08,	08,	10,	08,	09,	1,	3,	; h2o r5west
;	10,	10,	08,	10,	08,	09,	1,	3,	; h2o r5east
;	8,	10,	08,	10,	03,	03,	1,	3,	; h2o r6bottom
;	8,	10,	08,	08,	03,	04,	1,	3,	; h2o r6south
;	8,	10,	10,	10,	03,	04,	1,	3,	; h2o r6north
;	8,	08,	08,	10,	03,	04,	1,	3,	; h2o r6west
;	10,	10,	08,	10,	03,	04,	1,	3,	; h2o r6east
;									

```

;          8, 10, 16, 18, 03, 03, 1, 3, ; h2o r8bottom
;          8, 10, 16, 16, 03, 04, 1, 3, ; h2o r8south
;          8, 10, 18, 18, 03, 04, 1, 3, ; h2o r8north
;          8, 08, 16, 18, 03, 04, 1, 3, ; h2o r8west
;          10, 10, 16, 18, 03, 04, 1, 3, ; h2o r8east

holes =   8, 10, 08, 10, 08, 09, 1, ; h2oresr5
          0, 0, 0, 0, 0, 1,
          8, 10, 08, 10, 03, 04, 1, ; h2oresr6
          0, 0, 0, 0, 0, 1,
          8, 10, 16, 18, 03, 04, 1, ; h2oresr8
          0, 0, 0, 0, 0, 1,
          7, 08, 05, 15, 08, 09, 1, ; h2r5 res
          0, 0, 0, 0, 0, 1,
.
          4, 10, 01, 02, 12, 15, 1, ; airr5
          0, 0, 0, 1, 0, 0,
          4, 10, 01, 02, 04, 06, 1, ; airr6
          0, 0, 0, 1, 0, 0,
          4, 10, 26, 27, 04, 06, 1, ; airr8
          0, 0, 1, 0, 0, 0,
.
          5, 07, 11, 13, 08, 09, 1, ; smpr5
          0, 0, 0, 0, 0, 1,
          5, 07, 11, 13, 01, 02, 1, ; smpr6
          0, 0, 0, 0, 0, 1,
          5, 07, 19, 21, 08, 09, 1, ; smpr7
          0, 0, 0, 0, 0, 1,
          5, 07, 19, 21, 01, 02, 1, ; smpr8
          0, 0, 0, 0, 0, 1,
.
areardef = 05, 08, 2,05, 09,09, 1, 1.000, 4*0.0, ; ue56b
          06, 09, 15,15, 09,15, 1, 0.771, 4*0.0, ; ue57
          06, 09, 23,24, 09,09, 1, 0.896, 4*0.0, ; ue78a
          04, 04, 24,25, 04,05, 1, 0.934, 4*0.0, ; ue38a
          04, 04, 19,20, 07,08, 1, 0.863, 4*0.0, ; einstieg
          04, 04, 19,20, 04,05, 1, 0.934, 4*0.0, ; ue38c
          06, 08, 15,15, 06,07, 1, 0.870, 4*0.0, ; ue68
          04, 04, 13,14, 07,08, 1, 0.598, 4*0.0, ; ueh2
          04, 04, 10,11, 04,05, 1, 0.934, 4*0.0, ; ue36c
          04, 04, 07,08, 07,08, 1, 0.749, 4*0.0, ; ueh1
          04, 04, 03,05, 04,05, 1, 0.706, 4*0.0, ; ueh1
          05, 07, 11, 13, 09, 09, 1, 4.141e-3, 4*0.0, ; smpr5
          05, 07, 11, 13, 02, 02, 1, 4.141e-3, 4*0.0, ; smpr6
          05, 07, 19, 21, 09, 09, 1, 4.141e-3, 4*0.0, ; smpr7
          05, 07, 19, 21, 02, 02, 1, 4.141e-3, 4*0.0, ; smpr8
.

```

```

mat = 'n2', 'o2', 'h2', 'h2o', 'h2ol',
.
gasdef(1, 1)= 1, 10, 1, 27, 1, 18,1,1.e+6, 301.15,2,0.,0.,
               'n2', 0.78947,'o2', 0.21053,'h2', 0.,'h2o', 0.,'h2ol', 0.,
;TOTAL
gasdef(1, 2)= 4, 10, 2, 15, 9, 18,1,1.e+6, 301.15,2,0.,0., ;R5
               'n2', 0.78947,'o2', 0.21053,'h2', 0.,'h2o', 0.,'h2ol', 0.,
.

```

```

gasdef(1, 3)= 4, 10, 15, 26, 9, 18, 1, 1.e+6, 301.15, 2, 0., 0., ;R7
  'n2', 0.78947, 'o2', 0.21053, 'h2', 0., 'h2o', 0., 'h2ol', 0.,
gasdef(1, 4)= 4, 10, 2, 15, 2, 8, 1, 1.e+6, 301.15, 2, 0., 0., ;R6
  'n2', 0.78947, 'o2', 0.21053, 'h2', 0., 'h2o', 0., 'h2ol', 0.,
gasdef(1, 5)= 1, 4, 1, 27, 6, 12, 1, 1.e+6, 301.15, 2, 0., 0., ;R1
  'n2', 0.78947, 'o2', 0.21053, 'h2', 0., 'h2o', 0., 'h2ol', 0.,
gasdef(1, 6)= 1, 4, 1, 27, 1, 06, 1, 1.e+6, 303.15, 2, 0., 0., ;R3
  'n2', 0.78947, 'o2', 0.21053, 'h2', 0., 'h2o', 0., 'h2ol', 0.,
gasdef(1, 7)= 4, 10, 15, 26, 2, 8, 1, 1.e+6, 301.15, 2, 0., 0., ;R8
  'n2', 0.78947, 'o2', 0.21053, 'h2', 0., 'h2o', 0., 'h2ol', 0.,
gasdef(1, 8)= 5, 08, 2, 5, 8, 9, 1, 1.e+6, 301.15, 2, 0., 0., ;UE56
  'n2', 0.78947, 'o2', 0.21053, 'h2', 0., 'h2o', 0., 'h2ol', 0.,
gasdef(1, 9)= 6, 09, 23, 24, 8, 9, 1, 1.e+6, 301.15, 2, 0., 0., ;UE78
  'n2', 0.78947, 'o2', 0.21053, 'h2', 0., 'h2o', 0., 'h2ol', 0.,
gasdef(1,10)= 7, 08, 05, 15, 8, 9, 1, 1.e+6, 323., 2, 0., 1.e+99,
  'n2', 0., 'o2', 0., 'h2', 1., 'h2o', 0., 'h2ol', 0., ;h2r5
gasdef(1,11)= 3, 4, 15, 26, 3, 4, 1, 1.e+6, 323., 2, 0., 1.e+99,
  'n2', 0., 'o2', 0., 'h2', 1., 'h2o', 0., 'h2ol', 0., ;H2S
gasdef(1,12)= 8, 10, 08, 10, 8, 9, 1, 1.e+6, 373.15, 2, 0., 1.e+99,
  'n2', 0., 'o2', 0., 'h2', 0., 'h2o', 1., 'h2ol', 0., ;H2oR5
gasdef(1,13)= 8, 10, 08, 10, 3, 4, 1, 1.e+6, 373.15, 2, 0., 1.e+99,
  'n2', 0., 'o2', 0., 'h2', 0., 'h2o', 1., 'h2ol', 0., ;H2oR6
gasdef(1,14)= 8, 10, 16, 18, 3, 4, 1, 1.e+6, 373.15, 2, 0., 1.e+99,
  'n2', 0., 'o2', 0., 'h2', 0., 'h2o', 1., 'h2ol', 0., ;H2oR8

gasdef(1,15)= 4, 10, 01, 02, 12, 15, 1, 1.e+6, 298.15, 2, 0., 1.e+99,
  'n2', 0.78947, 'o2', 0.21053, 'h2', 0., 'h2o', 0., 'h2ol', 0., ;airr5
gasdef(1,16)= 4, 10, 01, 02, 04, 06, 1, 1.e+6, 298.15, 2, 0., 1.e+99,
  'n2', 0.78947, 'o2', 0.21053, 'h2', 0., 'h2o', 0., 'h2ol', 0., ;airr6
gasdef(1,17)= 4, 10, 26, 27, 04, 06, 1, 1.e+6, 298.15, 2, 0., 1.e+99,
  'n2', 0.78947, 'o2', 0.21053, 'h2', 0., 'h2o', 0., 'h2ol', 0., ;airr8

gasdef(1,18)= 2, 03, 01, 27, 00, 01, 1, 1.e+6, 298.15, 2, 0., 1.e+99,
  'n2', 0.78947, 'o2', 0.21053, 'h2', 0., 'h2o', 0., 'h2ol', 0., ;smpr1
gasdef(1,19)= 5, 07, 11, 13, 08, 09, 1, 1.0002757e+6, 298.15, 2, 0., 1.e+99,
  'n2', 0.78947, 'o2', 0.21053, 'h2', 0., 'h2o', 0., 'h2ol', 0., ;smpr5
gasdef(1,20)= 5, 07, 11, 13, 01, 02, 1, 1.0006492e+6, 298.15, 2, 0., 1.e+99,
  'n2', 0.78947, 'o2', 0.21053, 'h2', 0., 'h2o', 0., 'h2ol', 0., ;smpr6
gasdef(1,21)= 5, 07, 19, 21, 08, 09, 1, 1.0002757e+6, 298.15, 2, 0., 1.e+99,
  'n2', 0.78947, 'o2', 0.21053, 'h2', 0., 'h2o', 0., 'h2ol', 0., ;smpr7
gasdef(1,22)= 5, 07, 19, 21, 01, 02, 1, 1.0006492e+6, 298.15, 2, 0., 1.e+99,
  'n2', 0.78947, 'o2', 0.21053, 'h2', 0., 'h2o', 0., 'h2ol', 0., ;smpr8

; Damper initial condition.
gasdef(1,23)= 0, 6, 1, 0, 0, 0, 0, 1.e+6, 298.15, 2, 0., 0.0,
  'n2', 0.78947, 'o2', 0.21053, 'h2', 0., 'h2o', 0., 'h2ol', 0.,

; Damper west boundary condition.
gasdef(1,24)= 0, 1, 1, 0, 0, 0, 0, 1.000678e+6, 298.15, 2, 0., 1.e+99,
  'n2', 0.78947, 'o2', 0.21053, 'h2', 0., 'h2o', 0., 'h2ol', 0.,

; Leakage path initial condition.
gasdef(1,25)= 0, 6, 2, 0, 0, 0, 0, 1.e+6, 298.15, 2, 0., 0.0,
  'n2', 0.78947, 'o2', 0.21053, 'h2', 0., 'h2o', 0., 'h2ol', 0.,
gasdef(1,26)= 0, 6, 3, 0, 0, 0, 0, 1.e+6, 298.15, 2, 0., 0.0,

```

```

'n2', 0.78947,'o2', 0.21053,'h2', 0.,'h2o', 0.,'h2ol', 0.,
gasdef(1,27)= 0, 6, 4, 0, 0, 0, 1.e+6, 298.15, 2, 0., 0.0,
'n2', 0.78947,'o2', 0.21053,'h2', 0.,'h2o', 0.,'h2ol', 0.,
gasdef(1,28)= 0, 6, 5, 0, 0, 0, 1.e+6, 298.15, 2, 0., 0.0,
'n2', 0.78947,'o2', 0.21053,'h2', 0.,'h2o', 0.,'h2ol', 0.,
gasdef(1,29)= 0, 6, 6, 0, 0, 0, 1.e+6, 298.15, 2, 0., 0.0,
'n2', 0.78947,'o2', 0.21053,'h2', 0.,'h2o', 0.,'h2ol', 0.,
gasdef(1,30)= 0, 6, 7, 0, 0, 0, 1.e+6, 298.15, 2, 0., 0.0,
'n2', 0.78947,'o2', 0.21053,'h2', 0.,'h2o', 0.,'h2ol', 0.,
gasdef(1,31)= 0, 6, 8, 0, 0, 0, 1.e+6, 298.15, 2, 0., 0.0,
'n2', 0.78947,'o2', 0.21053,'h2', 0.,'h2o', 0.,'h2ol', 0.,
gasdef(1,32)= 0, 6, 9, 0, 0, 0, 1.e+6, 298.15, 2, 0., 0.0,
'n2', 0.78947,'o2', 0.21053,'h2', 0.,'h2o', 0.,'h2ol', 0.,
gasdef(1,33)= 0, 6,10, 0, 0, 0, 1.e+6, 298.15, 2, 0., 0.0,
'n2', 0.78947,'o2', 0.21053,'h2', 0.,'h2o', 0.,'h2ol', 0.,
gasdef(1,34)= 0, 6,11, 0, 0, 0, 1.e+6, 298.15, 2, 0., 0.0,
'n2', 0.78947,'o2', 0.21053,'h2', 0.,'h2o', 0.,'h2ol', 0.,
gasdef(1,35)= 0, 6,12, 0, 0, 0, 1.e+6, 298.15, 2, 0., 0.0,
'n2', 0.78947,'o2', 0.21053,'h2', 0.,'h2o', 0.,'h2ol', 0.,
gasdef(1,36)= 0, 6,13, 0, 0, 0, 1.e+6, 298.15, 2, 0., 0.0,
'n2', 0.78947,'o2', 0.21053,'h2', 0.,'h2o', 0.,'h2ol', 0.,
gasdef(1,37)= 0, 6,14, 0, 0, 0, 1.e+6, 298.15, 2, 0., 0.0,
'n2', 0.78947,'o2', 0.21053,'h2', 0.,'h2o', 0.,'h2ol', 0.,

; Leakage path east boundary condition.

gasdef(1,38)= 5, 6, 2, 0, 0, 0, 1.000372e+6, 298.15, 2, 0., 1.e+99,
'n2', 0.78947,'o2', 0.21053,'h2', 0.,'h2o', 0.,'h2ol', 0.,
gasdef(1,39)= 5, 6, 3, 0, 0, 0, 1.000372e+6, 298.15, 2, 0., 1.e+99,
'n2', 0.78947,'o2', 0.21053,'h2', 0.,'h2o', 0.,'h2ol', 0.,
gasdef(1,40)= 5, 6, 4, 0, 0, 0, 1.000372e+6, 298.15, 2, 0., 1.e+99,
'n2', 0.78947,'o2', 0.21053,'h2', 0.,'h2o', 0.,'h2ol', 0.,
gasdef(1,41)= 5, 6, 5, 0, 0, 0, 1.000372e+6, 298.15, 2, 0., 1.e+99,
'n2', 0.78947,'o2', 0.21053,'h2', 0.,'h2o', 0.,'h2ol', 0.,
gasdef(1,42)= 5, 6, 6, 0, 0, 0, 1.000320e+6, 298.15, 2, 0., 1.e+99,
'n2', 0.78947,'o2', 0.21053,'h2', 0.,'h2o', 0.,'h2ol', 0.,
gasdef(1,43)= 5, 6, 7, 0, 0, 0, 1.000320e+6, 298.15, 2, 0., 1.e+99,
'n2', 0.78947,'o2', 0.21053,'h2', 0.,'h2o', 0.,'h2ol', 0.,
gasdef(1,44)= 5, 6, 8, 0, 0, 0, 1.000320e+6, 298.15, 2, 0., 1.e+99,
'n2', 0.78947,'o2', 0.21053,'h2', 0.,'h2o', 0.,'h2ol', 0.,
gasdef(1,45)= 5, 6, 9, 0, 0, 0, 1.000181e+6, 298.15, 2, 0., 1.e+99,
'n2', 0.78947,'o2', 0.21053,'h2', 0.,'h2o', 0.,'h2ol', 0.,
gasdef(1,46)= 5, 6,10, 0, 0, 0, 1.000181e+6, 298.15, 2, 0., 1.e+99,
'n2', 0.78947,'o2', 0.21053,'h2', 0.,'h2o', 0.,'h2ol', 0.,
gasdef(1,47)= 5, 6,11, 0, 0, 0, 1.000181e+6, 298.15, 2, 0., 1.e+99,
'n2', 0.78947,'o2', 0.21053,'h2', 0.,'h2o', 0.,'h2ol', 0.,
gasdef(1,48)= 5, 6,12, 0, 0, 0, 1.000181e+6, 298.15, 2, 0., 1.e+99,
'n2', 0.78947,'o2', 0.21053,'h2', 0.,'h2o', 0.,'h2ol', 0.,
gasdef(1,49)= 5, 6,13, 0, 0, 0, 1.000125e+6, 298.15, 2, 0., 1.e+99,
'n2', 0.78947,'o2', 0.21053,'h2', 0.,'h2o', 0.,'h2ol', 0.,
gasdef(1,50)= 5, 6,14, 0, 0, 0, 1.000080e+6, 298.15, 2, 0., 1.e+99,
'n2', 0.78947,'o2', 0.21053,'h2', 0.,'h2o', 0.,'h2ol', 0.,

vbc(1,1) = 08, 10, 08, 10, 09, 09, 1, 1, 0., 1.e+99, ;h2or5
vbc(1,2) = 08, 10, 08, 10, 04, 04, 1, 2, 0., 1.e+99, ;h2or6
vbc(1,3) = 08, 10, 16, 18, 04, 04, 1, 3, 0., 1.e+99, ;h2or8

```

```

vbc(1,4) = 04, 04, 15, 26, 3, 4, 1, 5, 0., 1.e+99, ;h2r8
vbc(1,5) = 07, 08, 05, 15, 9, 9, 1, 6, 0., 1.e+99, ;h2r5

vbc(1,6) = 04, 10, 02, 02, 12, 15, 1, 7, 0., 1.e+99, ;airr5
vbc(1,7) = 04, 10, 02, 02, 04, 06, 1, 8, 0., 1.e+99, ;airr6
vbc(1,8) = 04, 10, 26, 26, 04, 06, 1, 9, 0., 1.e+99, ;airr8

vbc(1,9) = 02, 03, 01, 27, 01, 01, 1, 10, 0., 1.e+99, ;smpr1
vbc(1,10) = 05, 07, 11, 13, 09, 09, 1, 10, 4212., 21348., ;smpr5
vbc(1,11) = 05, 07, 11, 13, 02, 02, 1, 10, 12960., 21132., ;smpr6
vbc(1,12) = 05, 07, 19, 21, 09, 09, 1, 10, 12960., 21492., ;smpr7
vbc(1,13) = 05, 07, 19, 21, 02, 02, 1, 10, 12960., 21240., ;smpr8

vbc(1,14) = 06, 08, 03, 03, 12, 15, 1, 11, 2484., 11844., ;ventr5
vbc(1,15) = 06, 08, 03, 03, 04, 06, 1, 12, 6444., 11844., ;ventr6
vbc(1,16) = 06, 08, 25, 25, 04, 06, 1, 13, 2484., 11844., ;ventr8
vbc(1,17) = 06, 08, 25, 25, 12, 15, 1, 13, 6444., 6840., ;ventr7

; vbc(1,19) = 01, 02, 02, 03, 01, 01, 1, 14, 24806., 40000., ;vsmpr1
; vbc(1,4) = 01, 02, 02, 03, 01, 01, 1, 14, 12960., 20952., ;vsmpr1

vvalue = 0., 0., 0., 0., 0., 0., 0., 0.,
          0., 119.66, 107.69, -107.69, 0.,

; pbc(1,1) = 1, 2, 2, 3, 1, 1, 1, 0., 12960.,
; pbc(1,2) = 1, 2, 2, 3, 1, 1, 1, 20952., 24806.,

pbc(1,1) = 5, 7, 11, 13, 09, 09, 1, 21348., 40000.,
pbc(1,2) = 5, 7, 11, 13, 02, 02, 1, 21132., 40000.,
pbc(1,3) = 5, 7, 19, 21, 09, 09, 1, 21492., 40000.,
pbc(1,4) = 5, 7, 19, 21, 02, 02, 1, 21240., 40000.,
pbc(1,5) = 1, 1, 1, 0, 0, 0, 0., 1.e+99, ; For damper
pbc(1,6) = 2, 2, 2, 0, 0, 0, 0., 1.e+99, ; For leak duct 2
pbc(1,7) = 2, 2, 3, 0, 0, 0, 0., 1.e+99, ; For leak duct 3
pbc(1,8) = 2, 2, 4, 0, 0, 0, 0., 1.e+99, ; For leak duct 4
pbc(1,9) = 2, 2, 5, 0, 0, 0, 0., 1.e+99, ; For leak duct 5
pbc(1,10) = 2, 2, 6, 0, 0, 0, 0., 1.e+99, ; For leak duct 6
pbc(1,11) = 2, 2, 7, 0, 0, 0, 0., 1.e+99, ; For leak duct 7
pbc(1,12) = 2, 2, 8, 0, 0, 0, 0., 1.e+99, ; For leak duct 8
pbc(1,13) = 2, 2, 9, 0, 0, 0, 0., 1.e+99, ; For leak duct 9
pbc(1,14) = 2, 2, 10, 0, 0, 0, 0., 1.e+99, ; For leak duct 10
pbc(1,15) = 2, 2, 11, 0, 0, 0, 0., 1.e+99, ; For leak duct 11
pbc(1,16) = 2, 2, 12, 0, 0, 0, 0., 1.e+99, ; For leak duct 12
pbc(1,17) = 2, 2, 13, 0, 0, 0, 0., 1.e+99, ; For leak duct 13
pbc(1,18) = 2, 2, 14, 0, 0, 0, 0., 1.e+99, ; For leak duct 14

zeroddef(1,1) = 4, 4, 15, 26, 3, 4, 1, ;source interface
zeroddef(1,2) = 08, 10, 08, 10, 09, 09, 1, ;h2o source
zeroddef(1,3) = 08, 10, 08, 10, 04, 04, 1, ;h2o source
zeroddef(1,4) = 08, 10, 16, 18, 04, 04, 1, ;h2o source
zeroddef(1,5) = 07, 08, 05, 15, 09, 09, 1, ;h2r5

zeroddef(1,6) = 04, 10, 02, 02, 12, 15, 1, ;airr5
zeroddef(1,7) = 04, 10, 02, 02, 04, 06, 1, ;airr6
zeroddef(1,8) = 04, 10, 26, 26, 04, 06, 1, ;airr8

```

```

zeroddef(1,9) = 02, 03, 01, 27, 01, 01, 1, ;smpr1

zeroddef(1,10) = 05, 07, 11, 13, 09, 09, 1, ;smpr5
zeroddef(1,11) = 05, 07, 11, 13, 02, 02, 1, ;smpr6
zeroddef(1,12) = 05, 07, 19, 21, 09, 09, 1, ;smpr7
zeroddef(1,13) = 05, 07, 19, 21, 02, 02, 1, ;smpr8

zeroddef(1,14) = 01, 02, 02, 03, 01, 01, 1, ;smpr1

subsodef(1,1) = 3, 4, 15, 26, 3, 4, 1, ;source volume
subsodef(1,2) = 08, 10, 08, 10, 08, 09, 1, ;h2o source
subsodef(1,3) = 08, 10, 08, 10, 03, 04, 1, ;h2o source
subsodef(1,4) = 08, 10, 16, 18, 03, 04, 1, ;h2o source
subsodef(1,5) = 07, 08, 05, 15, 08, 09, 1, ;h2r5

subsodef(1,6) = 04, 10, 01, 02, 12, 15, 1, ;airr5
subsodef(1,7) = 04, 10, 01, 02, 04, 06, 1, ;airr6
subsodef(1,8) = 04, 10, 26, 27, 04, 06, 1, ;airr8

subsodef(1,09) = 05, 07, 11, 13, 08, 09, 1, ;smpr5
subsodef(1,10) = 05, 07, 11, 13, 01, 02, 1, ;smpr6
subsodef(1,11) = 05, 07, 19, 21, 08, 09, 1, ;smpr7
subsodef(1,12) = 05, 07, 19, 21, 01, 02, 1, ;smpr8

```

\$end

M E S H

\$meshgn

```

iblock = 1,

xgrid =
0.0000e+00, 1.0000e+02, 1.8500e+02, 2.6500e+02, 2.7980e+02, 2.9000e+02,
3.3000e+02, 3.5500e+02, 4.0000e+02, 4.3000e+02,
ygrid =
0.0000e+00, 1.5000e+01, 3.5000e+01, 4.7000e+01, 5.4845e+01, 5.7479e+01,
6.3000e+01, 7.5000e+01, 9.0000e+01, 1.0500e+02, 1.2000e+02, 1.3500e+02,
1.5000e+02, 1.6500e+02, 1.8000e+02, 1.9500e+02, 2.1000e+02, 2.2500e+02,
2.4000e+02, 2.5500e+02, 2.7000e+02, 2.8500e+02, 3.0000e+02, 3.1500e+02,
3.3000e+02, 3.4500e+02, 3.6000e+02,
zgrid =
-1.3000e+02, -1.0000e+02, -5.0000e+01, 0.0000e+00, 5.0000e+01, 1.0000e+02,
1.5000e+02, 1.9000e+02, 2.2500e+02, 2.7500e+02, 2.8500e+02, 3.0000e+02,
3.3450e+02, 3.4950e+02, 3.9000e+02, 4.1375e+02, 4.3871e+02, 4.6500e+02,

```

\$end

H E A T T R A N S F E R & C O N D E N S A T I O N

\$rheat

```

ihtflag = 1,
teta     = 1.0,

ircomb = 1,
rcombdef = 4.5, 5.6, 13,14, 1, 185.37, 2, -4, 0.0, 0.0,

nhtesink=5,
nhteslab=20,
nhtewall=10,

matbdy = 1,

icond= 1,
const1 = 4.0,
tslab0=-1.,
tsink0=299.15,
twall0=-1.-

walldef(1,1) = 1,30.0, 0.0, 0.0, 0.5,
walldef(1,2) = 2, 0.5, 0.0, 0.0, 0.0,
walldef(1,3) = 1, 30., -1., -1., 0.0, ;h2 r5 adiabatic
walldef(1,4) = 2, 10., -0.1, 296., 0.0, ; sump graben

cfilmdef = 4, 05, 02, 26, 02, 02, 1, 10., ; smp Graben
      5, 07, 02, 11, 02, 02, 1, 10., ; smp Graben
      5, 07, 13, 19, 02, 02, 1, 10., ; smp Graben
      5, 07, 21, 26, 02, 02, 1, 10., ; smp Graben
      7, 08, 02, 26, 02, 02, 1, 10., ; smp Graben

nsumpppts = -4,

sumptime = 0.0, 4000., 5000., 1.e+99,
sumptemp = 27., 45., 70., 70.,

sinkdef= 9, 10, 24, 25, 4, 5,1,2,1.698e+4, 6.,0.0,299.15,0.,4*0.0.,;U89
      9, 10, 2, 3, 4, 5,1,2,1.698e+4, 6.,0.0,299.15,0.,4*0.0.,;U69
      9, 10, 14, 15, 7, 8,1,2,.996e+4, 6.,0.0,299.15,0.,4*0.0.,;R69A
      9, 10, 9, 10, 7, 8,1,2,.996e+4, 6.,0.0,299.15,0.,4*0.0.,;R69B
      9, 10, 16, 17, 15, 16,1,2,3.3e+4, 6.,0.0,299.15,0.,4*0.0.,;U79H
      9, 10, 17, 18, 15, 16,1,2,1.65e+4, 6.,0.0,299.15,0.,4*0.0.,;u79F
      9, 10, 24, 25, 15, 16,1,2,3.3e+4, 6.,0.0,299.15,0.,4*0.0.,;u79E
      9, 10, 25, 26, 15, 16,1,2,1.65e+4, 6.,0.0,299.15,0.,4*0.0.,;u79C
      9, 10, 6, 7, 15, 16,1,2,5.28e+4, 6.,0.0,299.15,0.,4*0.0.,;u59D
      9, 10, 10, 11, 15, 16,1,2,5.28e+4, 6.,0.0,299.15,0.,4*0.0.,;u59C
      4, 5, 25, 26, 15, 16,1,2,1.698e+4, 6.,0.0,299.15,0.,4*0.0.,;u27A
      4, 5, 21, 22, 15, 16,1,2,1.698e+4, 6.,0.0,299.15,0.,4*0.0.,;u27B
      4, 5, 18, 19, 15, 16,1,2,1.698e+4, 6.,0.0,299.15,0.,4*0.0.,;u27C
      4, 5, 12, 13, 15, 16,1,2,1.698e+4, 6.,0.0,299.15,0.,4*0.0.,;u25A
      4, 5, 8, 9, 15, 16,1,2,1.698e+4, 6.,0.0,299.15,0.,4*0.0.,;u25B
      4, 5, 2, 3, 15, 16,1,2,1.698e+4, 6.,0.0,299.15,0.,4*0.0.,;u25C
      8, 9, 25, 26, 17, 18,1,2,4.932e+4, 6.,0.0,299.15,0.,4*0.0.,;u79A
      8, 9, 16, 17, 17, 18,1,2,4.932e+4, 6.,0.0,299.15,0.,4*0.0.,;u79B
      8, 9, 13, 14, 17, 18,1,2,13.482e+4, 6.,0.0,299.15,0.,4*0.0.,;u59A
      8, 9, 4, 5, 17, 18,1,2,10.932e+4, 6.,0.0,299.15,0.,4*0.0.,;u59B

```

```
tslabbc = 299.15,
slabthk = 30.99,
dxslabc = 0.1,

$end
-----
G R A P H I C S
-----
$grafic

thdt = 5.,

pnt(1,1) = 5, 1, 1, 1,
pnt(1,2) = 05, 27, 18, 1,
pnt(1,3) = 8, 1, 1, 1,
pnt(1,4) = 08, 27, 18, 1,
pnt(1,5) = 1, 1, 13, 1,
pnt(1,6) = 10, 27, 13, 1,
pnt(1,7) = 01, 01, 05, 1,
pnt(1,8) = 10, 27, 05, 1,
pnt(1,9) = 1, 7, 1, 1,
pnt(1,10)= 10, 07, 18, 1,
pnt(1,11)= 1, 6, 01, 1,
pnt(1,12)= 10, 06, 18, 1,
pnt(1,13)= 8, 6, 2, 1,
pnt(1,14)= 08, 06, 18, 1,
pnt(1,15)= 05, 24, 02, 1,
pnt(1,16)= 05, 24, 18, 1,
pnt(1,17)= 05, 06, 09, 1,
pnt(1,18)= 05, 06, 18, 1,
pnt(1,19)= 01, 24, 01, 1,
pnt(1,20)= 10, 24, 18, 1,
pnt(1,21)= 09, 01, 01, 1,
pnt(1,22)= 09, 27, 18, 1,
pnt(1,23)= 10, 09, 03, 1,
pnt(1,24)= 10, 09, 18, 1,
pnt(1,25)= 1, 1, 12, 1,
pnt(1,26)= 10, 27, 12, 1,
pnt(1,27)= 1, 11, 1, 1,
pnt(1,28)= 10, 11, 18, 1,
pnt(1,29)= 1, 12, 1, 1,
pnt(1,30)= 10, 12, 18, 1,

ht1dp(1,1) = 08, 09, 18, 1, 'slab', 'top',
ht1dp(1,2) = 08, 21, 18, 1, 'slab', 'top',
ht1dp(1,3) = 10, 03, 18, 1, 'slab', 'south',
ht1dp(1,4) = 10, 15, 18, 1, 'wall', 'north',
ht1dp(1,5) = 10, 07, 16, 1, 'sink',
ht1dp(1,6) = 10, 25, 5, 1, 'sink',
ht1dp(1,7) = 10, 3, 5, 1, 'sink',
ht1dp(1,8) = 10, 15, 8, 1, 'sink',
ht1dp(1,9) = 10, 10, 8, 1, 'sink',
ht1dp(1,10) = 10, 17, 16, 1, 'sink',
ht1dp(1,11) = 10, 18, 16, 1, 'sink',
```

```

ht1dp(1,12) = 10, 25, 16, 1, 'sink',
ht1dp(1,13) = 10, 26, 16, 1, 'sink',
ht1dp(1,14) = 10, 7, 16, 1, 'sink',
ht1dp(1,15) = 10, 11, 16, 1, 'sink',
ht1dp(1,16) = 5, 26, 16, 1, 'sink',
ht1dp(1,17) = 5, 22, 16, 1, 'sink',
ht1dp(1,18) = 5, 19, 16, 1, 'sink',
ht1dp(1,19) = 5, 13, 16, 1, 'sink',
ht1dp(1,20) = 5, 9, 16, 1, 'sink',
ht1dp(1,21) = 5, 3, 16, 1, 'sink',
ht1dp(1,22) = 9, 26, 18, 1, 'sink',
ht1dp(1,23) = 9, 17, 18, 1, 'sink',
ht1dp(1,24) = 9, 14, 18, 1, 'sink',
ht1dp(1,25) = 9, 5, 18, 1, 'sink',
; ht1dp(1,6) = 09, 10, 09, 1, 'wall', 'west',
; ht1dp(1,7) = 09, 18, 04, 1, 'wall', 'west',

pld = 13, 14, 'wn', 0,
      15, 16, 'wn', 0,
      13, 14, 'vf', 'h2',
      15, 16, 'vf', 'h2',
      13, 14, 'vf', 'h2o',
      15, 16, 'vf', 'h2o',
      17, 18, 'vf', 'h2',
      17, 18, 'vf', 'h2o',
      17, 18, 'wn', 0,
      23, 24, 'wn', 0,
      23, 24, 'vf', 'h2o',

v2d(1,1)      = 01, 02, 1,
v2d(1,2)      = 3, 4, 1,
v2d(1,3)      = 5, 6, 1,
v2d(1,4)      = 7, 8, 1,
v2d(1,5)      = 9, 10, 1,
v2d(1,6)      = 11, 12, 1,
v2d(1,7)      = 19, 20, 1,
v2d(1,8)      = 21, 22, 1,
v2d(1,9)      = 25, 26, 1,
v2d(1,10)     = 27, 28, 1,
v2d(1,11)     = 29, 30, 1.

c2d(1,1)      = 01, 02, 'vf', 'h2',
c2d(1,2)      = 3, 4, 'vf', 'h2',
c2d(1,3)      = 5, 6, 'vf', 'h2',
c2d(1,4)      = 7, 8, 'vf', 'h2',
c2d(1,5)      = 9, 10, 'vf', 'h2',
c2d(1,6)      = 11, 12, 'vf', 'h2',
c2d(1,7)      = 19, 20, 'vf', 'h2',
c2d(1,8)      = 01, 02, 'vf', 'h2o',
c2d(1,9)      = 3, 4, 'vf', 'h2o',
c2d(1,10)     = 5, 6, 'vf', 'h2o',
c2d(1,11)     = 7, 8, 'vf', 'h2o',
c2d(1,12)     = 9, 10, 'vf', 'h2o',
c2d(1,13)     = 11, 12, 'vf', 'h2o',
c2d(1,14)     = 19, 20, 'vf', 'h2o',

```

```

c2d(1,15)      =  01,  02,  'tk',  0,
c2d(1,16)      =  3,   4,  'tk',  0,
c2d(1,17)      =  5,   6,  'tk',  0,
c2d(1,18)      =  7,   8,  'tk',  0,
c2d(1,19)      =  9,  10,  'tk',  0,
c2d(1,20)      = 11,  12,  'tk',  0,
c2d(1,21)      = 19,  20,  'tk',  0,

thp(1,1)        = 05,  06,  13,  1,  'vdotz',  0, ;2
thp(1,2)        = 05,  06,  13,  1,  'vf',  'h2', ;3
thp(1,3)        = 05,  06,  13,  1,  'tk',  0, ;4
thp(1,4)        = 05,  06,  13,  1,  'wn',  0, ;5
thp(1,5)        = 05,  06,  15,  1,  'vdotx',  0, ;6
thp(1,6)        = 05,  06,  15,  1,  'vf',  'h2', ;7
thp(1,7)        = 05,  06,  15,  1,  'tk',  0, ;8
thp(1,8)        = 05,  06,  15,  1,  'wn',  0, ;9
thp(1,9)        = 05,  06,  13,  1,  'vf',  'h2', ;10
thp(1,10)       = 05,  06,  14,  1,  'vf',  'h2', ;11
thp(1,11)       = 05,  06,  15,  1,  'vf',  'h2', ;12
thp(1,12)       = 05,  06,  17,  1,  'vf',  'h2', ;13

10, 15,  9,  1,  'delt',  0, ;14

8,  9,  16,  1,  'vf',  'h2', ; 15 5KH270M17
8, 21, 16,  1,  'vf',  'h2', ; 16 7KH090M17
5,  8, 17,  1,  'vf',  'h2', ; 17 MKH295I19
7,  4,  9,  1,  'vf',  'h2', ; 18 6KH318U30
8, 24,  9,  1,  'vf',  'h2', ; 19 8KH046U30
2,  2,  4,  1,  'vf',  'h2', ; 20 3KH000M10
2,  2,  8,  1,  'vf',  'h2', ; 21 3KH000M30
8, 21,  5,  1,  'vf',  'h2', ; 22 8KH090M13
8,  9,  5,  1,  'vf',  'h2', ; 23 6KH270M13
5,  6, 13,  1,  'wn',  0, ; 24 MVT000M0
5,  6, 13,  1,  'tc',  0, ; 25 MTL000M00
5,  6, 14,  1,  'tc',  0, ; 26 MTL000M020
5,  6, 14,  1,  'tc',  0, ; 27 MTL001M020
5,  6, 17,  1,  'tc',  0, ; 28 MTL000M08
8,  9, 18,  1,  'tc',  0, ; 29 5TS270M22
8,  9, 14,  1,  'tc',  0, ; 30 5TS270M12
8,  9, 10,  1,  'tc',  0, ; 31 5TS270M02
8,  9,  8,  1,  'tc',  0, ; 32 6TS270M27
8,  9,  6,  1,  'tc',  0, ; 33 6TS270M17
8,  9,  3,  1,  'tc',  0, ; 34 6TS270M05
8, 13, 18,  1,  'tc',  0, ; 35 5TS210M22
8, 13, 14,  1,  'tc',  0, ; 36 5TS210M12
8, 13, 10,  1,  'tc',  0, ; 37 5TS210M02
8, 16, 15,  1,  'tc',  0, ; 38 7TS180U15
8, 16, 10,  1,  'tc',  0, ; 39 7TS180U05
8,  3, 18,  1,  'tc',  0, ; 40 5TS335M22
8,  3, 14,  1,  'tc',  0, ; 41 5TS335M12
7,  4,  9,  1,  'tc',  0, ; 42 6TS318U30
8, 21, 18,  1,  'tc',  0, ; 43 7TS090M22
8, 21, 14,  1,  'tc',  0, ; 44 7TS090M12
8, 21, 10,  1,  'tc',  0, ; 45 7TS090M02
8, 21,  8,  1,  'tc',  0, ; 46 8TS090M27

```

```

8, 21, 6, 1, 'tc', 0, ; 47 8TS090M17
8, 21, 3, 1, 'tc', 0, ; 48 8TS090M05
2, 2, 10, 1, 'tc', 0, ; 49 3TS000M40
2, 2, 8, 1, 'tc', 0, ; 50 3TS000M30
2, 2, 6, 1, 'tc', 0, ; 51 3TS000M20
2, 2, 4, 1, 'tc', 0, ; 52 3TS000M10
10, 9, 17, 1, 'pn', 0, ; 53 5PL270A12
09, 9, 09, 1, 'wn', 0, ; 54 h2or5
09, 09, 04, 1, 'wn', 0, ; 55 h2or6
09, 17, 04, 1, 'wn', 0, ; 56 h2or8
05, 02, 14, 1, 'vn', 0, ; 57 airr5
05, 02, 05, 1, 'vn', 0, ; 58 airr6
05, 26, 05, 1, 'vn', 0, ; 59 airr8
06, 12, 09, 1, 'wn', 0, ; 60 smpr5
06, 12, 02, 1, 'wn', 0, ; 61 smpr6
06, 20, 09, 1, 'wn', 0, ; 62 smpr7
06, 20, 02, 1, 'wn', 0, ; 63 smpr8

8, 14, 03, 1, 'tc', 0, ; 64 smp graben
8, 14, 03, 1, 'vf', 'h2o', , 65 smp graben
8, 17, 03, 1, 'tc', 0, ; 66 smp graben
8, 17, 03, 1, 'vf', 'h2o', , 67 smp graben
4, 1, -1, -1, 'un', 0, ; damper velocity
4, 1, -1, -1, 'mdotx', 0, ; damper mass flow rate
3, 2, -1, -1, 'mdotx', 0, ; leakage duct 2 mass flow rate
3, 3, -1, -1, 'mdotx', 0, ; leakage duct 3 mass flow rate
3, 4, -1, -1, 'mdotx', 0, ; leakage duct 4 mass flow rate
3, 5, -1, -1, 'mdotx', 0, ; leakage duct 5 mass flow rate
3, 6, -1, -1, 'mdotx', 0, ; leakage duct 6 mass flow rate
3, 7, -1, -1, 'mdotx', 0, ; leakage duct 7 mass flow rate
3, 8, -1, -1, 'mdotx', 0, ; leakage duct 8 mass flow rate
3, 9, -1, -1, 'mdotx', 0, ; leakage duct 9 mass flow rate
3, 10, -1, -1, 'mdotx', 0, ; leakage duct 10 mass flow rate
3, 11, -1, -1, 'mdotx', 0, ; leakage duct 11 mass flow rate
3, 12, -1, -1, 'mdotx', 0, ; leakage duct 12 mass flow rate
3, 13, -1, -1, 'mdotx', 0, ; leakage duct 13 mass flow rate
3, 14, -1, -1, 'mdotx', 0, ; leakage duct 14 mass flow rate

htthp(1,1) = 08, 09, 18, 1, 'slab', 'top', ; 68 W7TS270M22 (29)
htthp(1,2) = 08, 21, 18, 1, 'slab', 'top', ; 69 W7TS090M22 (43)
; htthp(1,4) = 09, 10, 09, 1, 'wall', 'west', ; 73
htthp(1,3) = 08, 17, 03, 1, 'wall', 'bottom', ; 79 smp graben

; htthp(1, 3) = 08, 03, 14, 1, 'slab', 'south', ; 70 W7TS335M12 (41)
; htthp(1, 4) = 09, 10, 09, 1, 'slab', 'north', ; 71
; htthp(1, 5) = 09, 10, 09, 1, 'wall', 'bottom', ; 72
; htthp(1, 6) = 09, 10, 09, 1, 'wall', 'west', ; 73
; htthp(1, 7) = 09, 18, 04, 1, 'wall', 'west', ; 74
; htthp(1, 8) = 07, 10, 09, 1, 'slab', 'bottom', ; 75
; htthp(1, 9) = 08, 10, 10, 1, 'slab', 'bottom', ; 76
; htthp(1,10) = 08, 15, 17, 1, 'wall', 'south', ; 77
; htthp(1,10) = 08, 14, 03, 1, 'wall', 'bottom', ; 78 ;smp graben
; htthp(1,10) = 08, 17, 03, 1, 'wall', 'bottom', ; 79 ;smp graben

```

\$end

P A R T I C L E S

\$parts

\$end

S P E C I A L

\$special

\$end

8.2.4. Battelle Containment HYJET Test JX7

8.2.4.1. Summary.

Purpose
Validation of the capability to model small- and large-scale effects (turbulent jet and convection in the containment) within one calculation.
Success Metrics
The GASFLOW-calculated hydrogen concentrations will agree with the experimentally measured helium concentrations in the BMC.
Problem Description
Test JX7 involved the full BMC, except for banana room R7, with a total gas volume of 600 m ³ . Helium with a total mass of 9.25 kg was injected upward in 200 s near the bottom of banana room R6 (see Figure 8-18). The nozzle had a diameter of 95 mm and an average injection jet velocity of 42 m/s. The nozzle was positioned under vertically overflow openings from R6 to R5 and to the dome. A jet formed that extended all the way from the source location into the dome region. Helium concentrations were measured at selected locations within the BMC.
Relationship to Code Models and Methods
See Table 7-1.
Relationship to PIRT Phenomena
Code Version and Modifications
GASFLOW 2.1.0.11. No modifications were made to the 2.1.0.11 source.
Hardware and Operating System
CRAY-J90 UNICOS operating system.
Compiler, Version, and Optimization Level
CRAY Fortran 90, Version 3.0.0.1.
Runtime Statistics: Total Run Time; Grind Time Problem took 2 weeks to complete.
Results and Conclusions The GASFLOW results agree with experimental results.

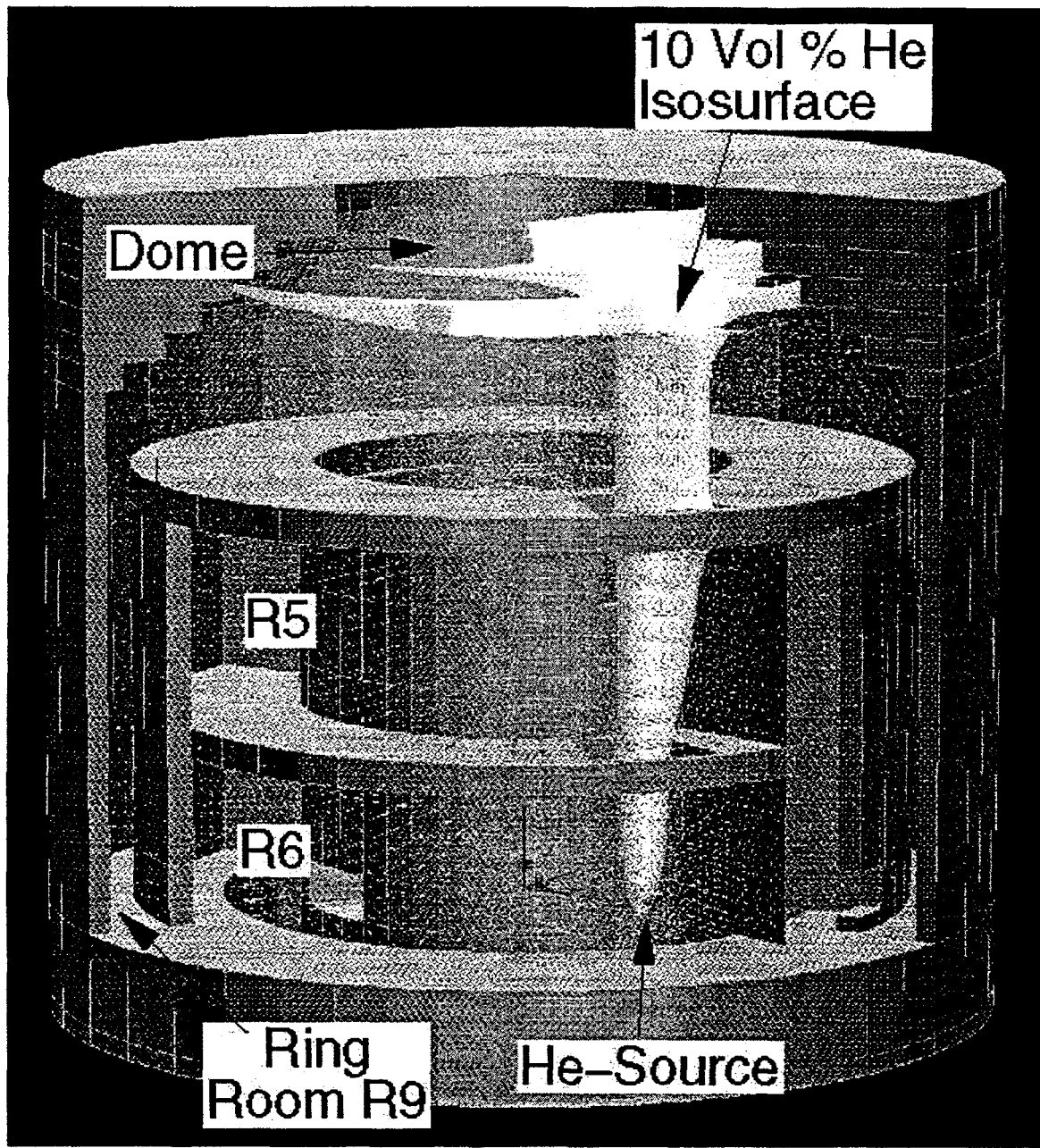


Fig. 8-22. Helium jet in BMC during Hyjet test Jx7 at 50 s (GASFLOW-Kismet)

8.2.4.2. Test Description. Test JX7 involved the full BMC, except for banana room R7, with a total gas volume of 600 m^3 . Helium with a total mass of 9.25 kg was injected upward in 200 s near the bottom of R6 (see Figure 8-18). The nozzle had a diameter of 95 mm and an average injection jet velocity of 42 m/s. The nozzle was positioned under vertically overflow openings from banana room R6 to banana room R5 and to the dome. A jet formed that extended all the way from the source location into the dome region. Helium concentrations were measured at selected locations within the BMC.

8.2.4.3. GASFLOW Calculations.

8.2.4.3.1. **GASFLOW Input Model.** The calculations were performed with GASFLOW, Version 2.1.0.11. No local updates or modifications were made to the code. The GASFLOW model uses 50,000 computational cells, with small cells around the nozzle and in the jet. The nozzle is represented by one single cell. The algebraic turbulence model was used for this calculation.

8.2.4.3.2. **GASFLOW Results.** The helium jet formed in the BMC extended all the way from the source location into the dome region and is displayed in Figure 8-22 at 50 s after the start of helium injection as the isosurface for 10 vol % helium. As can be seen in Figure 8-22, the helium stratifies as a cloud in the containment dome. In the experimental data it was found that the jet axis was shifted slightly due to the geometry of the BMC for this test.

Figure 8-23 is a comparison of the GASFLOW calculation with the measured data for the helium concentration at four sensor locations (i.e., in the dome, near the bottom of the central room, and in the upper and lower part of the ring room). In general, GASFLOW predicts the dominate trends well and predicts the helium stratification consistently with the data. Good agreement also is obtained in the central room and in the lower part of the ring room. The overprediction of the helium concentration in the dome region can be attributed to insufficient air entrainment along the jet surface.

In the upper overflow opening from R5 to the dome there was a flow coming down outside the jet. This was predicted by GASFLOW and observed in the experimental data (see Figure 8-24). However, from Figures 8-25 and 8-26, it can be seen that GASFLOW was not entraining enough air into the jet.

8.2.4.4. **Conclusions and Recommendations.** The GASFLOW, Version 2.1.0.11 results are in agreement with the test results, as required by the success metric.

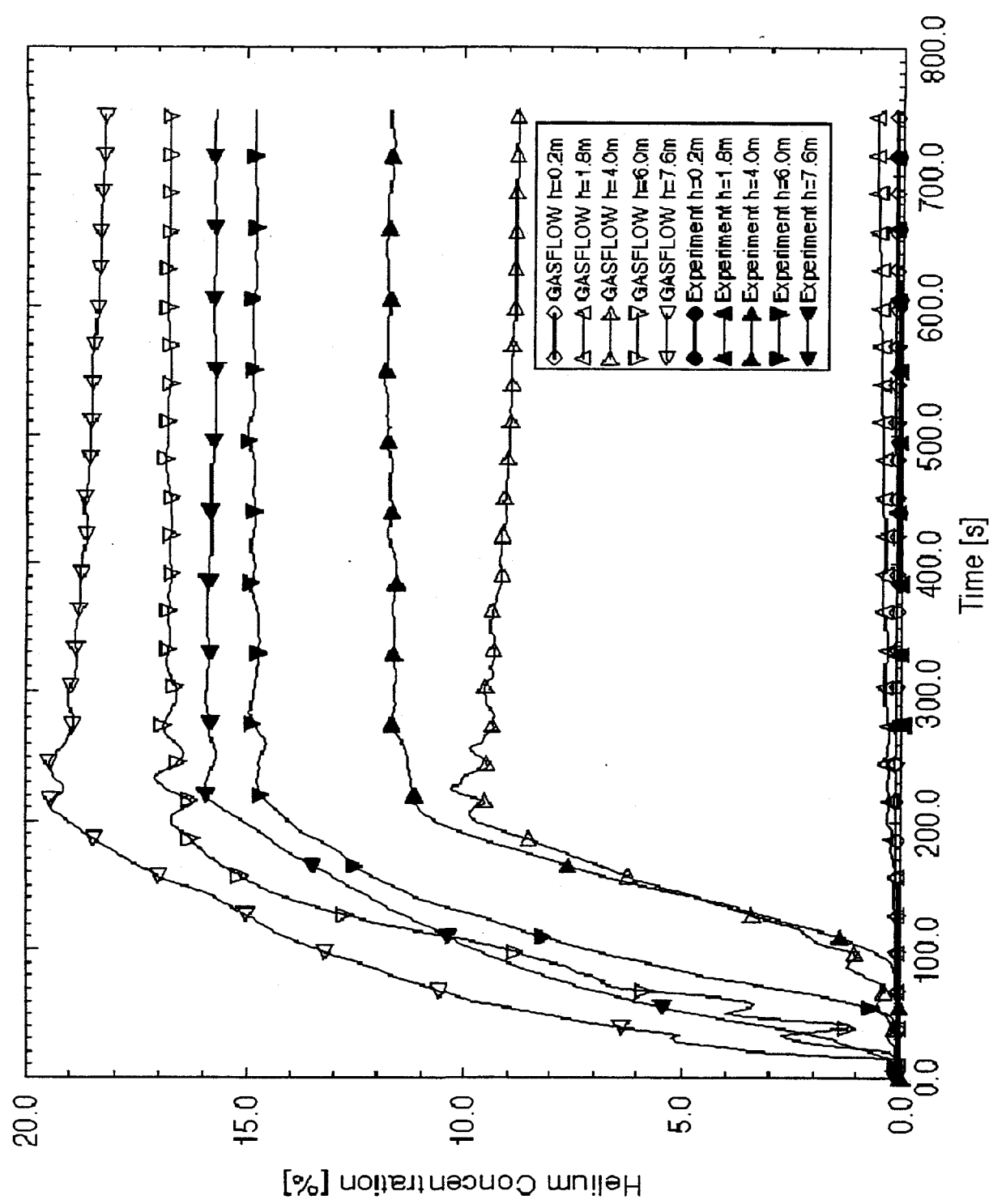


Fig. 8-23. He concentrations as a function of time at selected axial levels

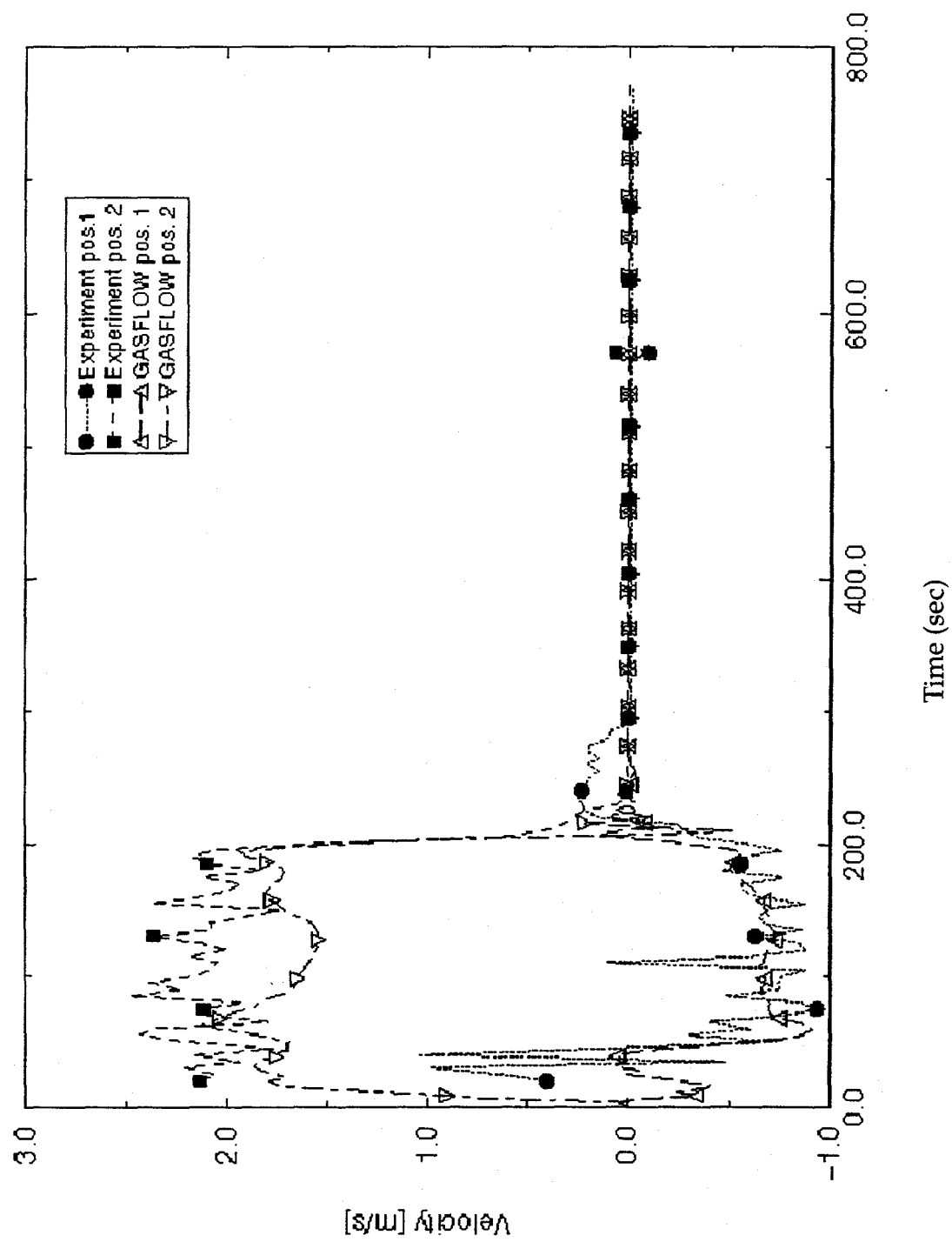


Fig. 8-24. He concentrations as a function of time at two different positions

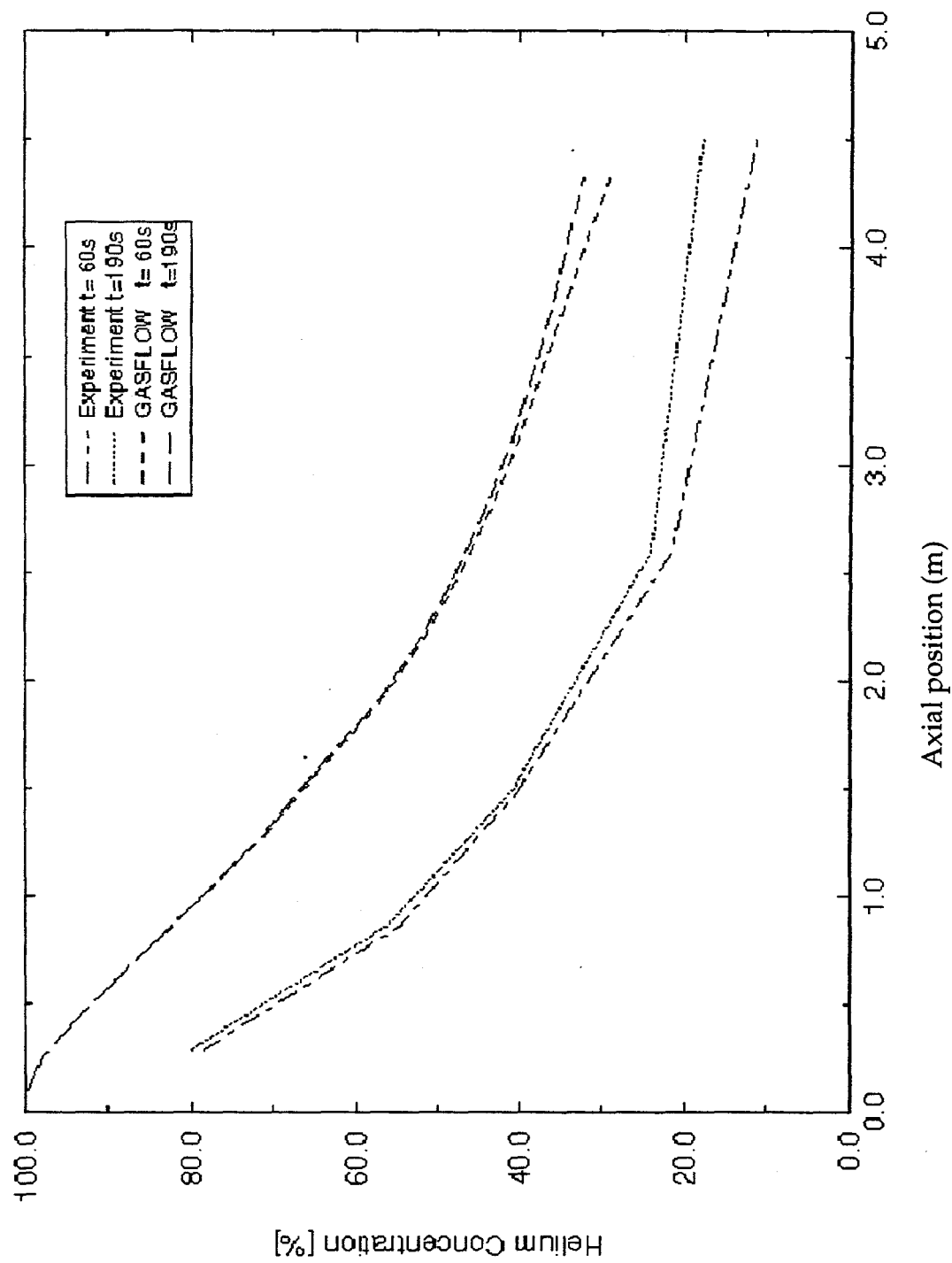


Fig. 8-25. He concentrations as a function of axial position at two different times

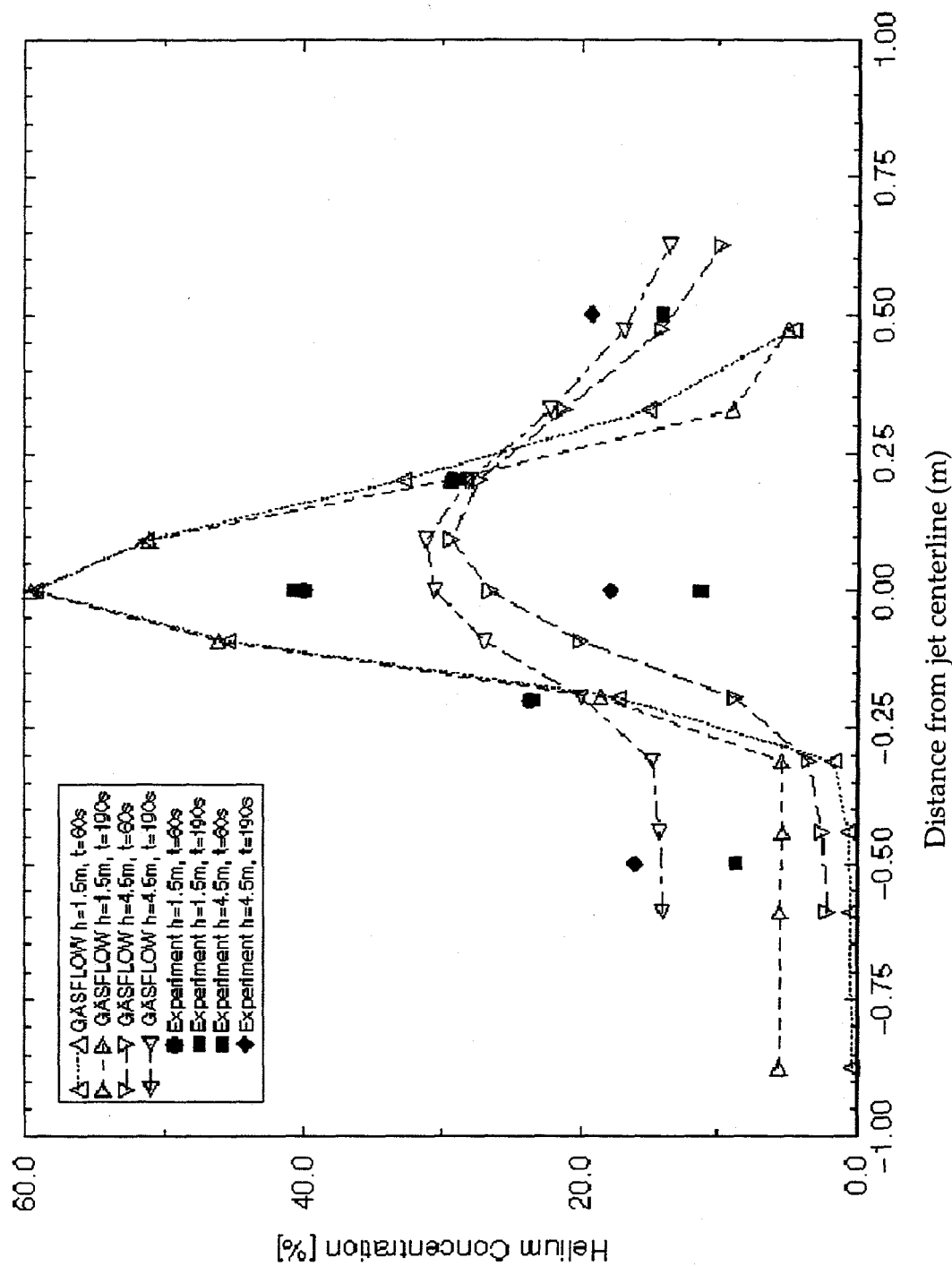


Fig. 8-26. He concentrations as a function of radial position from the jet center line at two different times and two different axial positions

8.2.4.5. Input File Listing.

3D-Battelle HYJET-Experiment

NOTES: 3-D domain

Number of fluid cells = 31 x 52 x 39 = 62868 for the
coordinate dimension r, theta, and z, respectively.

\$innet

\$end

\$xput

nrsdump = 0,

iburn = 0,

cyl = 1.,

idiffmom = 1,
idiffme = 1,

ieopt = 1,
trange = 'low',
icopt = 2,
itopt = 1,

tmodel = 'alg',
; fractke = 0.25,

autot = 1.0,
delt0 = 0.015,
deltmin = 1.000e-9,
deltmax = 1.0,

epsi0 = 1.000e-06,
epsimax = 1.000e-06,
epsimin = 1.000e-06,
itdowndt = 350,
itupdt = 350,
itmax = 1000,

gx = 0.0,
gy = 0.0,
gz = -980.0,

lpr = 1,
ittyfreq = 1,
plttdt = 25., ; pgf
prttdt = 1000.0, ; gfout
tddt = 250.0, ; gfd
velmx = 2.5,

```
; maxcyc = -56,  
maxcyc = 1000000000,  
; twfin = 0.1,  
twfin = 800.,
```

```
ibs = 4,  
ibn = 4,  
ibe = 1,  
ibw = 1,  
ibb = 1,  
ibt = 1,
```

```
mobs= 7, 11, 1, 52, 1, 8, 1, 1, ; inner zylinder lower part  
7, 11, 2, 4, 8, 11, 1, 1, ; inner zylinder lower part  
7, 11, 7, 9, 8, 11, 1, 1, ; inner zylinder lower part  
7, 11, 11, 13, 8, 11, 1, 1, ; inner zylinder lower part  
7, 11, 15, 16, 8, 11, 1, 1, ; inner zylinder lower part  
7, 11, 18, 25, 8, 11, 1, 1, ; inner zylinder lower part  
7, 11, 28, 51, 8, 11, 1, 1, ; inner zylinder lower part  
7, 11, 1, 52, 11, 16, 1, 1, ; inner zylinder lower part  
7, 11, 1, 12, 16, 18, 1, 1, ; inner zylinder lower part  
7, 11, 14, 52, 16, 18, 1, 1, ; inner zylinder lower part  
7, 11, 1, 52, 18, 21, 1, 1, ; inner zylinder lower part  
  
6, 7, 1, 52, 11, 14, 1, 1,  
  
9, 11, 1, 52, 21, 24, 1, 1, ; inner zylinder upper part  
9, 11, 1, 22, 24, 26, 1, 1, ; inner zylinder upper part  
9, 11, 24, 41, 24, 26, 1, 1, ; inner zylinder upper part  
9, 11, 47, 52, 24, 26, 1, 1, ; inner zylinder upper part  
9, 11, 1, 52, 26, 27, 1, 1, ; inner zylinder upper part  
  
10, 26, 1, 38, 27, 29, 1, 1, ; roof R4,R5,R7  
10, 13, 38, 47, 27, 29, 1, 1, ; roof R4,R5,R7  
24, 26, 38, 47, 27, 29, 1, 1, ; roof R4,R5,R7  
10, 26, 47, 52, 27, 29, 1, 1, ; roof R4,R5,R7  
11, 12, 1, 52, 26, 27, 1, 1,  
  
24, 26, 1, 52, 1, 9, 1, 1, ; outer zylinder  
24, 26, 2, 6, 9, 12, 1, 1, ; outer zylinder  
24, 26, 7, 40, 9, 12, 1, 1, ; outer zylinder  
24, 26, 44, 51, 9, 12, 1, 1, ; outer zylinder  
24, 26, 1, 52, 12, 29, 1, 1, ; outer zylinder  
  
11, 31, 1, 52, 1, 2, 1, 1, ; bottom  
18, 31, 1, 52, 2, 8, 1, 1, ; bottom  
  
11, 24, 3, 38, 18, 19, 1, 1, ; seeling R5/R6  
11, 12, 38, 47, 18, 19, 1, 1, ; seeling R5/R6  
23, 24, 38, 47, 18, 19, 1, 1, ; seeling R5/R6  
11, 24, 47, 50, 18, 19, 1, 1, ; seeling R5/R6  
  
; 30, 31, 1, 52, 32, 33, 1, 1, ; inclind  
; 29, 31, 1, 52, 33, 34, 1, 1, ; inclind
```

```

;      27, 31, 1, 52, 34, 35, 1, 1, ; inclind
;      23, 31, 1, 52, 35, 36, 1, 1, ; inclind
;      20, 31, 1, 52, 36, 37, 1, 1, ; inclind
;      14, 31, 1, 52, 37, 38, 1, 1, ; inclind
;      10, 31, 1, 52, 38, 39, 1, 1, ; inclind

```

```

30, 31, 1, 52, 32, 33, 1, 1, ; inclind
29, 31, 1, 52, 33, 34, 1, 1, ; inclind
26, 31, 1, 52, 34, 35, 1, 1, ; inclind
23, 31, 1, 52, 35, 36, 1, 1, ; inclind
20, 31, 1, 52, 36, 37, 1, 1, ; inclind
15, 31, 1, 52, 37, 38, 1, 1, ; inclind
10, 31, 1, 52, 38, 39, 1, 1, ; inclind

```

```
17, 21, 40, 44, 1, 10, 1, 1, ; source box
```

walls	=	11, 18, 3, 3, 2, 8, 1, 1, ; R4, R8 u.R7
		11, 24, 3, 3, 8, 27, 1, 1, ; R4, R8 u.R7
		11, 18, 50, 50, 2, 8, 1, 1, ; R4, R6 u.R5
		11, 24, 50, 50, 8, 27, 1, 1, ; R4, R6 u.R5
		11, 18, 20, 20, 2, 8, 1, 1, ; R8 u. R7, R6 u.R5
		11, 24, 20, 20, 8, 27, 1, 1, ; R8 u. R7, R6 u.R5
		18, 19, 42, 43, 10, 10, 1, 2, ; source
		18, 19, 42, 42, 10, 11, 1, 2, ; source
		18, 19, 43, 43, 10, 11, 1, 2, ; source
		18, 18, 42, 43, 10, 11, 1, 2, ; source
		19, 19, 42, 43, 10, 11, 1, 2, ; source
		21, 21, 40, 44, 10, 11, 1, 2, ; source plate
		21, 22, 40, 44, 11, 11, 1, 2, ; source plate
		22, 22, 40, 44, 11, 12, 1, 2, ; source plate
		22, 23, 40, 44, 12, 12, 1, 2, ; source plate
		23, 23, 40, 44, 12, 13, 1, 2, ; source plate
		23, 24, 40, 44, 13, 13, 1, 2, ; source plate

areardef	=	;	U 34
		7, 7, 4, 5, 8, 11, 1, 0.1669, ; U 38 A	
		7, 7, 8, 11, 8, 11, 1, 0.9054, ; U 38 B	
		7, 7, 12, 13, 8, 11, 1, 0.2413, ; U 38 C	
		7, 7, 14, 15, 8, 11, 1, 0.5694, ; U 38 C	
		7, 7, 16, 18, 8, 11, 1, 0.9054, ; U 38 D	
		8, 8, 4, 5, 8, 11, 1, 0.1669, ; U 38 A	
		8, 8, 8, 11, 8, 11, 1, 0.9054, ; U 38 B	
		8, 8, 12, 13, 8, 11, 1, 0.2413, ; U 38 C	
		8, 8, 14, 15, 8, 11, 1, 0.5694, ; U 38 C	
		8, 8, 16, 18, 8, 11, 1, 0.9054, ; U 38 D	
		9, 9, 4, 5, 8, 11, 1, 0.1669, ; U 38 A	
		9, 9, 8, 11, 8, 11, 1, 0.9054, ; U 38 B	
		9, 9, 12, 13, 8, 11, 1, 0.2413, ; U 38 C	

9,	9,	14,	15,	8,	11,	1,	0.5694,	; U 38 C
9,	9,	16,	18,	8,	11,	1,	0.9054,	; U 38 D
10,	10,	4,	5,	8,	11,	1,	0.1669,	; U 38 A
10,	10,	8,	11,	8,	11,	1,	0.9054,	; U 38 B
10,	10,	12,	13,	8,	11,	1,	0.2413,	; U 38 C
10,	10,	14,	15,	8,	11,	1,	0.5694,	; U 38 C
10,	10,	16,	18,	8,	11,	1,	0.9054,	; U 38 D
11,	11,	4,	5,	8,	11,	1,	0.1669,	; U 38 A
11,	11,	8,	11,	8,	11,	1,	0.9054,	; U 38 B
11,	11,	12,	13,	8,	11,	1,	0.2413,	; U 38 C
11,	11,	14,	15,	8,	11,	1,	0.5694,	; U 38 C
11,	11,	16,	18,	8,	11,	1,	0.9054,	; U 38 D
7,	7,	25,	26,	8,	11,	1,	0.5431,	; U 36 C
7,	7,	27,	28,	8,	11,	1,	0.4998,	; U 36 C
8,	8,	25,	26,	8,	11,	1,	0.5431,	; U 36 C
8,	8,	27,	28,	8,	11,	1,	0.4998,	; U 36 C
9,	9,	25,	26,	8,	11,	1,	0.5431,	; U 36 C
9,	9,	27,	28,	8,	11,	1,	0.4998,	; U 36 C
10,	10,	25,	26,	8,	11,	1,	0.5431,	; U 36 C
10,	10,	27,	28,	8,	11,	1,	0.4998,	; U 36 C
11,	11,	25,	26,	8,	11,	1,	0.5431,	; U 36 C
11,	11,	27,	28,	8,	11,	1,	0.4998,	; U 36 C
24,	24,	1,	2,	9,	12,	1,	0.4388,	; U 49 A
24,	24,	51,	52,	9,	12,	1,	0.4388,	; U 49 A
25,	25,	1,	2,	9,	12,	1,	0.4388,	; U 49 A
25,	25,	51,	52,	9,	12,	1,	0.4388,	; U 49 A
26,	26,	1,	2,	9,	12,	1,	0.4388,	; U 49 A
24,	24,	6,	7,	9,	12,	1,	0.7735,	; U 89
25,	25,	6,	7,	9,	12,	1,	0.7735,	; U 89
26,	26,	6,	7,	9,	12,	1,	0.7735,	; U 89
								; U 69
7,	7,	16,	12,	13,	18,	1,	0.2248,	; Estg
8,	8,	16,	12,	13,	18,	1,	0.2248,	; Estg
9,	9,	16,	12,	13,	18,	1,	0.2248,	; Estg
10,	10,	16,	12,	13,	18,	1,	0.2248,	; Estg
11,	11,	16,	12,	13,	18,	1,	0.2248,	; Estg
9,	9,	22,	24,	24,	26,	1,	0.5612,	; U 25 A
9,	9,	41,	42,	24,	26,	1,	0.3170,	; U 25 C
10,	10,	22,	24,	24,	26,	1,	0.5612,	; U 25 A
10,	10,	41,	42,	24,	26,	1,	0.3170,	; U 25 C
11,	11,	22,	24,	24,	26,	1,	0.5612,	; U 25 A
11,	11,	41,	42,	24,	26,	1,	0.3170,	; U 25 C
								; U 56 B
13,	24,	38,	39,	27,	27,	1,	0.8893,	; U 59 B
13,	24,	38,	39,	28,	28,	1,	0.8893,	; U 59 B
13,	24,	38,	39,	29,	29,	1,	0.8893,	; U 59 B

```

ihystat = 0,

; iroomdef(1,1)= 1,31, 1, 52, 1, 39, 1, +1, ; all
; iroomdef(1,2)= 11,24, 3, 20, 18, 27, 1, -1,
; iroomdef(1,3)= 1,11, 1, 52, 1, 29, 1, +2, ; R 3
; iroomdef(1,4)= 24,31, 1, 52, 1, 29, 1, +3, ; R 9 r
; iroomdef(1,5)= 1,31, 1, 52, 29, 39, 1, +4, ; R 9 d
; iroomdef(1,6)= 11,24, 1, 3, 1, 27, 1, +5, ; R 4
; iroomdef(1,7)= 11,24, 50, 52, 2, 27, 1, +5, ; R 4
; iroomdef(1,8)= 11,24, 20, 50, 18, 27, 1, +6, ; R 8
; iroomdef(1,9)= 11,24, 20, 50, 1, 18, 1, +7, ; R 6
; iroomdef(1,10)=11,24, 3, 20, 1, 18, 1, +8, ; R 5

mat = 'air', 'he',

gasdef(1,1) = 0, 32, 0, 53, 0, 40, 1, 1.011e+06, 308.15, 2, ; full
0., 0., 'air', 1.0000, 'he', 0.0000,

gasdef(1,2) = 1, 10, 1, 52, 1, 14, 1, 1.011e+06, 302.75, 2, ; R3 U
0., 0., 'air', 0.9994, 'he', 0.0006,
gasdef(1,3) = 1, 6, 1, 52, 14, 21, 1, 1.011e+06, 304.05, 2, ; R3 M
0., 0., 'air', 0.9991, 'he', 0.0009,
gasdef(1,4) = 6, 10, 1, 52, 14, 21, 1, 1.011e+06, 307.75, 2, ; R3 M
0., 0., 'air', 0.9991, 'he', 0.0009,
gasdef(1,5) = 1, 8, 1, 52, 21, 29, 1, 1.011e+06, 305.35, 2, ; R3 O
0., 0., 'air', 0.9989, 'he', 0.0011,
gasdef(1,6) = 8, 10, 1, 52, 21, 29, 1, 1.011e+06, 306.85, 2, ; R3 O
0., 0., 'air', 0.9989, 'he', 0.0011,

gasdef(1,7) = 10, 12, 3, 20, 1, 19, 1, 1.011e+06, 302.95, 2, ; R8 i
0., 0., 'air', 0.9991, 'he', 0.0009,
gasdef(1,8) = 12, 23, 3, 20, 1, 19, 1, 1.011e+06, 305.05, 2, ; R8 g
0., 0., 'air', 0.9991, 'he', 0.0009,
gasdef(1,9) = 23, 25, 3, 20, 1, 19, 1, 1.011e+06, 302.95, 2, ; R8 a
0., 0., 'air', 0.9991, 'he', 0.0009,

gasdef(1,10)= 25, 27, 1, 52, 1, 19, 1, 1.011e+06, 302.45, 2, ; R9 RR U i
0., 0., 'air', 0.9989, 'he', 0.0011,
gasdef(1,11)= 27, 30, 1, 52, 1, 19, 1, 1.011e+06, 302.85, 2, ; R9 RR U m
0., 0., 'air', 0.9989, 'he', 0.0011,
gasdef(1,12)= 30, 31, 1, 52, 1, 19, 1, 1.011e+06, 301.25, 2, ; R9 RR U a
0., 0., 'air', 0.9989, 'he', 0.0011,

gasdef(1,13)= 25, 27, 1, 52, 19, 29, 1, 1.011e+06, 304.15, 2, ; R9 RR O i
0., 0., 'air', 0.9989, 'he', 0.0011,
gasdef(1,14)= 27, 30, 1, 52, 19, 29, 1, 1.011e+06, 304.15, 2, ; R9 RR O m
0., 0., 'air', 0.9989, 'he', 0.0011,
gasdef(1,15)= 30, 31, 1, 52, 19, 29, 1, 1.011e+06, 304.05, 2, ; R9 RR O a
0., 0., 'air', 0.9989, 'he', 0.0011,

gasdef(1,16)= 1, 22, 1, 52, 29, 35, 1, 1.011e+06, 305.35, 2, ; R9 K U g
0., 0., 'air', 0.9993, 'he', 0.0007,

```

```

gasdef(1,17)= 22, 31, 1, 52, 29, 35, 1, 1.011e+06, 306.05, 2, ; R9 K U a
0., 0., 'air', 0.9993, 'he', 0.0007,
gasdef(1,18)= 1, 31, 1, 52, 29, 39, 1, 1.011e+06, 305.85, 2, ; R9 K O
0., 0., 'air', 0.9987, 'he', 0.0013,
gasdef(1,19)= 12, 23, 20, 50, 19, 29, 1, 1.011e+06, 305.55, 2, ; R5 g
0., 0., 'air', 0.9990, 'he', 0.0010,
gasdef(1,20)= 10, 12, 20, 50, 19, 29, 1, 1.011e+06, 304.75, 2, ; R5 i
0., 0., 'air', 0.9990, 'he', 0.0010,
gasdef(1,21)= 23, 25, 20, 50, 19, 29, 1, 1.011e+06, 304.75, 2, ; R5 a
0., 0., 'air', 0.9990, 'he', 0.0010,
gasdef(1,22)= 12, 23, 20, 50, 1, 19, 1, 1.011e+06, 303.55, 2, ; R6 g
0., 0., 'air', 0.9986, 'he', 0.0014,
gasdef(1,23)= 10, 12, 20, 50, 1, 19, 1, 1.011e+06, 303.05, 2, ; R6 i
0., 0., 'air', 0.9986, 'he', 0.0014,
gasdef(1,24)= 23, 25, 20, 50, 1, 19, 1, 1.011e+06, 303.05, 2, ; R6 a
0., 0., 'air', 0.9986, 'he', 0.0014,
gasdef(1,25)= 18, 19, 42, 43, 10, 11, 1, -19431201.,; source
300.15, 2, 0., 1000., 'he', 1.0000,
; vbc(1,1) = 18, 19, 42, 43, 11, 11, 1, 3, 0., 1000.,
; vbc(1,1) = 18, 19, 42, 43, 11, 11, 1, 1, 0., 50.,
; vbc(1,2) = 18, 19, 42, 43, 11, 11, 1, 3, 50., 80.,
; vbc(1,3) = 18, 19, 42, 43, 11, 11, 1, 2, 80., 240.,
; vbc(1,4) = 18, 19, 42, 43, 11, 11, 1, 3, 240., 250.,
; vbc(1,5) = 18, 19, 42, 43, 11, 11, 1, 1, 250., 800.,
; vvalue = 0.0, 4023.0, 2011.0,
mbc(1,1) = 18, 19, 42, 43, 11, 11, 1, 151, 0., 1000.,
mvalue = 0.0,
; time(sec) mdot(gm/s) Integral(mdot*delt)(gm)
mtab = 0.0, 0.0, ; 0.0
50.0, 0.0, ; 0.0
60.0, 25.0, ; 125.0
62.0, 25.0, ; 175.0
70.0, 45.0, ; 455.0
72.0, 45.0, ; 545.0
80.0, 49.0, ; 921.0
243.0, 48.1, ; 8834.65
254.0, 0.0, ; 9099.2
1000.0, 0.0, ; 9099.2
; turbdef(1,1) = 0, 32, 0, 53, 0, 40, 1, 1, 1, 0, 0.0, 0.0,
; turbdef(1,2) = 18, 19, 42, 43, 10, 11, 1, 2, 2, 0, 50.0, 250.0,

```

```

; tkeval = 0.01, 15000.,
; epsval = 0.09, 5500.,

subsodef(1,1) = 18, 19, 42, 43, 10, 11, 1,
zeroddef(1,1) = 18, 19, 42, 43, 11, 11, 1,

```

\$end

M E S H

\$meshgn

iblock = 1,

nkx=9,

xl(1) = 0.0, xc(1)= 185.0, nxl(1)=6, nxr(1)=0, dxmn(1)=	22.5,
xl(2) = 185.0, xc(2)= 228.0, nxl(2)=2, nxr(2)=2, dxmn(2)=	19.9,
xl(3) = 265.0, xc(3)= 265.0, nxl(3)=0, nxr(3)=1, dxmn(3)=	9.0e99 ,
xl(4) = 280.0, xc(4)= 280.0, nxl(4)=0, nxr(4)=1, dxmn(4)=	9.0e99 ,
xl(5) = 293.0, xc(5)= 293.0, nxl(5)=0, nxr(5)=1, dxmn(5)=	9.0e99 ,
xl(6) = 309.0, xc(6)= 364.2, nxl(6)=5, nxr(6)=0, dxmn(6)=	8.4,
xl(7) = 364.2, xc(7)= 364.2, nxl(7)=0, nxr(7)=4, dxmn(7)=	10.0,
xl(8) = 415.0, xc(8)= 415.0, nxl(8)=0, nxr(8)=1, dxmn(8)=	9.0e99,
xl(9) = 430.0, xc(9)= 460.0, nxl(9)=2, nxr(9)=5, dxmn(9)=	17.5,
xl(10)= 560.0,	

nky=9,

yl(1) = 0.00, yc(1)= 8.23, nyl(1)= 1, nyrr(1)= 6, dy mn(1)= 5.224,	
yl(2) = 55.00, yc(2)= 55.00, nyl(2)= 0, nyrr(2)= 12, dy mn(2)= 9.0e99,	
yl(3) = 180.00, yc(3)= 180.00, nyl(3)= 0, nyrr(3)= 6, dy mn(3)= 9.0e99,	
yl(4) = 240.00, yc(4)= 313.60, nyl(4)= 12, nyrr(4)= 0, dy mn(4)= 3.13,	
yl(5) = 313.60, yc(5)= 324.33, nyl(5)= 4, nyrr(5)= 0, dy mn(5)= 1.75,	
yl(6) = 324.33, yc(6)= 324.33, nyl(6)= 0, nyrr(6)= 1, dy mn(6)= 9.0e99,	
yl(7) = 325.67, yc(7)= 325.67, nyl(7)= 0, nyrr(7)= 4, dy mn(7)= 1.75,	
yl(8) = 335.00, yc(8)= 335.00, nyl(8)= 0, nyrr(8)= 3, dy mn(8)= 3.50,	
yl(9) = 346.54, yc(9)= 346.54, nyl(9)= 0, nyrr(9)= 2, dy mn(9)= 9.0e99,	
yl(10)= 360.00,	

; nky=6,

; yl(1)= 0.00, yc(1)= 0.00, nyl(1)= 0, nyrr(1)= 7, dy mn(1)= 6.50,	
; yl(2)= 55.00, yc(2)= 55.00, nyl(2)= 0, nyrr(2)= 18, dy mn(2)= 9.0e99,	
; yl(3)= 235.00, yc(3)= 313.60, nyl(3)= 12, nyrr(3)= 0, dy mn(3)= 3.13,	
; yl(4)= 313.00, yc(4)= 324.33, nyl(4)= 4, nyrr(4)= 0, dy mn(4)= 1.75,	
; yl(5)= 324.33, yc(5)= 324.33, nyl(5)= 0, nyrr(5)= 1, dy mn(5)= 9.0e99,	
; yl(6)= 325.67, yc(6)= 325.67, nyl(6)= 0, nyrr(6)= 9, dy mn(6)= 1.75,	
; yl(7)= 360.00,	

; nky=7,

; yl(1)= 0.00, yc(1)= 0.00, nyl(1)= 0, nyrr(1)= 7, dy mn(1)= 6.50,	
; yl(2)= 55.00, yc(2)= 55.00, nyl(2)= 0, nyrr(2)= 18, dy mn(2)= 9.0e99,	
; yl(3)= 235.00, yc(3)= 324.33, nyl(3)= 16, nyrr(3)= 0, dy mn(3)= 1.75,	

```

; yl(4)= 324.33, yc(4)= 324.33, nyl(4)= 0, nyr(4)= 1, dymn(4)= 9.0e99,
; yl(5)= 325.67, yc(5)= 325.67, nyl(5)= 0, nyr(5)= 4, dymn(5)= 1.75,
; yl(6)= 335.00, yc(6)= 335.00, nyl(6)= 0, nyr(6)= 1, dymn(6)= 9.0e99,
; yl(7)= 339.58, yc(7)= 339.58, nyl(7)= 0, nyr(7)= 4, dymn(7)= 4.33,
; yl(8)= 360.00,

; nky=5,
; yl(1)= 0.00, yc(1)= 0.00, nyl(1)= 0, nyr(1)= 7, dymn(1)= 6.50,
; yl(2)= 55.00, yc(2)= 55.00, nyl(2)= 0, nyr(2)= 18, dymn(2)= 9.0e99,
; yl(3)= 235.00, yc(3)= 324.33, nyl(3)= 16, nyr(3)= 0, dymn(3)= 1.75,
; yl(4)= 324.33, yc(4)= 324.33, nyl(4)= 0, nyr(4)= 1, dymn(4)= 9.0e99,
; yl(5)= 325.67, yc(5)= 325.67, nyl(5)= 0, nyr(5)= 9, dymn(5)= 1.75,
; yl(6)= 360.00,

nkz=13,
z1(1) =-130.00, zc(1) = -90.00, nzl(1) = 2, nzs(1) = 0, dzmn(1) = 19.0,
z1(2) = -90.00, zc(2) = -90.00, nzl(2) = 0, nzs(2) = 5, dzmn(2) = 9.0e99,
z1(3) = 0.00, zc(3) = 53.20, nzl(3) = 3, nzs(3) = 0, dzmn(3) = 17.5,
z1(4) = 53.20, zc(4) = 53.20, nzl(4) = 0, nzs(4) = 3, dzmn(4) = 9.0e99,
z1(5) = 104.00, zc(5) = 104.00, nzl(5) = 0, nzs(5) = 4, dzmn(5) = 18.5,
z1(6) = 195.00, zc(6) = 195.00, nzl(6) = 0, nzs(6) = 1, dzmn(6) = 9.0e99,
z1(7) = 230.00, zc(7) = 230.00, nzl(7) = 0, nzs(7) = 2, dzmn(7) = 9.0e99,
z1(8) = 285.00, zc(8) = 285.00, nzl(8) = 0, nzs(8) = 6, dzmn(8) = 9.0e99,
z1(9) = 475.00, zc(9) = 475.00, nzl(9) = 0, nzs(9) = 2, dzmn(9) = 9.0e99,
z1(10)= 515.00, zc(10)= 515.00, nzl(10)= 0, nzs(10)= 1, dzmn(10)= 9.0e99,
z1(11)= 550.00, zc(11)= 550.00, nzl(11)= 0, nzs(11)= 3, dzmn(11)= 9.0e99,
z1(12)= 630.00, zc(12)= 630.00, nzl(12)= 0, nzs(12)= 5, dzmn(12)= 30.5,
z1(13)= 790.00, zc(13)= 790.00, nzl(13)= 0, nzs(13)= 1, dzmn(13)= 9.0e99,
z1(14)= 850.00,

```

\$end

G R A P H I C S

\$grafic

```

; thdt = 0.05,
; thdt = 0.01,
; thdt = 1.00,

; pnt(1,1) = 19, 43, 12, 1,
; pnt(1,2) = 19, 43, 37, 1,
; pnt(1,3) = 1, 43, 1, 1,
; pnt(1,4) = 31, 43, 39, 1,
; pnt(1,5) = 19, 20, 1, 1,
; pnt(1,6) = 19, 50, 39, 1,
; pnt(1,7) = 1, 1, 11, 1,
; pnt(1,8) = 31, 52, 11, 1,
; pnt(1,9) = 1, 1, 15, 1,
; pnt(1,10)= 31, 52, 15, 1,

```

```
; pnt(1,11)= 1, 1, 25, 1,  
; pnt(1,12)= 31, 52, 25, 1,  
; pnt(1,13)= 1, 1, 35, 1,  
; pnt(1,14)= 31, 52, 35, 1,  
  
; pnt(1,15) = 12, 43, 14, 1,  
; pnt(1,16) = 24, 43, 14, 1,  
; pnt(1,17) = 12, 43, 15, 1,  
; pnt(1,18) = 24, 43, 15, 1,  
; pnt(1,19) = 13, 43, 18, 1,  
; pnt(1,20) = 23, 43, 18, 1,  
; pnt(1,21) = 13, 43, 19, 1,  
; pnt(1,22) = 23, 43, 19, 1,  
; pnt(1,23) = 14, 43, 29, 1,  
; pnt(1,24) = 24, 43, 29, 1,  
; pnt(1,25) = 9, 43, 35, 1,  
; pnt(1,26) = 23, 43, 35, 1,  
; pnt(1,27) = 9, 43, 36, 1,  
; pnt(1,28) = 23, 43, 36, 1,
```

```
pnt(1,1) = 19, 43, 12, 1,  
pnt(1,2) = 19, 43, 37, 1,
```

```
pnt(1,3) = 1, 43, 1, 1,  
pnt(1,4) = 31, 43, 39, 1,  
pnt(1,5) = 19, 20, 1, 1,  
pnt(1,6) = 19, 50, 39, 1,  
pnt(1,7) = 1, 1, 11, 1,  
pnt(1,8) = 31, 52, 11, 1,  
pnt(1,9) = 1, 1, 15, 1,  
pnt(1,10)= 31, 52, 15, 1,  
pnt(1,11)= 1, 1, 25, 1,  
pnt(1,12)= 31, 52, 25, 1,  
pnt(1,13)= 1, 1, 35, 1,  
pnt(1,14)= 31, 52, 35, 1,
```

```
pnt(1,15) = 11, 43, 14, 1,  
pnt(1,16) = 24, 43, 14, 1,  
pnt(1,17) = 11, 43, 15, 1,  
pnt(1,18) = 24, 43, 15, 1,  
pnt(1,19) = 12, 43, 18, 1,  
pnt(1,20) = 23, 43, 18, 1,  
pnt(1,21) = 12, 43, 19, 1,  
pnt(1,22) = 23, 43, 19, 1,  
pnt(1,23) = 13, 43, 29, 1,  
pnt(1,24) = 24, 43, 29, 1,  
pnt(1,25) = 8, 43, 35, 1,  
pnt(1,26) = 24, 43, 35, 1,  
pnt(1,27) = 8, 43, 36, 1,  
pnt(1,28) = 23, 43, 36, 1,
```

v2d(1,1)	=	3,	4,	1,				
v2d(1,2)	=	5,	6,	1,				
v2d(1,3)	=	7,	8,	1,				
v2d(1,4)	=	9,	10,	1,				
v2d(1,5)	=	11,	12,	1,				
v2d(1,6)	=	13,	14,	1,				
c2d(1,1)	=	3,	4,	'vf',	'he',			
c2d(1,2)	=	5,	6,	'vf',	'he',			
c2d(1,3)	=	7,	8,	'vf',	'he',			
c2d(1,4)	=	9,	10,	'vf',	'he',			
c2d(1,5)	=	11,	12,	'vf',	'he',			
c2d(1,6)	=	13,	14,	'vf',	'he',			
p1d(1,1)	=	1,	2,	'vf',	'he',			
p1d(1,2)	=	15,	16,	'vf',	'he',			
p1d(1,3)	=	17,	18,	'vf',	'he',			
p1d(1,4)	=	19,	20,	'vf',	'he',			
p1d(1,5)	=	21,	22,	'vf',	'he',			
p1d(1,6)	=	23,	24,	'vf',	'he',			
p1d(1,7)	=	25,	26,	'vf',	'he',			
p1d(1,8)	=	27,	28,	'vf',	'he',			
p1d(1,9)	=	1,	2,	'wn',	0,			
thp(1,1)	=	10,	23,	25,	1,	'un',	0,	;U 25 C
thp(1,2)	=	08,	27,	10,	1,	'un',	0,	;U 36 C
thp(1,3)	=	25,	2,	11,	1,	'un',	0,	;U 49 A
thp(1,4)	=	25,	52,	11,	1,	'un',	0,	;U 49 A
thp(1,5)	=	25,	42,	11,	1,	'un',	0,	;U 69
thp(1,6)	=	25,	7,	11,	1,	'un',	0,	;U 89
thp(1,7)	=	10,	23,	25,	1,	'un',	0,	;U 25 A
thp(1,8)	=	19,	43,	27,	1,	'wn',	0,	;U 59 B
thp(1,9)	=	21,	40,	27,	1,	'wn',	0,	;U 59 B
thp(1,10)	=	16,	46,	27,	1,	'wn',	0,	;U 59 B
thp(1,11)	=	16,	40,	27,	1,	'wn',	0,	;U 59 B
thp(1,12)	=	21,	46,	27,	1,	'wn',	0,	;U 59 B
thp(1,13)	=	31,	30,	31,	1,	'pn',	0,	; 157
thp(1,14)	=	2,	20,	10,	1,	'vf',	'he',	; 125
thp(1,15)	=	2,	20,	18,	1,	'vf',	'he',	; 126
thp(1,16)	=	2,	20,	25,	1,	'vf',	'he',	; 127
thp(1,17)	=	18,	30,	24,	1,	'vf',	'he',	; 128
thp(1,18)	=	18,	30,	13,	1,	'vf',	'he',	; 129
thp(1,19)	=	18,	12,	13,	1,	'vf',	'he',	; 131
thp(1,20)	=	28,	30,	13,	1,	'vf',	'he',	; 121
thp(1,21)	=	28,	30,	24,	1,	'vf',	'he',	; 122
thp(1,22)	=	2,	20,	32,	1,	'vf',	'he',	; 123
thp(1,23)	=	2,	20,	38,	1,	'vf',	'he',	; 124

thp(1,24)	= 25, 42, 11, 1, 'vf', 'he', ; U 69
thp(1,25)	= 19, 43, 19, 1, 'vf', 'he', ;U 56 B
thp(1,26)	= 18, 42, 14, 1, 'vf', 'he', ;jet h=0.5 A
thp(1,27)	= 18, 44, 14, 1, 'vf', 'he', ;jet h=0.5 B
thp(1,28)	= 18, 42, 19, 1, 'vf', 'he', ;jet h=1.5 A
thp(1,29)	= 18, 44, 19, 1, 'vf', 'he', ;jet h=1.5 B
thp(1,30)	= 19, 43, 28, 1, 'vf', 'he', ;U 59 B
thp(1,31)	= 17, 40, 28, 1, 'vf', 'he', ;jet h=4.5 A
thp(1,32)	= 17, 46, 28, 1, 'vf', 'he', ;jet h=4.5 B
thp(1,33)	= 16, 38, 36, 1, 'vf', 'he', ;jet h=6.4 A
thp(1,34)	= 16, 49, 36, 1, 'vf', 'he', ;jet h=6.4 B
thp(1,35)	= 2, 20, 10, 1, 'tk', 0, ; 24
thp(1,36)	= 2, 20, 18, 1, 'tk', 0, ; 26
thp(1,37)	= 2, 20, 25, 1, 'tk', 0, ; 28
thp(1,38)	= 18, 30, 24, 1, 'tk', 0, ; 34
thp(1,39)	= 18, 30, 13, 1, 'tk', 0, ; 31
thp(1,40)	= 18, 12, 13, 1, 'tk', 0, ; 30
thp(1,41)	= 28, 30, 13, 1, 'tk', 0, ; 5
thp(1,42)	= 28, 30, 24, 1, 'tk', 0, ; 7
thp(1,43)	= 2, 20, 32, 1, 'tk', 0, ; 10
thp(1,44)	= 2, 20, 38, 1, 'tk', 0, ; 14
thp(1,45)	= 25, 42, 11, 1, 'tk', 0, ; U 69
thp(1,46)	= 19, 43, 19, 1, 'tk', 0, ;U 56 B
thp(1,47)	= 19, 41, 19, 1, 'tk', 0, ;U 56 B
thp(1,48)	= 19, 45, 19, 1, 'tk', 0, ;U 56 B
thp(1,49)	= 16, 43, 19, 1, 'tk', 0, ;U 56 B
thp(1,50)	= 22, 43, 19, 1, 'tk', 0, ;U 56 B
thp(1,51)	= 19, 43, 28, 1, 'tk', 0, ;U 59 B
thp(1,52)	= 19, 41, 28, 1, 'tk', 0, ;U 59 B
thp(1,53)	= 19, 45, 28, 1, 'tk', 0, ;U 59 B
thp(1,54)	= 16, 43, 28, 1, 'tk', 0, ;U 59 B
thp(1,55)	= 22, 43, 28, 1, 'tk', 0, ;U 59 B
thp(1,56)	= 9, 27, 10, 1, 'tk', 0, ;U 36 C
thp(1,57)	= 10, 24, 25, 1, 'tk', 0, ;U 25 A
thp(1,58)	= 10, 43, 25, 1, 'tk', 0, ;U 25 C
thp(1,59)	= 10, 46, 25, 1, 'tk', 0, ;U 25 C
thp(1,60)	= 19, 43, 11, 1, 'vf', 'he', ; jet
thp(1,61)	= 19, 43, 12, 1, 'vf', 'he', ; jet
thp(1,62)	= 19, 43, 13, 1, 'vf', 'he', ; jet
thp(1,63)	= 19, 43, 14, 1, 'vf', 'he', ; jet
thp(1,64)	= 19, 43, 15, 1, 'vf', 'he', ; jet
thp(1,65)	= 19, 43, 16, 1, 'vf', 'he', ; jet

thp(1,66)	= 19, 43, 17, 1, 'vf', 'he', ; jet
thp(1,67)	= 19, 43, 18, 1, 'vf', 'he', ; jet
thp(1,68)	= 19, 43, 19, 1, 'vf', 'he', ; jet
thp(1,69)	= 19, 43, 20, 1, 'vf', 'he', ; jet
thp(1,70)	= 19, 43, 21, 1, 'vf', 'he', ; jet
thp(1,71)	= 19, 43, 22, 1, 'vf', 'he', ; jet
thp(1,72)	= 19, 43, 23, 1, 'vf', 'he', ; jet
thp(1,73)	= 19, 43, 24, 1, 'vf', 'he', ; jet
thp(1,74)	= 19, 43, 25, 1, 'vf', 'he', ; jet
thp(1,75)	= 19, 43, 26, 1, 'vf', 'he', ; jet
thp(1,76)	= 19, 43, 27, 1, 'vf', 'he', ; jet
thp(1,77)	= 19, 43, 28, 1, 'vf', 'he', ; jet
thp(1,78)	= 19, 43, 29, 1, 'vf', 'he', ; jet
thp(1,79)	= 19, 43, 30, 1, 'vf', 'he', ; jet
thp(1,80)	= 19, 43, 31, 1, 'vf', 'he', ; jet
thp(1,81)	= 19, 43, 32, 1, 'vf', 'he', ; jet
thp(1,82)	= 19, 43, 33, 1, 'vf', 'he', ; jet
thp(1,83)	= 19, 43, 34, 1, 'vf', 'he', ; jet
thp(1,84)	= 19, 43, 35, 1, 'vf', 'he', ; jet
thp(1,85)	= 19, 43, 36, 1, 'vf', 'he', ; jet
thp(1,86)	= 19, 43, 13, 1, 'tk', 0, ; jet
thp(1,87)	= 19, 43, 14, 1, 'tk', 0, ; jet
thp(1,88)	= 19, 43, 15, 1, 'tk', 0, ; jet
thp(1,89)	= 19, 43, 16, 1, 'tk', 0, ; jet
thp(1,90)	= 19, 43, 17, 1, 'tk', 0, ; jet
thp(1,91)	= 19, 43, 18, 1, 'tk', 0, ; jet
thp(1,92)	= 19, 43, 19, 1, 'tk', 0, ; jet
thp(1,93)	= 19, 43, 22, 1, 'tk', 0, ; jet
thp(1,94)	= 19, 43, 23, 1, 'tk', 0, ; jet
thp(1,95)	= 19, 43, 28, 1, 'tk', 0, ; jet
thp(1,96)	= 19, 43, 29, 1, 'tk', 0, ; jet
thp(1,97)	= 19, 43, 30, 1, 'tk', 0, ; jet
thp(1,98)	= 19, 43, 34, 1, 'tk', 0, ; jet
thp(1,99)	= 19, 43, 35, 1, 'tk', 0, ; jet
thp(1,100)	= 19, 43, 36, 1, 'tk', 0, ; jet
thp(1,101)	= 11, 43, 14, 1, 'vf', 'he', ; jet
thp(1,102)	= 12, 43, 14, 1, 'vf', 'he', ; jet
thp(1,103)	= 13, 43, 14, 1, 'vf', 'he', ; jet
thp(1,104)	= 14, 43, 14, 1, 'vf', 'he', ; jet
thp(1,105)	= 15, 43, 14, 1, 'vf', 'he', ; jet
thp(1,106)	= 16, 43, 14, 1, 'vf', 'he', ; jet
thp(1,107)	= 17, 43, 14, 1, 'vf', 'he', ; jet
thp(1,108)	= 18, 43, 14, 1, 'vf', 'he', ; jet
thp(1,109)	= 19, 43, 14, 1, 'vf', 'he', ; jet
thp(1,110)	= 20, 43, 14, 1, 'vf', 'he', ; jet
thp(1,111)	= 21, 43, 14, 1, 'vf', 'he', ; jet
thp(1,112)	= 22, 43, 14, 1, 'vf', 'he', ; jet
thp(1,113)	= 23, 43, 14, 1, 'vf', 'he', ; jet
thp(1,114)	= 24, 43, 14, 1, 'vf', 'he', ; jet
thp(1,115)	= 11, 43, 15, 1, 'vf', 'he', ; jet
thp(1,116)	= 12, 43, 15, 1, 'vf', 'he', ; jet
thp(1,117)	= 13, 43, 15, 1, 'vf', 'he', ; jet
thp(1,118)	= 14, 43, 15, 1, 'vf', 'he', ; jet

thp(1,119)	=	15,	43,	15,	1,	'vf',	'he',	;	jet
thp(1,120)	=	16,	43,	15,	1,	'vf',	'he',	;	jet
thp(1,121)	=	17,	43,	15,	1,	'vf',	'he',	;	jet
thp(1,122)	=	18,	43,	15,	1,	'vf',	'he',	;	jet
thp(1,123)	=	19,	43,	15,	1,	'vf',	'he',	;	jet
thp(1,124)	=	20,	43,	15,	1,	'vf',	'he',	;	jet
thp(1,125)	=	21,	43,	15,	1,	'vf',	'he',	;	jet
thp(1,126)	=	22,	43,	15,	1,	'vf',	'he',	;	jet
thp(1,127)	=	23,	43,	15,	1,	'vf',	'he',	;	jet
thp(1,128)	=	24,	43,	15,	1,	'vf',	'he',	;	jet
thp(1,129)	=	12,	43,	18,	1,	'vf',	'he',	;	jet
thp(1,130)	=	13,	43,	18,	1,	'vf',	'he',	;	jet
thp(1,131)	=	14,	43,	18,	1,	'vf',	'he',	;	jet
thp(1,132)	=	15,	43,	18,	1,	'vf',	'he',	;	jet
thp(1,133)	=	16,	43,	18,	1,	'vf',	'he',	;	jet
thp(1,134)	=	17,	43,	18,	1,	'vf',	'he',	;	jet
thp(1,135)	=	18,	43,	18,	1,	'vf',	'he',	;	jet
thp(1,136)	=	19,	43,	18,	1,	'vf',	'he',	;	jet
thp(1,137)	=	20,	43,	18,	1,	'vf',	'he',	;	jet
thp(1,138)	=	21,	43,	18,	1,	'vf',	'he',	;	jet
thp(1,139)	=	22,	43,	18,	1,	'vf',	'he',	;	jet
thp(1,140)	=	23,	43,	18,	1,	'vf',	'he',	;	jet
thp(1,141)	=	12,	43,	19,	1,	'vf',	'he',	;	jet
thp(1,142)	=	13,	43,	19,	1,	'vf',	'he',	;	jet
thp(1,143)	=	14,	43,	19,	1,	'vf',	'he',	;	jet
thp(1,144)	=	15,	43,	19,	1,	'vf',	'he',	;	jet
thp(1,145)	=	16,	43,	19,	1,	'vf',	'he',	;	jet
thp(1,146)	=	17,	43,	19,	1,	'vf',	'he',	;	jet
thp(1,147)	=	18,	43,	19,	1,	'vf',	'he',	;	jet
thp(1,148)	=	19,	43,	19,	1,	'vf',	'he',	;	jet
thp(1,149)	=	20,	43,	19,	1,	'vf',	'he',	;	jet
thp(1,150)	=	21,	43,	19,	1,	'vf',	'he',	;	jet
thp(1,151)	=	22,	43,	19,	1,	'vf',	'he',	;	jet
thp(1,152)	=	23,	43,	19,	1,	'vf',	'he',	;	jet
thp(1,153)	=	13,	43,	29,	1,	'vf',	'he',	;	jet
thp(1,154)	=	14,	43,	29,	1,	'vf',	'he',	;	jet
thp(1,155)	=	15,	43,	29,	1,	'vf',	'he',	;	jet
thp(1,156)	=	16,	43,	29,	1,	'vf',	'he',	;	jet
thp(1,157)	=	17,	43,	29,	1,	'vf',	'he',	;	jet
thp(1,158)	=	18,	43,	29,	1,	'vf',	'he',	;	jet
thp(1,159)	=	19,	43,	29,	1,	'vf',	'he',	;	jet
thp(1,160)	=	20,	43,	29,	1,	'vf',	'he',	;	jet
thp(1,161)	=	21,	43,	29,	1,	'vf',	'he',	;	jet
thp(1,162)	=	22,	43,	29,	1,	'vf',	'he',	;	jet
thp(1,163)	=	23,	43,	29,	1,	'vf',	'he',	;	jet
thp(1,164)	=	24,	43,	29,	1,	'vf',	'he',	;	jet
thp(1,165)	=	13,	43,	29,	1,	'vf',	'he',	;	jet
thp(1,166)	=	14,	43,	29,	1,	'vf',	'he',	;	jet
thp(1,167)	=	15,	43,	29,	1,	'vf',	'he',	;	jet
thp(1,168)	=	16,	43,	29,	1,	'vf',	'he',	;	jet
thp(1,169)	=	17,	43,	29,	1,	'vf',	'he',	;	jet
thp(1,170)	=	18,	43,	29,	1,	'vf',	'he',	;	jet
thp(1,171)	=	19,	43,	29,	1,	'vf',	'he',	;	jet

```

thp(1,172) = 20, 43, 29, 1, 'vf', 'he', ; jet
thp(1,173) = 21, 43, 29, 1, 'vf', 'he', ; jet
thp(1,174) = 22, 43, 29, 1, 'vf', 'he', ; jet
thp(1,175) = 23, 43, 29, 1, 'vf', 'he', ; jet
thp(1,176) = 24, 43, 29, 1, 'vf', 'he', ; jet

thp(1,177) = 8, 43, 36, 1, 'vf', 'he', ; jet
thp(1,178) = 9, 43, 36, 1, 'vf', 'he', ; jet
thp(1,179) = 10, 43, 36, 1, 'vf', 'he', ; jet
thp(1,180) = 11, 43, 36, 1, 'vf', 'he', ; jet
thp(1,181) = 12, 43, 36, 1, 'vf', 'he', ; jet
thp(1,182) = 13, 43, 36, 1, 'vf', 'he', ; jet
thp(1,183) = 14, 43, 36, 1, 'vf', 'he', ; jet
thp(1,184) = 15, 43, 36, 1, 'vf', 'he', ; jet
thp(1,185) = 16, 43, 36, 1, 'vf', 'he', ; jet
thp(1,186) = 17, 43, 36, 1, 'vf', 'he', ; jet
thp(1,187) = 18, 43, 36, 1, 'vf', 'he', ; jet
thp(1,188) = 19, 43, 36, 1, 'vf', 'he', ; jet
thp(1,189) = 20, 43, 36, 1, 'vf', 'he', ; jet
thp(1,190) = 21, 43, 36, 1, 'vf', 'he', ; jet
thp(1,191) = 22, 43, 36, 1, 'vf', 'he', ; jet
thp(1,192) = 23, 43, 36, 1, 'vf', 'he', ; jet

```

\$end

P A R T I C L E S

\$parts

\$end

H E A T T R A N S F E R & C O N D E N S A T I O N

\$rheat

ihtflag = 1,

nhtesink=5,
nhteslab=20,
nhtewall=10,

matbdy = 1,

icond= 1,
tslab0=-1,
tsink0=-1,
twall0=-1,

walldef(1,1) = 1,30.0, 0.0, 0.0, 0.5,
walldef(1,2) = 2, 0.5, -0.1, -0.1, 0.0,

tslabbc = 298.15,
dxslabc = 0.1,

\$end

S P E C I A L

\$special

\$end

8.2.5. HDR Test T31.5

8.2.5.1. Summary.

Purpose
Validation of the capability to model full-scale containment during simulated accident conditions.
Success Metrics
The GASFLOW-calculated light-gas concentrations and containment pressure will agree with the experimentally measured light-gas concentrations and containment pressure in the Heißdampfreaktor (HDR).
Problem Description
Test T31.5 simulated the steam and hydrogen release after a large-break (LB) loss-of-coolant accident (LOCA) in the containment of the former HDR.
Relationship to Code Models and Methods
See Table 7-1.
Relationship to PIRT Phenomena
Code Version and Modifications
GASFLOW 2.1.0.13.
Hardware and Operating System
CRAY-J90 UNICOS operating system.
Compiler, Version, and Optimization Level
CRAY Fortran 90, Version 3.0.0.1.
Runtime Statistics: Total Run Time, Grind Time
Problem took 2 weeks to complete..
Results and Conclusions
The GASFLOW results agree with experimental results.

8.2.5.2. Test Description. The HDR building (Ref. 8-5) near Frankfurt, Germany, is a full-scale containment facility designed to provide experimental data on simulated reactor accident situations. The containment consists of a steel shell that is 60 m high and 20 m in diameter and has a free volume of 11 300 m³. This steel shell is surrounded by a secondary concrete shell, with an annular gap between. Vertical cross-sectional

views of the containment at two angles, presented in Figure 8-27, show the spiral and standard staircases. The HDR facility has a multicompartamental geometry (72 compartments) with a large number of steel structures (total interior steel surface area in excess of 15 000 m²) and a very large dome with a volume of ~5000 m³. Overall, ~200 passageways interconnect the compartments.

The experiment chosen for the code assessment discussed in this document, Test T31.5, is an LBLOCA and a hydrogen distribution experiment that lasted for ~1 h. This experiment was selected as one of the Organization for Economic Cooperation and Development (OECD)/Committee on the Safety of Nuclear Installations (CSNI) International Standard Problems and was called ISP-23.

In the experiment, a blowdown of the HDR pressure vessel occurring for 50 s with the injection of 30 Mg (where 1 Mg = 1000 kg) of steam-water mixture into the containment. (The flow Reynolds number at the peak blowdown rate was 2.1×10^7 .) Then a superheated steam release at a rate of 2.2 kg/s ($Re = 2.8 \times 10^6$) occurred roughly 21 to 36 min after the blowdown began. The superheated steam release was followed immediately by a release of light gas (15% hydrogen and 85% helium on a volume basis) at 0.24 kg/s ($Re = 1.9 \times 10^5$) from 36 to 48 min after the beginning of the blowdown. For safety reasons, hydrogen was diluted by helium to form the light gas in this experiment to reduce the flammability of the gas mixture. A time sequence of these events in the experiment is presented in Table 8-2. The blowdown and gas releases were at about the 22-m-height level. Figure 8-28 shows (1) a vertical, cross-sectional view of the containment showing the room where the blowdown and gas releases took place and (2) details of the blowdown and gas release pipes. The blowdown pipe has a diameter of 43.5 cm and is pointed nearly vertically upward, whereas the gas release pipe is 8 cm in diameter and is directed inward horizontally. Pressure, temperature, and volume fractions of air, steam, and light gas were measured at various locations as a function of time. These experimental measurements were used for the assessment of the GASFLOW calculations.

TABLE 8-2 TIME SEQUENCE OF EVENTS IN THE HDR T31.5 EXPERIMENT

TIME	EVENT
0 sec	BLOWDOWN (simulating LBLOCA) 30 Mg total
50 sec	(NO SOURCE INJECTION)
21 min	SUPERHEATED STEAM RELEASE 2 Mg total
36 min	RELEASE OF LIGHT GAS MIXTURE (15% H ₂ , 85% He) 168 kg total
48 min	

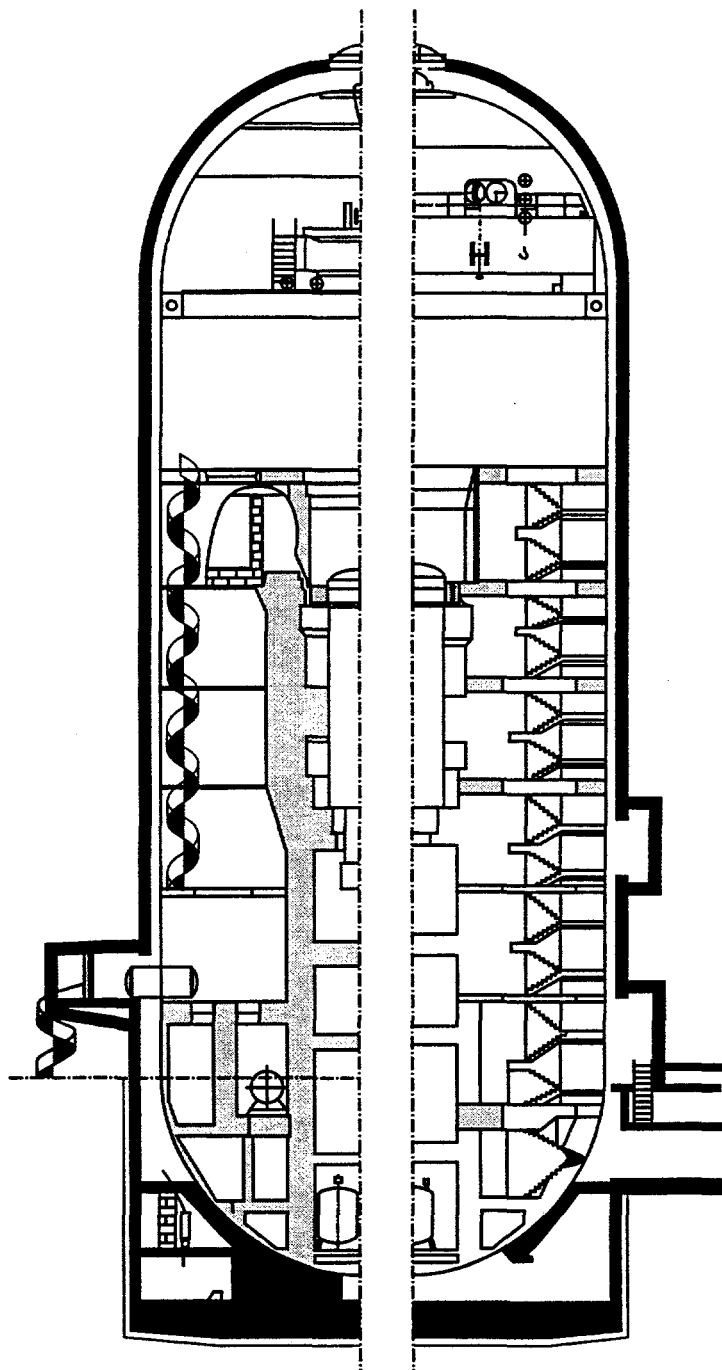


Fig. 8-27. Cross-sectional view of the HDR containment building at two angles. The cross section on the right shows the standard staircase; the spiral staircase is visible on the left

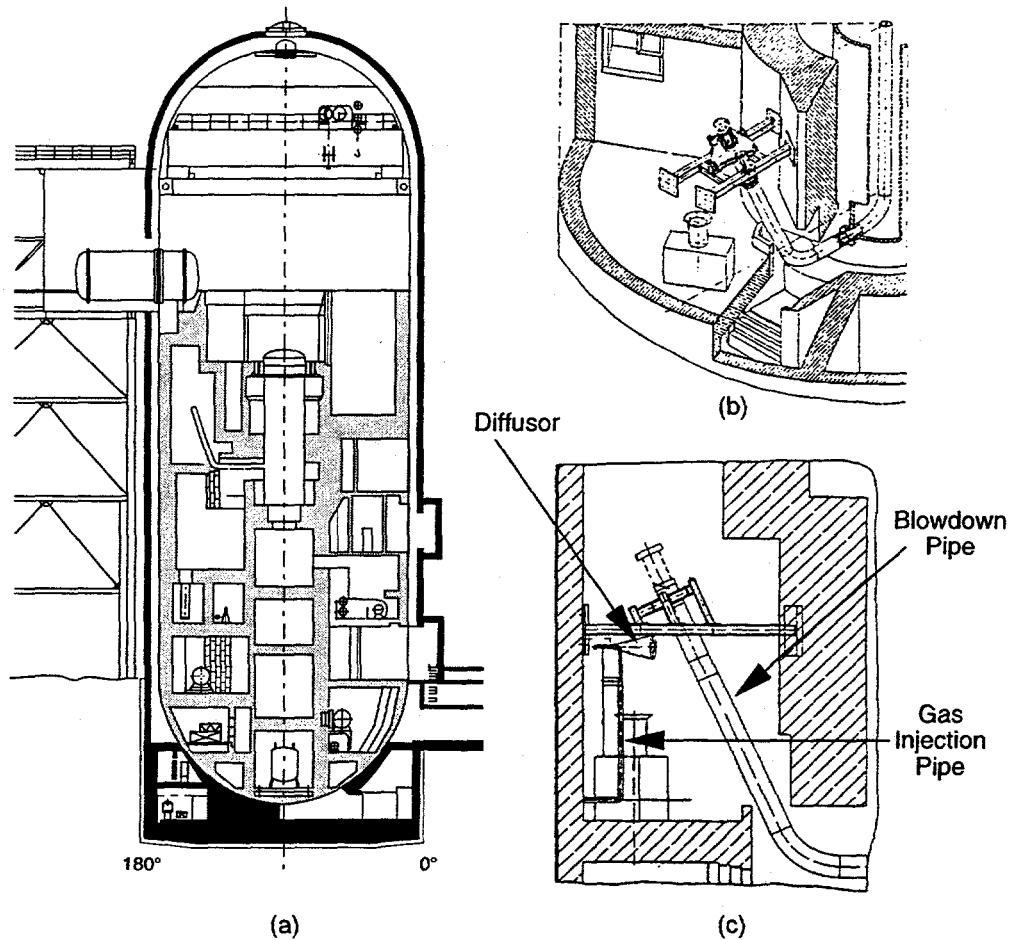


Fig. 8-28. (a) Cross-sectional view of the HDR containment facility showing the blowdown room. The blowdown pipe can be seen in the middle, extending from the left side of the pressure vessel; (b) perspective drawing of the blowdown room; and (c) details of the blowdown pipe, gas injection pipe, and diffusor

8.2.5.3. GASFLOW Calculations.

8.2.5.3.1. GASFLOW Input Model. GASFLOW can model 3D geometries in cylindrical or rectangular coordinates. In the case of the HDR containment, using cylindrical geometry is more appropriate. The containment building is represented by a 3D mesh consisting of 11 radial cells, 40 axial cells, and 24 azimuthal cells (giving a total of 12,300 computational cells) with variable mesh spacing. Figure 8-28 shows the computational mesh.

In the model, the blocked cells are specified by mesh obstacle definitions and the flow barriers are specified by wall definitions. The flow obstacles and barriers combine to model all of the major floors and walls in the containment building. Although the inertial barriers have zero thickness in the computational mesh, heat conduction calculations for these solid structures are based on an average thickness of 1 m for the concrete walls and floors and 3 cm for the outer cylindrical steel shell. In this modeling procedure, we physically represent all of the compartments. The flow areas (doors,

connections, and other openings) among compartments are simulated using the GASFLOW fractional area capability.

We have modeled the effects of internal structures (e.g., steel structures in various rooms in the HDR containment) that are too fine to be resolved by using distributed heat sinks. Distributed heat sinks are specified by defining the total exposed surface area and average half-thickness over a region of the computational space. (The half-thickness specification is used because the heat conduction calculation in these distributed heat sinks assumes symmetry at the center line.) From the heat sink specification, the code calculates the free-gas volume within the defined region and distributes the solid heat sinks evenly over all the included fluid cells. We have chosen to subdivide the HDR containment into horizontal disks extending radially from the center line to the steel shell (radial position of 10 m) and axially between the edges of each vertical computational cell.

In addition to the model geometry and nodalization, other parameters are needed to specify the calculation. The experiment involves five main gas species—nitrogen and oxygen from the air, water vapor, and helium and hydrogen from the light gas (15% hydrogen and 85% helium). We modeled the light gas and air as two species with thermodynamic properties given by the weighted averages of the constituent properties. (However, modeling the five gas species separately is possible in GASFLOW, if desired.) Therefore, the transport of only three gas components (air, steam, and light gas) was calculated. The hydrogen concentration presented in the discussion of results was obtained by multiplying the calculated light-gas concentration by 15%.

An important part of the calculation involves an isentropic expansion model to determine the correct amount of steam received by the containment, based on the measured blowdown source data. The HDR experiment T31.5 involves an LB blowdown of the pressure vessel followed by a superheated steam release and then by a light-gas release. The LB blowdown injected 30 Mg of a two-phase, steam-water mixture into the containment in 50 s. GASFLOW includes a homogeneous-equilibrium model that simulates the isentropic expansion and condensation of steam as the blowdown source is injected into the containment.

8.2.5.3.2. GASFLOW Results. During the blowdown, the peak of the containment pressures occurs near the source location in the breakroom. However, the flow driven by the overpressures leads to a rapid equilibration throughout the containment so that differences between the various pressure readings in the containment become only marginal after 1 min. The rapid pressure equilibration throughout the containment is predicted also in GASFLOW and is in good agreement with the data. The direct use of the blowdown data gave pressure peaks from the GASFLOW analysis that match the measured data near the source location rather well. The data point compared in Figure 8-30 refers to the pressure sensor CP7407 located somewhat below the source location.

The calculated pressure decay after the blowdown is also in good agreement with the measured data. However, after 5 min GASFLOW starts predicting slower pressure

decays than what was measured in the test. The difference levels off at 0.08 bars and remains fairly stable after ~15 min.

The second steam-injection phase at 21 min stops the pressure decay, whereas the light-gas release after 36 min actually leads to a slight increase. Both tendencies are reflected also in the results from GASFLOW. One explanation for the higher value of the asymptotic pressure is the lack of a film relocation model. The film vaporization model provides a continuous steam source that slows down the pressure decay but that should be cut off as dryout occurs.

The calculated temperature histories throughout the containment reflect the fact that the asymptotic pressures are somewhat higher. Their values early in the transient are in fair agreement with the measured data in the middle and upper regions of the containment, yet as the system approaches more stable conditions they are getting too high by ~10°C (Figure 8-30). The temperature increase after 20 min near the source location reflects the energy added in the second steam-injection phase, but it occurs only locally. In the bottom region of the containment, the predicted temperatures are overpredicted throughout the transient by 20 to 25°C. This overprediction of the bottom temperatures occurred also in the earlier analyses with the Hydrogen Mixing Study. There are three effects that could be responsible for this.

The steam flow to the bottom may be overpredicted due to too little resistance to the downward flow. However, the fact that the overprediction occurs also when the exact flow areas are applied points to another mechanism. In the new homogeneous equilibrium model, the relocating steam carries a significant amount of water droplets. As the steam condenses on the cold surfaces in the bottom region, it can be partly replaced by vaporization of the hot-water droplets, thus keeping the pressure higher. However, this effect does not have a large influence on the temperature because the liquid droplets contribute very little to the overall internal energy of the gas field, which is dominated by the latent heat of the steam. Also, these droplets are dispersed quickly in this GASFLOW simulation. The third reason, which seems to be the more likely one, is that a significant amount of water collects in this lower region. After flowing over fairly cold walls with high heat capacities, the water may arrive there in a rather cold state, thus providing an additional heat sink. GASFLOW has no liquid tracking model for a mechanistic simulation of this recollecting liquid. Attempts to relocate a fraction of the dispersed water from the upper regions with a lower temperature at the bottom have been made, but overall this could not explain the early overprediction of the temperatures. More work is in progress in this area.

The long-time development of the pressure and temperatures is controlled also by the heat transfer to the steel shell. The cooling of this shell by circulating air in the annulus and the heat transfer to the concrete shell are simulated mechanistically in GASFLOW, whereas the simulation may well have been used as parameter in other codes to adjust for the correct pressure and time dependence. The heat transfer to the annulus and from there to the concrete shell needs to be reviewed also in GASFLOW. It is surprising how little the concrete shell is heated up from the applied convective heat-transfer

correlation. Unfortunately, no data exist for the concrete shell, which would have allowed us to check the convective cooling simulated in the annulus.

The light gas that is released after 36 min is shown to move up rapidly into the dome region, whereas only small fractions move downward. GASFLOW results show excellent agreement with the measured light-gas concentration in the spiral staircase and the dome region (Figure 8-31). The light-gas concentrations from GASFLOW are overpredicted at the 26.5-m level. However, this occurs in a region close to the source where the concentration gradients vary strongly. Also, the selection of the GASFLOW computational volume that represents the location of the measurement point is rather difficult in this region. The experimental results are also fairly well matched at the 12-m level of the spiral staircase. The experimental data report some light-gas concentrations of 0.5 vol % near the 0-m level after 60 min. The predicted light-gas concentration from GASFLOW at this low level is very small, although it shows some increase with time at a level that is several orders of magnitude below the experimental data.

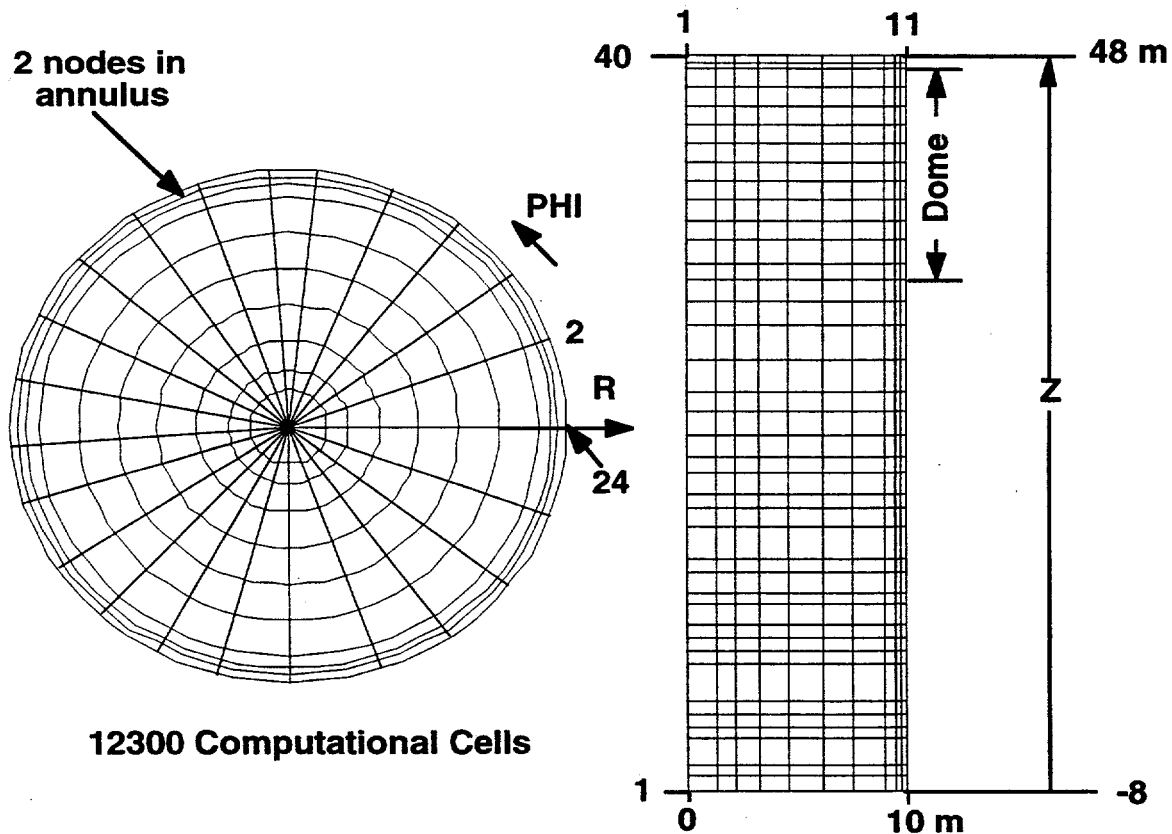


Fig. 8-29. Noding diagram

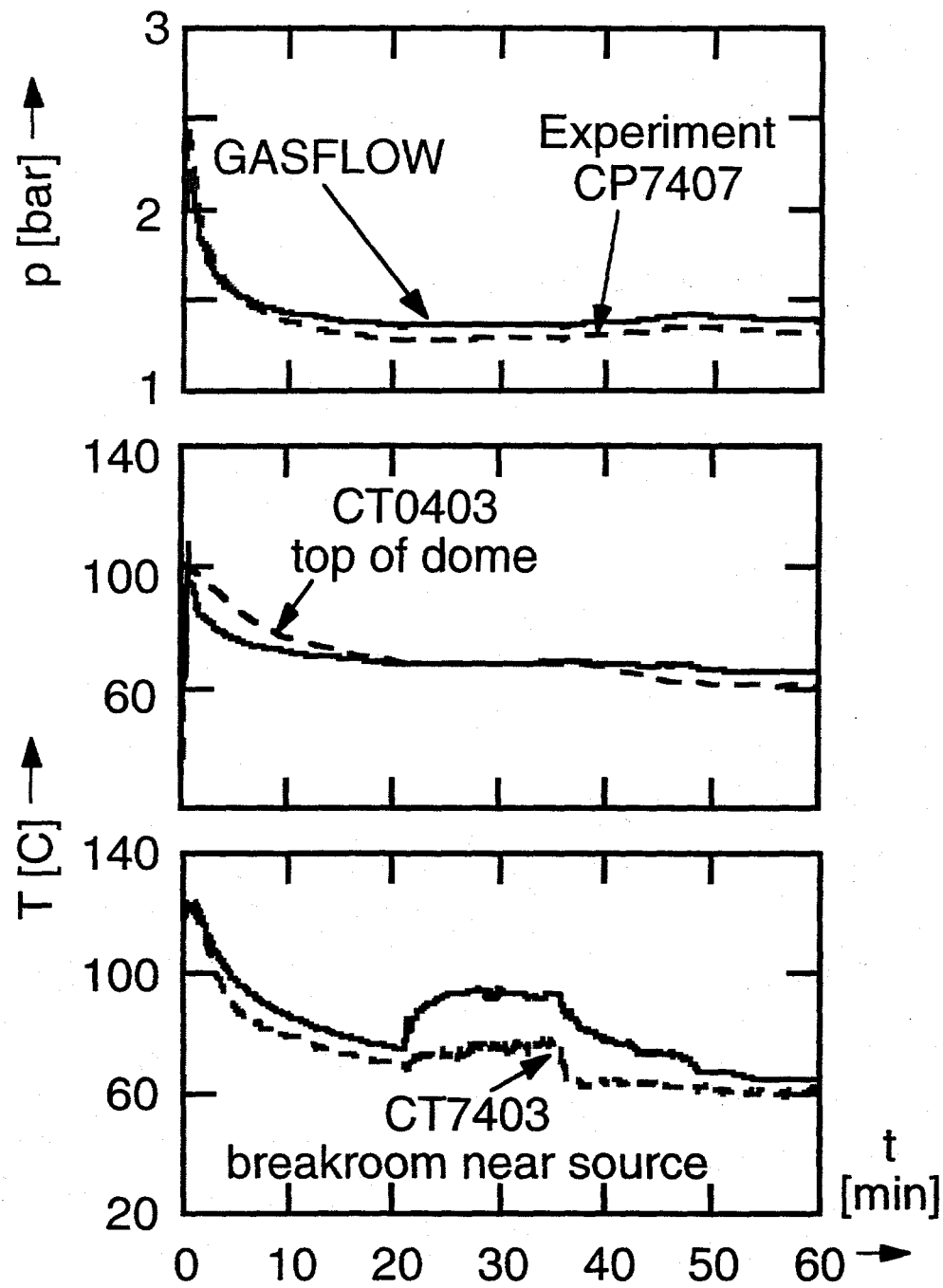


Fig. 8-30. HDR test T31.5 pressures and temperatures; test data vs results from GASFLOW 2.1

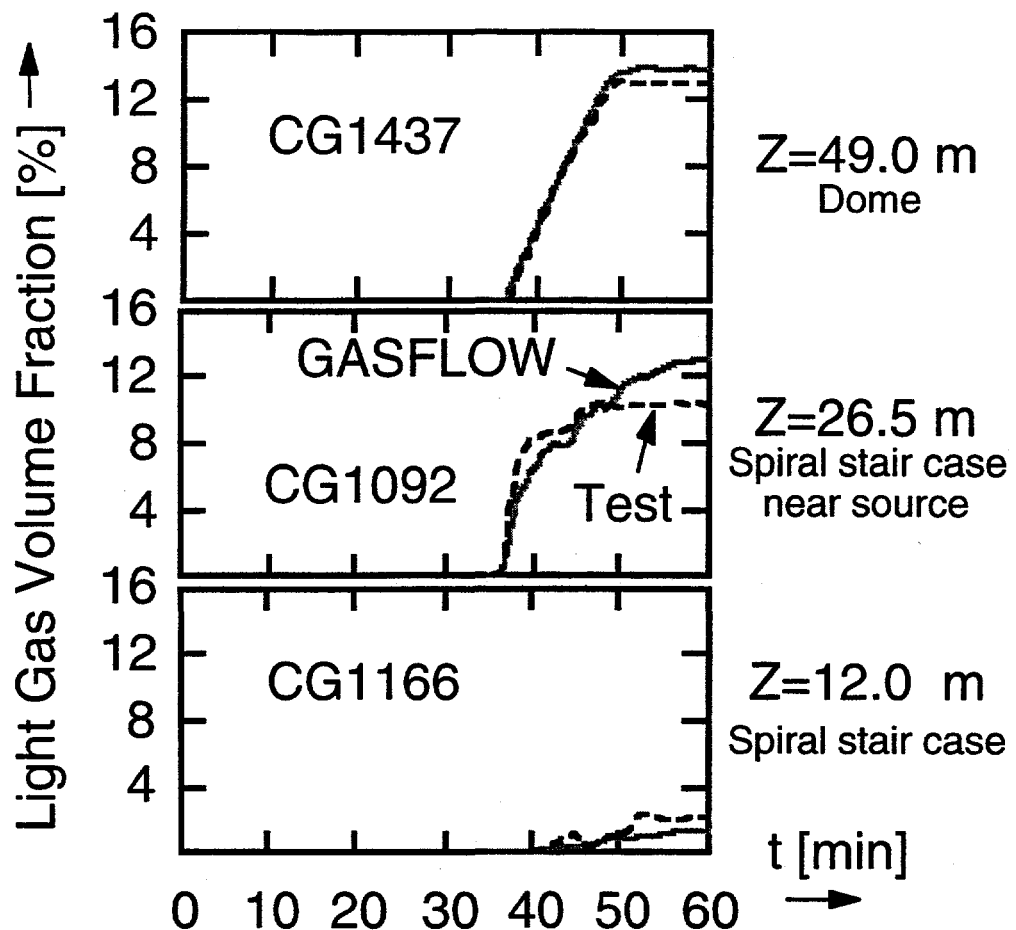


Fig. 8-31. Light-gas (15% hydrogen, 95% helium) volume fractions in HDR test T31.5; test data vs results from GASFLOW 2.1

8.2.5.4. Conclusions and Recommendations.

The GASFLOW, Version 2.1.0.13 results are in agreement with the test results, as required by the success metric.

8.2.6. Phebus Test

8.2.6.1. Summary

Purpose
Validation of the GASFLOW condensation model.
Success Metrics
Prediction of the quasi-steady containment vessel pressure, which is determined by the condensation rate in the test.
Problem Description
The Phebus thermal-hydraulic tests (Figure 8-32) consist of a total of four steady-state experiments. The initial conditions in each case were a pressure of 1.936 bars, a temperature of 110°C, and an atmosphere containing 47.952 vol % nitrogen, 39.26 vol % steam, and 12.788 vol % oxygen. During these tests, the pressure inside the vessel was measured for various rates of steam injections and different values of thermal boundary conditions (Table 8-3).
Relationship to Code Models and Methods
See Table 7-1.
Relationship to PIRT Phenomena
See Table 6.1.
Code Version and Modifications
GASFLOW 2.1.0.13 with no updates.
Hardware and Operating System
CRAY-J90 UNICOS operating system.
Compiler, Version, and Optimization Level
CRAY Fortran 90, Version 3.0.0.1.
Runtime Statistics: Total Run Time, Grind Time
Results and Conclusions
The GASFLOW results agree with experimental results.

8.2.6.2. Test Description. The Phebus containment vessel REPF 502 with its free-gas volume of ~10 m³ represents a 1/5000 scale model in volume of an actual PWR

containment vessel (Figure 8-32). Its total height and inner diameter extend to ~5.7 m and 1.8 m, respectively. It is equipped with a double-skinned outer wall; an organic liquid flowing through this annulus maintains a homogeneous temperature of ~110°C on the inner-wall surface (Table 8-3). Three condenser rods having an outer diameter of 0.15 m are attached to the top vault in positions 120° apart at a distance 0.24 m from the center line. The rods have a total length of 2.50 m. Their upper part, with a length of 1.70 m, is the so-called "wet condenser," where steam condenses on steel walls kept at an almost uniform temperature of ~70°C. The lower part, with a length of 0.80 m, contains the so-called "dry condenser," which is heated to a similar temperature at the vessel walls to prevent condensation. Steam and hydrogen can be injected through a feed pipe, which is centrally located in the lower part of the vessel. A sump at the bottom of the vault contains water, the temperature of which can be controlled.

The Phebus thermal-hydraulic tests consist of a total of four steady-state experiments. The initial conditions in each case were a pressure of 1.936 bars, a temperature of 110°C, and an atmosphere containing 47.952 vol % nitrogen, 39.26 vol % steam, and 12.788 vol % oxygen. During these tests, the pressure inside the vessel was measured for various rates of steam injections and different values of thermal boundary conditions (Table 8-3).

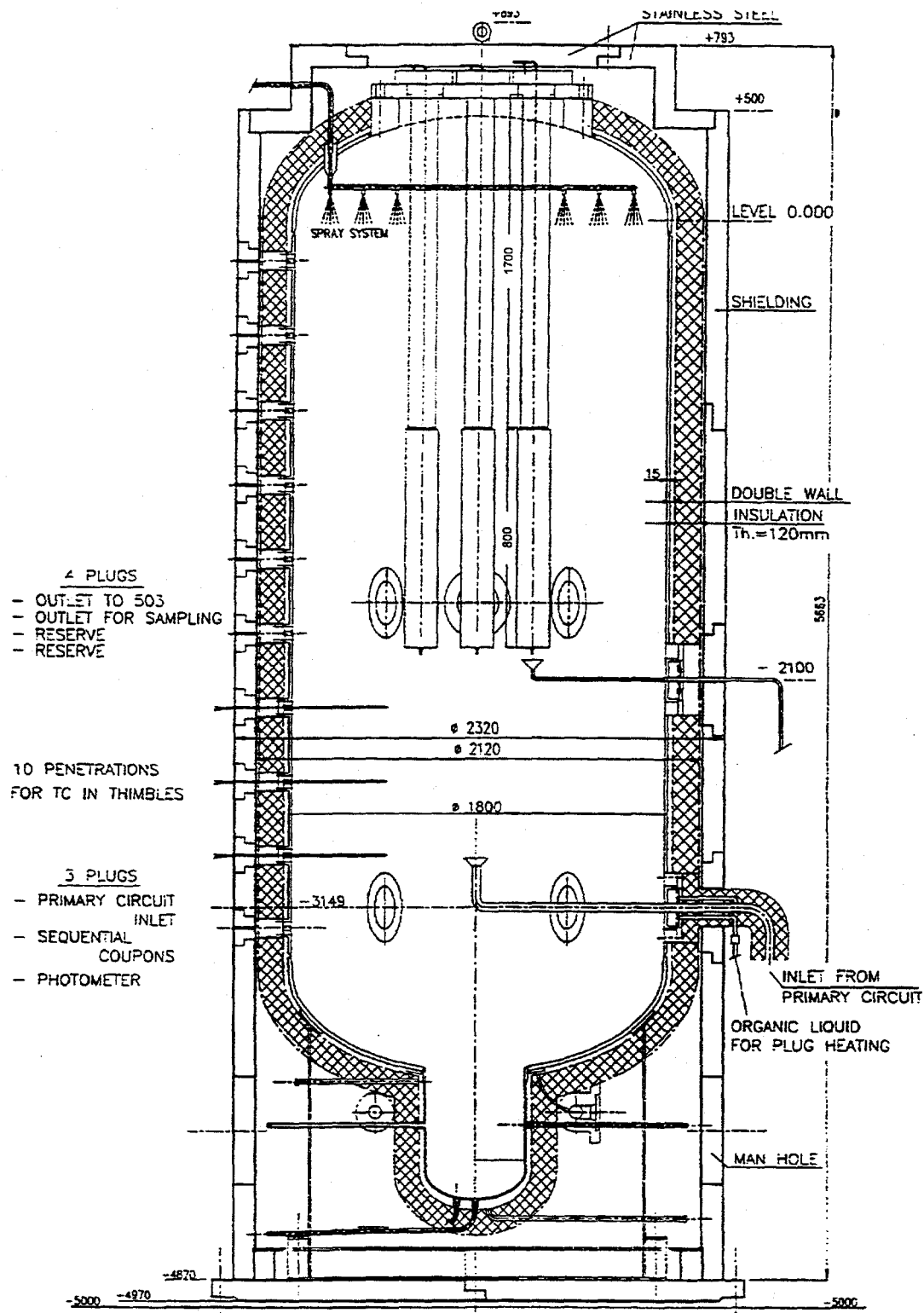


Fig. 8-32. Phebus Containment Vessel REPF 502

TABLE 8-3 Parameters and Results for the Steady-State Thermal-Hydraulic Tests

		Test 6A	Test 10A	Test 4A	Test 4B
Experimental Conditions	Steam Source (g/s)	1	2	4	4
	Pressure (bar)	1.652	1.814	2.322	2.008
	Temperature (°C)	114.17	117.04	124.82	120.21
	Dry Condenser Temperature (°C)	108 110 98	108 109 108	107 110 104	98 100 96
	Wet Condenser Temperature (°C)	75	77	91	81
	Vessel Wall Temperature (°C)	111	111	111	101
	Sump Surface Temperature (°C)	89	89	91	90
Gasflow Results (previous)	pfinal stationary (bar)	1.65	1.814	2.322	2.008
	pfinal cons1 = 4 (bar)	1.66	1.852	2.62	2.23
	pfinal cons1 = 4 Film Enhancement (bar)	1.652	1.796	2.42	2.13
Recalculation	pfinal cons1 = 4 Film Enhancement (bar)	1.644	1.753	2.213	1.952

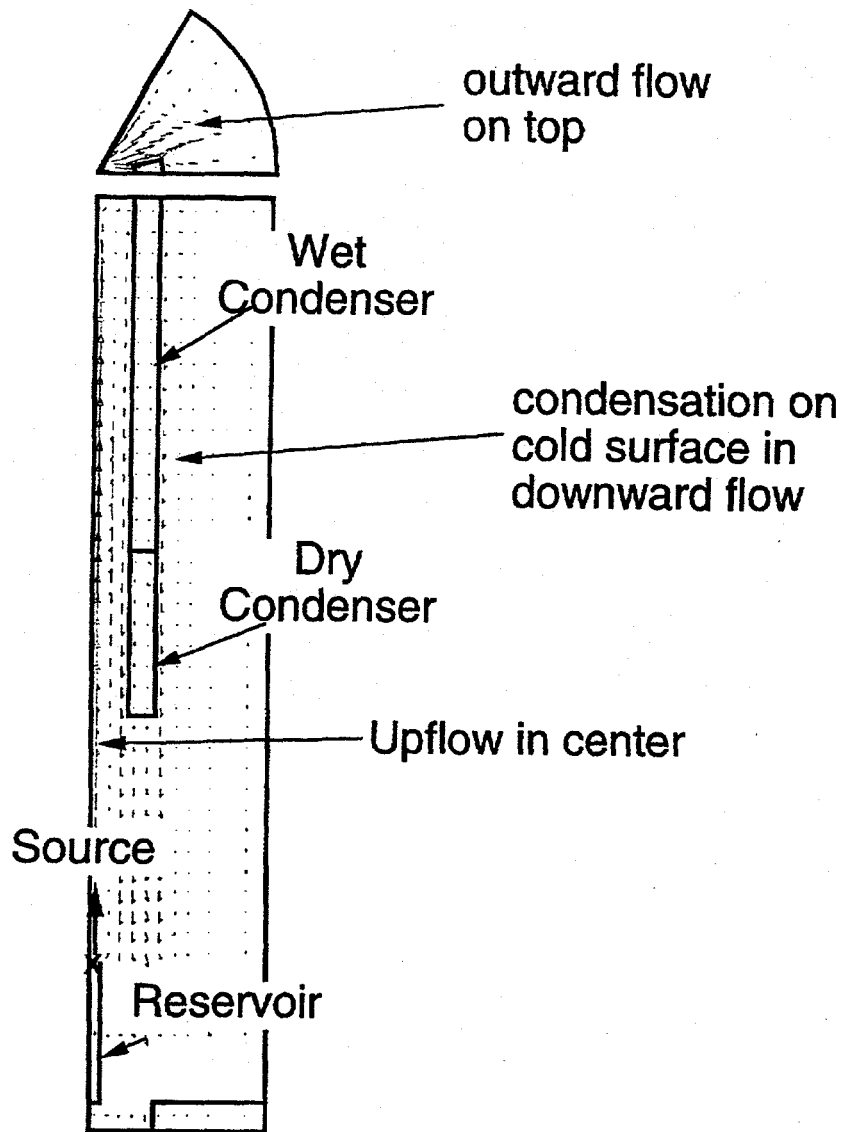


Fig. 8-33. Characteristic flow field from GASFLOW

8.2.6.3. GASFLOW Calculations.

8.2.6.3.1. GASFLOW Input Model. For the analysis with GASFLOW, a 3D model of the vessel was set up representing a 60° sector with 11 radial, 5 azimuthal, and 13 axial nodes in cylindrical coordinates (Figure 8-33). Free-slip conditions were applied to all boundary surfaces. The condensation multiplier was set to the standard value of 4.0, and a correction factor suggested by Bird-Stewart-Lightfoot⁸⁻⁶ was used.

8.2.6.3.2. GASFLOW Results. The calculations performed for laminar flow were extended to a problem time of 3600 s, which was sufficient to reach steady-state pressure levels (Table 8-3). The Phebus thermal-hydraulic tests were used to validate the GASFLOW condensation option, with the condensation parameters set to standard values. The calculated final pressures during the condensation process come close to the measured ones (Table 8-3).

8.2.6.4. Conclusions and Recommendations. The GASFLOW, Version 2.1.0.13 results are in agreement with the test results, as required by the success metric.

8.2.6.5. Input File Listing.

Input Data for Phebus Test# 10A

```
pheb-a10h2 rerun with pdv work term cons1=4.0
n7 lam 12 apr 93 / nov 97
gf-hdr
-----
$innet
$end
$xput

nrsdump = 0,
autot = 1.0,
cyl = 1.0,
delt0 = 0.0002,
deltmin = 7.000e-05,
deltmax = 1.000,
epsi0 = 1.000e-05,
epsimax = 1.000e-05,
epsimin = 1.000e-05,
gz = -980.0,
itdowndt = 500,
itupdt = 500,
itmax = 1000,
lpr = 1,
maxcyc = 900000,
ittyfreq = 200,
nu = 0.15,
prandtl = 0.7,
schmidt = 0.45,
muoption = 1,
tmodel = 'none',
idiffmom = 0,
idiffme = 0,
pltdt = 5000.000,
prtdt = 5000.00,
twfin = 3600.0,
tddt = 5000.0000,
velmx = 5.0,
ibb = 1,
ibn = 1,
ibs = 1,
ibw = 1,
ibe = 1,
ibt = 1,

sortami = 1,
mat = 'n2', 'h2o', 'h2', 'h2ol', 'o2',
```

```

gasdef(1,1)= 1, 11, 1, 06, 1, 12, 1, 1.936e+6, 383.15, 2, 0., 0.,
              'n2', 0.47952, 'h2o', 0.3926, 'h2', 0., 'h2ol', 0.,
              'o2', 0.12788,
gasdef(1,2)= 1, 02, 1, 06, 02, 03, 1, 1.814e+6, 390.19, 2, 0., 1.e+9,
              'h2o', -102,
vbc          = 1, 2, 1, 6, 3, 3, 1, 1, 0., 1.e+9,
vvalue        = 0.0,
zeroddef(1,1) = 1, 2, 1, 6, 3, 3, 1, ; reservoir
subsodef(1,1) = 1, 2, 1, 6, 2, 3, 1, ; reservoir

walls = 6, 11, 1, 06, 2, 2, 1, 1, ; vessel bottom
        1, 6, 1, 6, 1, 1, 1, 2, ; sump surface
        6, 6, 1, 6, 1, 2, 1, 3, ; sump side
        11, 11, 1, 6, 2, 12, 1, 3, ; vessel side
        01, 11, 1, 6, 12, 12, 1, 4, ; vessel top
        04, 06, 2, 2, 06, 08, 1, 5, ; dry condenser
        04, 04, 1, 2, 06, 08, 1, 6, ; dry condenser
        06, 06, 1, 2, 06, 08, 1, 7, ; dry condenser
        04, 06, 2, 2, 08, 12, 1, 8, ; wet condenser
        04, 04, 1, 2, 08, 12, 1, 9, ; wet condenser
        06, 06, 1, 2, 08, 12, 1, 10, ; wet condenser
        04, 06, 1, 2, 06, 06, 1, 11, ; dry condenser
        04, 06, 1, 2, 08, 08, 1, 12, ; wet condenser
        01, 02, 1, 6, 02, 02, 1, 00, ; blow down res.
        02, 02, 1, 6, 02, 03, 1, 00, ; blow down res.
        01, 02, 2, 02, 02, 03, 1, 00, ; blow d. res.
        01, 02, 3, 03, 02, 03, 1, 00, ; blow d. res.
        01, 02, 4, 04, 02, 03, 1, 00, ; blow d. res.
        01, 02, 5, 05, 02, 03, 1, 00, ; blow d. res.
        01, 02, 6, 06, 02, 03, 1, 00, ; blow d. res.

turbdef(1,1)= 1, 12, 1, 07, 1, 13, 1, 1, 1, 0, 0.0, 0.0,
turbdef(1,2)= 11, 12, 0, 07, 0, 13, 1, 2, 2, 0, 0., 1.e+9,
turbdef(1,3)= 0, 12, 6, 07, 0, 13, 1, 2, 2, 0, 0., 1.e+9,
turbdef(1,4)= 0, 12, 0, 07, 12, 13, 1, 2, 2, 0, 0., 1.e+9,
turbdef(1,5)= 0, 01, 0, 07, 00, 13, 1, 2, 2, 0, 0., 1.e+9,
turbdef(1,6)= 0, 12, 0, 01, 00, 13, 1, 2, 2, 0, 0., 1.e+9,
turbdef(1,7)= 0, 12, 0, 07, 00, 01, 1, 2, 2, 0, 0., 1.e+9,
tkeval      = 1., 1.0,
epsval      = 1., 1.0,

```

\$end

heat - transfer

\$rheat

```

ihtflag = 1,
matbdy = 0,

```

```

cbulkrlx = 0.001,
```

```

filmth   = 5.,
crelax   = 3.3e-2,
rholiqmx = 0.0,
cons1    = 4.0,

nhteslab = 10,
nhtewall = 22,

tsink0 =-287.,
tslab0 =-343.15,
twall0 =-343.15,

walldef(1,1) = 2, 1., 384.15, 0.0,0.01, ;vessel bottom
walldef(1,2) = 2, 0.1, 362.15, 0.0,0.01, ;sump surface top
walldef(1,3) = 2, 1., 0., 384.15,0.01, ;sump side+vessel side
walldef(1,4) = 2, 1., 0., 384.15,0.01, ;vessel top
walldef(1,5) = 2, 1., 381.48, 0.,0.01, ;dry condenser south
walldef(1,6) = 2, 1., 0., 381.48,0.01, ;dry condenser east
walldef(1,7) = 2, 1., 381.48, 0.,0.01, ;dry condenser west
walldef(1,8) = 2, 1., 350.15, 0.,0.01, ;wet condenser south
walldef(1,9) = 2, 1., 0., 350.15,0.01, ;wet condenser east
walldef(1,10) = 2, 1., 350.15, 0.,0.01, ;wet condenser west
walldef(1,11) = 2, 1., 0., 381.48,0.01, ;dry condenser top
walldef(1,12) = 2, 1., 350.15, 0.,0.01, ;wet condenser top

slabthk = 100.,
$end
-----
```

m e s h

```

$meshgn

iblock = 1,
xgrid =
0.0000e+00, 5.7867e+00, 1.1573e+01, 1.7360e+01, 2.4005e+01, 3.0650e+01,
3.7150e+01, 4.3650e+01, 5.0662e+01, 6.4685e+01, 8.5720e+01,
ygrid =
0.0000e+00, 1.2259e+01, 2.4194e+01, 3.6130e+01, 4.8065e+01, 6.0000e+01,
zgrid =
0.0000e+00, 1.3880e+01, 8.1180e+01, 1.2115e+02, 1.6111e+02, 2.0108e+02,
2.4108e+02, 2.8108e+02, 3.2358e+02, 3.6608e+02, 4.0858e+02, 4.5108e+02,
```

```
$end
-----
```

g r a p h i c s

```
$grafic
-----
```

```
thdt = 5.,
```

```
igrid = 0,
```

```

pnt = 1, 1, 05, 1,
      11, 06, 05, 1,
      01, 01, 10, 1,
      11, 06, 10, 1,
      01, 02, 01, 1,
      11, 02, 12, 1,
      04, 02, 01, 1,
      04, 02, 12, 1,
      01, 02, 12, 1,
      11, 02, 12, 1,
      01, 01, 12, 1,
      11, 06, 12, 1,

p1d = 7, 8, 'tk', 0,
      7, 8, 'vf', 'h2o',
      7, 8, 'vf', 'h2',
      9,10, 'tk', 0,
      9,10, 'vf', 'h2o',
      9,10, 'vf', 'h2',

ht1dp = 4, 02, 10, 1, 'wall', 'east',
        4, 02, 07, 1, 'wall', 'east',
        5, 02, 06, 1, 'wall', 'top',
        7, 02, 10, 1, 'wall', 'west',
        11, 02, 12, 1, 'wall', 'east',
        11, 02, 12, 1, 'wall', 'top',

v2d = 1, 2, 1,
      3, 4, 1,
      5, 6, 1,
      11, 12, 1,

c2d = 1, 2, 'vf', 'h2o',
      3, 4, 'vf', 'h2o',
      5, 6, 'vf', 'h2o',
      11, 12, 'vf', 'h2o',
      1, 2, 'vf', 'h2',
      3, 4, 'vf', 'h2',
      5, 6, 'vf', 'h2',
      11, 12, 'vf', 'h2',
      11, 12, 'tk', 0,

thp(1,1) = 04, 02, 05, 1, 'tk', 0, ; 2
            04, 02, 05, 1, 'vf', 'h2o', ; 3
            04, 02, 05, 1, 'pn', 0, ; 4
            04, 02, 05, 1, 'psat', 0, ; 5
            04, 02, 10, 1, 'tk', 0, ; 6
            04, 02, 10, 1, 'vf', 'h2o', ; 7
            04, 02, 10, 1, 'pn', 0, ; 8
            04, 02, 10, 1, 'psat', 0, ; 09
            04, 02, 12, 1, 'tk', 0, ; 10
            04, 02, 12, 1, 'vf', 'h2o', ; 11
            04, 02, 12, 1, 'pn', 0, ; 12
            04, 02, 12, 1, 'psat', 0, ; 13

```

```

04, 02, 05, 1, 'vf', 'h2', ; 14
04, 02, 10, 1, 'vf', 'h2', ; 15
04, 02, 12, 1, 'vf', 'h2', ; 16
07, 02, 12, 1, 'vf', 'h2', ; 17
04, 02, 12, 1, 'rh', 0, ; 18
04, 02, 05, 1, 'rh', 0, ; 19
02, 04, 03, 1, 'rsn', 'h2o', ; 20
02, 04, 03, 1, 'wn', 0, ; 21
htthp(1,1) = 04, 02, 10, 1, 'wall', 'east', ; 22
04, 02, 07, 1, 'wall', 'east', ; 23
07, 02, 10, 1, 'wall', 'west', ; 24
07, 02, 07, 1, 'wall', 'west', ; 25
02, 02, 02, 1, 'wall', 'bottom', ; 26
07, 02, 03, 1, 'wall', 'bottom', ; 27
$end

$special

$end
$parts

$end
-----
```

Sortam - File:

```

GF2.1 Sortam File for Phebus a10 with 2g h2o/s const
NCOLS
2
ivvalues ivtypes
1 1
0 1
time, s mdot, g/s xih2o
0.0000E+00 3.3333E-01 1.0000E+00
9.0000E+03 3.3333E-01 1.0000E+00
```

8.3. References

- 8-1 S. Gordon and B. J. McBride, "Computer Program for Calculation of Complex Chemical Equilibrium Compositions, Rocket Performance, Incident and Reflected Shocks, and Chapman-Jouget Detonations," NASA Special Publication SP-273 (1971).
- 8-2 K. L. Cashdollar et al., "Laboratory Flammability Studies of Mixtures of Hydrogen, Nitrous Oxide, and Air," Westinghouse Hanford Company report WHC-SD-WM-ES-219 (1992).
- 8-3 M. P. Sherman, S. R. Tieszen, and W. B. Benedick, "FLAME Facility: The Effect of Obstacles and Transverse Venting on Flame Acceleration and Transition to Detonation for Hydrogen-Air Mixtures at Large Scale," US Nuclear Regulatory Commission report NUREG/CR-5275 (April 1989).
- 8-4 T. K. Sherwood, R. L. Pigford, and C. R. Wilke, *Mass Transfer* (McGraw-Hill, New York, 1975), p. 23.
- 8-5 L. Wolf and L. Valencia, "Results of the Preliminary Hydrogen Distribution Experimentat HDR and Future Experiments for Phase III," 16th Water Reactor Safety Information Meeting, Gaithersburg, Maryland, October 1988, 189-222, Vol. 5, (NUREG/CP-0097) (March 1989).
- 8-6 R. B. Bird, W. E. Stewart, and E. N. Lightfoot, *Transport Phenomena* (John Wiley and Sons, New York, 1960).